

**THE EVOLUTION OF NUCLEAR MICROSATELLITE DNA MARKERS AND
THEIR FLANKING REGIONS USING RECIPROCAL COMPARISONS
WITHIN THE AFRICAN MOLE-RATS (RODENTIA: BATHYERGIDAE)**

A Dissertation

by

COLLEEN MARIE INGRAM

Submitted to the Office of Graduate Studies of
Texas A&M University
in partial fulfillment of the requirements for the degree of
DOCTOR OF PHILOSOPHY

August 2005

Major Subject: Genetics

**THE EVOLUTION OF NUCLEAR MICROSATELLITE DNA MARKERS AND
THEIR FLANKING REGIONS USING RECIPROCAL COMPARISONS
WITHIN THE AFRICAN MOLE-RATS (RODENTIA: BATHYERGIDAE)**

A Dissertation

by

COLLEEN MARIE INGRAM

Submitted to the Office of Graduate Studies of
Texas A&M University
in partial fulfillment of the requirements for the degree of

DOCTOR OF PHILOSOPHY

Approved by:

Chair of Committee,	Rodney L. Honeycutt
Committee Members,	James B. Woolley
	John W. Bickham
	Clare A. Gill
Chair of Genetics Faculty,	Geoffrey M. Kapler

August 2005

Major Subject: Genetics

ABSTRACT

The Evolution of Nuclear Microsatellite DNA Markers and Their Flanking Regions
Using Reciprocal Comparisons within the African Mole-rats (Rodentia: Bathyergidae).

(August 2005)

Colleen Marie Ingram, B.S., California State University, Long Beach

Chair of Advisory Committee: Dr. Rodney L. Honeycutt

Microsatellites are repetitive DNA characterized by tandem repeats of short motifs (2 – 5 bp). High mutation rates make them ideal for population level studies. Microsatellite allele genesis is generally attributed to strand slippage, and it is assumed that alleles are caused only by changes in repeat number. Most analyses are limited to alleles (electromorphs) scored by mobility only, and models of evolution rarely account for homoplasmy in allele length. Additionally, insertion/deletion events (indels) in the flanking region or interruptions in the repeat can obfuscate the accuracy of genotyping.

Many investigators use microsatellites, designed for a focal species, to screen for genetic variation in non-focal species. Comparative studies have shown different mutation rates of microsatellites in different species, and even individuals. Recent studies have used reciprocal comparisons to assess the level of polymorphism of microsatellites between pairs of taxa.

In this study, I investigated the evolution of microsatellites within a phylogenetic context, using comparisons within the rodent family Bathyergidae. Bathyergidae represents a monophyletic group endemic to sub-Saharan Africa and relationships are

well supported by morphological and molecular data. Using mitochondrial and nuclear DNA, a robust phylogeny was generated for the Bathyergidae. From my results, I proposed the new genus, *Coetomys*.

I designed species-specific genotyping and microsatellite flanking sequence (MFS) primers for each genus. Sequencing of the MFS provided direct evidence of the evolutionary dynamics of the repeat motifs and their flanking sequence, including rampant electromorphic homoplasy, null alleles, and indels. This adds to the growing body of evidence regarding problems with genotype scores from fragment analysis. A number of the loci isolated were linked with repetitive elements (LTRs and SINEs), characterized as robust phylogenetic characters. Results suggest that cryptic variation in microsatellite loci are not trivial and should be assessed in all studies.

The phylogenetic utility of the nucleotide variation of the MFS was compared to the well-resolved relationships of this family based on the 12S/TTR phylogeny. Variation observed in MFS generated robust phylogenies, congruent with results from 12S/TTR. Finally, a number of the indels within the MFS provided a suite of suitable phylogenetic characters.

DEDICATION

I dedicate this body of work to my parents, who have always encouraged me to explore my interests, no matter what direction I decided to take, and opening up the world to me from the beginning, including camping and an appreciation for the natural world. To Sally, who has given me so much, including the strength to be my own person and push to the end. To my Nana and Aunt Do, who weren't here but I hope would be proud. To my precious Hildie, who was with me until the end, giving me tail wags, nudges, and kisses when I needed them most. And of course, to the love of my life, Laurence, who sees in me something that I often can't, helps me find my words, inspires me to be the best scientist that I can be, and so much more...

ACKNOWLEDGEMENTS

I would like to acknowledge and thank the following people: Rodney Honeycutt, my advisor, for his previous hard work in amassing the specimen collection necessary for this study and who took me in, allowing me the independence I needed to solidify this body of work; my committee members, John Bickham, who is always a friendly face and provided me with one of my many teaching positions; James Woolley, who provided me with a strong foundation in phylogenetics and whose chuckles always brightened my day; and special thanks to Clare Gill, who picked up the slack in the Davis lab and gave me a place to do molecular evolution in an Animal Science lab. Her support and encouragement were paramount to my success during my graduate experience at A&M. A special thanks to Hynek Burda, University of Essen, while not a committee member, has acted in an adjunct capacity and has been extremely supportive throughout this project. Thank you to Colette Abbey, of the Gill lab, for her laboratory assistance and for enduring my numerous questions. I would like to thank Duane Schlitter, for his outstanding collection of African small mammal references. Thank you to Ron Adkins, for his assistance with running r8s. And a special thanks to Anthony Cognato for stepping up and providing me with employment when no one else would, allowing me to survive my last year and complete my dissertation, and to both him and his wife, April Harlin-Cognato, for their friendship, empathy, and appreciation for life outside of College Station. A number of individuals and institutions provided samples from their collections and museums: (1) D. Schlitter and S. McLaren, Carnegie Museum of Natural History, (2) D. Kock, Senckenberg Museum, and (3) I.R. Rautenbach,

Transvaal Museum. For assistance in field collections, I want to thank: W.N. Chitaukali, T. Dhliwayo, G.L. Dryden, B.H. Erasmus, M. Kawalika, J.-L. Meier, I.R. Rautenbach, A. Scharff, D. Schlitter, R. Sumbera, and P. Van Daele. I also want to thank the numerous collaborators in this ongoing project, including H. Burda, P. Dammann, S. Braude, D. Schlitter, M. Allard, E. Nevo, M. Kawalika, D. Kock, I. Rautenbabach, B. Erasmus, W. Chitikauli, R. Sumbera, P. van Daele, and A. Scharff.

Special thanks to my parents, Judd and Nancy Ingram, who have given me so much support, encouragement and enthusiasm for my research. Thank you to Sally Tolle, my other mom, who is such a strong woman, who applauded me for tolerating her son, and who shows a passion and excitement for my research endeavors as if I were her own kid. And most of all, to my love, Laurence, who I could not have done this without, thank you for helping me throughout every aspect of this project, from literature searches, through long nights in the lab, to editing, for laughing at me when I need to be laughed at, holding me up when I have doubts, believing in my abilities even more than I do, and showing such excitement with each new result.

TABLE OF CONTENTS

	Page
ABSTRACT	iii
DEDICATION	v
ACKNOWLEDGEMENTS	vi
TABLE OF CONTENTS.....	viii
LIST OF TABLES.....	xi
LIST OF FIGURES	xiv
 CHAPTER	
I INTRODUCTION.....	1
II MOLECULAR PHYLOGENETICS AND TAXONOMY OF THE AFRICAN MOLE-RATS, GENUS <i>CRYPTOMYS</i> AND THE NEW GENUS <i>COETOMYS</i> GRAY, 1864.....	11
1. Introduction	11
2. Materials and Methods.....	18
2.1. Taxon sampling and DNA isolation.....	18
2.2. PCR amplification and nucleotide sequencing.....	18
2.3. Data analyses	21
3. Results.....	24
3.1. Phylogenetic relationships based on 12S rRNA gene	24
3.2. Phylogenetic relationships based on TTR intron 1 ...	28
3.3. Phylogenetic relationships based on combined datasets	30
4. Discussion	32
4.1. Corrections to previous taxonomic designations	32
4.2. Chromosomal diversity	33
4.3. Comments on the status of the genus <i>Cryptomys</i>	36
4.4. Divergence estimates	40
4.5. Phylogenetic and biogeographic implications.....	42
4.6. Patterns of intrageneric variation.....	44
5. Conclusions	47

CHAPTER	Page
III	DEVELOPMENT AND CHARACTERIZATION OF NOVEL MICROSATELLITE MARKERS FOR THE SIX GENERA OF BATHYERGIDAE (RODENTIA) AND THEIR UTILITY IN OTHER MEMBERS OF THE FAMILY 48
	1. Introduction 48
	2. Materials and Methods 53
	2.1. Microsatellite library and primer construction 53
	2.2. Taxon sampling 55
	2.3. Microsatellite amplification, genotyping, and sequencing 56
	2.4. Data analyses 56
	3. Results and Discussion 57
	3.1. Amplification and variation within focal taxa 57
	3.2. Application and variation in non-focal taxa 61
	4. Conclusions 70
IV	CHARACTERIZING MICROSATELLITE LOCI AND THEIR PRIMER SITES BY DIRECT SEQUENCING: MOTIF DECAY, ELECTROMORPHIC HOMOPLASY, AND NULL ALLELES 71
	1. Introduction 71
	2. Materials and Methods 73
	2.1. Genomic library and primer construction 73
	2.2. Screening of genotyping and flanking sequence primer sets 74
	2.3. Data analyses (Characterization of loci) 76
	3. Results 80
	3.1. Genotyping 80
	3.2. Characterization of the microsatellite motifs and their immediate flanking sequences 89
	4. Discussion 147
	4.1. Comparison of microsatellite panels based on genotyping data 147
	4.2. Comparisons of repeat motifs and the function of sequence data 149
	4.3. Is ascertainment bias a problem? 150
	4.4. Electromorphic size homoplasy 150
	4.5. Null alleles 151
	4.6. Rare genomic changes (RGC) 152
	5. Conclusions 153

CHAPTER	Page
V	THE UTILITY OF MICROSATELLITE FLANKING SEQUENCES AS DATA IN PHYLOGENETIC RECONSTRUCTION..... 155
	1. Introduction 155
	2. Materials and Methods..... 159
	2.1. Taxon sampling and DNA isolation..... 159
	2.2. Microsatellite flanking region amplification and sequencing..... 159
	2.3. Data analyses 161
	3. Results 163
	3.1. Success of sequencing effort across MFS loci 163
	3.2. Phylogenetic analyses of 16 microsatellite flanking sequences..... 163
	3.3. Combined data sets 182
	4. Discussion 185
	4.1. Utility of flanking sequences in phylogenetic reconstruction 185
	4.2. Combined analysis 186
	5. Conclusions 187
VI	SUMMARY 188
	REFERENCES..... 191
	APPENDIX..... 210
	VITA..... 211

LIST OF TABLES

TABLE	Page
2.1	Estimation of the ages of the lineages within the family Bathyergidae using non-parameteric rate smoothing..... 41
3.1	Characterization of seven polymorphic microsatellite loci isolated from <i>Heliophobius argenteocinereus</i> 58
3.2	Characterization of 6 polymorphic microsatellite loci isolated from <i>Georychus capensis</i> 59
3.3	Characterization of 5 polymorphic microsatellite loci isolated from <i>Bathyergus suillus</i> 62
3.4	Characterization of 5 polymorphic microsatellite loci isolated from <i>Cryptomys hottentotus</i> 63
3.5	Characterization of 5 polymorphic microsatellite loci isolated from <i>Coetomys mechowii</i> 64
3.6	Characterization of seven polymorphic microsatellite loci isolated from <i>Heterocephalus glaber</i> 65
3.7	Number of alleles observed at each microsatellite loci designed from <i>Heliophobius argenteocinereus</i> (Harg), <i>Georychus capensis</i> (Gcap), <i>Bathyergus suillus</i> (Bsuil), <i>Cryptomys hottentotus</i> (Chott), <i>Coetomys mechowii</i> (Cmech), and <i>Heterocephalus glaber</i> (Hglab). 67
4.1	Observed and expected heterozygosities (obs/exp) calculated using data from microsatellite loci designed from <i>Heliophobius argenteocinereus</i> (Harg), <i>Georychus capensis</i> (Gcap), <i>Bathyergus suillus</i> (Bsuil), <i>Cryptomys hottentotus</i> (Chott), <i>Coetomys mechowii</i> (Cmech), and <i>Heterocephalus glaber</i> (Hglab)..... 78
4.2	Range of alleles observed at microsatellite loci designed from <i>Heliophobius argenteocinereus</i> (Harg), <i>Georychus capensis</i> (Gcap), <i>Bathyergus suillus</i> (Bsuil), <i>Cryptomys hottentotus</i> (Chott), <i>Coetomys mechowii</i> (Cmech), and <i>Heterocephalus glaber</i> (Hglab). 79
4.3	Comparison of number of loci with the longest alleles, number of loci with the highest number of alleles, and range of alleles for focal and non-focal taxa for each microsatellite panel. 90

TABLE	Page
4.4 Observed sequence length, repeat motif, indels, additional repetitive regions, and changes in the primer sites for locus Harg02.	91
4.5 Observed sequence length, repeat motif, and indels documented for locus Harg03.....	93
4.6 Observed sequence length, repeat motif, indels, additional repetitive regions, and changes in the primer sites for locus Harg07.	95
4.7 Observed sequence length, repeat motif, indels, additional repetitive regions, and changes in the primer sites for locus Gcap01.....	97
4.8 Observed sequence length, repeat motif, indels, additional repetitive regions, and changes in the primer sites for locus Gcap07.....	99
4.9 Observed sequence length, repeat motif, indels, additional repetitive regions, and changes in the primer sites for locus Bsuil01.....	101
4.10 Observed sequence length, repeat motif, indels, and changes in the primer sites for locus Bsuil04.....	103
4.11 Observed sequence length, repeat motif, indels, and changes in the primer sites for locus Bsuil06.....	105
4.12 Observed sequence length, repeat motif, indels, and changes in the primer sites for locus Chott01.	107
4.13 Observed sequence length, repeat motif, indels, and changes in the primer sites for locus Chott03.	109
4.14 Observed sequence length, repeat motif, indels, and changes in the primer sites for locus Chott08.	111
4.15 Observed sequence length, repeat motif, indels, additional repetitive regions, and changes in the primer sites for locus Cmech03.	113
4.16 Observed sequence length, repeat motif, indels, additional repetitive regions, and changes in the primer sites for locus Cmech04.	115
4.17 Observed sequence length, repeat motif, indels, and changes in the primer sites for locus Cmech09.....	117

TABLE	Page
4.18 Observed sequence length, repeat motif, indels, additional repetitive regions, and changes in the primer sites for locus Cmech11.	119
4.19 Observed sequence length, repeat motif, indels, and changes in the Hglab10-R primer site for locus Hglab10.....	121
4.20 Microsatellite loci with confirmation of null alleles	124
4.21 Detection of electromorphic homoplasies.....	127
5.1 Phylogenetic use of microsatellite flanking sequences (MFS).	164

LIST OF FIGURES

FIGURE	Page
2.1 Sampling localities for specimens.....	13
2.2 12S rRNA maximum-likelihood phylogeny under GTR + Γ + I.....	25
2.3 TTR Intron I maximum-likelihood phylogeny under HKY85 + Γ	29
2.4 Combined data (12S rRNA and TTR Intron I) maximum-likelihood phylogeny under GTR + Γ + I.....	31
2.5 Diploid numbers (2N) mapped on the 12S rRNA phylogeny.....	35
4.1 Two scenarios of microsatellite flanking sequence (MFS) primer design. ..	75
4.2 Microsatellite repeat motif of Harg02 plotted on the phylogeny based on Ingram et al. 2004.....	92
4.3 Microsatellite repeat motif of Harg03 plotted on the phylogeny based on Ingram et al. 2004.....	94
4.4 Microsatellite repeat motif of Harg07 plotted on the phylogeny based on Ingram et al. 2004.....	96
4.5 Microsatellite repeat motif of Gcap01 plotted on the phylogeny based on Ingram et al. 2004.....	98
4.6 Microsatellite repeat motif of Gcap07 plotted on the phylogeny based on Ingram et al. 2004.....	100
4.7 Microsatellite repeat motifs of Bsui101 plotted on the phylogeny based on Ingram et al. 2004.....	102
4.8 Microsatellite repeat motif of Bsui104 plotted on the phylogeny based on Ingram et al. 2004.....	104
4.9 Microsatellite repeat motif of Bsui106 plotted on the phylogeny based on Ingram et al. 2004.....	106
4.10 Microsatellite repeat motif of Chott01 plotted on the phylogeny based on Ingram et al. 2004.....	108

FIGURE	Page
4.11 Microsatellite repeat motif of Chott03 plotted on the phylogeny based on Ingram et al. 2004.....	110
4.12 Microsatellite repeat motif of Chott08 plotted on the phylogeny based on Ingram et al. 2004.....	112
4.13 Microsatellite repeat motif of Cmech03 plotted on the phylogeny based on Ingram et al. 2004.....	114
4.14 Microsatellite repeat motif of Cmech04 plotted on the phylogeny based on Ingram et al. 2004.....	116
4.15 Microsatellite repeat motif of Cmech09 plotted on the phylogeny based on Ingram et al. 2004.....	118
4.16 Microsatellite repeat motif of Cmech11 plotted on the phylogeny based on Ingram et al. 2004.....	120
4.17 Microsatellite repeat motif of Hglab10 plotted on the phylogeny based on Ingram et al. 2004.....	122
5.1 Bsuil06 microsatellite flanking sequence maximum-likelihood phylogeny under GTR	165
5.2 Cmech03 microsatellite flanking sequence maximum-likelihood phylogeny under K80.....	166
5.3 Cmech09 microsatellite flanking sequence maximum-likelihood phylogeny under TrN + G.....	167
5.4 Bsuil01 microsatellite flanking sequence maximum-likelihood phylogeny under K80+G.....	168
5.5 Cmech04 microsatellite flanking sequence maximum-likelihood phylogeny under K80 + G.....	169
5.6 Harg03 microsatellite flanking sequence maximum-likelihood phylogeny under K80.....	170
5.7 Harg02 microsatellite flanking sequence maximum-likelihood phylogeny under K80.....	171

FIGURE	Page
5.8 Harg07 microsatellite flanking sequence maximum-likelihood phylogeny under K80.....	172
5.9 Chott03 microsatellite flanking sequence maximum-likelihood phylogeny under HKY85.....	173
5.10 Gcap07 microsatellite flanking sequence maximum-likelihood phylogeny under K80.....	175
5.11 Chott01 microsatellite flanking sequence maximum-likelihood phylogeny under K81uf + G	176
5.12 Chott08 microsatellite flanking sequence maximum-likelihood phylogeny under GTR	177
5.13 Cmech11 microsatellite flanking sequence maximum-likelihood phylogeny under TrN.....	178
5.14 Gcap01 microsatellite flanking sequence maximum-likelihood phylogeny under K80.....	179
5.15 Bsui104 microsatellite flanking sequence maximum-likelihood phylogeny under HKY85	180
5.16 Hglab10 microsatellite flanking sequence maximum-likelihood phylogeny under K80.....	181
5.17 Combined maximum-likelihood phylogeny of Cmech04, Gcap01, and Hglab10 under TVM + G	183
5.18 Combined maximum-likelihood phylogeny of all 16 microsatellite flanking sequence (MFS) loci under TVM + G	184

CHAPTER I

INTRODUCTION

Microsatellites are regions of DNA containing simple sequence motifs (2-6 bp in length) that are repeated in tandem up to 100 times (Tautz, 1993; Zhivotovsky and Feldman, 1995). Currently, microsatellite loci are considered the marker of choice for population genetics (Bowcock et al., 1994; Gardner et al., 2000; Sunnucks, 2000). In addition, they have been used extensively for paternity and kinship assessment (Altet et al., 2001), forensic identification (Edwards et al., 1992), epidemiology of infectious diseases (Wang et al., 2001), and genome mapping (Causse et al., 1994; Dib et al., 1996; Su and Willems, 1996). Many microsatellite loci are characterized by moderate to high levels of polymorphism associated with the repeat region and sequence conservation in the flanking regions where site-specific PCR (polymerase chain reaction) primers can be made for the amplification of orthologous loci across individuals within a species. In addition, many loci isolated from one species (the focal species) can be used in genetic studies of related species (non-focal species), thus providing a high yield of genetic information with little start-up investment (Clisson et al., 2000; Glenn et al., 1996; Fitzsimmons et al., 1995; Jordan et al., 2002; Moore et al., 1991).

This dissertation follows the style of *Molecular Phylogenetics and Evolution*.

Microsatellites are ideal for intraspecific and population level studies because of their high mutation rate that has been documented to be 10^{-5} to 10^{-2} per generation (Edwards et al., 1992; Macaubas et al., 1997). Other markers that have been applied to studies at similar levels of taxonomic divergence (allozymes, mtDNA, etc.) usually cannot provide sufficient variation when comparing closely related individuals (Fitzsimmons et al., 1995). The high mutation rate observed in microsatellites is due to increases or decreases in the number of repeat units as a result of either slip-strand mispairing or unequal crossing-over (Levinson and Gutman, 1987). Slip-strand mispairing (SSM) occurs during the process of DNA replication, when the DNA polymerase is believed to “slip,” causing the newly synthesized fragment of DNA to become misaligned with the template. For continued replication of the template strand, the two strands must be realigned. If the realignment is not perfect, then a mutation will be generated, generally resulting in changes to the number of tandem repeat elements. It is expected that SSM will occur in microsatellites at an increased rate due to their repetitive nature (Streisinger et al., 1966). The instability of microsatellite DNA also has been attributed to unequal crossing-over (UCO) within the microsatellite repeat. It is believed that misalignment along the repeating sequence of homologous chromosomes during meiosis increases the likelihood of UCO. While multiple studies support the SSM model to account for the majority of mutation events in microsatellite DNA (Levinson and Gutman, 1987; Macaubas et al., 1997; Schlötterer and Tautz, 1992; Strand et al., 1993), UCO has been shown to be a contributor to the instability of these regions, as evidenced by changes in the flanking regions (Gardner et al., 2000; Jin et al.,

1996; Primmer et al., 1998).

Although SSM and UCO explain the mechanism by which new mutations, or alleles, can be produced in microsatellite DNA, an adequate evolutionary model is necessary for the quantitative assessment of genetic variation within and between populations. Two of the most frequently applied models are the infinite alleles model (IAM: Kimura and Crow, 1964) and the stepwise mutation model (SMM: Kimura and Ohta, 1978). These models both assume that mutation rate is constant across all loci and for all alleles at a single locus (Goldstein et al., 1995b; Shriver et al., 1993; Slatkin, 1995; Valdes et al., 1993). The IAM assumes no homoplasy with each new mutation creating a novel allele (Estoup and Cornuet, 1999). Therefore, if two alleles are identical by state (IBS), then they must also be identical by descent (IBD). Data analyzed under IAM are limited to alleles (electromorphs) scored by mobility only, without information about repeat number. While this model is not realistic because mutations in these loci and restrictions in maximum length make homoplasy virtually inevitable, it is useful as a standard (or null) for comparison with other models. The SMM explains mutations as single additions or deletions of the repeat unit due to strand slippage (Valdes et al., 1993). Therefore, alleles that are identical by state are not assumed to be IBD, allowing for size homoplasy (Estoup et al., 1995). Although the IAM and SMM are extreme models, they are incorporated into most of the statistical/analytical software available to analyze microsatellite data, with the assumption that the true model falls somewhere between the two extremes. Recently, additional models have been developed or revisited as a means of explaining the intermediate distributions of microsatellite alleles

found in natural populations. The *K*-allele Model (KAM: Crow and Kimura, 1970; Crow, 1986) was the first modification of the IAM and is receiving renewed consideration in the search for more appropriate models. Like the IAM, the KAM defines each mutation event as unique, resulting in a novel allele, but places limitations on the number of alleles possible (Estoup and Cornuet, 1999). The Two-Phase Model (TPM: Di Rienzo et al., 1994) allows for gain/loss of *X* number of repeats, assuming that single step changes are most frequent, but allowing for larger jumps in repeat number. While modifications of this model provide allowances for rate variation between loci and an allele length ceiling (Feldman et al., 1997), no current models address the known complexities of microsatellite DNA evolution.

Many different factors have been shown to influence mutation rates of microsatellites. Variation in mutation rates across multiple loci or within different lineages is common (Crozier et al., 1999; Gardner et al., 2000; Primmer and Ellegren, 1998; Weber and Wong, 1993). It also has been suggested that rates can vary among alleles at a single locus (Jin et al., 1996). Alleles with greater number of repeats generally demonstrate increased mutation rates (Macaubas et al., 1997; Primmer et al., 1996a; Weber, 1990). Longer repeat stretches offer more opportunities for slippage events resulting in a positive correlation between allele size and mutation rate at a locus (Primmer et al., 1998). Through the use of cell lines and deep pedigrees, several studies support a bias toward expansions in repeat number (Amos et al., 1996; Ellegren, 2000; Primmer et al., 1998, 1996a; Weber and Wong, 1993). This expansion appears to be limited by as yet undefined mechanisms, enforcing upper limits on allele sizes (Bowcock

et al., 1994; Garza et al., 1995; Primmer et al., 1998). Mutation rates and the direction of mutations have been shown to differ between sexes in both human and non-human studies (Primmer et al., 1998; Weber and Wong, 1993). The structure of the repeat array can influence mutation rates (Estoup et al., 1995). In general, disease-causing trinucleotide loci have shown the highest mutation rates, followed by dinucleotide, non-disease trinucleotide, and tetranucleotide loci in decreasing order (Chakraborty et al., 1997; Schug et al., 1998). A number of studies, however, found extraordinarily high mutation rates in rare non-disease-causing tetranucleotide loci (Gardner et al., 2000; Primmer et al., 1996a). Complex repeats have been documented to have slower mutation rates than intact repeat motifs (Chung et al., 1993; Estoup et al., 1995). Interrupting point mutations within a repeat motif are believed to slow down mutation rate and have been linked to the “death” of microsatellite loci (Chung et al., 1993; Macaubas et al., 1997). Among individuals, mutation rates have been shown to increase in heterozygotes with large size differences between alleles, relative to heterozygotes with small size differences (heterozygote instability)(Amos et al., 1996). The base composition of flanking sequences also has been shown to influence mutation rate and high GC content of flanking regions appears to be negatively-correlated with allelic diversity (Glenn et al., 1996).

Although these markers can provide the necessary amount of polymorphism at the population level, there are problems with their current application, usually as the result of limited knowledge of the markers being used (Primmer et al., 1998). One problem with the current use of microsatellite markers is that the complexity in the

repeat patterns of loci is not usually accounted for in either model selection or the interpretation of results. Studies that use perfect dinucleotide repeats, have shown support for the stepwise mutation model, although most are limited to species-specific markers in population level work (Bell and Jurka, 1997). Any expansion to comparisons at higher taxonomic levels could be compromised by lineage-specific mutation rates. To reduce costs, microsatellite primers previously designed for a focal species are used to screen for genetic variation in non-focal species (Fitzsimmons et al., 1995; Glenn et al., 1996; Jordan et al., 2002; Moore et al., 1991). Any successfully amplified loci that show any degree of polymorphism are then included, under the assumption that the nature of variation at each microsatellite locus will be comparable to that of the species from which the primers were originally designed. It is assumed that detectable “alleles” are caused only by changes in repeat number. More importantly, most investigators score electromorphs as alleles, based on migration of an amplified fragment (fragment analysis). Scoring alleles by product length alone cannot detect “cryptic” electromorphic homoplasy of alleles. When microsatellite alleles are sequenced, it has often been discovered that the variability is due to an insertion/deletion (indel) event within the flanking sequence or varying changes along a complex repeat motif (*e.g.*, $(CA)_8(CG)_{10}$ to $(CA)_9(CG)_{10}$ versus $(CA)_8(CG)_{10}$ to $(CA)_8(CG)_{11}$) (Angers and Bernatchez, 1997; Colson and Goldstein, 1999; Estoup et al., 1995; Jin et al., 1996; Ortí et al., 1997; Schlötterer, 2001; van Oppen et al., 2000). If undetected, this homoplasy will lead to inaccurate measurements of population statistics (heterozygosity, diversity, effective population size, migration rates, etc.). Additionally, most models assume that

markers have equal mutation rates, both among sites and among taxa. Comparative studies have shown that the mutation rates at microsatellite loci are not equal in different species, populations, and even individuals (Cooper et al., 1998; Crawford et al., 1998; Glenn et al., 1996; Rubinsztein et al., 1995; van Oppen et al., 2000). A recurring observation is higher levels of polymorphism in the taxa from which the markers were originally designed, suggesting increased mutation rates in the focal species. These trends have usually been explained as a result of an ascertainment bias toward higher levels of polymorphism in the focal species due to the qualifiers (amplification success, product length, number of repeats, etc.) used for the initial selection of a locus as a marker for the focal species (Ellegren et al., 1995; Jordan et al., 2002; Primmer et al., 1996b). One caveat to accepting ascertainment bias alone, as an explanation for the differences in the levels of polymorphism observed, is that most studies examine the behavior of proven markers (previously designed for a focal taxon) in other related taxa without reciprocal tests. Since most previous studies compared only two taxa (focal versus non-focal), they are limited in their ability to uncover the mechanisms responsible for differences in levels of polymorphism. While many of these studies may show true ascertainment bias, they fail to provide unbiased data for alternative explanations. Recent studies do not support the ascertainment bias hypothesis, but rather support directional evolution in which a particular species would tend to gain or lose repeats across all loci in concert (Cooper et al., 1998; Crawford et al., 1998; Ellegren et al., 1995; Estoup et al., 1995; Zhu et al., 2000).

Recently the utility of microsatellites as phylogenetic markers has been assessed

(Arévalo et al., 2004; Jin et al., 1996; Ortí et al., 1997; Schlötterer, 2001; Zardoya et al., 1996). The results were mixed with some microsatellites showing sound phylogenetic information, particularly imperfections within the repeat motif, while the utility of perfect repeats was limited to closely related taxa (Zhu et al., 2000). Although these studies have provided more information on the value of microsatellites as informative genetic markers, each was limited to few loci, analogous to earlier work with single locus mtDNA gene trees (Avise, 1994).

The goal of this study is to investigate the evolutionary processes of microsatellite DNA within a phylogenetic context using reciprocal comparisons within and among the genera of African mole-rats (Bathyergidae: Rodentia). Many characteristics make Bathyergidae an ideal model for evolutionary studies. African mole-rats represent a monophyletic group endemic to sub-Saharan Africa and relationships among the genera are well supported by morphological, chromosomal, and nuclear and mitochondrial DNA sequence data (Chapter II; Allard and Honeycutt, 1992; Faulkes et al., 1997; Honeycutt et al., 1987; Ingram et al., 2004; Janecek et al., 1992; Walton et al., 2000). Prior to the current study, there were five recognized genera: *Heterocephalus* (1 sp) and *Heliophobius* (1 sp), which are restricted in distribution to Eastern Africa; *Bathyergus* (2 sp) and *Georychus* (1 sp), which are limited to southern Africa; and, the broadly distributed and specious genus *Cryptomys* (11 species currently recognized), whose range extends from Ghana in west Africa to southern Sudan and northern Angola in east Africa, and south to the Cape Province of South Africa (Aguilar, 1993; Burda et al., 1999; Faulkes et al., 1997; Honeycutt et al., 1987; Macholán et al.,

1993; Walton et al., 2000). Within *Cryptomys*, were two well-defined monophyletic clades: the southern *hottentotus* species group and the *mechowii* group that includes all other forms (Bennett and Faulkes, 2000; Walton et al., 2000). All species of the family are strictly fossorial and have been much studied due to their unique life histories (Bennett and Faulkes, 2000; Sherman, et al., 1991). As with other families of fossorial rodents, bathyergids exhibit high levels of chromosomal evolution. All species in *Heterocephalus*, *Georychus*, *Bathyergus* and the *C. hottentotus* group have fixed diploid numbers, ranging from 54 to 60. A recent paper describes a second karyotype within *Heliophobius* (Scharff et al., 2001). In contrast, the *C. mechowii* group shows high levels of chromosomal evolution (ranging from 40 to 72), coupled with lower levels of sequence divergence, suggesting the rapid and isolating effect of changes in chromosome number (Ingram et al., 2004). Among bathyergids, population structure ranges from solitary to the highly structured social system of the naked mole-rat, *Heterocephalus*. The genus *Heterocephalus* was the first mammalian species to be documented as eusocial, with colonies showing a definitive caste system analogous to the social insects (Jarvis, 1981). Because of their varying life histories, differences in effective population size, and chromosomal evolution, this family is ideal for investigating the evolution of microsatellites and their flanking regions.

Previous molecular and morphological studies have focused on relationships among genera and the placement of Bathyergidae, relative to other families of hystricognath rodents (Allard and Honeycutt, 1992; Faulkes et al., 1997; Honeycutt et al., 1987; Janecek et al., 1992; Walton et al., 2000). Although molecular data have

contributed to the resolution of relationships among genera in Bathyergidae and the placement of the family relative to other families, few studies have been conducted on geographic variation within either genera or species. For instance, considerable allozyme (Filippucci et al., 1997, 1994; Janacek et al., 1992; Nevo et al., 1987), chromosome (Burda et al., 1999), and nucleotide sequence variation (Faulkes et al., 1997; Walton et al., 2000) has been reported in *Cryptomys*, yet no study has thoroughly documented patterns of genetic variation throughout the distribution of the genus. In Chapter II, a well-supported phylogeny is recovered for the family using both mitochondrial (12S rRNA) and nuclear (Intron 1 of Transthyretin) DNA markers. This phylogeny provides evidence for the elevation of the *mechowii* species group to the genus *Coetomys* and an independent phylogenetic framework of the relationships of the genera and species of Bathyergidae.

To examine the evolution of microsatellite DNA within this phylogenetic framework, species-specific genotyping primers were designed for each genus (Chapter III). In addition to genotyping primers, primers were designed outside of the genotyping fragment so the evolutionary dynamics of the repeat motifs and their flanking sequence could be investigated (Chapter IV). Additionally, the microsatellite flanking sequences (MFS) were tested for their utility in phylogenetic reconstruction when compared to the well-resolved relationships of this family based on the 12S/TTR phylogeny (Chapter V).

CHAPTER II
MOLECULAR PHYLOGENETICS AND TAXONOMY OF THE AFRICAN
MOLE-RATS, GENUS *CRYPTOMYS* AND THE NEW GENUS *COETOMYS*
GRAY, 1864*

1. Introduction

African mole-rats of the family Bathyergidae represent a monophyletic group of subterranean rodents endemic to sub-Saharan Africa. Two members of this family, *Heterocephalus* and *Cryptomys*, have received extensive attention due to their unique life histories and ecology (e.g., Bennett and Faulkes, 2000; Lacey et al., 2000; Nevo, 1999; Nevo and Reig, 1990; Sherman et al., 1991). Among members of the family, social structure ranges from solitary (*Bathyergus*, *Georychus*, *Heliophobius*) to the highly-structured social system of the naked mole-rat, *Heterocephalus glaber*, the first mammalian species to be documented as eusocial (Jarvis, 1981). Currently, there are 5 recognized genera, 4 of which have relatively low species diversity. These taxa include: 1) the monotypic genus *Heterocephalus*, restricted to eastern Africa; 2) the monotypic genus *Heliophobius* occurring in eastern and southeastern Africa; 3) the monotypic genus *Georychus*, which is endemic to South Africa and 4) *Bathyergus*, containing two species found in Namibia and South Africa. In contrast, the fifth genus, *Cryptomys*,

*Reprinted with permission from “Molecular phylogenetics and taxonomy of the African mole-rats, genus *Cryptomys* and the new genus *Coetomys* Gray, 1864”: by CM Ingram, H Burda, and RL Honeycutt, 2004. *Molecular Phylogenetics and Evolution*, 31: 997– 1014. 2005 by Elsevier Inc.

contains 11 currently recognized species, and displays a broad but disjunct distribution extending from Ghana and Nigeria in west Africa to the southern Sudan in east Africa (within the Sudanian vegetation phytochorion, cf., White 1983), and from southern Congo and southern Tanzania to the Western Cape Province of South Africa (i.e., throughout the Zambebian, Kalahari-Highveld, Karoo-Namib and Cape phytochoria) (Fig. 2.1a-c: also, Bennett and Faulkes, 2000; Burda, 2001; Honeycutt et al., 1991). All species of the genus *Cryptomys* are social and some can be considered eusocial (cf., Bennett and Faulkes, 2000; Burda et al., 2000; Burda and Kawalika, 1993; Jarvis and Bennett, 1993; Jarvis et al., 1994). In addition, this genus displays considerable chromosomal variation (diploid numbers ranging from 40-78: Burda, 2001) and complex patterns of morphological variation, especially relative to size and color patterns (Honeycutt et al., 1991; Rosevear, 1969).

Previous molecular and morphological studies have focused on relationships among genera and the placement of Bathyergidae relative to other families of hystricognath rodents (Allard and Honeycutt, 1992; Faulkes et al., 1997; Honeycutt et al., 1987; Janecek et al., 1992; Walton et al., 2000). Although molecular data have contributed to the resolution of relationships among genera of Bathyergidae and the placement of the family relative to other families, few studies have been conducted on geographic variation within either genera or species. For instance, considerable allozyme (Filippucci et al., 1994, 1997; Janacek et al., 1992; Nevo et al., 1987), chromosome (Burda et al., 1999), and nucleotide sequence variation (Faulkes et al.,

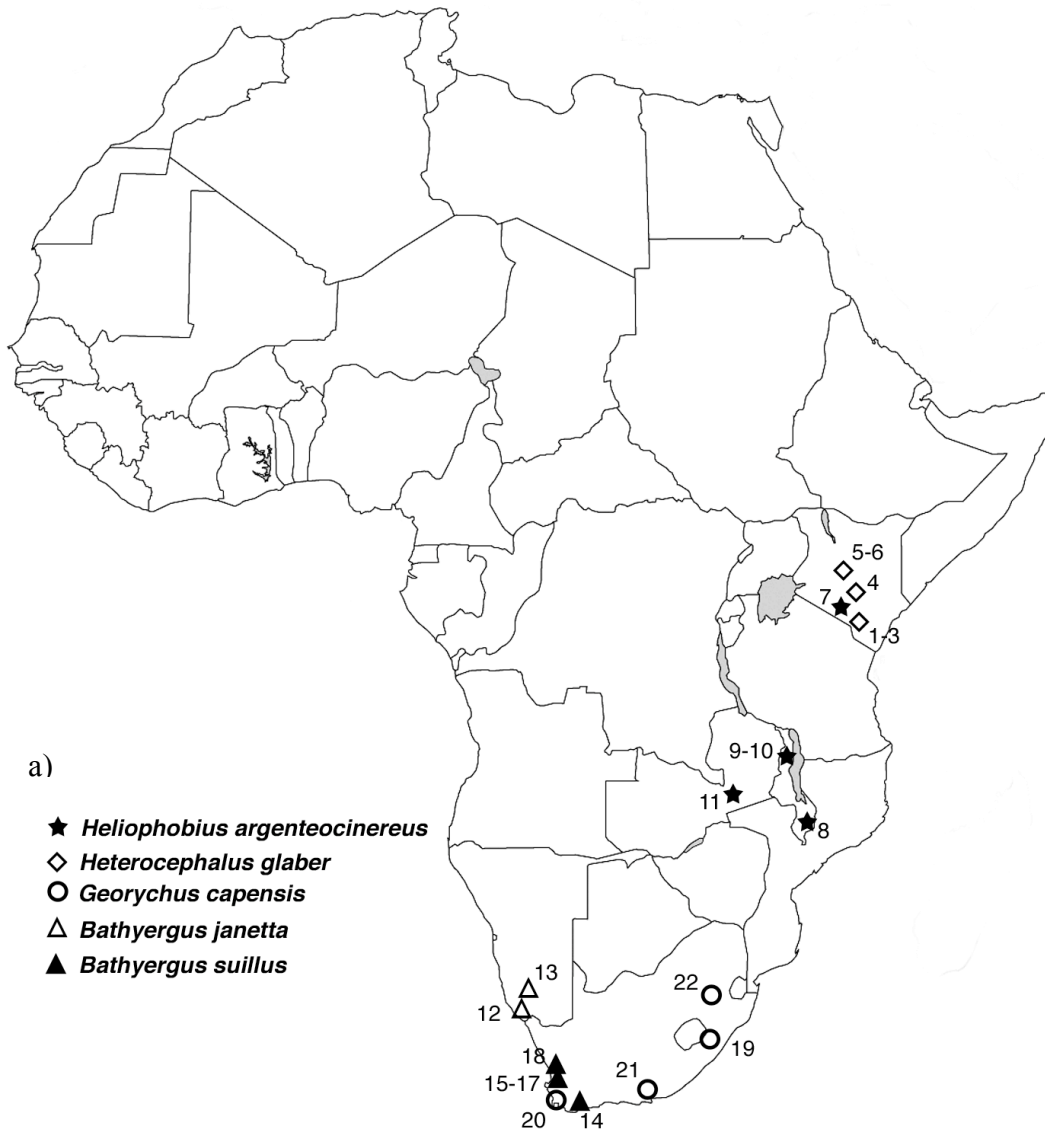


Fig. 2.1 Sampling localities for specimens. Sample numbers correspond to the specimens listed in the Appendix. a) *Heterocephalus*, *Heliophobius*, *Bathyergus*, *Georychus* specimens used in this study.

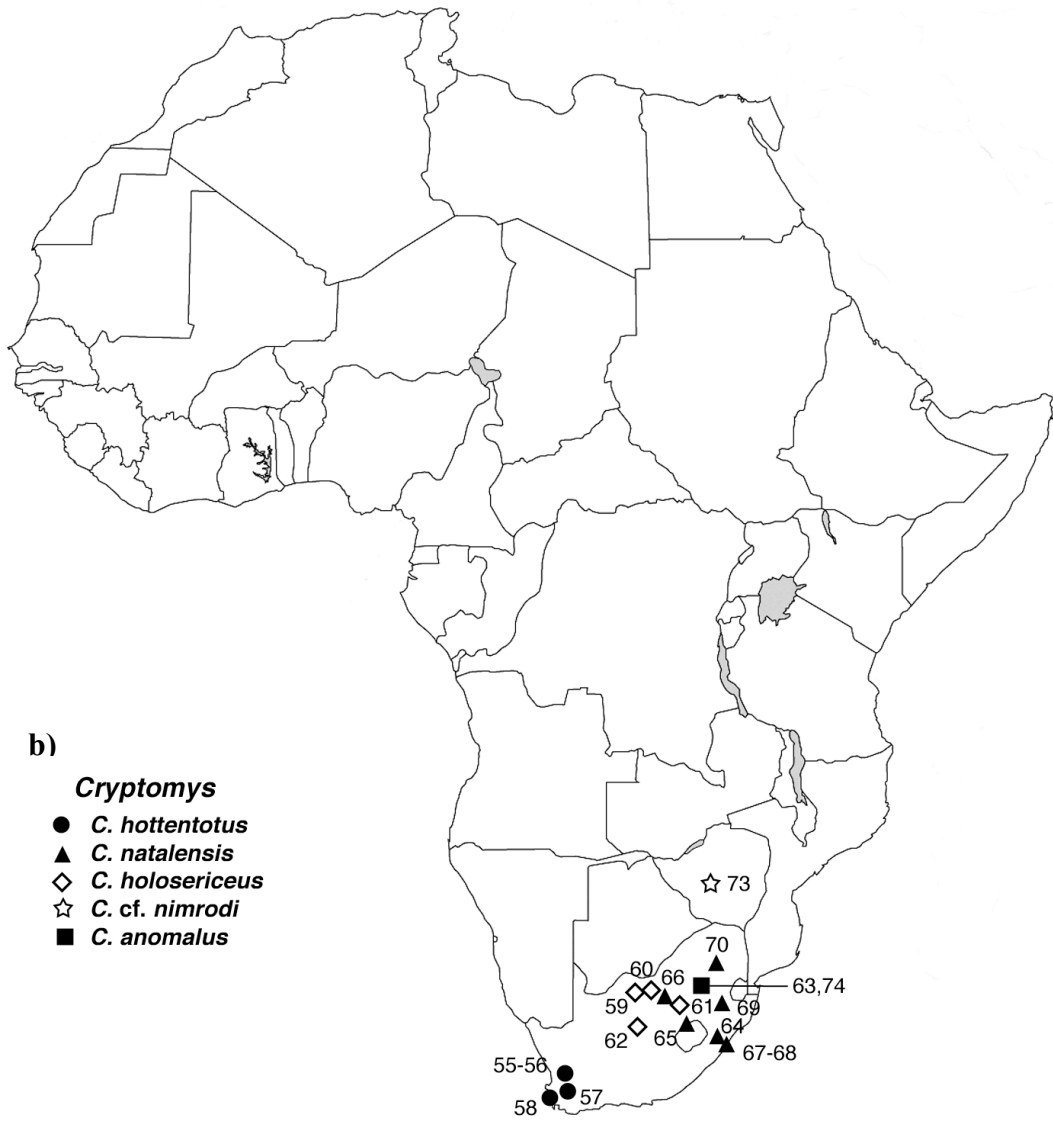


Fig. 2.1 continued. b) *Cryptomys* (*hottentotus* group) specimens used in this study.

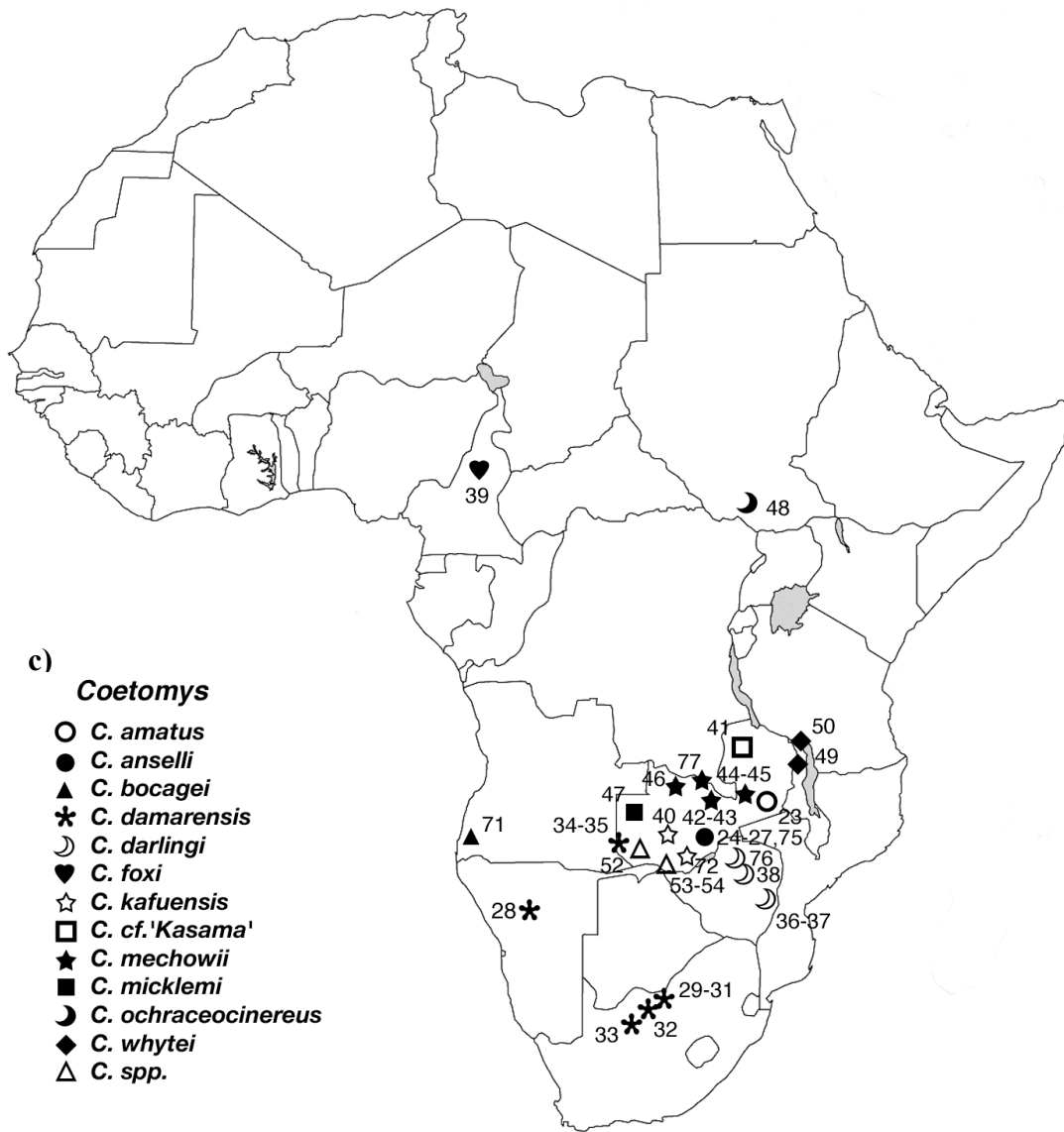


Fig. 2.1 continued. c) *Coetomys* (*mechowii* group) specimens used in this study.

1997; Walton et al., 2000) has been reported in *Cryptomys*, yet no study has thoroughly documented patterns of genetic variation throughout the range of the genus.

In terms of taxonomy and phylogenetics, the genus *Cryptomys* is problematic for several reasons (cf., Honeycutt et al., 1991). First, *Cryptomys* is the most broadly distributed bathyergid genus. The current distribution of the genus presumably reflects the influence of past climatic and geologic events associated with alterations of the African landscape (Grubb et al., 1999). Therefore, an understanding of relationships among populations and species of *Cryptomys* will provide phylogeographic information that can be compared to historical changes that influenced the biogeography of African flora and fauna since the Miocene. Second, as with other fossorial rodents such as *Ctenomys* in South America, *Thomomys* and *Geomys* in North America, and *Spalax* in the eastern Mediterranean, patterns of morphological and genetic variation in *Cryptomys* make the delineation of species boundaries difficult (Bennett and Faulkes, 2000; Honeycutt et al., 1991; Rosevear, 1969). For instance, the number of recognized species of *Cryptomys* ranges between 1 to 49 depending on whether the particular taxonomic treatment of morphological variation emphasized lumping (Ellerman et al., 1940) or splitting (Allen, 1939; Roberts, 1951). The latest detailed taxonomic treatment of *Cryptomys* recognized seven species: *C. bocagei*, *C. damarensis*, *C. foxi*, *C. hottentotus*, *C. mechowii*, *C. ochraceocinereus*, and *C. zechi* (Honeycutt et al., 1991). Subsequent to this study, several subspecies have been elevated to species status (*C. darlingi* and *C. amatus*: Aguilar, 1993; Macholán et al., 1998, respectively), and two species were recently described (*C. anseli* and *C. kafuensis*: Burda et al., 1999). Third, karyotypic

variation in *Cryptomys* is pronounced with diploid numbers ranging from 40 to 78 (*C. mechowii* and *C. damarensis*: Macholán et al., 1993; Nevo et al., 1986, respectively). Indeed, several studies have used chromosomal variation as a yardstick for species recognition (Aguilar, 1993; Burda et al., 1999; Macholán et al., 1998). Nevertheless, no study has investigated relationships among all the various chromosomal forms. Finally, *Cryptomys* is highly social, with some forms approaching eusociality similar to the naked mole-rat, *Heterocephalus glaber* (Burda and Kawalika, 1993; Burda et al., 2000; Jarvis and Bennett, 1993). Such aspects of behavioral ecology may influence the partitioning of genetic variation within species, especially if animals/colonies display restricted dispersal and populations are highly subdivided.

The objective of this paper is to use nucleotide sequences from nuclear and mitochondrial genomes to generate a molecular phylogeny of populations and presumptive species of bathyergids with emphasis on *Cryptomys*. The use of data from both nuclear and mitochondrial sequences will provide independent support for phylogenetic relationships. This molecular phylogeny will be used as an interpretive framework for examining the evolutionary relationships in this group with brief discussion on patterns of geographic variation, the delineation of species boundaries, and chromosomal evolution.

2. Materials and Methods

2.1. *Taxon sampling and DNA isolation*

Representatives of *Cryptomys* species and subspecies were collected throughout their distribution. Several specimens from other bathyergid genera and species also were sampled. For *Cryptomys*, samples were examined from 41 localities of which 11 had been sampled previously (Appendix; Fig. 2.1b-c). DNA from either frozen liver and/or skin samples preserved in ethanol (70%) was isolated by proteinase-K digestion followed by either phenol/chloroform extraction or QIAGEN DNAEasy spin columns (Qiagen Inc., Valencia, CA). Skin samples from museum specimens, representing species in geographic areas not previously available, were attained from the Transvaal, Senckenberg, and Carnegie Museums (Appendix). For museum specimens, DNA was extracted using a modified phenol:chloroform extraction, where precautionary steps were taken to prevent contamination (Glenn et al., 2002). All protocols were performed in a separate room from other extractions or PCR experiments. Negative controls were used to identify potential contamination of museum extractions.

2.2. *PCR amplification and nucleotide sequencing*

To allow for the inclusion of museum samples and published sequences from previous studies (Allard and Honeycutt, 1992; Bennett and Faulkes, 2000; Faulkes et al., 1997; Walton et al., 2000), our sequencing efforts focused on the mitochondrial 12S ribosomal RNA (rRNA) gene and intron 1 of the nuclear transthyretin gene (TTR). Due

to lower observed levels of sequence variation, only a subset of specimens were examined for TTR.

The polymerase chain reaction (PCR) was used to amplify an 1140 base pair (bp) fragment of the mitochondrial 12S rRNA gene. Initial amplification was performed using two universal primers, L651 and 12GH (Nedbal et al., 1994), and reaction conditions consisted of an initial denaturation at 94°C for five min, followed by 35 cycles of a 94°C for 30 sec, 52°C for 30 sec, and 72°C for 30 sec, with a final extension at 72°C degrees for ten min. Amplification of the correct fragment length was confirmed by electrophoresis of PCR product (5µl) with a size standard marker on 1% minigels, stained with ethidium bromide, and visualized under UV light. PCR products were cleaned using QIAquick Spin PCR purification spin columns and following a standard protocol (Qiagen Inc., Valencia, CA).

Both strands of the PCR product were sequenced using the PCR primers, as well as four internal primers: Ha12S, L109, H147, and 12EL (Nedbal et al., 1994). Cycle sequencing reactions were performed using ABI Prism BigDye Terminator v3.0 chemistry (Applied Biosystems, Foster City, CA), with 25 cycles of 97°C for 30 secs, 50°C for five sec, and 60°C for two min. Excess terminator dye, oligonucleotides, and polymerase were removed by centrifugation at 3000 rpm through a Sephadex G-50 matrix (Sigma-Aldrich, Inc.). Sequencing reactions were electrophoresed and analyzed on an ABI 377 XL automated sequencer. Sequence data were imported into Sequencer v3.0 (Gene Codes Corporation, Ann Arbor, MI) for alignment and contig assembly for

each individual. Once the entire sequence was confirmed by overlapping reads, the contigs were exported in Nexus file format into PAUP* v4.0b10 (Swofford, 2002).

Due to the poor quality of DNA extracted from museum samples, three small overlapping fragments (avg length = 418 bp) of the 12S rRNA gene were amplified using three primer pairs (L651-Ha12S, L109-H147, and 12EL-12GH). Conditions of PCR and sequencing reactions for the three smaller fragments were the same as those described for the complete 12S fragment. Sequences from independent PCR amplifications were used to confirm sequences. For some museum samples, the DNA was too degraded to produce a complete contig. In all reactions, multiple negative controls were included, both from the extraction and PCR reaction to ensure that there was no contamination. Subsequent to multiple alignment in ClustalX (Thompson et al., 1997), sequences were aligned by eye to a 12S alignment of previously sequenced and analyzed hystricognath dataset (ongoing study in the Honeycutt lab) based on the secondary structure proposed by Springer and Douzery (1996). Previously sequenced individuals (Allard and Honeycutt, 1992; Faulkes et al., 1997; Walton et al. 2000) were included to increase sample size and geographic representation and allow for comparison to these studies. Although some published sequences were shorter than those acquired in the current study, they were included with missing sites (145-188 bp missing, 14-19%).

Primers PreAlb(F) and PreAlb(R) were used to amplify intron 1 of the transthyretin gene (modified from Tsuzuki et al., 1985). Additional primers, BR6 and HF3, designed for the family Bathyergidae (Walton et al. 2000), were used to sequence

both strands. The sequencing protocol was the same as that described for the 12S rRNA gene. Sequences were aligned by eye to the previous alignment of Walton et al. (2000).

2.3. Data analyses

A 156 bp fragment, containing an invariable portion of the Valine tRNA, was excluded from all 12S sequences prior to analysis. To account for the phylogenetic information of insertions and deletions (indels), gaps were treated as missing and an interleaved matrix, coding presence/absence of phylogenetically informative gaps, was added to the end of the aligned sequences. For the 12S rDNA data, stems and loops (determined from the secondary structure alignment) were partitioned and tested for congruence using the partition homogeneity test (PHT: Farris et al., 1995) implemented in PAUP*.

Maximum-parsimony (MP) and maximum-likelihood (ML) analyses were performed using PAUP* v4.0b10 (Swofford, 2002). Based on phylogenetic affinities recovered in previous studies (Allard and Honeycutt, 1992; Huchon and Douzery, 2001; Nedbal et al., 1994), two phiomorphs, *Thryonomys swinderianus* and *Petromus typicus*, were chosen as outgroup taxa for the 12S rRNA and TTR analyses. Under MP, all analyses were performed using the heuristic search option with 1,000 replicate searches, random addition of taxa, and tree bisection and reconnection (TBR) branch swapping, with the steepest descent option not in effect. When equally-weighted heuristic searches failed to recover a single MP tree, additional MP analyses were performed with characters successively-weighted (Farris, 1969) by their rescaled consistency index (RC;

Farris, 1989). Bootstrap proportions (Felsenstein, 1985) and decay indices (Bremer, 1988) were used as relative measures of nodal support. Bootstrap analyses were initiated using 1,000 replicates, each with 10 random addition sequences and TBR branch-swapping using PAUP*. Decay indices were generated using TreeRot v.2 (Sorenson, 1999).

To determine the appropriate model of evolution for maximum-likelihood (ML) and Bayesian (BA) analyses, a hierarchical likelihood ratio test (hLRT) was performed using MODELTEST v3.06 (Posada and Crandall, 1998). For ML and BA, only one outgroup (*Thryonomys*) was used. A search, using the parameters estimated from the MP tree and employing the heuristic search option, was used to obtain a ML tree. Using an iterative approach, additional heuristic searches were performed using the parameters recovered in the prior search until the likelihood value stabilized (Sullivan and Swofford, 1997). Bootstrap support for the ML tree was determined using the "fast" stepwise addition option. The MP and ML trees were compared using the Shimodaira-Hasagawa (S-H) test (Shimodaira and Hasagawa, 1999) in PAUP*.

Congruence of the phylogenetic signal for the 12S and TTR data was determined by trimming the 12S dataset to include only those taxa for which TTR sequences also were available. These datasets were compared for combinability with the PHT. Based on sufficient homogeneity, datasets were then combined and analyzed together with characters coded as missing for incomplete sequences.

Bayesian posterior probabilities were calculated using the Metropolis-coupled Markov chain Monte Carlo (MCMCMC) sampling approach in MrBayes v3.01

(Huelsenbeck and Ronquist, 2001). Four independent searches were performed for each dataset; each search consisted of a cold chain and 3 heated chains (temp = 0.2). All searches started with random trees and uniform prior probabilities for all possible trees. For all datasets, Markov chains were run for 1×10^6 generations and trees were sampled every 100 generations. To determine appropriate burn-in values, an initial run of 35,000 generations was performed to check for stationarity of the likelihood values. The “burnin” value was conservatively set at 500, the first 500 (50,000 generations) trees were eliminated from the approximation of posterior probabilities. The trees retained from each run were combined and a 50% majority rule consensus tree was produced. For the 12S gene, and combined 12S and TTR sequences, the data were analyzed under the general time-reversible model (Yang, 1994) with site-specific rate variation (GTR+SS) (stems:loops:TTR), or corrected for invariable sites and among site rate variation using a discrete gamma distribution (GTR+ Γ +I). The TTR dataset was analyzed under the HKY+ Γ model (Hasagawa et al., 1985).

To test for clock-like behavior, ML scores with and without the enforcement of a molecular clock were compared using a likelihood ratio test (LRT; Felsenstein, 1985) in PAUP*. Tajima’s relative rate test (RRT, 1-D method; Tajima, 1993a) was performed to identify operational taxonomic units (OTUs) that deviated from a clock-like rate of substitution. For the RRT, *P*-values were corrected using the Bonferroni method to account for multiple pairwise comparisons.

To evaluate congruence between the molecular phylogeny and previously described patterns of chromosomal variation, MacClade v4.05 (Maddison and

Maddison, 2000) was used to map diploid number from known karyotypes (Burda, 2001) onto the molecular phylogeny.

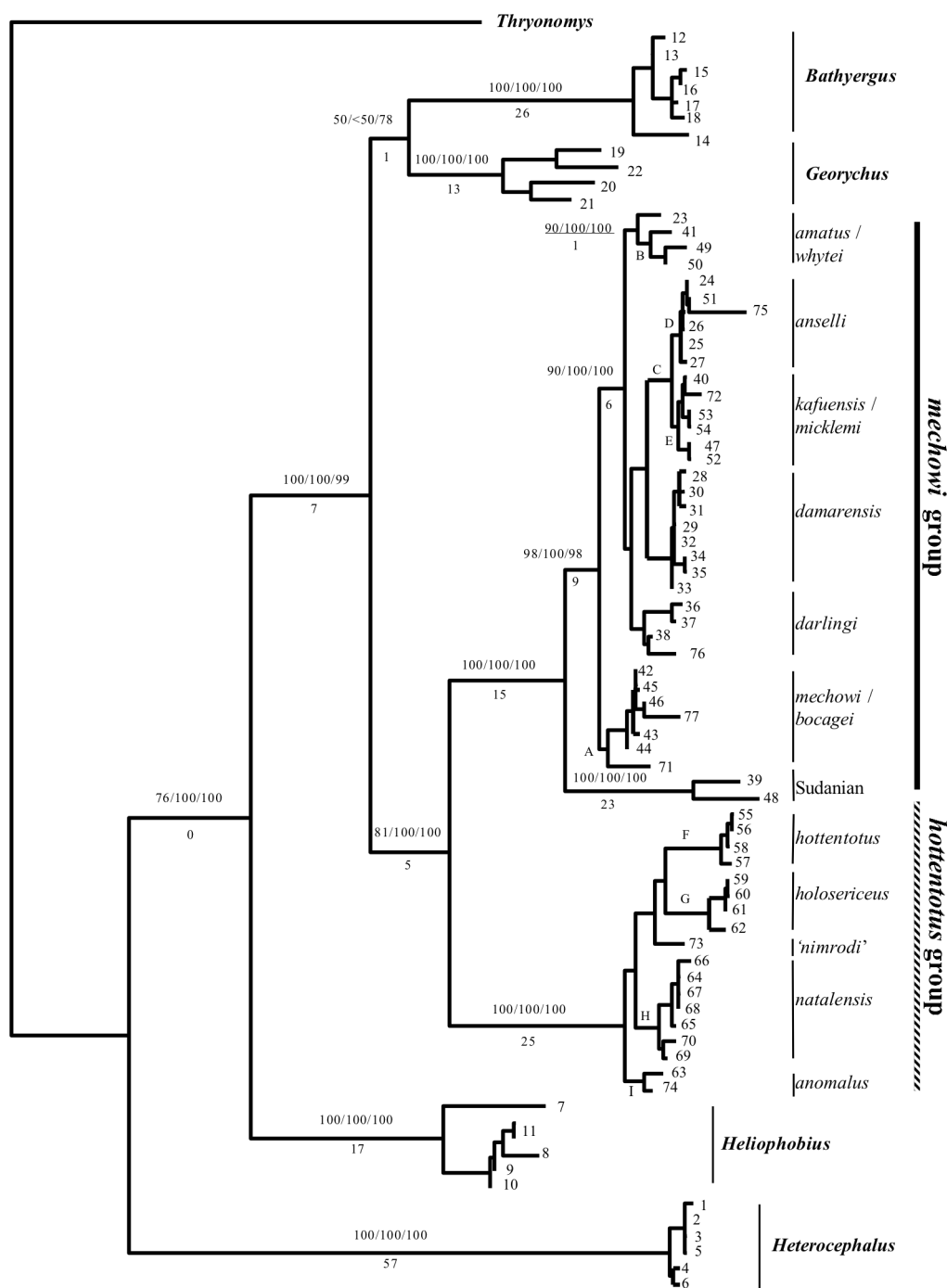
3. Results

3.1. Phylogenetic relationships based on 12S rRNA gene

Approximately 1140 bp of the 12S rRNA gene were analyzed for 77 samples, and 156 bp were excluded from further analyses. Of the 1,050 remaining characters (984 nucleotides and 66 indels), 597 (47%) were variable and 382 (64% of 597) were parsimony-informative.

Average corrected (GTR+ Γ +I) pairwise sequence differences between the ingroup and outgroup taxa ranged from 38.8-65.2% (mean = 51.3%). The average corrected pairwise sequence differences observed among and within the ingroup genera were 34.0% ($R = 15.0 - 73.4\%$) and 10.5% ($R = 0.1 - 24.6\%$), respectively. In *Cryptomys*, the average pairwise differences between the karyotypically stable *hottentotus* species group and the taxa within the large, karyotypically-diverse *mechowii* species group was 18.5% ($R = 13.8-24.6\%$). Pairwise differences within each of these two clades (*hottentotus* species group and *mechowii* species group) were 4.2% ($R = 0.1-7.5\%$) and 4.7% ($R = 0.1-14.6$), respectively.

A heuristic search under maximum-parsimony (equal-weights) recovered 20 equally-parsimonious trees (not shown: TL = 1435, CI = 0.511, RI= 0.876). Successively-weighted MP (by RC) recovered a single tree (not shown, see Fig. 2.2: TL = 1435, CI = 0.511, RI= 0.876). All currently recognized genera formed well-supported



monophyletic groups: *Heterocephalus* (Bootstrap proportions (BP) = 100, Decay Indices (DI) = 57), *Heliophobius* (BP = 100, DI = 17), *Bathyergus* (BP = 100, DI = 26), *Georychus* (BP = 100, DI = 13), and *Cryptomys* (BP = 81, DI = 5). In this tree, *Heterocephalus* was basal to the remaining genera with *Heliophobius* as sister to a clade containing *Bathyergus*, *Georychus* and *Cryptomys*.

Within *Cryptomys*, two divergent clades (*hottentotus* species group and *mechowii* species group) were recovered in all 20 trees, with differences representing small rearrangements of lineages within the *mechowii* clade (not shown). *Cryptomys holosericeus*, *C. hottentotus*, *C. natalensis*, *C. nimrodi* and *C. anomalus* ('pretoriae') formed the monophyletic *hottentotus* species group (BP = 100%, DI = 25), and the remaining species of *Cryptomys* formed the monophyletic *mechowii* species group (BP = 98, DI = 15). Included in the *mechowii* species group is the Sudanian clade (*C. foxi* + *C. ochraceocinereus*). These two taxa formed a monophyletic group (BP = 100, DI = 23) sister to other taxa of the *mechowii* species group (BP = 98, DI = 9). Monophyly of a clade containing *Cryptomys mechowii* and *C. bocagei* also was supported (BP = 86, DI = 2). Although the *amatus/whytei* clade was not strongly supported (BP = 63, DI = 1), monophyly of the internal clade containing *C. 'Kasama'* and *C. whytei* was strongly supported (BP = 95, DI = 4). An *anselli/kafuensis* clade had strong support (BP = 100, DI = 10), but the monophyly of each species was only weakly supported (BP = 53, DI = 0 and BP = 66, DI = 1, respectively).

Under ML, the general time-reversible (Yang, 1994), corrected for among-site rate variation using the discrete gamma distribution and invariable sites (GTR+ Γ +I), was

significantly better than all simpler models (MODELTEST; p -value < 0.001). In addition, the GTR+ Γ +I model, the general time-reversible model corrected for site-specific rate variation (GTR+SS), was used in ML and Bayesian analyses of the 12S data. The heuristic likelihood search recovered the same topology as the MP search (Fig. 2.2, $-\ln = 7335.29$), and branches leading to each genus were long (0.036-0.279) relative to branch lengths observed within each genus (0.001-0.026). An exception is *Cryptomys sensu lato* with the two divergent lineages defined by branch lengths of 0.083 and 0.056 (*hottentotus* species group and *mechowii* species group, respectively). Another long branch was observed in the Sudanian clade (*C. foxi* + *C. ochraceocinereus*, BL = 0.061).

For the Bayesian analyses of the 12S data, the GTR+SS model generated higher posterior probabilities (PP). Incorporating site-specific rates for stems and loops produced the same topology supported by both the MP and ML analyses. In both Bayesian analyses and ML analysis, a *Bathyergus* + *Georychus* clade was recovered, but with weak to moderate support (PP = 53 and 78, GTR+SS and GTR+ Γ +I, respectively; ML BP < 50). In all analyses, the Sudanian clade (*C. foxi* + *C. ochraceocinereus*) was basal within the *mechowii* species group clade. This placement was strongly supported (MP BP = 100, DI = 23; ML BP = 100; PP = 100).

The null hypothesis of equal rates among lineages was not supported by the ($-\ln L_0 = 7438.83$, $-\ln L_1 = 7363.00$, $p < 0.001$), thus suggesting that lineages are not evolving in a clock-like manner. The conservative Tajima 1-D RRT (with Bonferroni correction) failed to detect significant rate heterogeneity.

3.2. Phylogenetic relationships based on TTR intron 1

DNA sequences of approximately 986 bp were analyzed from 27 bathyergids: new specimens of *Cryptomys* representing 16 new sequences (this study) in addition to the 12 reported by Walton et al. (2000). Of the 1081 characters (1046 nucleotides and 35 indels), 382 (64%) of 597 variable characters were parsimony-informative.

Average corrected (HKY+ Γ) pairwise sequence difference between the ingroup and outgroup taxa was 23.1% ($R = 18.9-25.5\%$). Corrected sequence divergence among and within the ingroup genera ranged from 3.6-15.6% (mean = 8.6%) and 0.1-4.6% (mean = 2.1%), respectively. Average corrected pairwise differences between the *hottentotus* species group and *mechowii* species group was 3.9% ($R = 3.0- 4.6\%$). Average pairwise difference within each of these two clades was 1.2% ($R = 1.5-1.6\%$) and 0.4% ($R = 0.1-0.8\%$), respectively.

A heuristic search under an equally-weighted MP analysis recovered two most-parsimonious trees (not shown, see Fig. 2.3: TL = 446, CI = 0.872, RI = 0.936). Successive-weighting (by RC) recovered a single tree (not shown, see Fig. 2.3: TL = 446, CI = 0.872, RI = 0.936). Although fewer taxa were represented in the transthyretin (TTR) dataset, the topology matched that obtained with the 12S dataset. Branching order of the genera within the family were consistent with previous studies and the 12S rRNA sequences. *Heterocephalus* (BP = 100, DI = 34) was basal to a clade containing the other genera (BP = 100, DI = 29) with *Heliophobius* (BP = 100, DI = 18) sister to a *Bathyergus*, *Georychus* + *Cryptomys* clade. Although the monophyly of each genus (*Bathyergus*, *Georychus*, and *Cryptomys*) was well supported (BP = 100, DI = 18; BP =

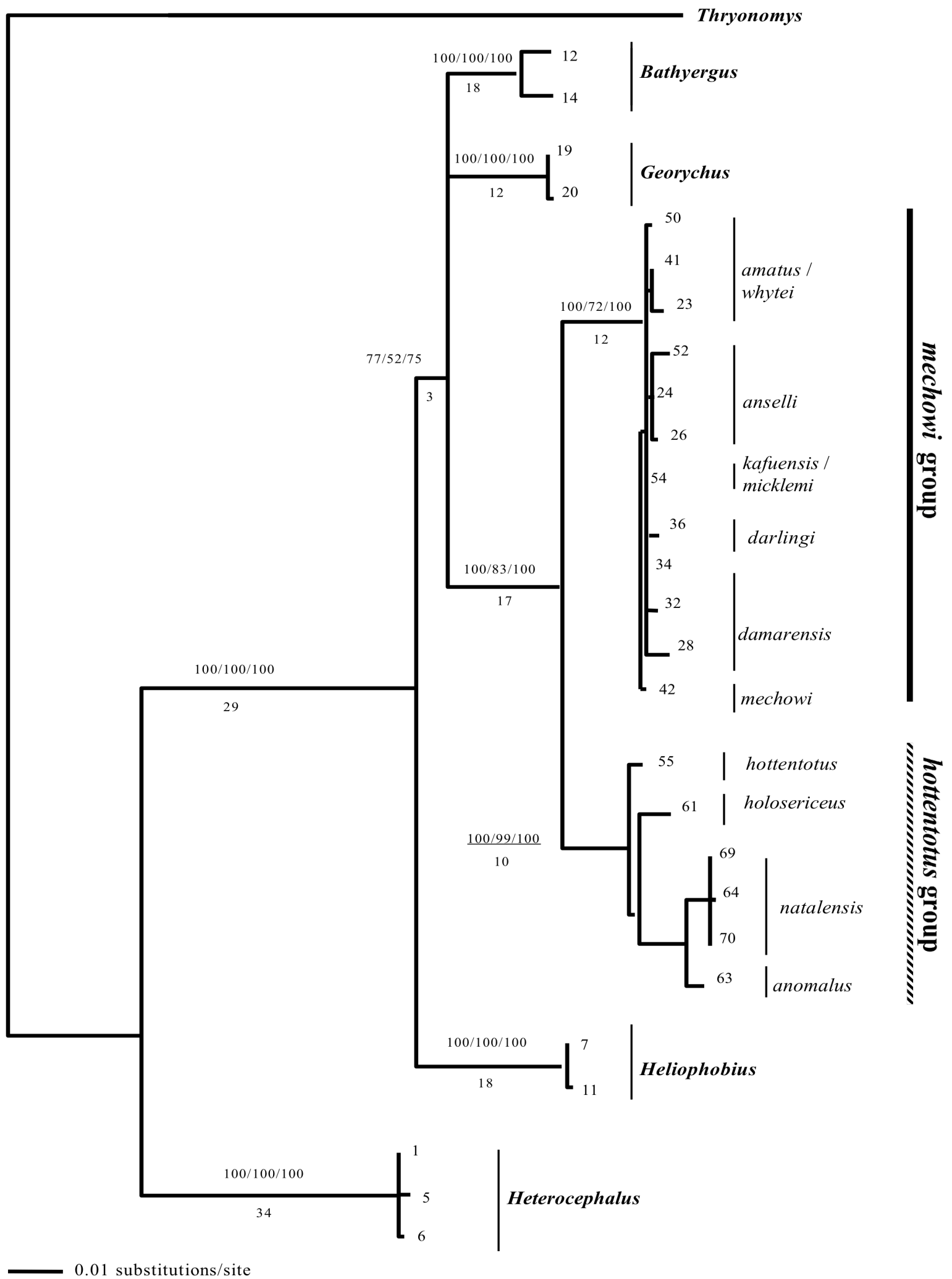


Fig. 2.3 TTR Intron I maximum-likelihood phylogeny under HKY85 + Γ ($-\ln L = 3241.73$, $\alpha = 0.8512$). Successively-weighted maximum-parsimony (by RC) recovered the same topology. For all major branches, values above branches refer to MP bootstrap proportions, ML bootstrap proportions, and Bayesian posterior probabilities, respectively; values below branches represent Bremer decay indices under MP. Numbers correspond to the specimens listed in Appendix.

100, DI = 12; BP = 100, DI = 17, respectively), the relationship among the 3 genera remained unresolved. Within *Cryptomys*, the two divergent and monophyletic lineages were recovered (*hottentotus* clade: BP = 100, DI = 10; *mechowii* clade: BP = 100, DI = 12).

For TTR, the HKY+ Γ model was significantly better than all simpler models (p -value < 0.001) and was used for the ML and BA analyses. ML and BA analyses recovered identical topologies to that recovered by MP (with successive-weighting). All genera and the two clades within *Cryptomys* were strongly supported by ML bootstrap proportions and posterior probabilities of 100% (Fig. 2.3).

As with the 12S data, LRT revealed significant rate heterogeneity ($-\ln L_0 = 3244.90$, $-\ln L_1 = 3269.37$, p -value < 0.001). The Tajima 1-D relative rate test failed to detect significant rate heterogeneity (after Bonferroni correction: $\alpha = 0.0001$).

3.3. Phylogenetic relationships based on combined datasets

To allow comparisons between the mitochondrial and nuclear gene data, the phylogeny based on 12S was trimmed to include only samples represented in the TTR dataset. Based on the S-H test, the ML trees from each dataset were not significantly different (p -value = 1.000), although the 12S tree showed more phylogenetic structure. A PHT (1000 replications) suggested that the datasets were homogeneous ($p = 1.00$). This result and strong overall topological congruence between the recovered phylogenies provided support for analyses of the combined dataset. To achieve a better geographic representation of the species, all 36 sequences of TTR were included in the combined

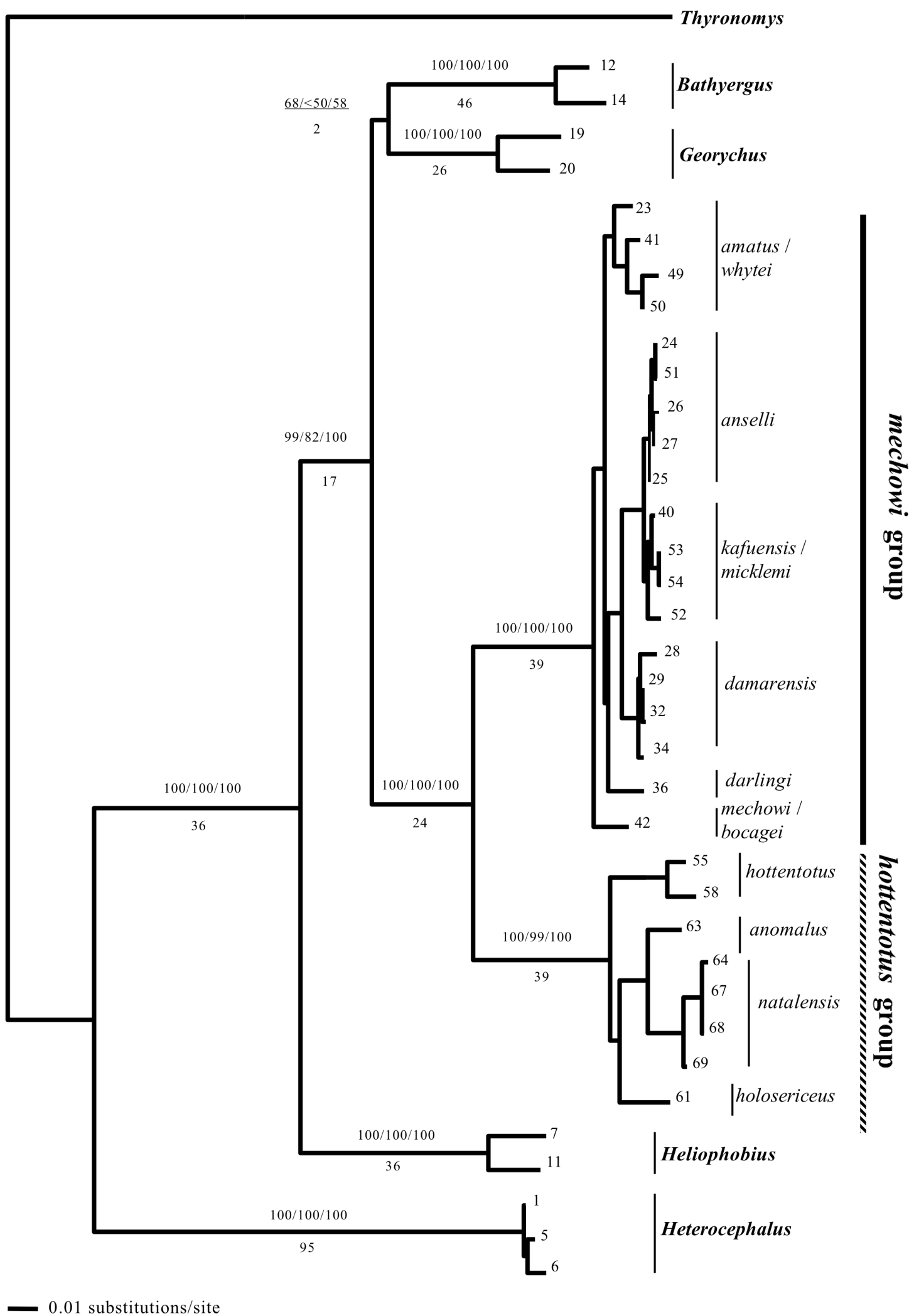


Fig. 2.4 Combined data (12S rRNA and TTR Intron I) maximum-likelihood phylogeny under GTR + Γ + I ($-\ln L = 10053.88$, $\alpha = 0.5885$, proportion of invariable sites = 0.3404). Unweighted maximum-parsimony recovered the same topology. For all major branches, values above branches refer to MP bootstrap proportions, ML bootstrap proportions, and Bayesian posterior probabilities, respectively; values below branches represent Bremer decay indices under MP. Numbers correspond to the specimens listed in Appendix.

analyses. The combined MP analysis resulted in a single tree (Fig. 2.4: TL=1395, CI = 0.674, RI = 0.847), recovering the same relationships found in the single gene analyses. *Bathyergus* and *Georchus* formed a monophyletic clade, again with only weak support (BP = 68, DI = 2). ML and Bayesian analyses (both under GTR+G+I) recovered the same tree with strong support for the monophyly of the genera as well as the *hottentotus* and *mechowii* species groups (Fig. 2.4).

4. Discussion

4.1. Corrections to previous taxonomic designations

Since previous molecular phylogenetic studies either emphasized intergeneric relationships (Allard and Honeycutt, 1992; Faulkes et al., 1997; Honeycutt et al., 1987; Janecek et al., 1992; Walton et al., 2000) or had limited geographic and taxonomic sampling within a genus (Faulkes et al., 1997), broad patterns of variation could not be detected. This lack of sampling, coupled with taxonomic problems associated with *Cryptomys*, has led to several cases of potential errors in assignment of specimens to particular species. By sampling from type localities of currently recognized species, our study identified discrepancies in the assignment of some specimens. A sample from Zambia (H650) was designated as *C. cf. bocagei* by Walton et al. (2000) for the 12S rRNA gene (Accession #AF290211). Based on our current 12S rRNA tree (Fig. 2.2), this specimen should be assigned to *C. anseli*. *C. amatus* (AF012234) from Faulkes et al. (1997) also should be assigned to *C. anseli* as it grouped within the *C. anseli* clade of the 12S phylogeny, is located within *C. anseli*'s range, and shares the same karyotype

($2N = 68$: Aguilar, unpublished data; Bennett and Faulkes, 2000) as *C. anelli*. *C. 'choma'* (AF012217) was recovered within the *kafuensis* clade. It apparently does not share the same karyotype ($2N = 50$: Aguilar, unpublished data; Bennett and Faulkes, 2000), and may in fact be distinct from *kafuensis*, but more data will be required.

The two species of dune mole-rats (*Bathyergus suillus* and *B. janetta*) did not form clades as was expected. The Cape dune mole-rat (*B. suillus*) from Allard and Honeycutt (1992; Accession M63564) was not recovered with the *B. suillus* samples. This may be explained by two scenarios: 1) there is more variability within this genus, warranting the recognition of additional taxa, or 2) a tissue sample was assigned to the wrong museum voucher. Additional sampling within the distribution of *Bathyergus* is required to resolve this discrepancy and the phylogenetic relationships within this genus.

To prevent additional misidentifications, new species descriptions should be based on the most currently recognized taxa, phylogenetic affinity, chromosome morphology, geographic distribution, and molecular genetics. The 12S phylogeny, which incorporates previous genetic samples, could be used as the framework for future species identification and taxonomic designations.

4.2. Chromosomal diversity

Chromosomal diversity within the Bathyergidae has been a topic of interest for the past 25 years. Based on the karyotypes of *Heterocephalus* and *Heliophobius* specimens from Kenya, George (1979) concluded that the family Bathyergidae was karyotypically stable ($2N = 60$, mostly biarmed chromosomes, $NF = 118-120$). To date,

Heterocephalus has revealed a stable diploid number of 60, but individuals from Kenya and Somalia show length differences in chromosomal arms (Capanna and Merani, 1980). Recently, a new karyotype ($2N = 62$) was discovered in Zambian populations of *Heliophobius argenteocinereus* (Scharff et al., 2001), revealing slight chromosomal diversity not documented in previous studies. This new karyotype may be representative of *Heliophobius argenteocinereus*, while George's Kenyan sample may represent *H. spalax* (Thomas, 1910).

The relative chromosomal stability in bathyergids was further corroborated by the low levels of chromosomal variation ($2N = 54-56$, $NF = 104-108$: Nevo et al., 1986) for *Bathyergus janetta*, *B. suillus*, *Cryptomys hottentotus*, *Georychus capensis*. The only exception was *C. damarensis* with a $2N = 74-78$ and $NF = 92-96$ (Nevo et al., 1986). Subsequent studies have documented a large amount of chromosomal diversity within the *mechowii* species group of *Cryptomys sensu lato*, with diploid number ranging from 40 to 78 in *C. mechowii* (Macholán et al., 1993) and *C. damarensis* (Nevo et al., 1986), respectively. As the number of known karyotypes has increased, complexity of chromosomal evolution and the patterns of diversification within the family have increased. Several new species descriptions are based on fixed novel karyotypes (Aguilar, 1993; Burda et al., 1999; Chitaukali et al., 2001; Kawalika et al., 2001; Macholán et al., 1998). Although changes in chromosome number and morphology may be an important isolating mechanism, karyotypic comparisons alone have not provided information on phylogenetic relationships and/or patterns of chromosomal change. In order to resolve this, diploid numbers were plotted on the current phylogeny (Fig. 2.5).

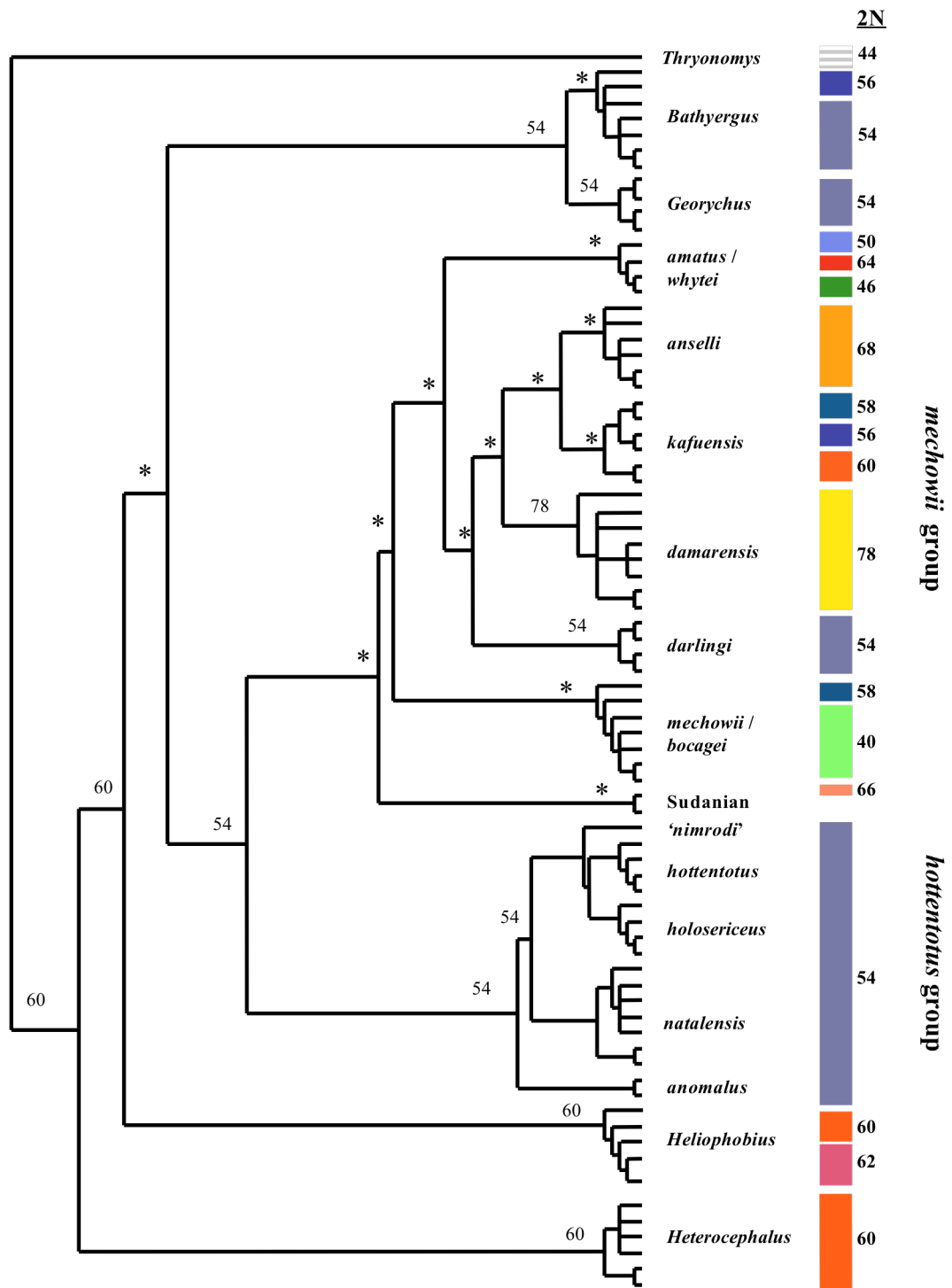


Fig. 2.5 Diploid numbers (2N) mapped on the 12S rRNA phylogeny. Ancestral states at the major nodes were estimated using MacClade v4.05, * refer to ambiguous nodes.

Due to the strong congruence of the nuclear and mitochondrial datasets, the larger 12S phylogeny was selected to represent our hypothesis for the phylogenetic relationships among bathyergids. While functional in defining clades, no clear phylogenetic pattern is apparent, with the exception of marked chromosomal diversity in the *mechowii* species group. Chromosomal rearrangements appear to be correlated with speciation (or at least coincide with it), although there is no clear pattern of evolution (*e.g.*, fissions or fusions, increase or decrease in chromosome numbers). Much of the current genetic diversity of this species group has evolved from the Zambebian region, where the high level of chromosomal evolution has been documented (Burda, 2001). To date, direct comparisons of published karyotypes have been limited by the quality of the chromosome preparations and staining techniques (Burda et al., 1999). Without differential staining (G-banding), it is difficult to derive a cladistically-based chromosome phylogeny.

4.3. Comments on the status of the genus *Cryptomys*

Within the currently recognized genus *Cryptomys*, two reciprocally-monophyletic clades (*hottentotus* species group and *mechowii* species group) were consistently recovered, with strong support from both the mitochondrial and nuclear genes (Figure 2.2 and 2.3). *C. hottentotus*, *C. holosericeus*, *C. natalensis*, and *C. anomalus* (cf. '*pretoriae*') form a monophyletic group separate from other *Cryptomys* species (the *mechowii* species group), many of which were previously considered subspecies of *C. hottentotus*. Average corrected pairwise distances between these two

clades based on both nuclear and mtDNA data (TTR = 3.9%, 12S = 18.5 %) are equivalent to the level of sequence divergence observed between other genera (*i.e.*, *Bathyergus* and *Georychus*: TTR = 3.7%, 12S = 18.8%). This level of divergence was observed also by Bennett and Faulkes (2000) for 12S and cytochrome *b* sequences.

The two divergent lineages within *Cryptomys* have been noted in numerous genetic studies (Faulkes et al., 1997; Filippucci et al., 1994, 1997; Janecek et al., 1992; Nevo et al., 1987; Walton et al., 2000). This was first observed in comparisons of allozyme data that produced relatively large genetic distances between two South African species, *C. damarensis* (of the *mechowii* species group) and *C. hottentotus* (Nevo et al., 1987). While several authors have suggested the recognition of both groups as distinct genera, no study to date has provided sufficient data to support this recommendation (Faulkes et al., 1997; Filippucci et al., 1994; Honeycutt et al., 1991).

Based on our nuclear and mitochondrial DNA analyses, and support from other data (allozymes, chromosomes, and other nuclear and mtDNA data), we propose the recognition of two genera *Coetomys* Gray, 1864 and *Cryptomys*. This change in classification is supported by: 1) reciprocal monophyly of the two lineages based on independent nuclear and mitochondrial datasets and multiple analyses, 2) the level of sequence divergence observed between these two lineages for both nuclear and mitochondrial markers, relative to that observed for other genera (*i.e.*, *Bathyergus* and *Georychus*), 3) different modes and patterns of chromosomal evolution with *Cryptomys* being karyotypically-conserved ($2N = 54$) and *Coetomys* exhibiting high karyotypic diversity with diploid numbers ranging from 40-78.

4.3.1. *Coetomys* Gray, 1864 *gen. nov.*

Etymology. *Coetus* = aggregation, society plus *mys* = mouse, *Coetomys* = “social mouse”. The name expresses one of the most striking characteristics of mole-rats of this genus – their (eu)sociality which is pointed out by all students of the biology of these rodents (cf., Bennett and Faulkes, 2000; Burda et al., 2000). Noteworthy that *C. damarensis*, *C. anelli*, and *C. mechowii*, the most studied representatives of the genus *Coetomys*, are considered to be more social, living in larger family groups than *Cryptomys hottentotus* (Burda et al., 2000; Jarvis and Bennett, 1993).

Type species. *Bathyergus damarensis*, Ogilby, 1838: When originally described as a subgenus of *Georchus*, no type species was designated, but *B. caecutiens*, Licht and *B. damarensis*, Ogilby 1838, were both included. Since *B. caecutiens* is no longer recognized as a valid species (Honeycutt et al., 1991), we select *B. damarensis*, Ogilby 1838 as the type species of this genus.

Type specimen.- B.M. 149

Type locality : Usakos, Namibia (Damaraland)

Genus diagnosis – At the current state of knowledge, and due to large interspecific and intraspecific polymorphism, the genus cannot be clearly separated from the genus *Cryptomys* on grounds of morphological or morphometric traits. The genus (and its separation from other genera) can be characterized by allozyme (Filippucci et al., 1994, 1997; Nevo et al., 1987) and molecular (nuclear and mitochondrial) markers described in this study and relevant papers cited above. This genus has high karyotypic

diversity with diploid numbers ranging from 40-78 and is distributed in sub-Saharan Africa, south to the Limpopo River where it is substituted by the genus *Cryptomys*. Mole-rats of the genus *Coetomys* seem to be characterized by their social and mating system: monogamy with helpers and pronounced philopatry. Living in larger families, where only one parental pair is reproducing and offspring are engaged in cooperative burrowing and foraging denoted as eusociality in at least some members of the genus. Prenatal and postnatal development in *Coetomys* seems to be slower/longer than in *Cryptomys* (cf., Bennett and Faulkes, 2000). Note, however, that data on social and reproductive biology are still missing for many species of this genus.

Included species. – *C. amatus* Wroughton, 1907; *C. anelli* Burda et al., 1999; *C. bocagei* De Winton, 1897; *C. damarensis* Ogilby, 1838; *C. darlingi* Thomas, 1895; *C. foxi* Thomas, 1911; *C. kafuensis* Burda et al., 1999; *C. mechowii* Peters, 1881; *C. micklei* Chubb, 1909; *C. ochraceocinereus* Heuglin, 1864; *C. whytei* Thomas, 1897; *C. zechi* Matschie, 1900. Additionally, a *Coetomys* species from Kasama in Zambia (Kawalika et al., 2001) is yet to be formally described.

4.3.2. *Cryptomys* Gray, 1864

Etymology. *Cryptos* = hidden plus *mys* = mouse, *Cryptomys* = “hidden mouse”.

The genus name refers to the fossorial natural history of members of this family.

Type species. *Georychus holosericeus* Wagner, 1843

Type specimen. Leipzig Museum, Germany

Type locality. Graaff-Reinet, Northern Province, South Africa

Genus diagnosis – To date, all members of this genus are characterized by a stable diploid number ($2N = 54$). *Cryptomys* is distributed in southern Africa, primarily south of the Limpopo River to the Cape of Good Hope, with the exception of *C. cf. nimrodi* which occurs in Zimbabwe. There are no clear morphological characters to distinguish *Cryptomys* from *Coetomys*.

Included species. *C. anomalus* Roberts, 1913; *C. holosericeus* Wagner, 1843; *C. hottentotus* Lesson, 1826; *C. natalensis* Roberts, 1913.

4.4. Divergence estimates

Like other lineages of African rodents, the fossil record for Bathyergidae is not well represented in the geologic record. Only a few taxa have been recovered from the early and middle Miocene (Lavocat, 1978), and extant genera do not appear prior to the mid-Pliocene (Denys and Jaeger, 1992). The earliest known fossils, *Proheliophobius* and *Richardus*, were recovered from early to mid-Miocene formations of Kenya and Uganda (Lavocat, 1973, 1988). Therefore, calibration points that can be used to estimate divergence times are limited. Based on the rate of nucleotide substitutions per site per year in the 12S rRNA gene and assuming a molecular clock, Allard and Honeycutt (1992) estimated origin of the family to be approximately 38 MYA. Likelihood ratio

Table 2.1. Estimation of the ages of the lineages within the family Bathyergidae using non-parametric rate smoothing (Sanderson, 2003). Calibration based on 20-19 MYA for the divergence of *Heliophobius* (*Proheliophobius*) lineage.

Split	12S	TTR	Both
<i>Heterocephalus</i> - All	26.19-24.88	52.61-49.98	34.75-33.01
<i>Heliophobius</i> - S.African	20-19	20-19	20-19
<i>Georychus</i> - S.African	16.96-16.12	17.21-16.34	16.96-16.11
<i>Bathyergus</i> - <i>Cryptomys sensu lato</i>	15.77-14.98	17.21-16.35	16.20-15.39
<i>Cryptomys sensu scripto</i> - <i>Coetomys</i>	12.48-11.86	10.91-10.37	11.97-11.37
<i>Coetomys</i>	6.59-6.26	4.82-4.58	6.23-5.92
<i>Cryptomys sensu scripto</i>	4.62-4.39	5.00-4.75	4.99-4.74

tests revealed that both datasets, 12S rRNA and TTR, violate the assumption of a molecular clock. Divergence dates were therefore estimated using a nonparametric rate smoothing method (r8s, Sanderson, 2003). This method allows for a unique substitution rate for each branch of the tree rather than the single rate enforced under the molecular clock scenario. To allow for comparisons between the two datasets, the trimmed phylogeny from the combined dataset was used and divergence dates were estimated for each dataset (Table 2.1). Based on the available fossil evidence and dating of the sites (Lavocat, 1973), a date of 20-19 MYA was used as a calibration point for the divergence of the *Heliophobius* lineage (A. Winkler, per. comm.). Dates estimated from

12S substitution rates for the basal nodes were typically earlier than estimates from TTR, although this relationship is reversed in the *Coetomys*+*Cryptomys* clade (Table 1).

Based on these dates, the hypothesized North-South migration through a proposed “arid corridor” would have occurred 17 – 16MYA during the early/mid-Miocene. A rapid radiation resulting in the differentiation of *Bathyergus*, *Georychus*, *Cryptomys*, and *Coetomys* is estimated to have occurred in the early Miocene (17 – 15MYA), and the divergence of *Coetomys* from *Cryptomys* is estimated to have occurred during the mid-Miocene, 12 – 10MYA. These estimates are much earlier than that predicted by the fossil record. These data support the hypothesized origin of the family in East Africa (Lavocat, 1973). Connection of the eastern taxa with the South African genera has been hypothesized as the product of a migration through an arid corridor as supported by current distribution patterns and fossil evidence. The sister-group relationship between *Heliophobius* and the common ancestor of the South African genera suggests a single migration event into the Cape region of South Africa.

4.5. Phylogenetic and biogeographic implications

Separate and combined analyses produced the same overall topology. Within the family Bathyergidae, relationships among genera are similar to those recovered in previous studies (Allard and Honeycutt, 1992; Faulkes et al., 1997; Walton et al., 2000). In all analyses, *Heterocephalus* is basal to the clade of remaining genera (*Heliophobius*, *Bathyergus*, *Georychus*, *Cryptomys* and *Coetomys*). Within this clade, the East African genus, *Heliophobius*, is sister to the remaining genera. As in previous studies (Walton et

al., 2000), relationships among *Bathyergus*, *Georchus*, and *Cryptomys* + *Coetomys* remain poorly resolved. The inability to resolve relationships among these three lineages, even with multiple genes, suggests a rapid radiation similar to those experienced by other groups of fossorial rodents in North and South America (Smith, 1998; Sudman and Hafner, 1992). The separation of *Coetomys* from *Cryptomys* roughly follows the borders between the Zambezian and the Kalahari-Highveld phytochoria (cf., White, 1983), and the pattern of flow of the PaleoZambezi River. Historically, the Upper Zambezi continued its southern course, crossing what is now Botswana to join either the Oranje system or the Limpopo (cf., Thomas and Shaw, 1988). This would have provided a barrier separating the ancestral stock into what would become *Cryptomys* and *Coetomys*, allowing for subsequent northern expansion of *Coetomys*.

Within *Coetomys*, the Sudanian species, *C. foxi* and *C. ochraceocinereus* are sister to all of the Zambezian species. Although the affinity of Sudanian taxa has been suggested by morphology and geographic proximity (Honeycutt et al., 1991), their placement within the genus has not been examined with genetic data. Expansion of the rainforest has provided a geographic barrier, isolating this northern stock from the East Africa taxa. Subsequently, in the late Pleistocene/early Pliocene, the Middle Zambezi developed, linking the Upper Zambezi and Lower Zambezi (cf., Thomas and Shaw, 1988), thus separating *C. damarensis* and *C. darlingi*.

The radiation of recent species within the Zambezian region may have occurred in the Pleistocene, as supported by allozyme data (Filippucci et al., 1994, 1997; Nevo et al., 1987), coinciding with dramatic geomorphological changes producing physical

barriers (Thomas and Shaw, 1988) and dramatic climatic and vegetational changes forming ecological barriers (Adams, 2001). Both of these factors lead to habitat fragmentation and speciation by vicariance.

4.6. *Patterns of intrageneric variation*

Silvery mole-rats (*Heliophobius*) from Kenyan on one side and Zambian and Malawian samples on the other side of the Rift Valley are divergent (12S corrected pairwise difference = 7.3%), and this is reflected in a slightly different karyotype found in Zambia (Scharff et al., 2001). Nevertheless, since sampling was limited to a few localities within their area of occurrence, additional sampling across their entire distribution is required prior to any formal taxonomic decisions.

Among Cape mole-rats (*Georychus*), there are at least two well-supported lineages: Cape Region (Eastern + Western Cape Province) and Transvaal/Natal (Mpumalanga + Kwazulu-Natal Province). Two previous studies (mtDNA RFLP: Honeycutt et al., 1987; allozymes: Nevo et al., 1987) documented a substantial amount of genetic distance between the two regions. Both studies recommended further investigation into the relationships within *Georychus*, and we are currently assessing the genetic patterns of additional samples from across the distribution.

Within *Cryptomys (sensu stricto)*, the pattern of variation is similar to that reported by Faulkes et al. (1997). Based on the larger 12S phylogeny, there appears to be five monophyletic lineages that show geographic cohesion: *anomalous* (cf. '*pretoriae*'), *natalensis*, *nimrodi*, *holosericeus* (North-West/Free State), and *hottentotus*

(Western Cape/Northern Cape). All of these clades have strong support (MP BP = 100, DI = 6 - 11; ML BP = 89 - 99, PP = 97-100) with the exception of *nimrodi*, which is limited to the single sample from Faulkes et al. (1997). Our *anomalus* clade is represented by specimens from Pretoria and surrounding areas (Appendix, Figs. 2.1-2.4). Faulkes et al. (1997) referenced animals collected in Pretoria as *Cryptomys 'pretoriae'*, but De Graaff (1964) included *C. pretoriae* Roberts, 1913 as a synonym under *C. anomalus* Roberts, 1913. We follow De Graaff's recommendation. The North-West/Free State clade (Figs. 2.2-2.4) roughly corresponds to *C. holosericeus* Wagner, 1843 supporting the taxonomy of Roberts (1951) and De Graaff (1964). De Graaff (1964) questioned the validity of Graaff-Reinet (Cape Province = Northern Province) as the true type locality for *C. holosericeus* based on the distribution of the known localities of all *C. holosericeus* museum specimens. We believe the specimens considered here as *C. holosericeus* are representative samples from within its true distribution.

The genus *Coetomys* has the largest geographic distribution. Within this genus, there are six well-defined clades: Sudanian, *mechowii/bocagei*, *darlingi*, *damarensis*, *anselli/kafuensis*, and *amatus/whytei*. The Sudanian clade is sister to all other *Coetomys*. This clade includes *C. foxi* and *C. ochraceocinereus*. The *C. foxi* samples are from Cameroon (Williams et al., 1983), and other authors have referred to them as *C. ochraceocinereus* (Bennett and Faulkes, 2000; Honeycutt et al., 1991). While the genetic divergence between these two taxa is relatively high, a more complete sampling throughout this geographic region (Ghana, Nigeria, Cameroon, Central African

Republic, Southern Sudan, Northern Zaire, North-east Uganda) is necessary prior to any conclusions about phylogenetic relationships within this clade as well as their relationship to the unsampled species, *C. zechi*. The only available karyotype for this clade is for *C. foxi* ($2N = 66/70$; Williams et al., 1983).

The west-Zambeian *mechowii/bocagei* clade consists of two recognized species and is sister to the other Zambeian clades. While the placement of *C. bocagei* within this clade has weak support (MP BP = 86, DI = 2; ML BP = 62, PP = 84/<50), additional samples of *C. bocagei* may help resolve its phylogenetic position. The monophyly of *C. mechowii* is well supported (MP BP = 100, DI = 5; ML BP = 81, PP = 100/100). The north-eastern Zambeian *amatus/whytei* clade (MP BP = 100, DI = 1; ML BP = 61, PP = 99/100) contains three taxa, *C. amatus* ($2N = 50$; Macholán et al., 1998), *C. sp.* ‘Kasama’ ($2N = 64$; Kawalika et al., 2001), and *C. whytei* ($2N = 46$; Chitaukali et al., 2001). The monophyly of both southern species, *C. darlingi* (MP BP = 100, DI = 1; ML BP = <50, PP = 98-100) and *C. damarensis* (MP BP = 100, DI = 7; ML BP = 93, PP = 100), is supported.

While there is strong support for the central Zambeian *anselli/kafuensis* clade (MP BP = 100, DI = 10; ML BP = 100, PP = 100), relationships within this clade are not well resolved. There appear to be at least three species, *C. anseli* ($2N = 68$; Burda et al., 1999), *C. kafuensis* ($2N = 58$; Burda et al., 1999), and *C. micklemei* ($2N = 58$; Meier, 2001), although we expect more will be identified with the addition of samples from this region of Zambia (Van Daele et al., in prep).

5. Conclusions

Although this study does not provide exhaustive sampling across the entire distribution of the Bathyergidae, it presents the most robust genetic representation of the family to date. Additional data continue to identify complexities in the evolutionary history of this group. Instead of fitting the accepted taxonomic views of Ellerman et al. (1940) and DeGraaff (1964, 1981) (*i.e.*, Faulkes et al., 1997; Honeycutt et al., 1991; McKenna et al., 1998; Nevo et al., 1987; Nowak, 1999), the level of diversity appears to reflect the species-rich classification scheme of Roberts (1951). More detailed sampling/analysis, including the development of a chromosomal evolution hypothesis, is required to fully understand the relationships within each genus and formulate a complete biogeographic history.

CHAPTER III
DEVELOPMENT AND CHARACTERIZATION OF NOVEL
MICROSATELLITE MARKERS FOR THE SIX GENERA OF
BATHYERGIDAE (RODENTIA) AND THEIR UTILITY IN OTHER MEMBERS
OF THE FAMILY

1. Introduction

African mole-rats (family Bathyergidae) represent a monophyletic group of subterranean rodents endemic to sub-Saharan Africa. Within Bathyergidae, there are currently six recognized genera; *Heterocephalus*, *Heliophobius*, *Bathyergus*, *Georchus*, *Cryptomys*, and *Coetomys* (Ingram et al., 2004). Bathyergidae has received extensive attention due to their varying social structures that range from solitary (*Bathyergus*, *Georchus*, *Heliophobius*) to the highly structured social system of the naked mole-rat, *Heterocephalus glaber*.

Among the solitary species of Bathyergidae is the Silvery mole-rat, *Heliophobius argenteocinereus*. *Heliophobius* is currently recognized as a monotypic genus endemic to eastern and southeastern Africa and distributed in Kenya, Tanzania, Zambia, Malawi, and Mozambique (Burda, 2001). Recent research has focused on their burrowing activity (e.g. Sumbera et al., 2003), parasites (e.g. Tenora et al., 2003), or phylogenetic studies of the family Bathyergidae (e.g. Ingram et al., 2004). Their phylogenetic position within the family has been well supported, but there has been no investigation of the intra-generic relationships. Within the genus, a high degree of genetic variation

has been observed (Ingram et al., 2004). *Heliophobius* samples from Kenya and Malawi/Zambia, on opposite sides of the Rift Valley, are markedly divergent at the molecular level (12S rRNA: ML divergence = 7.3%), and this is reflected in distinct karyotypes found in Zambia versus Kenya (Scharff et al., 2001).

The Cape mole-rat, *Georychus capensis*, is also a solitary species, occurring in sandy or loose soil of South Africa. Its distribution is coastal, consisting of disjunct populations. Although *Georychus* is recognized as a monotypic genus, there are at least two well-supported lineages, Cape Region (including the eastern Cape) and Transvaal/Natal, which show a substantial amount of genetic divergence (Honeycutt et al., 1987; Ingram et al., 2004; Nevo et al., 1987). Research on *Georychus* has been limited to investigations of their physiology {e.g. circadian rhythms (Oosthuizen et al., 2003), reproductive biology (Bennett and Jarvis, 1988), visual systems (Omlin, 1997)} and environmental conditions (Roper et al., 2001). There has been recent focus on the phylogenetic relationships within Bathyergidae (Faulkes et al., 2004; Ingram et al., 2004), but no studies have focused on the genetics within *Georychus*. With high genetic divergence documented between disjunct populations, investigation of typical population parameters is essential.

The genus *Bathyergus* is comprised of two species, the Cape dune mole-rat, *B. suillus* and the Namaqua dune mole-rat, *B. janetta*. Both species are solitary, endemic to South Africa or South Africa and Namibia, respectively. Dune mole-rats have the largest body size of the bathyergids reaching up to 2000 g, with the average weight of 933 g and 635g for males and females, respectively (Jarvis and Bennett, 1991). Unlike

the other members of this family that rely solely on their incisors for excavating their burrow systems, *Bathyergus* primarily use the clawed forefoot (Bennett and Faulkes, 2000). While the position of *Bathyergus* within the family has been investigated (Faulkes et al., 2004; Honeycutt et al., 1987; Ingram et al., 2004; Walton et al., 2000), few studies have focused on the relationships within *Bathyergus*. The available information of the social organization and behavior of this genus has been obtained through observation (Davies and Jarvis, 1986; Lovegrove, 1986). Genotypic information, through microsatellite data, could provide insight into the social structure and mating patterns, as well as the amount of gene flow, migration patterns, and other population parameters. Population level genetic studies will be helpful in the ongoing studies of the evolution of sociality in Bathyergidae since *B. janetta* is a solitary species and is found in arid habitats which are usually occupied by the species exhibiting more social behavior.

The common mole-rat, *Cryptomys hottentotus*, is endemic to South Africa. *C. hottentotus* is described as social in nature (Bennett and Faulkes, 2000). Social structure and other aspects of behavioral ecology likely influence the partitioning of genetic variation within species, especially if animals or colonies display restricted dispersal, resulting in highly subdivided populations (Nevo et al., 1990). *Cryptomys*, in particular, has been the focus of recent studies due to a relatively high amount of species diversity compared to the other genera of the family (Faulkes et al., 2004; Ingram et al., 2004).

All species of the genus *Coetomys* are social, with some forms approaching eusociality similar to the naked mole-rat (e.g., *C. mechowii*, Burda and Kawalika, 1993).

Coetomys, currently contains eleven recognized species in a broad but disjunct distribution extending from Ghana and Nigeria in west Africa to the southern Sudan in east Africa and from southern Congo and southern Tanzania, south to the Limpopo River where it is replaced by members of *Cryptomys*. The delineation of species boundaries among *Coetomys* species based on morphological variation is problematic, but unlike other members of the family, *Coetomys* displays considerable species-specific chromosomal variation ($2N = 40-78$: Burda, 2001). The Zambezi region has been proposed as the center of origin for *Coetomys* with the highest species per area density for the entire family (Burda, 2001). For this reason, I developed an array of microsatellite loci for the well-characterized Zambian giant mole-rat, *Coetomys mechowii*.

The naked mole-rat or sand puppy, *Heterocephalus glaber*, has received much attention due to its unique life history and ecology. They are fossorial rodents that live in extensive burrow systems in the semi-arid deserts of Ethiopia, Somalia, and Kenya. *H. glaber* was the first eusocial mammal to be described (Jarvis, 1981), and the evolution of eusociality in mammals has been a popular topic since this discovery. Previous molecular studies revealed significantly low levels of genetic diversity in both mitochondrial DNA and nuclear minisatellite markers (Faulkes et al., 1990; Honeycutt et al., 1991; Reeve et al., 1990). The high relatedness within colonies was interpreted as supporting the hypothesis that inbreeding was an important genetic factor leading to the evolution of eusociality (e.g., Freeman and Herron, 1998). More recent studies have documented a preference for outbreeding (Braude, 2000; Cizek, 2000) and propose that

the high levels of relatedness and low levels of genetic variation reported in previous studies (Faulkes et al., 1990; Honeycutt et al., 1991; Reeve et al., 1990) may have been sampling error (Braude, 2000).

Burland et al. (2001) reported a panel of microsatellite markers for *Cryptomys*, seven isolated from *C. damarensis* and four from *C. hottentotus*. Subsequent to this study, the clade containing *C. damarensis* was elevated to the genus *Coetomys* (Ingram et al., 2004). All seven microsatellite markers reported for *C. damarensis* were polymorphic in *C. mechowii*, my focal species for *Coetomys*.

To date, no species-specific microsatellite primers have been reported for *Heterocephalus*, *Heliophobius*, *Georychus*, or *Bathyergus*. Burland et al. (2001) demonstrated cross-species amplification of their microsatellite markers. Of their eleven loci, only two successfully amplified in a small sample of *H. glaber* (5-6 individuals): one (DMR1) from *Coetomys (Cryptomys) damarensis* had five alleles, while the other, CH2 from *Cryptomys hottentotus* was monomorphic in *H. glaber*. Four of seven loci developed for *Coetomys (Cryptomys) damarensis* and all four loci developed for *Cryptomys hottentotus* amplified in a small sample of *H. argenteocinereus* (4-8 individuals). Although amplification was successful in eight loci, two of the eight were monomorphic. In *Georychus capensis* (1-5 individuals), six of seven loci developed for *Coetomys (Cryptomys) damarensis* and all four loci developed for *Cryptomys hottentotus* successfully amplified with the number of alleles at each locus ranging from 2-6. In *Bathyergus*, four of seven loci developed from *Coetomys (Cryptomys) damarensis* and three of four loci developed from *Cryptomys hottentotus* amplified in a

small sample of *B. suillus* (1-6 individuals). Amplification was more successful in *B. janetta* (2-5 individuals) with six of seven and four of four loci, respectively.

Here I present six polymorphic species-specific markers designed from *Heterocephalus glaber*, five designed from *Bathyergus suillus*, seven loci designed from *Heliophobius argenteocinereus*, six loci designed from *Georychus capensis*, five additional *Cryptomys hottentotus* loci, five loci developed for *C. mechowii*, and test their application across the other species in Bathyergidae.

2. Materials and Methods

2.1. Microsatellite library and primer construction

Six individuals were selected for genomic DNA library construction: *Heterocephalus* (H034), *Heliophobius* (H046), *Georychus* (TM38353), and *Bathyergus* (TM41494), *Cryptomys* (TM38375) and *Coetomys* (Z9). Genomic DNA was digested with *Pst* I and size selected to eliminate fragments outside the range of 400-1500 bp. Fragments were ligated using T4 ligase into pBluescript plasmid and transformed into DH10 β Electrocomp *E. coli* (Stratagene). Cells were grown on Amp⁺ LB agar plates with standard blue/white screening. Colonies with inserts were transferred into 96-well plates and cultured in Amp⁺ LB broth with 1% freezing medium for permanent storage. Colonies were transferred and grown on nylon membrane, the cells and DNA were denatured and fixed to the membranes, and probed with the following repeat motifs: (GT)₁₈, (CT)₁₈, (GTCT)₈, (CA)₁₈, (GA)₁₈, and (GTAA)₈. For recombinants containing microsatellites, plasmid DNA was purified via organic miniprep, and the insert DNA

was sequenced using the pUC primers (pUC-F, pUC-R). PCR amplifications were conducted in 50 μ L reactions with a final concentration of 2.5U of *EX-Taq* polymerase (Takara: Fisher Scientific), 1X *EX-Taq* Buffer w/ $MgCl_2$ (Takara), 0.25 mM dNTPs (Takara), 0.1 μ M of each primer. Reaction conditions included an initial 2 min denaturation at 95 $^{\circ}C$, followed by 35 cycles of 95 $^{\circ}C$ for 30 s, 52 $^{\circ}C$ for 30 s, and 72 $^{\circ}C$ for 30 s, with a final extension time of 7 min at 72 $^{\circ}C$. Fragment length was determined by electrophoresis of PCR product (5 μ l) with a size standard on 1% agarose minigels, stained with ethidium bromide, and visualized under UV light. This allowed for the confirmation that the plasmid contained an insert. For PCR products greater than 500 bp in length, the product were cleaned using QIAquick Spin PCR purification spin columns, following a standard protocol (Qiagen Inc., Valencia, CA). Clean PCR products were sequenced in both directions using pUC primers. Cycle sequencing reactions were performed using ABI Prism BigDye Terminator v3.0 chemistry (Applied Biosystems), with 25 cycles of 97 $^{\circ}C$ for 30 s, 50 $^{\circ}C$ for 5 s, and 60 $^{\circ}C$ for 2 min. Excess terminator dye, oligonucleotides, and polymerase were removed by centrifugation at 3000 g through a Sephadex G-50 matrix (Sigma-Aldrich, Inc.). Sequencing reactions were electrophoresed and analyzed on an ABI 377 XL automated sequencer. Sequence data were imported into SEQUENCHER v4.2 (Gene Codes Corporation, Ann Arbor, MI) for alignment and contig assembly for each clone.

Once the entire sequence was confirmed by overlapping reads, contigs were exported as FASTA files. Repeat regions of each contig were masked out of the sequence using RepeatMasker v3.0 (Smit et al., 2004) and searched with BLAST to

ensure absence of contamination in the sequence (e.g. dimerism with *E. coli*) and to identify any similarity to previously published sequences. PCR primers were designed in the flanking sequence of each microsatellite using Primer 0.5 (Whitehead Institute, MIT).

2.2. Taxon sampling

For *Heterocephalus*, a total of 79 Kenyan DNA samples were used: 30 from Meru (7 colonies), eight from Mbovo (3 colonies), and 41 (10 colonies) from Mtito Andei. A total of 76 *Heliophobius* samples were included: 34 individuals from Kenya and 42 individuals from Malawi/Zambia. A total of 47 individuals of *B. suillus* and 11 individuals of *B. janetta*, and a total of 28 *Georychus* samples were screened: 11 individuals from the Western Cape Province (WC), 14 individuals from the Eastern Cape Province (EC), and three individuals from the Mpumalanga (Transvaal) Province (TP). Four species of *Cryptomys* were included with a total of 11 *Cryptomys anomalus* (2 populations), 19 *C. holosericeus* (4 populations), 13 *C. hottentotus* (5 populations), and 24 *C. natalensis* (7 populations) samples. Five species of *Coetomys*, with a total of 75 individuals: two *Coetomys amatus* (1 population), five *C. anselli* (3 populations), 52 *C. damarensis* (10 populations), ten *C. mechowii* (4 populations) and six *C. whytei* (2 populations) samples. The individuals from which the microsatellite libraries were designed were included for each genus.

2.3. *Microsatellite amplification, genotyping, and sequencing*

All primer sets were screened via polymerase chain reaction (PCR) across all lineages of Bathyergidae to determine if each locus is conserved. If amplification of a locus was successful, then all available samples were genotyped using an ABI 377 automated sequencer using primers labeled with one of three fluorescent dyes: TET, FAM, or HEX. Approximately 20-100 ng of template DNA was amplified in 25 μ L reactions using 1.25U of EX-*Taq* polymerase (Takara: Fisher Scientific), and a final concentration of 1X EX-*Taq* Buffer (w/ $MgCl_2$)(Takara), 0.25 mM dNTPs (Takara), 0.1 μ M of fluorescent-labeled (forward) and unlabeled (reverse) primers. Reaction conditions included an initial 2 min denaturation at 95 $^{\circ}C$, followed by 35 cycles of 95 $^{\circ}C$ for 30 s, annealing temperature (Tables 3.1–3.6) for 30 s, and 72 $^{\circ}C$ for 30 s, with a final extension time of 7 min at 72 $^{\circ}C$. An internal size standard (MapMarker 400: BioVentures, Inc.) was run with every sample. Each locus was compiled and analyzed using GENOTYPER v.2.5 software (PE Applied Biosystems).

2.4. *Data analyses*

Both POPGENE v1.31 (Yeh and Boyle, 1997) and GENEPOP (Raymond and Roussett, 1995) were used to test for deviation from Hardy-Weinberg equilibrium (HWE) and assay linkage disequilibrium. When pairwise comparisons were made, *p*-values were adjusted using Bonferroni correction.

3. Results and Discussion

3.1. Amplification and variation within focal taxa

3.1.1. *Heliophobius*

The primer sequence, annealing temperature, number of alleles, and both observed (H_O) and expected (H_E) heterozygosities found at each locus are listed in Table 3.1. In the Kenyan samples, Harg01 and Harg07 were not in Hardy-Weinberg equilibrium (HWE; $p < 0.0001$). In the Malawi/Zambian samples, Harg03 and Harg08 were not at HWE. Both the Kenyan and Malawi/Zambian datasets consisted of pooled populations, which, when separated by sampling locality, met HWE except one Malawian population (Blantyre) that was not in HWE for Harg08. No loci were in linkage disequilibrium after pairwise testing (GENEPOP).

3.1.2. *Georychus*

Six primers designed from *Georychus capensis* are shown in Table 3.2, including primer sequence, number of alleles, and both observed (H_O) and expected (H_E) heterozygosities at each locus. Gcap01 and Gcap10 were the only loci that deviated from HWE (eastern Cape only). This sample consisted of individuals from multiple sampling sites in that region, that when separated by locality, met Hardy-Weinberg expectations. No linkage disequilibrium was detected. Mean number of alleles (\pm S.D.) per loci for the genus was 7.50 ± 3.39 . Mean observed heterozygosity (H_O) was 0.424 ± 0.260 .

Table 3.1 Characterization of seven polymorphic microsatellite loci isolated from *Heliopobius argenteocinereus*.

Primer Name	Sequence 5' - 3'	Dye	Annealing	Size of clones (bp) exp/obs	Repeats in cloned allele	Location*	Size			
			Temp (°C)				Range (bp)*	N _a *	H ₀ *	H _E *
Harg01	F: TACATATGGCAGGGCTGG	6-FAM	63	222/222	(GTT) ₈ ATT(GTT) ₂ ATT	Kenya	216 - 222	2	0.000	0.060
	Malawi					216 - 219	2	0.152	0.179	
Harg02	F: AAAGGAAAGGCAGGCAAG	HEX	61	324/323	(GTT) ₇ GT	Kenya	320 - 323	2	0.000	0.056
	Malawi					317 - 323	3	0.237	0.219	
Harg03	F: TCCACTGCCTCCCTCAAT	6-FAM	61	259/259	(GT) ₁₀ GC(GT) ₄	Kenya	258	1	0.000	0.000
	Malawi					272 - 296	12	0.600	0.901	
Harg07	F: ATGAGAGTTTCCTGATGTCCC	TET	54	171/171	(GT) ₁₅ GCTT(GT) ₅	Kenya	163 - 175	3	0.039	0.298
	Malawi					143 - 159	3	0.105	0.103	
Harg08	F: CTAAGGTTTTGGCTCTGACC	HEX	58	310/314	(GT) ₂₄	Kenya	304 - 322	6	0.526	0.795
	Malawi					297 - 322	13	0.667	0.891	
Harg10	F: CTTCCAGCTGTCACAGAGT	TET	61	195/195	(GTT) ₁₃	Kenya	192 - 195	2	0.333	0.419
	Malawi					177	1	0.000	0.000	
Harg11	F: CTGTGTCCTTCTCCTTCA	HEX	65	333/334	(GT) ₁₇	Kenya	334 - 346	5	0.600	0.822
	Malawi					-	-	-	-	

*For each locus, the allele size range, number of alleles (N_a), observed (H₀) and expected (H_E) heterozygosity are reported for *H. argenteocinereus* from Kenya and Malawi.

Table 3.2 Characterization of 6 polymorphic microsatellite loci isolated from *Georychus capensis*

Primer Name	Sequence 5' - 3'	Dye	Annealing Temp (°C)	Size of clones (bp) exp/obs	Repeats in cloned allele	Locality*	Size Range (bp)*	N _a *	H _o *	H _E *
Gcap01	F: CTTGTTGGGAAGTTTCACTCA R: AGTTCTGAGCCCAGCTGAC	TET	58	124/113	(GT) ₁₀ AT (GT) _k	CP	113 - 129	8	0.900	0.868
						EC	113 - 125	4	0.083	0.308
						TP	123 - 125	2	0.333	0.333
Gcap02	F: TATGTGTCTCAGCAGCCAAA R: ACATAGGTTAACAGCTGTGCG	6-FAM	58	417/294	(GT) ₁₇	CP	286 - 324	9	0.900	0.916
						EC	286 - 308	7	0.571	0.656
						TP	-	-	-	-
Gcap03	F: TTGATGAGGTGAAGCATAAGC R: CTACCCACTCTCGGGGAC	HEX	58	283	(GT) ₁₄	CP	286 - 288	2	0.000	0.533
						EC	284 - 284	2	0.000	0.667
						TP	284	1	0.000	0.000
Gcap04	F: GGGTGATGAGAGCATGTCTT R: CAGTGGGAAGAGTTTTAGATGG	6-FAM	58	167/159	(GTT) ₇	CP	163 - 173	4	0.455	0.688
						EC	161 - 167	2	0.071	0.071
						TP	161 - 167	3	0.333	0.733
Gcap07	F: TAAGGACACGGAGTAGGTGG R: AGTTCCCAAGTTGGTAAGG	HEX	58	242/218	(GT) ₂₁	CP	216 - 228	5	0.546	0.706
						EC	216 - 222	3	0.539	0.557
						TP	242 - 246	3	0.667	0.733
Gcap10	F: TAGTTTCCCCTTGTTC R: TAGGCTAAAAAGAAGCCTTGG	TET	58	162/163	(GT) ₁₉	CP	163 - 173	6	0.727	0.849
						EC	161 - 171	6	0.500	0.765
						TP	163 - 177	2	0.500	0.500

*For each locus, the allele size range, number of alleles (N_a), observed (H_o) and expected (H_E) heterozygosity are reported for *G. capensis* from western Cape (CP), eastern Cape (EC) and Mpumalanga (TP).

3.1.3. *Bathyergus*

Table 3.3 lists the primer sequence, annealing temperature, number of alleles and both observed (H_O) and expected (H_E) heterozygosities for each locus. For *B. suillus*, mean number of alleles per loci (\pm SD) was 11.8 ± 3.49 , and mean observed heterozygosity was 0.602 ± 0.2 . Bsuil01, Bsuil02, and Bsuil06 were not in Hardy-Weinberg equilibrium ($p < 0.0001$) when populations were pooled together, but when populations were separated by sampling locality, the loci met HWE in *B. suillus*. None of the loci were in linkage disequilibrium after pairwise testing using GENEPOP v3.4.

3.1.4. *Cryptomys*

Characterization of five microsatellite loci designed from *C. hottentotus* are listed in Table 3.4, including primer sequence, number of alleles, and both observed (H_O) and expected (H_E) heterozygosities at each locus. After Bonferroni correction to account for multiple pairwise comparisons, only Chott05, Chott06, and Chott08 were not at HWE in *C. natalensis*, and Chott08 did not meet HWE in *C. anomalus*. Once separated by localities, all loci met HWE, except a single population of *C. anomalus* for Chott08. No significant linkage disequilibrium was detected between loci. Mean number of alleles (\pm S.D.) per loci for the genus was 14.6 ± 2.61 and mean observed heterozygosity (H_O) was 0.538 ± 0.113 .

3.1.5. *Coetomys*

Primer sequence, number of alleles, and both observed (H_O) and expected (H_E) heterozygosities are listed in Table 3.5. After Bonferroni correction, Cmech03, Cmech06, Cmech09 and Cmech11 were not at HWE in *C. damarensis*, and Cmech06 did not meet HWE in *C. mechowii*. Once separated by localities, all loci met HWE. No significant linkage disequilibrium was detected among loci. Mean number of alleles (\pm SD) per loci for the genus was 13.6 ± 7.50 . Mean observed heterozygosity (H_O) was 0.400 ± 0.309 .

3.1.6. *Heterocephalus*

The primer sequence, annealing temperature, number of alleles, and both observed (H_O) and expected (H_E) heterozygosities found at each locus are listed in Table 3.6. After Bonferroni correction, only Hglab10 in Mtito Andei samples, and Hglab01 and Hglab03 in Meru samples were not in Hardy-Weinberg equilibrium (HWE; corrected $p < 0.0028$). All localities consist of multiple colonies, which may account for this deviation from HWE, as well as the fact that the mating system does not meet the assumption of random mating and colonies have very low N_e and overlapping generations. No loci were in linkage disequilibrium after pairwise testing (GENEPOP).

Table 3.3 Characterization of 5 polymorphic microsatellite loci isolated from *Bathyergerus suillus*.

Primer Name	Sequence 5' - 3'	Dye	Annealing Temp (°C)	Size of clones (bp) exp/obs	Repeats in cloned allele	Species*	Size Range (bp)*	N _a *	H ₀ *	H _E *
Bsuil01	F: GTCTACCCGTCTCCAGG	6-FAM	64.7	211/208	(GT) ₁₄ GC (GT) ₄	BS	194 - 216	10	0.404	0.827
	R: AACGTTCTCCTAATTCTCCTCC						BJ	192 - 204	3	0.091
Bsuil02	F: CAGGGAGAGGGTGGGTAG	6-FAM	56.4	198/131	(GT) ₁₄ GCAC (GT) ₅ TTGTG	BS	127 - 141	7	0.422	0.680
	R: CCTTTGTGAGCTCCATCAGT						BJ	123 - 135	5	0.300
Bsuil04	F: TTGCAACACAGAGGAACTGA	HEX	58.9	337/337	(GT) ₂₁	BS	321 - 353	14	0.838	0.872
	R: GTGGGTTGCTGATCTGTCTT						BJ	317 - 343	4	0.333
Bsuil05	F: CCTCTCTGACCCTGTGACAC	HEX	62.7	364/378	(GT) ₁₆ (GA) ₁₀	BS	360 - 396	16	0.787	0.923
	R: TCGAAGATCCCACCACAG						BJ	362 - 366	3	0.429
Bsuil06	F: TGTGGTCTCTTTCTTGGCTC	TET	63.9	253/242	(GT) ₂ GA (GT) ₁₆ G (GT) ₄	BS	238 - 266	12	0.558	0.873
	R: AACAGTGGAGGAGCTTTGTG						BJ	242	1	0.000

*For each locus, the allele size range, number of alleles (N_a), observed (H₀) and expected (H_E) are reported for both *B. suillus* (BS) and *B. janetta* (BJ).

Table 3.4 Characterization of 5 polymorphic microsatellite loci isolated from *Cryptomys hottentotus*.

Primer Name	Sequence 5' - 3'	Dye	Annealing Temp (°C)	Size of clones (bp) exp/obs	Repeats in cloned allele	Species*	Size			
							Range (bp)*	N _a *	H ₀ *	H _E *
Chott01	F: CCTCCCGTTACTTAGGGT R: CTGACATGCAAGGCTTTTG	HEX	58.9	281/279	(GT) ₁₉	<i>C.anomalus</i>	263-291	8	0.778	0.895
						<i>C.holosericeus</i>	263-293	10	0.632	0.873
						<i>C.hottentotus</i>	271-287	5	0.500	0.725
						<i>C.natalensis</i>	271-291	10	0.474	0.845
Chott03	F: TGCCTCAGTATAAGGCTAGAG(6-FAM R: ATGTTCAAGGACCTACAGGAGG	HEX	61	208/210	(GT) ₂ (GC) ₃ (GT) ₃ (GCGT) ₃ (GT) ₄ (GCGT) ₂ GTGC(GT) ₃ GCGTGCA(TGT)	<i>C.anomalus</i>	182-208	4	0.546	0.541
						<i>C.holosericeus</i>	156-238	9	0.556	0.832
						<i>C.hottentotus</i>	198-214	7	0.615	0.825
						<i>C.natalensis</i>	180-212	8	0.792	0.858
Chott05	F: ATCTAGAGAGGCTTGACCTGC R: GCTTGAGCAGTTTCTAAAATGC	HEX	63.9	302/303	(GT) ₁₃ (GC) ₃ (GT) ₃ GCGT	<i>C.anomalus</i>	283-307	7	0.750	0.858
						<i>C.holosericeus</i>	273-301	8	0.375	0.925
						<i>C.hottentotus</i>	283-303	5	0.571	0.593
						<i>C.natalensis</i>	285-301	4	0.250	0.767
Chott06	F: CTTGAAGGGGCTATGACAA R: GTATTCTTCCAAAGCAGTGG	6-FAM	58.9	265/267	(GT) ₁₈	<i>C.anomalus</i>	245-265	6	0.444	0.824
						<i>C.holosericeus</i>	247-273	6	0.833	0.802
						<i>C.hottentotus</i>	243-273	6	0.385	0.812
						<i>C.natalensis</i>	259-275	8	0.625	0.780
Chott08	F: CTCAGCCCTCACTACCC R: GTGTCTTCCCCCTTTTCTGT	TET	63.9	140/141	(GT) ₂₀	<i>C.anomalus</i>	113-123	3	0.000	0.554
						<i>C.holosericeus</i>	115-159	5	0.222	0.611
						<i>C.hottentotus</i>	115-147	8	0.692	0.843
						<i>C.natalensis</i>	115-155	12	0.478	0.897

*For each locus, the allele size range, number of alleles (N_a), observed (H₀) and expected (H_E) heterozygosity are reported for *C. anomalus*, *C.holosericeus*, *C.hottentotus*, and *C.natalensis*.

Table 3.5 Characterization of 5 polymorphic microsatellite loci isolated from *Coetomys mechowii*.

Primer Name	Sequence 5' - 3'	Dye	Annealing Temp (°C)	clones (bp) exp/obs	Repeats in cloned allele	Species*	Size Range (bp)*	N _a *	H ₀ *	H _E *
Cmech03	F: CATAAATAAGCAATAGCCC/ HEX R: CCAGAAGTGGAGGACTAGCA		58	294/294	(GT) ₁₆	<i>C.amatus</i>	300-304	2	0.667	0.000
						<i>C.anselli</i>	284-290	4	0.733	0.800
						<i>C.damarensis</i>	264-294	8	0.650	0.265
						<i>C.mechowii</i>	278-294	6	0.817	0.750
						<i>C.whytei</i>	284-306	9	0.955	0.833
Cmech04	F: GGAGTGGTGAGGACTGTGA(6-FAM R: TCTGACTGGAACCCATCACT		58	374/374	(GT) ₁₇	<i>C.amatus</i>	372-386	3	0.833	0.500
						<i>C.anselli</i>	376-390	6	0.929	1.000
						<i>C.damarensis</i>	354-396	15	0.924	0.898
						<i>C.mechowii</i>	370-390	7	0.901	0.571
						<i>C.whytei</i>	370-390	5	0.933	1.000
Cmech06	F: AGACGACTCTGTTTTTCGGTG TET R: CCAGTCTGTGCCTCTGAGAT		58	168/166	(GTT) ₈ (GCA) ₆	<i>C.amatus</i>	148	1	0.000	0.000
						<i>C.anselli</i>	160-163	2	0.536	0.750
						<i>C.damarensis</i>	142-169	7	0.743	0.385
						<i>C.mechowii</i>	148-169	4	0.634	0.222
						<i>C.whytei</i>	139-163	5	0.893	0.250
Cmech09	F: TGTCTTGGCTCCTAGGTCAG HEX R: CACCCCAACATTATACTCGC		58	296/310	(GT) ₁₀ (GT) ₂₁	<i>C.amatus</i>	310	1	0.000	0.000
						<i>C.anselli</i>	310	1	0.000	0.000
						<i>C.damarensis</i>	306-312	3	0.169	0.026
						<i>C.mechowii</i>	310-314	2	0.546	0.333
						<i>C.whytei</i>	308-310	2	0.667	0.000
Cmech11	F: GACAGTAGGCCGTAATGTGCTET R: CCACCTGTGGTTATCTCTCG		58	149/146	(GT) ₁₈	<i>C.amatus</i>	152-156	2	1.000	1.000
						<i>C.anselli</i>	146-150	3	0.733	0.200
						<i>C.damarensis</i>	132-150	7	0.770	0.212
						<i>C.mechowii</i>	140-154	6	0.842	0.500
						<i>C.whytei</i>	142-162	2	0.667	0.000

*For each locus, the allele size range, number of alleles (N_a), observed (H₀) and expected (H_E) heterozygosity are reported for *C. amatus*, *C. anseli*, *C. damarensis*, *C. mechowii*, and *C. whytei*.

Table 3.6 Characterization of seven polymorphic microsatellite loci isolated from *Heterocephalus glaber*.

Primer Name	Sequence 5' - 3'	Dye	Annealing Temp (°C)	Size of clones		Location*	Size			
				(bp)	exp/obs		Range (bp)*	N _a *	H ₀ *	H _E *
Hglab01	F:TCAGAGTGCTACCCAGGATC R:TACCAAAACTTGCAAAATTCA	6-FAM	58	228/231	(GTT) ₆ GT	Mtito Andei	231	1	0.000	0.000
						Mbovo	229 - 231	2	0.125	0.125
						Meru	231 - 235	3	0.513	0.08
Hglab03	F:GTCAGGTTGGCAGATTTTGA R:TGTGTGAGGGGGAGACAG	HEX	58	296/297	(GT) ₁₉ (GA) ₁₆ CA(GA) ₃ (GGGA) ₂ (GA) ₂ AAGAGGGG(GA) ₂	Mtito Andei	297	1	0.000	0.000
						Mbovo	315 - 323	5	0.733	0.626
						Meru	293 - 323	11	0.870	0.670
Hglab07	F:AACTGAAGTTCCTGTGCTGG R:TGAGGACACATTCTTCTTGG	TET	58	181/181	GTGA(GT) ₁₉ AT(GT) ₄	Mtito Andei	181	1	0.000	0.000
						Mbovo	169 - 183	3	0.396	0.429
						Meru	177 - 183	4	0.706	0.636
Hglab09	F:AGATTTGTTACCTCAATCC R:GTTTTGGTAAAGGCTTCTTGG	TET	58	168/170	(GT) ₁₃	Mtito Andei	168 - 172	3	0.499	0.353
						Mbovo	172 - 174	2	0.485	0.333
						Meru	170 - 174	3	0.192	0.207
Hglab10	F:ACCAAGGGAAATAAACCTGC R:TTCTTCTGTTCCTGTGGC	HEX	58	302/304	(GT) ₂₁	Mtito Andei	294 - 306	3	0.222	0.182
						Mbovo	294 - 304	3	0.275	0.143
						Meru	294 - 308	5	0.627	0.52
Hglab13	F:TCAGTTGGCTAGAGTGGGAG R:CCAGGTTTCTGAGCGACTAA	6-FAM	58	380/385	(GT) ₂₁	Mtito Andei	385	1	0.000	0.000
						Mbovo	383 - 385	2	0.536	0.25
						Meru	375 - 383	5	0.700	0.563

*For each locus, the allele size range, number of alleles (N_a), observed (H₀) and expected (H_E) heterozygosity are reported for *H. glaber* from Mtito Andei, Mbovo, and Meru.

3.2. Application and variation in non-focal taxa

3.2.1. *Heliophobius* (Harg) loci

Cross-amplification of all seven loci was tested in the other five genera of Bathyergidae (Table 3.7). A single locus, Harg01, amplified in the highly divergent basal member, *Heterocephalus glaber*, but high levels of non-specific binding resulted in no scorable genotypes. Although Harg07 amplified in all other species tested, the fragment was too large (>650 bp) for use in fragment analysis. Only Harg03 and Harg11 showed promise for use in other species of Bathyergidae. Harg02 failed to amplify in *Coetomys*, *Bathyergus*, *Georychus* or *Heterocephalus*, but showed polymorphism, with number of alleles ranging from 3-5, in all species of *Cryptomys* tested. Although limited in their use in other studies, this new suite of microsatellite markers provide a promising tool for detailed studies of *Heliophobius*.

3.2.2. *Georychus* (Gcap) loci

To test the applicability of these markers in other species of Bathyergidae, genotyping reactions were run across samples of 12 representative species. Successful amplification and number of alleles detected at each locus are listed in Table 3.7. A single locus, Gcap10, successfully amplified *Heterocephalus glaber*, and showed variability with 8 alleles. In the other four genera, *Bathyergus*, *Cryptomys*, *Heliophobius*, and *Coetomys*, only two markers failed to amplify all samples: Gcap02 in *Coetomys* and Gcap03 in *Cryptomys*. Overall, these markers show great promise for their application in genetics studies in all genera but the highly divergent *Heterocephalus*.

Table 3.7 Number of alleles observed at each microsatellite loci designed from *Heliophobius argenteocinereus* (Harg), *Georychus capensis* (Gcap), *Bathergus suillus* (Bsuil), *Cryptomys hottentotus* (Chott), *Coetomys mechowii* (Cmech), and *Heterocephalus glaber* (Hglab).

Locus	n =	Species											
		<i>Cryptomys anomalous</i>	<i>Cryptomys holosericeus</i>	<i>Cryptomys hottentotus</i>	<i>Cryptomys natalensis</i>	<i>Coetomys amatus</i>	<i>Coetomys anelli</i>	<i>Coetomys damarensis</i>	<i>Coetomys mechowii</i>	<i>Coetomys whytei</i>	<i>Bathergus janetta</i>	<i>Bathergus suillus</i>	<i>Georychus capensis</i>
Harg01	–	–	–	–	–	–	–	4	–	–	1	1	1
Harg02	4	3	5	4	–	–	–	–	–	–	–	–	–
Harg03	5	7	6	10	1	1	8	2	3	3	3	3	3
Harg07	>	>	>	>	>	>	>	>	>	>	>	>	>
Harg08	–	–	–	–	–	–	–	–	–	–	–	–	–
Harg10	–	–	–	–	–	–	–	–	–	–	–	–	–
Harg11	–	–	–	–	2	1	7	1	1	5	10	7	7
Gcap01	5	11	8	10	3	3	8	6	1	3	6	8	8
Gcap02	5	7	3	5	–	–	–	–	–	9	10	13	13
Gcap03	–	–	–	–	4	2	19	4	–	1	4	3	3
Gcap04	1	2	1	1	2	2	3	3	–	4	9	5	5
Gcap07	8	9	7	11	3	5	10	5	1	5	13	8	8
Gcap10	1	2	2	1	1	1	2	1	2	3	8	8	8
Bsuil01	1	3	1	2	2	3	5	3	7	3	10	2	2
Bsuil02	7	8	6	10	3	4	13	7	4	5	7	8	8
Bsuil04	2	1	2	3	1	3	4	5	5	4	14	8	8
Bsuil05	1	1	2	3	1	1	2	2	1	3	16	13	13
Bsuil06	10	8	5	5	–	–	–	–	–	1	12	10	10
Chott01	8	10	5	10	–	–	7	3	–	3	9	7	7
Chott03	4	9	7	8	4	4	17	7	4	6	10	7	7
Chott05	7	8	5	4	2	1	6	1	1	3	7	11	11
Chott06	6	6	6	8	1	1	11	4	4	1	1	1	1
Chott08	3	5	8	12	1	2	9	4	2	2	6	10	10
Cmech03	3	4	2	3	2	4	8	6	9	5	14	8	8
Cmech04	6	10	6	10	3	6	15	7	5	8	11	13	13
Cmech06	3	2	1	2	1	2	7	4	5	1	1	1	1
Cmech09	–	–	–	–	1	1	3	2	2	5	10	7	7
Cmech11	3	3	4	3	2	3	7	6	2	1	2	5	5
Hglab01	3	8	5	6	2	2	10	5	3	7	10	7	7
Hglab03	–	–	–	–	–	–	–	–	–	–	–	–	–
Hglab07	3	8	6	9	2	4	15	6	3	–	–	–	–
Hglab09	7	11	8	10	4	5	14	7	4	6	10	12	12
Hglab10	1	5	1	1	3	4	14	11	6	5	17	8	8
Hglab13	–	–	–	–	–	–	–	–	–	–	–	–	–

Numbers indicate the number of alleles

The highest number of alleles is highlighted green if in the focal species, blue in a congener, or red in a different genus.

– = amplification unsuccessful

+++ = multiple bands

> = fragment too large to analyze

3.2.3. *Bathyergus (Bsuil) loci*

All five loci were tested across other members of the family Bathyergidae (Table 3.7). None of the primers successfully amplified in the basal member of the family, *Heterocephalus glaber*. In *Heliophobius*, only Bsuil02 and Bsuil06 successfully amplified. These taxa are highly divergent from other members of the family at the molecular level (Ingram et al., 2004), so these results are not unexpected. In the more closely related genera, *Georychus*, *Cryptomys*, and *Coetomys*, all five markers amplified, except that Bsuil06 did not amplify in *Coetomys*. When amplification was successful, all loci were polymorphic within each genus, ranging from 2–16 alleles (Table 3.7). This new set of microsatellite markers provides a promising tool for detailed genetic studies of *Bathyergus*. The successful amplification of polymorphic loci across several species suggests their usefulness for other genetic studies.

3.2.4. *Cryptomys (Chott) loci*

Cross-species amplification was tested across 10 species representing the other five genera of Bathyergidae. Amplification success and number of alleles are listed in Table 3.7. Two loci (Chott05 and Chott06) amplified in the phylogenetically-divergent genus, *Heterocephalus*, but both were monomorphic. Three loci (Chott03, Chott05, Chott08) amplified in *Heliophobius* and showed some polymorphism with number of alleles ranging from three to five. All five loci successfully amplified across the more closely-related genera (*Bathyergus*, *Georychus*, and *Coetomys*), with number of alleles ranging from 1 to 17. Based on the success of cross-taxon amplification, these markers

will provide a promising tool for detailed studies of the genus *Cryptomys*, as well as other genera in Bathyergidae.

3.2.5. *Coetomys (Cmech) loci*

Cross-species amplification was tested across nine species representing the other five genera of Bathyergidae. Successful amplification and number of alleles are listed in Table 3.7. Only a single locus, Cmech04, amplified in the phylogenetically-divergent *Heterocephalus glaber*, and was polymorphic (3 alleles). Two loci (Cmech04, Cmech09) amplified in *Heliophobius* and showed high levels of polymorphism at locus Cmech04 with 21 alleles. All five loci successfully amplified across the more closely related genera (*Bathyergus*, *Georchus*, and *Cryptomys*), with number of alleles ranging from 1 to 15 (Table 3.7). This new suite of microsatellite loci provides a promising tool for detailed studies of the giant Zambian mole-rat, *Coetomys mechowii*, as well as other *Coetomys* species. The ability of these primers to amplify across several species suggests their potential for use in broader genetic studies across the family.

3.2.6. *Heterocephalus (Hglab) loci*

Cross-amplification of all seven *Heterocephalus* loci was tested in the other five genera of Bathyergidae (Table 3.7). In the closest member based on a recent phylogenetic study (Chapter II; Ingram et al. 2004), *Heliophobius*, five of the six primers successfully amplified with four showing polymorphism, ranging from 4-19 alleles in the samples screened. Hglab13 was the only locus that did not amplify in any of the other species tested. Hglab01, Hglab09, and Hglab10 successfully amplified across all

five genera with number of alleles ranging from one to 19. This new suite of microsatellite markers provides a promising tool for detailed studies of *Heterocephalus*, as well as providing at least 3 loci that can be applied in studies of other genera of the family Bathyergidae.

4. Conclusions

Because of the varying social structures found in Bathyergidae, with members ranging from solitary (*Heliophobius*, *Georychus*, *Bathyergus*) to social or eusocial (*Cryptomys*, *Coetomys*, *Heterocephalus*), detailed studies of each genus can provide valuable information for parameters that influence behavior changes. Genotypic data can provide insight into aspects of their biology that has not been observed, such as heterozygosity levels, levels of gene flow, and mating structure. The availability of molecular markers, such as microsatellite loci, will be invaluable to the further investigations into the breeding system of these taxa. Although the Burland et al. (2001) loci are available, the availability of species-specific primers will provide more robust markers for studies of the more basal members of the family (*Heterocephalus*, *Heliophobius*), rather than relying only on markers developed for genera that are phylogenetically-divergent that could introduce problems associated with ascertainment bias (Ellegren et al. 1995).

CHAPTER IV
CHARACTERIZING MICROSATELLITE LOCI AND THEIR PRIMER SITES
BY DIRECT SEQUENCING: MOTIF DECAY, ELECTROMORPHIC
HOMOPLASY, AND NULL ALLELES

1. Introduction

Microsatellites are regions of DNA consisting of simple sequence motifs (2 – 6 bp in length) that are repeated in tandem up to 100 times (Tautz, 1993; Zhivotovsky and Feldman, 1995). Currently, microsatellite loci are considered the marker of choice for population genetic studies (Bowcock et al., 1994; Gardner et al., 2000; Sunnucks, 2000). In addition, they have been used extensively for paternity and kinship assessment (Altet et al., 2001), forensic identification (Edwards et al., 1992), epidemiology of infectious diseases (Wang et al., 2001), and genome mapping (Causse et al., 1994; Dib et al., 1996; El Nahas et al., 2001; Su and Willems, 1996). Many microsatellite loci are characterized by moderate to high levels of polymorphism associated with the repeat region that is flanked by conserved stretches of nucleotides. These conserved flanking sequences provide specific PCR (polymerase chain reaction) priming sites that allow for the amplification of orthologous loci across individuals (usually within a species). In addition, many loci isolated from one species (the focal species) have been applied in genetic studies of related species (non-focal species), thus providing a high yield of genetic information with little start-up investment (Clisson et al., 2000; Fitzsimmons et al., 1995; Glenn et al., 1996; Jordan et al., 2002; Kim et al., 2004; Moore et al., 1991).

The use of cross-species primers assumes that a locus is evolving at the same rate and under the same mutational mechanism across different lineages, and that only changes in allele length within the motif are contributing to changes in electrophoretic migration when scored as a genotype. Nevertheless, several processes can cause violation of these assumptions. First, repeat motifs at the orthologous locus in the non-focal species can change in complexity from a simple repeat to one that is interrupted or consisting of multiple repeat motifs (Culver et al., 2001; Harr et al., 2000; Macaubas et al., 1997; Sibley et al., 2003; Synmonds and Lloyd, 2003; Zhu et al., 2000). Second, the flanking sequences adjacent to the repeat motif may experience insertion/deletion events (indels), causing either fragment sizes to be out of phase with the expected change in repeat length or mutations in phase with the repeat motif (Blankenship et al., 2002; Karhu et al., 2000; Shao et al., 2005). The latter case will result in electromorphic homoplasies. Third, mutations in either of the genotyping primer sites can result in failure to PCR amplify, either causing the locus to appear completely absent or increasing the frequency of null alleles (Pemberton et al., 1995). Finally, conservation of the primer sites can allow amplification, even in the absence of the microsatellite locus in non-focal taxa.

In this study, I have used a phylogenetic approach and reciprocal comparisons of microsatellite loci in focal and non-focal species to evaluate the processes of microsatellite evolution in a monophyletic group of African rodents (family Bathyergidae). All of these species are fossorial, and several show highly structured social systems. In addition, phylogenetic relationships and the biogeographic history of

the family are well established (Faulkes et al., 2004; Ingram et al., 2004). Several specific questions will be addressed including: 1) Do genotyping primers designed for one of six possible focal genera successfully amplify PCR products suitable for fragment analysis (genotyping in the non-focal taxa); 2) Do the levels of heterozygosity, number of alleles, and range of allele sizes observed across all taxa suggest an ascertainment bias associated with primer selection; 3) Does direct sequencing of the genotyping loci as part of larger microsatellite flanking sequences (MFS) reveal changes in the repeat motifs or indels within the genotyping fragments that contribute to estimated allele size of electromorphs; and 4) Does sequencing of the genotyping loci reveal the presence of undetected microsatellite alleles (null alleles) in taxa that fail to amplify the genotyping fragment?

2. Materials and Methods

2.1. Genomic library and primer construction

Genomic libraries and genotyping primers were constructed using the methods described in Chapter III. While designing the microsatellite primers described in Chapter III, if sufficient flanking sequence was available, additional primers lying outside of the genotyping fragment were designed to amplify larger fragments (500 – 800 bp) to allow for the sequencing of more nucleotides surrounding the repeat motif, as well as the documentation of any changes in the genotyping primer site that would lead to null alleles. For four microsatellite loci isolated from each taxon, both genotyping and microsatellite flanking sequence (MFS) primers were designed to amplify either

fragments containing primarily a microsatellite locus (ca. 100 – 450 bp) or larger fragments composed of the genotyping fragment and additional flanking sequence (ca. 500-800 bp). This strategy allowed for the assessment of changes in the microsatellite locus as well as changes in regions distal and proximal to the repeat motif. Depending on the amount of sequence available and the position of the microsatellite with respect to the original genotyping primers, flanking sequence primer sets were designed under two scenarios: 1) a single additional primer was designed to produce a 500 – 800 bp fragment when combined with one of the original genotyping primers; or 2) two new primers producing a 500 – 800 bp product bounding the original genotyping primers and the microsatellite (Fig. 4.1).

2.2. Screening of genotyping and flanking sequence primer sets

Both the original genotyping and flanking sequence primer sets for each locus were screened via PCR across representatives (same samples as Chapter III) from the six genera of Bathyergidae to determine if each locus was conserved. For the genotyping primers, if amplification of a locus was successful in a genus, then all available samples for that genus were genotyped using primers labeled with one of three fluorescent dyes: TET, FAM, or HEX on an ABI 377 automated sequencer. Genotyping parameters were the same as those described in Chapter III.

If the flanking sequence primers amplified successfully, then two representatives from each species were amplified. When possible, homozygotes (determined from genotypic analyses) were selected for sequencing. Approximately 20-100 ng of template

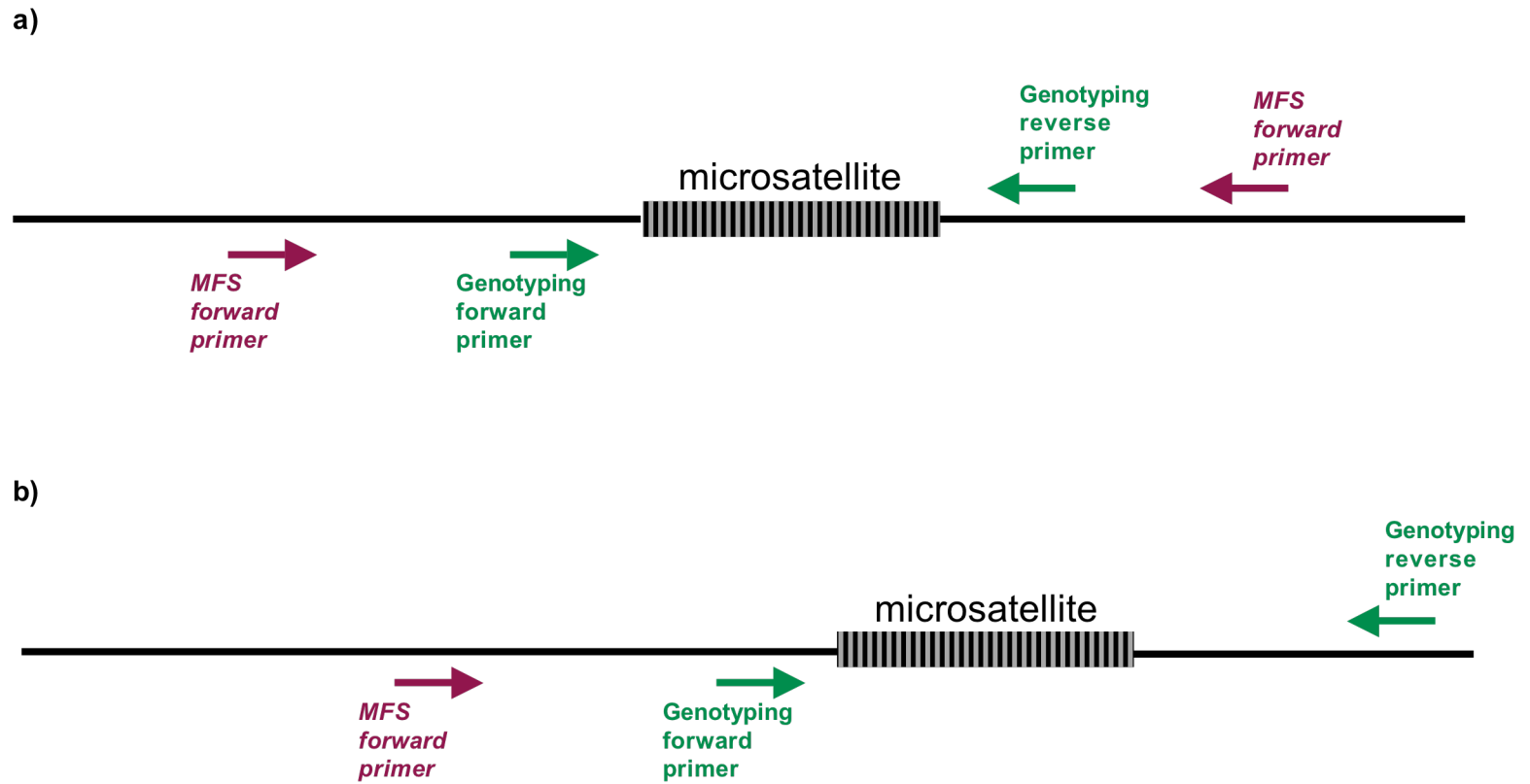


Fig. 4.1 Two scenarios of microsatellite flanking sequence (MFS) primer design. a) a single additional primer was designed to produce a 500 – 800 bp fragment when combined with one of the original genotyping primers; or b) two new primers producing a 500 – 800 bp product bounding the original genotyping primers and the microsatellite.

DNA was amplified in 50 μ L reactions containing 2.5 U of EX-*Taq* polymerase (Takara), 1X EX-*Taq* Buffer w/ MgCl₂ (Takara), 0.25 mM dNTPs (Takara), 0.1 μ M of primers. Reaction conditions included an initial 2 min denaturation at 95 °C, followed by 35 cycles of 95 °C for 30 s, 58 °C for 30 s, and 72 °C for 30 s, with a final extension time of 10 min at 72 °C. Amplification of the correct fragment length was confirmed by electrophoresis of the PCR product (5 μ l) with a size standard on 1% agarose minigels, stained with ethidium bromide, and visualized under UV light. PCR products were cleaned using QIAquick Spin PCR purification spin columns and following a standard protocol (Qiagen Inc., Valencia, CA).

Both strands of the PCR product were sequenced using the PCR primers. Each strand was sequenced at least two times for confirmation of the sequence. This was necessary since the quality of the sequence dramatically declines once the polymerase reaches the repeat region of the microsatellite. The cycle sequencing reactions, cleanup, assembly, and contig construction were identical to that described in Chapter III.

2.3. Data analyses (Characterization of loci)

2.3.1. Genotyping data

Genotyping data from GENOTYPER were imported into Microsoft Excel spreadsheets. The program CONVERT v1.31 (Glaubitz, 2004) was used to format files for POPGENE v1.31 (Yeh and Boyle, 1997) and GENEPOP (Raymond and Rousset, 1995). Both POPGENE and GENEPOP were used to calculate summary statistics for each species, such as the number of alleles and observed and expected heterozygosities

for each locus. The Wilcoxon Signed-Ranks test was used to test for the presence of an ascertainment bias in marker selection on the following characteristics of the microsatellite loci: 1) longest (genotyping fragment) allele; 2) highest number of alleles per genus; and 3) largest range of alleles. To calculate the range of alleles (integer value between the highest and lowest allele size), the step-wise mutation model (SMM) was applied. Under SMM, it is assumed that with adequate sampling, all possible alleles between the highest and lowest would be recovered in a given taxon (Kimura and Ohta, 1978; Valdes et al., 1993).

2.3.2. Sequencing data

Sequences were initially aligned using SEQUENCHER to establish a baseline alignment and confirm sequence homology. After a working alignment was built in SEQUENCHER, the file was imported into MacClade v3.02 (Maddison and Maddison, 2002). Fine-tuning of the alignments was performed visually using the plain molecular data matrix setting in MacClade. All internal genotyping primers for each locus were included in the alignment to identify any changes at the primer site. The boundaries of the repeat region at each locus were determined using RepeatMasker. The masked sequences were added to the alignments to delimit the range of the repeat region across all taxa. Gaps were added throughout alignments to account for unique indels, as well as any trackable changes in the repeat motif of each microsatellite locus.

Table 4.1 Observed and expected heterozygosities (obs/exp) calculated using data from microsatellite loci designed from *Heliophobius argenteocinereus* (Harg), *Georychus capensis* (Gcap), *Bathergus suillus* (Bsuil), *Cryptomys hottentotus* (Chott), *Coetomys mechowii* (Cmech), and *Heterocephalus glaber* (Hglab).

Locus	n =	Species												
		<i>Cryptomys anomalus</i>	<i>Cryptomys holosericeus</i>	<i>Cryptomys hottentotus</i>	<i>Cryptomys natalensis</i>	<i>Coetomys amatus</i>	<i>Coetomys anelli</i>	<i>Coetomys damarensis</i>	<i>Coetomys mechowii</i>	<i>Coetomys whytei</i>	<i>Bathergus janetta</i>	<i>Bathergus suillus</i>	<i>Georychus capensis</i>	<i>Heliophobius argenteocinereus</i>
Harg01	-	-	-	-	-	-	0.000/0.616	-	-	0.000/0.000	0.000/0.000	0.000/0.000	0.064 /0.560	-
Harg02	0.333/0.867	0.400/0.542	0.333/0.803	0.385/0.760	-	-	-	-	-	-	-	-	0.125/0.530	-
Harg03	0.556/0.758	0.400/0.830	0.333/0.819	0.565/0.880	0.000/0.000	0.000/0.000	0.077/0.341	0.000/0.356	0.250/0.679	0.125/0.425	0.065/0.180	0.039/0.527	0.214/0.576	-
Harg07	-	-	-	-	-	-	-	-	-	-	-	-	0.078/0.571	-
Harg08	-	-	-	-	-	-	-	-	-	-	-	-	0.667/0.890	-
Harg10	-	-	-	-	-	-	-	-	-	-	-	-	0.141/0.628	-
Harg11	-	-	-	-	0.000/0.667	0.000/0.000	0.103/0.228	0.000/0.000	0.000/0.000	0.600/0.867	0.857/0.884	0.286/0.729	0.600/0.822	-
Gcap01	0.091/0.836	0.737/0.866	0.846/0.862	0.600/0.833	1.000/0.833	0.500/0.833	0.717/0.768	0.833/0.849	0.000/0.000	0.167/0.591	0.500/0.683	0.440/0.716	0.263/0.711	-
Gcap02	0.100/0.668	0.105/0.731	0.000/0.303	0.050/0.519	-	-	-	-	-	0.750/0.933	0.689/0.780	0.708/0.838	0.212/0.279	-
Gcap03	-	-	-	-	1.000/1.000	0.000/0.5333	0.2414/0.9238	0.1667/0.5606	-	0.000/0.000	0.1053/0.3242	0.000/0.667	0.500/0.929	-
Gcap04	0.000/0.000	0.000/0.102	0.000/0.000	0.000/0.000	0.500/0.500	0.500/0.500	0.150/0.504	0.500/0.714	-	0.222/0.634	0.476/0.757	0.250/0.665	0.000/0.000	-
Gcap07	0.818/0.871	0.647/0.829	0.539/0.723	0.920/0.885	1.000/0.833	0.400/0.844	0.519/0.778	1.000/0.844	0.000/0.000	0.333/0.667	0.691/0.884	0.556/0.713	0.441/0.774	-
Gcap10	0.000/0.000	0.000/0.226	0.091/0.091	0.000/0.000	0.000/0.000	0.000/0.000	0.0233/0.0233	0.000/0.000	0.000/0.005	0.333/0.733	0.650/0.818	0.593/0.827	0.125/0.148	-
Bsuil01	0.000/0.000	0.167/0.652	0.000/0.000	0.000/0.667	0.000/0.6667	0.5000/0.8333	0.000/0.2503	0.2500/0.6071	0.3333/0.8788	0.0909/0.6450	0.404/0.827	0.000/0.073	-	-
Bsuil02	0.818/0.719	0.778/0.862	0.786/0.818	0.333/0.855	0.5000/0.8383	0.8000/0.7333	0.8400/0.8416	0.7143/0.8571	0.6667/0.8000	0.3000/0.7947	0.4222/0.6799	0.296/0.791	0.543/0.733	-
Bsuil04	1.000/0.571	0.091/0.091	0.000/0.303	0.000/0.394	0.000/0.000	0.7500/0.6786	0.5500/0.5231	0.5000/0.7737	0.3333/0.5758	0.3333/0.8667	0.8378/0.8715	0.625/0.768	-	-
Bsuil05	0.000/0.000	0.000/0.000	0.000/0.159	0.000/0.603	0.000/0.000	0.000/0.000	0.000/0.1313	0.000/0.3030	0.000/0.000	0.4286/0.6484	0.7872/0.9234	0.440/0.886	-	-
Bsuil06	0.778/0.915	0.474/0.834	0.071/0.569	0.087/0.570	-	-	-	-	-	0.000/0.000	0.5581/0.8733	0.400/0.806	0.327/0.680	0.099/0.627
Chott01	0.778/0.895	0.632/0.873	0.500/0.725	0.474/0.845	-	-	0.5333/0.8414	0.500/0.8333	-	0.2000/0.6158	0.5909/0.7239	0.600/0.804	-	-
Chott03	0.546/0.541	0.556/0.832	0.615/0.825	0.792/0.858	1.000/1.000	0.4000/0.7778	0.4902/0.7119	0.6000/0.8158	0.5000/0.7857	0.5455/0.7922	0.7083/0.8428	0.296/0.732	0.119/0.214	-
Chott05	0.750/0.858	0.375/0.925	0.571/0.593	0.250/0.767	1.000/1.000	0.000/0.000	0.0588/0.4394	0.000/0.000	0.000/0.000	0.000/0.7033	0.333/0.836	0.269/0.783	0.455/0.740	0.000/0.000
Chott06	0.444/0.824	0.833/0.802	0.385/0.812	0.625/0.780	0.000/0.000	0.000/0.000	0.1667/0.5316	0.1111/0.6078	0.000/0.000	0.000/0.000	0.000/0.000	0.000/0.000	-	0.000/0.000
Chott08	0.000/0.554	0.222/0.611	0.692/0.843	0.478/0.867	0.000/0.000	0.000/0.3556	0.0816/0.4761	0.000/0.000	0.000/0.5714	0.000/0.5000	0.234/0.782	0.200/0.695	0.048/0.300	-
Cmech03	0.364/0.329	0.235/0.480	0.077/0.077	0.000/0.581	0.000/0.667	0.800/0.733	0.265/0.650	0.750/0.817	0.833/0.955	0.250/0.708	0.354/0.767	0.536/0.809	-	-
Cmech04	0.556/0.745	0.813/0.885	0.357/0.839	0.462/0.870	0.500/0.833	1.000/0.927	0.898/0.924	0.571/0.901	1.000/0.933	0.546/0.883	0.651/0.858	0.692/0.855	0.541/0.874	0.000/0.153
Cmech06	0.000/0.329	0.000/0.314	0.000/0.000	0.000/0.075	0.000/0.000	0.7500/0.5357	0.3846/0.7431	0.2222/0.6340	0.2500/0.8929	0.000/0.000	0.000/0.000	0.000/0.000	-	-
Cmech09	-	-	-	-	0.000/0.000	0.000/0.000	0.026/0.169	0.333/0.546	0.000/0.667	0.333/0.778	0.488/0.818	0.259/0.638	0.000/0.589	-
Cmech11	0.091/0.255	0.053/0.323	0.000/0.381	0.074/0.419	1.000/1.000	0.200/0.733	0.212/0.770	0.500/0.842	0.000/0.667	0.000/0.000	0.023/0.023	0.000/0.733	-	-
Hglab01	0.778/0.601	0.556/0.832	0.583/0.696	0.130/0.593	0.500/0.500	0.600/0.556	0.367/0.661	0.571/0.813	0.500/0.833	0.444/0.837	0.435/0.773	0.304/0.767	0.245/0.636	0.020/0.204
Hglab03	-	-	-	-	-	-	-	-	-	-	-	-	0.000/0.487	0.270/0.771
Hglab07	0.400/0.574	0.625/0.800	0.636/0.788	0.652/0.877	1.000/0.667	0.400/0.800	0.727/0.885	0.800/0.911	0.333/0.600	-	-	-	0.406/0.649	0.165/0.238
Hglab09	0.700/0.837	0.389/0.891	0.417/0.830	0.625/0.853	1.000/1.000	0.600/0.844	0.730/0.911	0.625/0.883	0.333/0.867	0.556/0.804	0.667/0.811	0.567/0.841	0.660/0.859	0.281/0.623
Hglab10	0.0000/0.000	0.091/0.533	0.000/0.000	0.000/0.000	0.500/0.833	0.400/0.822	0.479/0.811	0.300/0.942	0.500/0.929	0.500/0.833	0.714/0.921	0.625/0.813	0.000/0.000	0.317/0.550
Hglab13	-	-	-	-	-	-	-	-	-	-	-	-	-	0.263/0.715

- = no successful amplification

Table 4.2 Range of alleles observed at microsatellite loci designed from *Heliophobius argenteocinereus* (Harg), *Georychus capensis* (Gcap), *Bathergus suillus* (Bsuil), *Cryptomys hottentotus* (Chott), *Coetomys mechowii* (Cmech), and *Heterocephalus glaber* (Hglab).

Locus	n =	Species												
		<i>Cryptomys anomalus</i>	<i>Cryptomys holosericeus</i>	<i>Cryptomys hottentotus</i>	<i>Cryptomys natalensis</i>	<i>Coetomys amatus</i>	<i>Coetomys anelli</i>	<i>Coetomys damarensis</i>	<i>Coetomys mechowii</i>	<i>Coetomys whytei</i>	<i>Bathergus janetta</i>	<i>Bathergus suillus</i>	<i>Georychus capensis</i>	<i>Heliophobius argenteocinereus</i>
Harg01		–	–	–	–	–	–	149–237	–	–	259	259	177	216–222
Harg02		308–338	305–335	308–335	308–335	–	–	–	–	–	–	–	–	317–323
Harg03		256–264	246–260	250–268	246–274	248	248	248–280	248–250	244–250	244–252	248–256	250–252	258–296
Harg07		–	–	–	–	–	–	–	–	–	–	–	–	143–175
Harg08		–	–	–	–	–	–	–	–	–	–	–	–	298–322
Harg10		–	–	–	–	–	–	–	–	–	–	–	–	177–195
Harg11		–	–	–	–	324–326	338	332–368	390	338	322–332	312–336	362–372	334–346
Gcap01		119–135	111–133	117–141	107–135	123–127	127–133	121–141	117–127	131	99–117	113–123	113–125	117–135
Gcap02		278–308	266–318	278–302	278–320	–	–	–	–	–	274–304	290–310	286–324	244–316
Gcap03		–	–	–	–	258–268	238–248	244–340	252–316	–	268	254–290	284–288	366–384
Gcap04		157	143–157	157	157	241–245	237–239	221–239	225–229	–	147–169	153–175	161–173	157
Gcap07		224–242	226–244	230–248	230–250	238–248	232–248	230–252	226–236	246	204–242	224–260	216–246	238–266
Gcap10		141	127–141	141–143	141	141	141	125–141	141	127–141	153–157	151–165	161–177	141–179
Bsuil01		182	182–250	182	182–206	214–222	216–224	182–216	194–214	204–221	192–204	194–216	206–214	–
Bsuil02		145–161	143–161	147–159	131–163	149–157	147–157	135–163	137–155	147–151	123–135	127–141	129–145	135–151
Bsuil04		311–313	311	311–313	309–313	307	299–307	299–307	297–305	299–307	317–343	321–353	315–347	–
Bsuil05		338	338	322–334	322–338	338	338	322–338	334–338	338	362–366	360–396	362–406	–
Bsuil06		234–272	242–290	234–314	234–264	–	–	–	–	–	242	238–266	240–262	246–280
Chott01		263–291	263–293	271–287	271–291	–	–	277–293	285–289	–	257–263	247–271	267–281	–
Chott03		182–208	156–238	198–214	180–212	154–160	138–168	154–204	160–208	156–170	142–154	134–154	146–174	154–158
Chott05		283–307	273–301	283–303	285–301	287–293	273	271–285	279	295	257–287	285–315	255–309	207–255
Chott06		245–265	247–273	243–273	259–275	251	253	243–273	243–253	245–251	239	239	239	–
Chott08		113–123	115–159	115–147	115–155	115	115–119	111–181	111–123	111–115	121–123	113–123	121–223	115–125
Cmech03		262–266	260–288	266–270	264–270	300–304	284–290	264–294	278–294	284–306	276–298	272–306	290–314	–
Cmech04		368–384	350–390	370–382	368–394	372–386	376–390	354–396	370–390	370–390	364–384	368–392	362–394	400–476
Cmech06		140–145	142–145	145	142–145	148	160–163	142–169	148–169	139–163	139	139	136	–
Cmech09		–	–	–	–	310	310	306–312	310–314	308–310	296–312	296–316	296–308	302–306
Cmech11		126–132	128–144	128–136	132–136	152–156	146–150	132–150	140–154	142–162	116	116	120–188	–
Hglab01		219–223	213–243	221–229	219–243	241–245	237–239	221–243	225–239	221–233	211–241	229–249	223–237	231–257
Hglab03		–	–	–	–	–	–	–	–	–	–	–	–	291–313
Hglab07		167–181	165–181	175–187	165–185	187–191	179–193	161–197	167–183	173–177	–	–	–	177–195
Hglab09		180–200	176–202	180–196	182–198	190–198	192–202	170–204	170–194	178–192	170–200	176–208	162–204	170–210
Hglab10		292	280–330	292	292	318–330	324–334	290–332	290–332	310–326	396–306	302–346	300–322	296
Hglab13		–	–	–	–	–	–	–	–	–	–	–	–	–

– = no successful amplification

3. Results

3.1. Genotyping

The number of alleles, range of allele size, and observed and expected heterozygosities for each locus are shown in Tables 3.7, 4.1 – 4.2. Since values of observed and expected heterozygosity were calculated from pooled populations within each species, the reduced levels of observed heterozygosity may be the result of admixture (Wahlund effect). In order to make comparisons across species/genera for each microsatellite locus, I used the number and range of electromorphic alleles as assessments of genetic variability.

3.1.1. *Heliophobius* (Harg) loci

For *Heliophobius*, seven microsatellite loci were characterized. Four of the seven genotyping loci were successful in amplifying taxa other than the focal species. No *Heliophobius* (Harg) genotyping primers amplified in *Heterocephalus glaber*, the basal member of the family.

Harg01 had low variation and little success in amplification. *Coetomys damarensis* had a higher number of alleles than the focal taxon, but consisted of only homozygotes. Harg02 amplified only in *Heliophobius* and *Cryptomys*. The amount of variation across *Cryptomys* was greater than observed in *Heliophobius*, which had only three alleles. Harg03 amplified in all genera, except *Heterocephalus*. The highest number of alleles was found in *Heliophobius* (13 alleles). Although Harg07 amplified in *Georchus*, *Bathyergus*, *Cryptomys*, and *Coetomys*, the fragment was too large (> 450

bp) to run as a genotype fragment (Table 3.7). Locus Harg08 and Harg10 successfully amplified only in *Heliophobius*. The most variable loci in *Heliophobius* were Harg03 and Harg08, both with 13 alleles. Hatg08 is the only *Heliophobius* locus that consists of a complex repeat (GT/GC). Harg11 amplified in all taxa, except *Heterocephalus* and *Cryptomys*. The variability was highest in *Bathyergus suillus* with 10 alleles and *Coetomys* showed a moderate amount of variation, with 1 – 7 alleles.

3.1.2. *Georychus* (Gcap) loci

For *Georychus*, six microsatellite loci were characterized. All *Georychus* loci consisted of simple GT dinucleotide repeats, except the trinucleotide repeat (GTT) found at the Gcap04 locus. The most basal member of the family, *Heterocephalus*, amplified only with the Gcap10 primer set. Although five of the six loci amplified across species of *Coetomys*, no samples of *C. whytei* (six individuals) amplified for any of the six *Georychus* loci.

For Gcap01, the number of alleles ranged from 3 – 11 alleles. The highest number of alleles (11) was observed in *Cryptomys holosericeus*. Genotyping Gcap02 was unsuccessful in *Heterocephalus* and all species of *Coetomys*. The number of alleles ranged from 3 (*C. hottentotus*) to 13 (*G. capensis*). Gcap03 amplified in *Heliophobius*, *Georychus*, *Bathyergus*, and all species of *Coetomys*, except *C. whytei*. The number of alleles ranged from one (*B. janetta*) to 19 (*C. damarensis*). Higher polymorphism and variability was documented in a non-focal genus, *Coetomys*. Gcap04 amplified in all species except for *H. glaber* and *C. whytei*. In *G. capensis* and both species of

Bathyergus, the polymorphism and variability were relatively high with the number of alleles ranging from 4 – 9. In *Cryptomys* and *Coetomys*, the variation was substantially lower with the number of alleles ranging from 1 – 3. For *Cryptomys*, no heterozygotes were observed. Gcap07 was consistently polymorphic across all species that it successfully amplified. The number of alleles ranged from 3 – 13 (mean number of alleles = 8) with *G. capensis* having the mean number of alleles. *B. suillus* and *H. argenteocinereus* shared the highest number of alleles. For Gcap10, the amount of polymorphism was skewed across the six genera. For *Heliophobius*, *Georchus*, and *Bathyergus*, the number of alleles ranged from 3 – 8 alleles. In *Cryptomys* and *Coetomys*, the number of alleles was much lower (1 – 2). Gcap10 was the only *Georchus* microsatellite locus to amplify *Heterocephalus*. The highest number of alleles was found in *Heterocephalus*, *G. capensis* and *B. suillus*.

3.1.3. *Bathyergus* (Bsuil) loci

For *Bathyergus*, five microsatellite loci were characterized. All Bsuil loci consisted of simple GT dinucleotide repeats, except Bsuil05 which consisted of a complex GT/GA dinucleotide repeat. None of the *Bathyergus* genotyping primers successfully amplified the basal member of the family, *Heterocephalus glaber*. Only two loci, Bsuil02 and Bsuil06, amplified in *Heliophobius*. All *Bathyergus* loci amplified in *Bathyergus*, *Georchus*, *Cryptomys*, and *Coetomys*, except Bsuil06 that did not amplify any species of *Coetomys*.

In Bsuil01, the number of alleles ranged from 1 to 10. The highest number of alleles was documented in the focal taxon, *B. suillus*. The number of alleles was much lower (3 alleles) in the sister species, *B. janetta*. In *G. capensis*, there were 2 alleles but no heterozygotes were observed. This locus was monomorphic in three of the four species of *Cryptomys*. Variation at this locus was inconsistent across the five species of *Coetomys*, with the number of alleles ranging from 2 to 7. Bsuil02 was the most variable *Bathyergus* locus. The number of alleles observed across the species sampled was 3 – 13 (mean number of alleles = 7). The level of variation seen in the four species of *Cryptomys* was relatively high with the number of alleles ranging from 6 to 10. The highest amount of polymorphism and variation was observed in the genus *Coetomys* with the number of alleles ranging from 3 to 13. *C. damarensis* had the highest number of alleles, while *B. suillus* showed the average number of alleles.

In the species for which Bsuil04 could be amplified, the number of alleles ranged from 1 to 14. The focal taxon, *B. suillus*, showed the highest number of alleles, but *B. janetta* had only 4 alleles. In the four species of *Cryptomys*, the number of alleles was low, ranging from 1 to 3. No heterozygotes were observed in three of the four species (*C. holosericeus*, *C. hottentotus*, and *C. natalensis*). In contrast, all individuals of *C. anomalus* were heterozygous at this locus.

For Bsuil05, the number of alleles ranged from 1 to 16. Most of the variation was observed in the focal taxon, *B. suillus*, and its closest relatives. The number of alleles (16) was highest in *B. suillus*, *G. capensis* had 13 alleles, and *B. janetta* again showed little variation with only 3 alleles. For both *Cryptomys* and *Coetomys*, there was

little variation at this locus. The number of alleles ranged from 1 to 3 and all individuals were homozygous. Bsuil06 did not amplify in either *Coetomys* or *Heterocephalus*. The number of alleles ranged from 1 to 13 (mean = 8), in the taxa in which it did amplify, *Heliophobius* had the most alleles, *B. suillus* had 12 alleles, and *B. janetta* was monomorphic at this locus. For *G. capensis*, the variation at this locus was high with 10 alleles.

3.1.4. *Cryptomys* (Chott) loci

For *Cryptomys*, five microsatellite loci were characterized. Three of the *Cryptomys* loci, Chott01, Chott06 and Chott08, were simple dinucleotide (GT) repeats, while the other two loci, Chott03 and Chott05, consisted of complex dinucleotide repeats. Only one genotyping locus, Chott05, successfully amplified all species sampled. At Chott01, amplification was not successful in *Heterocephalus*, *Heliophobius*, *Coetomys amatus*, *C. anelli*, or *C. whytei*. In the other taxa, number of alleles ranged from 3 to 10 (mean number of alleles = 7). Within the genus *Cryptomys*, the number of alleles ranged from 5 to 10. The highest number of alleles was observed in *C. holosericeus* and *C. natalensis*. Among *Coetomys*, Chott01 amplified only in *C. damarensis* and *C. mechowii* with 3 and 7 alleles, respectively.

Chott03 amplified in all species, except *H. glaber*. Across the five genera sampled, the number of alleles ranged from 3 to 17 (mean = 7). The highest amount of variation at this locus was not found in the focal species or its congeners. Within the focal genus, number of alleles ranged from 4 to 9. Across the five species of *Coetomys*,

number of alleles ranged from 4 to 17 with the highest number of alleles found in *Coetomys damarensis* (Table 3.7).

At Chott05, the number of alleles ranged from 1 to 11 (mean = 4). In *Heterocephalus*, Chott05 was monomorphic. The highest number of alleles was observed in *Georychus*. In *Cryptomys*, the number of alleles ranged from 4 – 7. Across the five species of *Coetomys*, the number of alleles ranged from 1 – 6. *Coetomys anseli*, *C. mechowii*, and *C. whytei* were all monomorphic, while both *C. amatus* individuals were heterozygotes.

Chott06 amplified in all species except *Heliophobius*. The number of alleles across all species sampled ranged from 1 – 11 (mean = 4). Chott06 was monomorphic in *Heterocephalus*, *Georychus*, both species of *Bathyergus*, and three species of *Coetomys* (*C. amatus*, *C. anseli*, and *C. whytei*). Within *Cryptomys*, the number of alleles ranged from 6 – 8. Across the five species of *Coetomys* sampled, the number of alleles ranged from 1 – 11. The highest number of alleles was not observed in the focal taxon, *Cryptomys hottentotus*, but in *Coetomys damarensis*. Chott08 amplified successfully in all species, except for *Heterocephalus glaber*. The number of alleles observed at this locus ranged from 1 - 12 (mean = 5). The highest number of alleles was observed in the congener, *C. natalensis*.

3.1.5. *Coetomys (Cmech) loci*

For *Coetomys*, five microsatellite loci were characterized. Four of the *Coetomys* genotyping loci, Cmech03, Cmech04, Cmech09 and Cmech11 consisted of simple

dinucleotide (GT) repeats and one locus, Cmech06, contained a complex trinucleotide (GTT/GCA) repeat. Only one locus, Cmech04, amplified across all species of bathyergids (Table 3.7). Two loci, Cmech04 and Cmech09, successfully amplified in *Heliophobius*, and all Cmech loci amplified in *Georychus*, *Bathyergus*, *Cryptomys*, and *Coetomys*, except Cmech09 that did not amplify in any species of *Cryptomys*. For the taxa that amplified Cmech03, number of alleles ranged from 2 – 14 (mean = 6). The number of alleles was substantially different (5 vs. 14) between the two species of *Bathyergus*. The highest number of alleles was found in *B. suillus* rather than the focal species. Cmech04 was the only *Coetomys* locus that could be amplified in all species. The number of alleles across all species ranged from 3 – 21 (mean = 9). In *Heterocephalus*, 3 alleles were identified and all individuals were homozygous. *Heliophobius* had the highest number of alleles. Neither polymorphism nor genetic variation was highest in the focal taxon, *C. mechowii*, as expected. *Heliophobius* was the most polymorphic with 21 alleles (Table 3.7).

The number of alleles at Cmech06 ranged from 1 – 7 (mean = 3). This locus was monomorphic in *Georychus capensis*, both species of *Bathyergus*, *Cryptomys hottentotus*, and *Coetomys amatus*. In the other three species of *Cryptomys* (*C. anomalus*, *C. holosericeus*, and *C. natalensis*), the number of alleles ranged from 2 to 3 alleles and all individuals were homozygous. With the exception of *C. amatus*, the number of alleles within *Coetomys* ranged from 2 to 7. The highest number of alleles was observed in *C. damarensis*.

Cmech09 did not amplify in *Heterocephalus glaber* or any species of *Cryptomys*. Across the species that amplified this locus, number of alleles ranged from 1 – 10 (mean = 4). In *Heliophobius*, 3 alleles were observed, but no heterozygotes. Within the genus *Coetomys*, two species (*C. amatus* and *C. anelli*) were monomorphic. Among the other three species, the number of alleles ranged from 2 – 3. At locus Cmech11, amplification was successful in all species, except *Heterocephalus* and *Heliophobius*. Across the taxa that amplified, number of alleles ranged from 1 – 7 (mean = 3). In *Georychus*, there were 5 alleles, but all individuals sampled were homozygous. The largest number of alleles was observed in *C. damarensis*.

3.1.6. *Heterocephalus (Hglab) loci*

For *Heterocephalus*, six microsatellite loci were characterized. Three of the Hglab genotyping loci (Hglab09, Hglab10, and Hglab13) consisted of simple dinucleotide (GT) repeats, Hglab01 contained a trinucleotide (GTT) repeat, and Hglab03 and Hglab07 both contained complex repeats. Three of the loci amplified in all species. Hglab13 amplified only in the focal species.

Across all species sampled, the number of alleles in Hglab01 ranged from 2 – 10 (mean = 6). In the focal taxon, the amount of variation at this locus was markedly low with 5 alleles. The highest polymorphism (number of alleles = 8) was seen in *C. damarensis*. Hglab03 only amplified in *Heterocephalus* and *Heliophobius*. In *Heliophobius*, there were 4 alleles, but all individuals were homozygous, while *Heterocephalus* had 15 alleles.

Three species did not successfully amplify with the Hglab07 genotyping primers (*B. janetta*, *B. suillus*, and *G. capensis*). Across the species that did amplify, the number of alleles ranged from 2 –15 (mean = 6). *Heterocephalus* had the average number of alleles (6), while *C. damarensis* had the highest (15 alleles). All species successfully amplified with the Hglab09 genotyping primers. Among all species sampled, number of alleles ranged from 4 to 19 (mean = 9). *Heliophobius* showed the highest variation at this locus. In the focal species, variation at this locus was again low with 5 alleles.

The number of alleles at Hglab10 ranged from 1 – 17 (mean = 6). *Heliophobius*, *C. anomalus*, *C. hottentotus*, and *C. natalensis* were monomorphic. The amount of variation in *Cryptomys spp.* was markedly low. *C. holosericeus*, the only species that showed polymorphism at this loci, had 5 alleles. The focal species had 8 alleles, and *B. suillus* had the highest number of alleles. Hglab13 only amplified in *Heterocephalus* with seven alleles. Although this locus was specific for the focal taxon, suggesting an ascertainment bias, when an Hglab locus could be amplified in the other bathyergid taxa, variation was always higher in a non-focal species.

3.1.7. Ascertainment bias

For each microsatellite panel, the number of loci with the longest alleles, highest number of alleles, and range of alleles for focal and non-focal taxa are shown in Table 4.3. If the largest allele, number of alleles, or range of alleles was observed in a congener it was still treated as being observed in the focal taxon, thereby possibly inflating an ascertainment bias. Nevertheless, no ascertainment bias was detected in any

of the three comparisons ($p = 0.562$, 0.438 , and 0.375 , respectively). A one-tail test comparing the range of alleles between the focal and non-focal taxa with the largest range at each locus found a significant difference between the two groups ($p = 0.027$). However, rather than supporting an ascertainment bias, the larger range was observed in a non-focal taxon.

3.2. Characterization of the microsatellite motifs and their immediate flanking sequences

Microsatellite flanking sequence (MFS) data was recovered for 16 of the 34 microsatellite loci. Information, including repeat motif, changes in primer sites, indels, and additional repetitive elements, is shown in Tables 4.4 – 4.19 for each individual sequenced. The repeat motif, genotyping fragment length, and genotyping success of each locus were plotted on the Bathyergidae phylogeny modified from Ingram et al., 2004 (Figs. 4.2 – 4.17). Due to potential errors in allele size based on the fragment analysis, the genotyping fragment lengths were calculated from the MFS data.

3.2.1. Heliophobius (Harg) loci

Three *Heliophobius* loci (Harg02, Harg03, and Harg07) were sequenced. Representatives of *Heliophobius*, *Bathyergus*, *Cryptomys*, and *Coetomys* were successfully sequenced for the Harg02 MFS locus (Table 4.4). In all individuals, the repeat motif was a perfect trinucleotide (GTT) repeat. In the immediate flanking sequence, there were seven regions identified that contributed to variation in the fragment size of the genotyping product. Four of these regions varied only between

Table 4.3 Comparison of number of loci with the longest alleles, number of loci with the highest number of alleles, and range of alleles for focal and non-focal taxa for each microsatellite panel. *P*-values for the Wilcoxon Signed-Ranks test is shown for each comparison.

a)	Number of loci with largest allele observed in		b)	Number of loci with highest number of alleles observed in		c)	Number of loci with largest range of alleles observed in	
	focal species	non focal		focal species	non focal		focal species	non focal
<i>Heterocephalus</i>	2	4	<i>Heterocephalus</i>	2	4	<i>Heterocephalus</i>	3	3
<i>Heliophobius</i>	5	2	<i>Heliophobius</i>	3	5	<i>Heliophobius</i>	5	2
<i>Bathyergus</i>	1	4	<i>Bathyergus</i>	2	4	<i>Bathyergus</i>	3	3
<i>Georychus</i>	1	5	<i>Georychus</i>	1	5	<i>Georychus</i>	0	6
<i>Cryptomys</i>	3	2	<i>Cryptomys</i>	4	1	<i>Cryptomys</i>	2	5
<i>Coetomys</i>	3	2	<i>Coetomys</i>	3	2	<i>Coetomys</i>	1	4

W+ = 7.50, W- = 13.50, N = 6, p <= 0.5625

W+ = 6, W- = 15, N = 6, p <= 0.4375

W+ = 2, W- = 8, N = 4, p <= 0.375

Table 4.4 Observed sequence length, repeat motif, indels, additional repetitive regions, and changes in the primer sites for locus Harg02. Expansions within a SINE element are included with other indels documented at this locus.

Taxa	Sample	GENOTYPE			Repeat motifs Target region	Indels		Expansion		Changes in primer site Harg02-F		
		Fragment length	Observed Seq length			A	TTT	T/A	w/in Sine	A	G	CAGGA (C) _n
<i>H. argenteocinereus</i>	H046	323	325	(GTT) ₇	X	X	13	-GG---	-	X	CAGGA (C) ₆	*****
<i>H. argenteocinereus</i>	H050	323	324	(GTT) ₇	X	X	13	-GG---	-	X	CAGGA (C) ₆	*****
<i>H. argenteocinereus</i>	HA24	320	322	(GTT) ₆	X	X	13	-GG---	-	X	CAGGA (C) ₆	*****
<i>B. suillus</i>	BS	NA	320	(GTT) ₃	-	X	11	-GG---	-	X	CAGGA (C) ₆	*****A****
<i>B. suillus</i>	BJ	NA	320	(GTT) ₃	-	X	11	-GG---	-	X	CAGGA (C) ₆	*****A****
<i>B. suillus</i>	N8	NA	320	(GTT) ₃	-	X	11	-GG---	-	X	CAGGA (C) ₆	*****A****
<i>C. hottentotus</i>	MCA324	NA	308	(GTT) ₆	X	-	12	AGG---	X	-	-	*****A****
<i>C. hottentotus</i>	TM38375	NA	315	(GTT) ₇	X	-	12	AGG---	X	-	-	*****A****
<i>C. holosericeus</i>	SP7552	305	308	(GTT) ₆	X	-	12	AGG---	X	-	-	*****A****
<i>C. natalensis</i>	CHN2	308	309	(GTT) ₅	X	X	12	AGG---	X	X	-	*****A****
<i>C. anaomalus</i>	SP7705	323/326	318	(GTT) ₁₀	X	X	12	AGG---	X	X	-	*****A****
<i>C. mechowii</i>	M71	NA	295	(GTT) ₂	X	X	13	GGGG--	-	X	-	*****A**G*
<i>C. kafuensis</i>	Z10	NA	295	(GTT) ₂	X	X	13	GGGG--	-	X	-	*****A**G*
<i>C. damarensis</i>	HW3084	NA	295	(GTT) ₂	X	X	13	GGGG--	-	X	-	*****A**G*
<i>C. 'Sekute'</i>	SEK	NA	295	(GTT) ₂	X	X	13	GGGG--	-	X	-	*****A**G*
<i>C. anelli</i>	Z4	NA	295	(GTT) ₂	X	X	13	GGGG--	-	X	-	*****A**G*
<i>C. amatus</i>	AMATUS1	NA	297	(GTT) ₂	X	X	13	GGGGGG	-	X	-	*****A**G*

NA - no amplification

* X denotes presence of sequence, - denotes absence

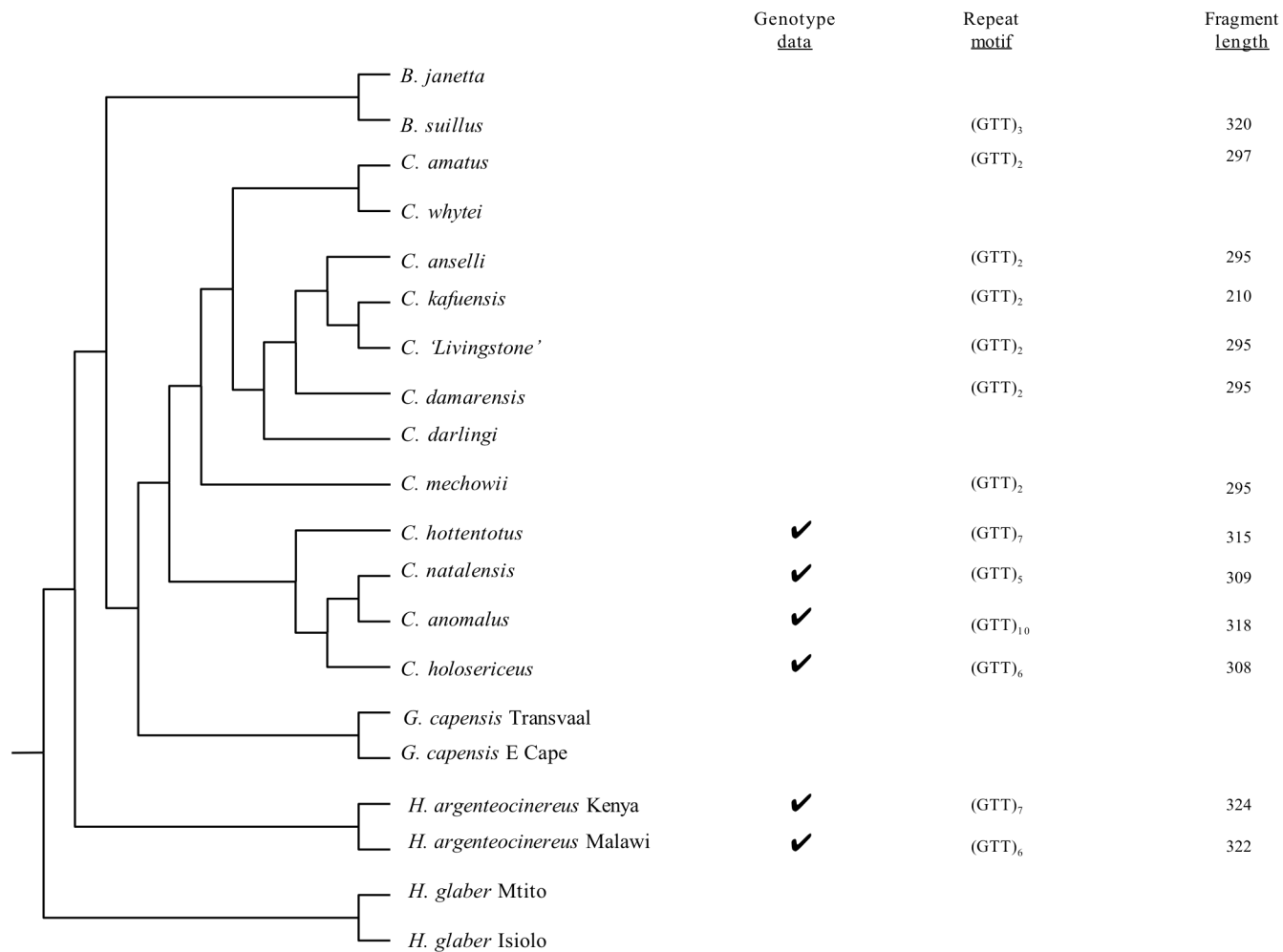


Fig. 4. 2 Microsatellite repeat motif of Harg02 plotted on the phylogeny based on Ingram et al. 2004. ✓ indicates successful genotyping amplification. Fragment length was determined from sequencing product size. For species with multiple samples, a representative was selected. Absence of a repeat motif indicates that no sequence data is available and does not suggest information about the repeat region itself.

Table 4.5 Observed sequence length, repeat motif, and indels documented for locus Harg03. No genotyping primer sites were available.

Taxa	Sample	GENOTYPE		Repeat motifs Target region	Indels		
		Fragment length	Observed Seq length		T	AC	TGGG
<i>H.argenteocinereus</i>	H046	258	259	(GT) ₁₀ GC (GT) ₃	X	-	X
<i>H.argenteocinereus</i>	H050	258	259	(GT) ₁₀ GC (GT) ₃	X	-	X
<i>B.suillus</i>	BS	252	252	(GT) ₃ AT (GT) ₅	X	X	X
<i>B.suillus</i>	TM41494	252	252	(GT) ₃ AT (GT) ₅	X	X	X
<i>G.capensis</i>	TM38354	252	251	(GT) ₃ AT (GT) ₅	-	X	X
<i>G.capensis</i>	TM38362	252	251	(GT) ₃ AT (GT) ₅	-	X	X
<i>C.hottentotus</i>	TM38375	255	258	(GT) ₁₄	X	-	-
<i>C.hottentotus</i>	MCA324	248	248	(GT) ₉	X	-	-
<i>C.mechowii</i>	Z9	250	252	(GT) ₃ AT (GT) ₇	X	-	-
<i>C.mechowii</i>	M71	248	250	(GT) ₃ AT (GT) ₅	X	-	-

* X denotes presence of sequence, - denotes absence

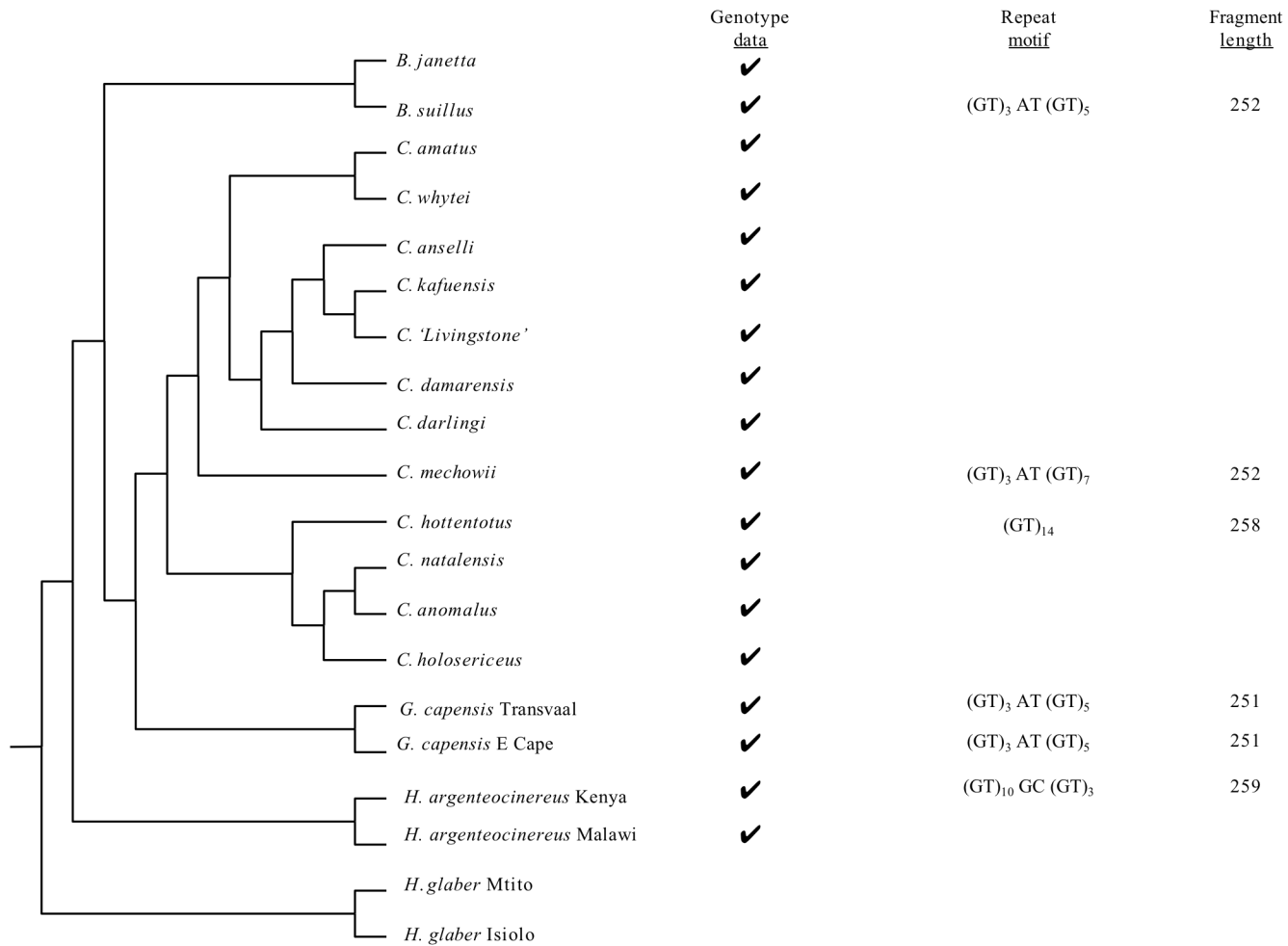


Fig. 4.3 Microsatellite repeat motif of Harg03 plotted on the phylogeny based on Ingram et al. 2004. ✓ indicates successful genotyping amplification. Fragment length was determined from sequencing product size. For species with multiple samples, a representative was selected. Absence of a repeat motif indicates that no sequence data is available and does not suggest information about the repeat region itself.

Table 4.6 Observed sequence length, repeat motif, indels, additional repetitive regions, and changes in the primer sites for locus Harg07. Included are indels that were found within the LTR that was discovered in all taxa except for *Heliophobius*.

Taxa	Sample	GENOTYPE		Repeat motifs Target region	Indels			Outside LTR				Primer sites	
		Fragment length	Observed Seq length		Insertions	W/In LTR	LTR	[GTTTGACTGTCTG]	[TTGGA]	GT	TGGGTGGCTAGG	139BP W/REPEAT	AG
<i>H. argenteocinereus</i>	H046	171/175	171	(GT) ₁₅ GCTT(GT) ₅	-	0	0	X	X	-	X	X	*****C***C**T*****
<i>H. argenteocinereus</i>	H050/H053	171	170	(GT) ₁₃ GCTT(GT) ₅	-	0	0	X	X	-	X	X	*****C***C**T*****
<i>H. argenteocinereus</i>	HA24	157	158	(GT) ₇ GCTT(GT) ₅	-	0	0	X	X	-	X	X	*****C***C**T*****
<i>B. suillus</i>	BS	NA- TOO BIG	588	(GT) ₅ ATATCATGT	X	-	X	-	X	-	-	X	*****C***C**T*****
<i>B. suillus</i>	TM41494	NA- TOO BIG	588	(GT) ₅ ATATCATGT	X	-	X	-	X	-	-	X	*****C***C**T*****
<i>B. janetta</i>	BJ	NA- TOO BIG	588	(GT) ₅ ATATCATGT	X	-	X	-	X	-	-	X	*****C***C**T*****
<i>B. janetta</i>	N8	NA- TOO BIG	588	(GT) ₅ ATATCATGT	X	-	X	-	X	-	-	X	*****C***C**T*****
<i>G. capensis</i>	GPPH2	NA- TOO BIG	599	(GT) ₅ ATGCATGCTT (GT) ₄ GCATGT	X	-	-	X	X	-	-	X	*****C***G**T*****
<i>G. capensis</i>	TM38354	NA- TOO BIG	603	(GT) ₈ GCGTGCTTGA(GT) ₃ GCATGT	X	-	-	X	X	X	-	X	*****C***G**T*****
<i>G. capensis</i>	TM41550	NA- TOO BIG	563	(GT) ₅ ATGCATGCTT (GT) ₄ GCATGT	X	-	-	X	X	-	-	X	*****C***G**T*****
<i>C. darlingi</i>	DAR	NA- TOO BIG	627	(GT) ₁₉ ATGT(GC) ₂ ATGT	X	X	-	X	-	-	X	-	*****C***G**T*****
<i>C. kafuensis</i>	Z10	NA- TOO BIG	622	(GT) ₁₈ (GC) ₂ ATGT	X	X	-	X	-	-	X	-	*****C***G**T*****
<i>C. damarensis</i>	CHD	NA- TOO BIG	624	(GT) ₁₇ ATGT(GC) ₂ ATGT	X	X	-	X	-	-	X	-	*****C***G**T*****
<i>C. 'Sekute'</i>	SEK	NA- TOO BIG	622	(GT) ₁₆ ATGT(GC) ₂ ATGT	X	X	-	X	-	-	X	-	*****C***G**T*****
<i>C. anselli</i>	Z4	NA- TOO BIG	618	(GT) ₁₄ ATGT(GC) ₂ ATGT	X	X	-	X	-	-	X	-	*****C***G**T*****
<i>C. amatus</i>	AMATUS 2	NA- TOO BIG	624	(GT) ₁₆ (GC) ₅ ATGT	X	X	-	X	-	-	X	-	*****C***G**T*****

NA - no amplification

* X = presence of sequence, - = absence

0 = no sequence in that region to compare

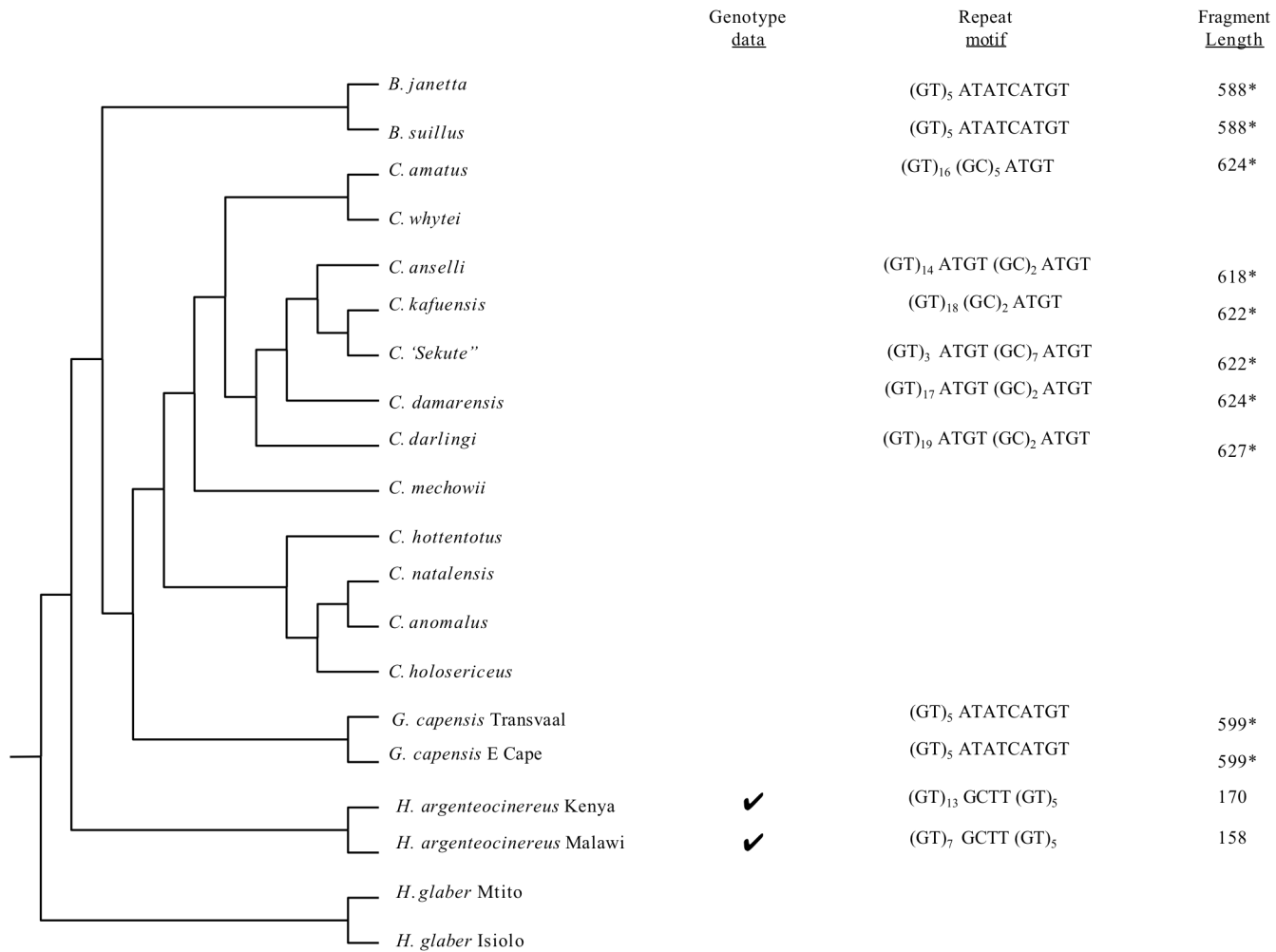


Fig. 4.4 Microsatellite repeat motif of Harg07 plotted on the phylogeny based on Ingram et al. 2004. ✓ indicates successful genotyping amplification. Fragment length was determined from sequencing product size and *denotes the insertion of an LTR of ~453bp. For species with multiple samples, a representative was selected. Absence of a repeat motif indicates that no sequence data is available and does not suggest information about the repeat region itself.

Table 4.7 Observed sequence length, repeat motif, indels, additional repetitive regions, and changes in the primer sites for locus Gcap01.

Taxa	Sample	GENOTYPE			Indel		PRIMER	
		Fragment length	Observed Seq length	Repeat motif	A	95 bp insertion	GCAP01-F	GCAP01-R
5'-CTTGGTGGGAAGTTTCACTCA-3' 5'-AGTTCTGAGCCCAGCTGAC-3'								
<i>H.glaber</i>	H025	NA	211	CTGTGTATGCGTGTATGTGTATGT	-	X	****C*****C*C*T****	*****AG*****
<i>H.glaber</i>	h006	NA	211	CTGTGTATGCGTGTATGTGTATGT	-	X	****C*****C*C*T****	*****AG*****
<i>H.glaber</i>	H875	NA	211	CTGTGTATGCGTGTATGTGTATGT	-	X	****C*****C*C*T****	*****AG*****
<i>H.glaber</i>	L4018	NA	211	CTGTGTATGCGTGTATGTGTATGT	-	X	****C*****C*C*T****	*****AG*****
<i>H.argenteocinereus</i>	H045/46/50	125	126	(GT) ₁₃ (GA) ₂ GT	-	-	*****C*****	*****
<i>H.argenteocinereus</i>	HA24	119	119	(GT) ₁₀ GAGT	X	-		
<i>H.argenteocinereus</i>	B4	119	117	(GT) ₉ GAGT	X	-	*****C*****	*****
<i>B.suillus</i>	TM41500	119	120	GTGC(GT) ₁₁	-	-	*****C*****	*****
<i>B.suillus</i>	BS	113	114	GTGC(GT) ₈	-	-	*****C*****	*****
<i>B.suillus</i>	TM38417	119	120	GTGC(GT) ₁₂	-	-	*****C*****	*****
<i>B.janetta</i>	BJ	117	118	GTGC(GT) ₁₀	-	-	*****C*****	*****
<i>B.janetta</i>	N8	117	118	GTGC(GT) ₁₀	-	-	*****C*****	*****
<i>G.capensis</i>	SP6063	127/129	128	(GT) ₁₇	-	-	*****C*****	*****
<i>G.capensis</i>	TM41550	123/125	124	(GT) ₁₆	-	-	*****C*****	*****
<i>G.capensis</i>	TM38357	113	114	(GT) ₁₀	-	-	*****C*****	*****
<i>G.capensis</i>	TM38362	121	122	(GT) ₁₄	-	-	*****C*****	*****
<i>C.hottentotus</i>	SP6230	127/133	128	(GT) ₁₇	-	-	*****C*****	*****
<i>C.hottentotus</i>	MCA324	125	122	(GT) ₁₄	-	-	*****C*****	*****
<i>C.hottentotus</i>	SP7520	133	132	(GT) ₁₉	-	-	*****C*****	*****
<i>C.holosericus</i>	SP7552	117/123	118	(GT) ₁₂	-	-	*****C*****	*****
<i>C.natalensis</i>	TM38464	135	118	(GT) ₁₂	-	-	*****C*****	*****
<i>C.natalensis</i>	CHN2	107	108	(GT) ₇	-	-	*****C*****	*****
<i>C.anaomalus</i>	SP7705	129	128	(GT) ₁₇	-	-	*****C*****	*****
<i>C.mechowii</i>	Z6/7	119	118	(GT) ₁₂	-	-	*****C*****	*****
<i>C.mechowii</i>	M71	NA	122	(GT) ₁₄	-	-	*****C*****	*****
<i>C.kafuensis</i>	Z10	121	122	(GT) ₁₄	-	-	*****C*****	*****
<i>C.damarensis</i>	Wessam0201	123/125	124	(GT) ₁₀ GC(GT) ₄	-	-	*****C*****	*****
<i>C.damarensis</i>	TM39469	123	122	(GT) ₁₄	-	-	*_*C*****C*****	*****
<i>C.damarensis</i>	SP7758	125	123	(GT) ₆ G(GT) ₃ GC(GT) ₄	-	-	*****C*****	*****
<i>C.'Sekute'</i>	LIV/SEN/SEK	121/123	122	(GT) ₁₄	-	-	*****C*****	*****
<i>C.whytei</i>	KAR1	NA	132	(GT) ₁₉	-	-	*****C*****	*****T*****
<i>C.anselli</i>	Z1	127/133	132	(GT) ₁₉	-	-	*****CC*****	*****
<i>C.anselli</i>	Z4	NA	132	(GT) ₁₉	-	-	*****C*****	*****
<i>C.amatus</i>	AMATUS	125/127?	126	(GT) ₁₇	-	-	*****C*****	*****T*****

NA - no amplification

* X denotes presence of sequence, - denotes absence

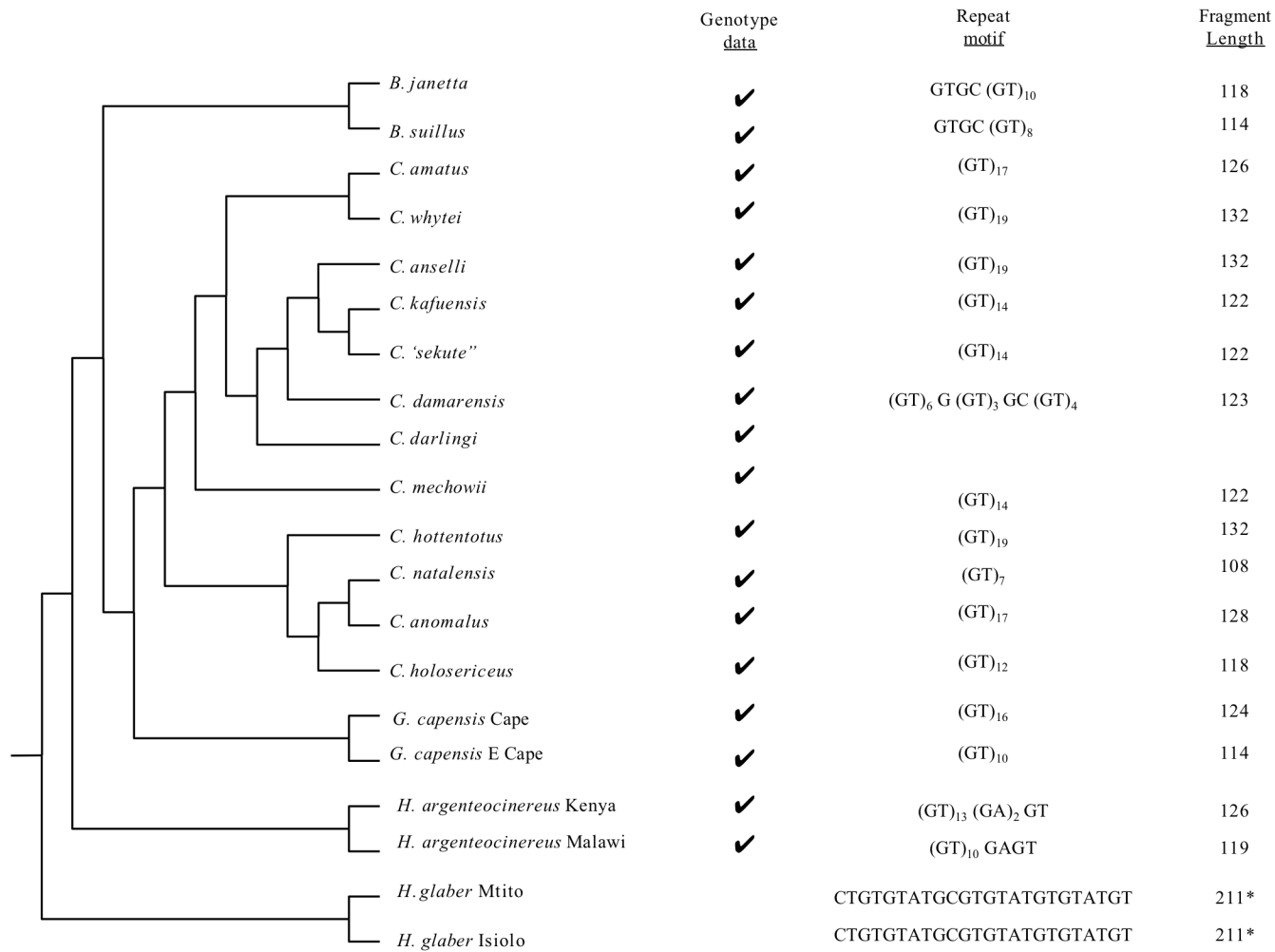


Fig. 4.5 Microsatellite repeat motif of Gcap01 plotted on the phylogeny based on Ingram et al. 2004. ✓ indicates successful genotyping amplification. Fragment length was determined from sequencing product size and * denotes the 95bp insertion (SINE) . For species with multiple samples, a representative was selected. Absence of a repeat motif indicates that no sequence data is available and does not suggest information about the repeat region itself.

Table 4. 8 Observed sequence length, repeat motif, indels, additional repetitive regions, and changes in the primer sites for locus Gcap07.

Taxa	Sample	GENOTYPE			Indel			Primer - GCAP07R
		Fragment length	Observed Seq length	Repeat motif	A	AA	A	5'-AGTTCCCAAGTTGGTAAGG-3'
<i>H. argenteocinereus</i>	H050	264	264	GTGC(GT) ₆ AT(GT) ₂₁ ATGT	X	X	-	*****G**
<i>H. argenteocinereus</i>	HA24	254/260	254	GTGC(GT) ₄ AT(GT) ₂₀	X	X	-	*****G**
<i>B. suillus</i>	TM41494	242/244	242	GTGC(GT) ₄ GC(GT) ₁₆	X	-	-	*****
<i>B. suillus</i>	BS	252/256	251	GTGC(GT) ₄ GC(GT) ₂₀	-	-	-	*****
<i>B. janetta</i>	BJ	238	238	GTGC(GT) ₄ GC(GT) ₁₄	-	-	-	*****
<i>G. capensis</i>	TM38354	216/218	216	(GT) ₈	X	X	-	*****
<i>G. capensis</i>	TM38353	216/218	242	(GT) ₂₁	X	X	-	*****
<i>G. capensis</i>	GPPH2	218	218	(GT) ₉	X	X	-	*****
<i>C. hottentotus</i>	TM38375	236/242	236	GTGA(GT) ₁₅	X	X	-	*****
<i>C. hottentotus</i>	MCA324	240	234	GTGA(GT) ₁₅	X	X	-	*****
<i>C. hottentotus</i>	TM38475	238/244	244	GTGA(GT) ₂₀	X	X	-	*****
<i>C. holosericeus</i>	TM41446	230/240	240	GTGA(GT) ₁₈	X	X	-	*****
<i>C. holosericeus</i>	SP7552	232/234	234	GTGA(GT) ₁₅	X	X	-	*****
<i>C. natalensis</i>	CHN2	230/250	230	(GT) ₁₅	X	X	-	*****
<i>C. natalensis</i>	TM38464	234/246	234	(GT) ₁₇	X	X	-	*****
<i>C. anaomalus</i>	SP7705	224/242	224	GTGA(GT) ₁₀	X	X	-	*****
<i>C. mechowii</i>	Z9	234/236	234	GTGACT(GT) ₁₄	X	X	-	*****T***
<i>C. darlingi</i>	DAR4	NA	226	GTGACT(GT) ₁₁	X	X	-	*****T***
<i>C. kafuensis</i>	Z10	234	234	GTGACT(GT) ₁₄	X	X	-	*****T***
<i>C. damarensis</i>	HW3084	236/240	236	GTGACT(GT) ₁₅	X	X	X	****T*****T***
<i>C. 'Sekute'</i>	C. 'sekute'	242	242	GTGACT(GT) ₁₈	X	X	-	*****T***
<i>C. anSELLi</i>	Z4	232/248	232	GTGACT(GT) ₁₃	X	X	-	*****T***
<i>C. amatus</i>	AMATUS2	238/240	238	GTGACT(GT) ₁₆	X	X	-	*****T***
<i>C. 'Livingstone'</i>	LIV	234	232	GTGACT(GT) ₁₃	X	X	-	*****T***

NA - no amplification

* X = presence of sequence, - = absence

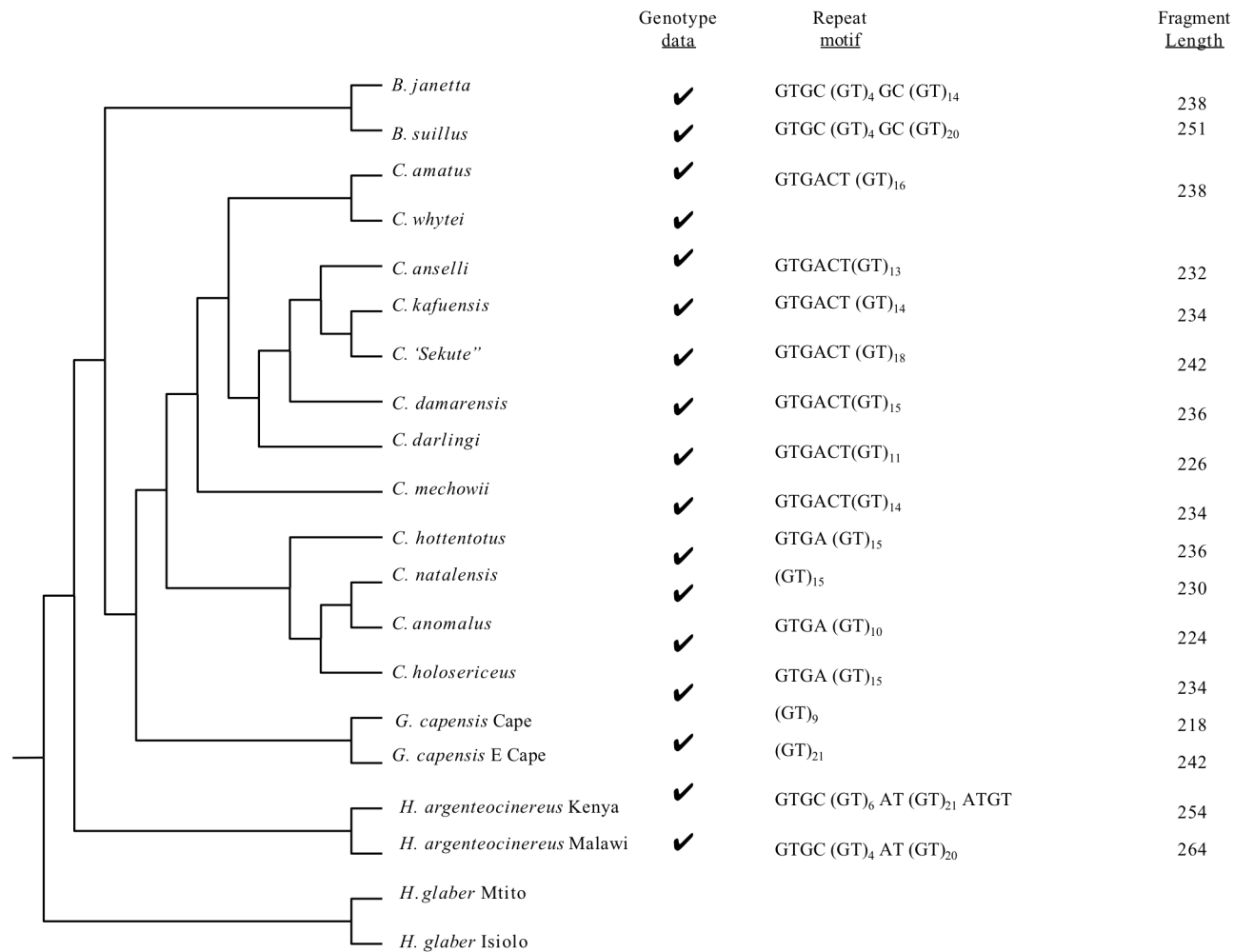


Fig. 4.6 Microsatellite repeat motif of Gcap07 plotted on the phylogeny based on Ingram et al. 2004. ✓ indicates successful genotyping amplification. Fragment length was determined from sequencing product size. For species with multiple samples, a representative was selected. Absence of a repeat motif indicates that no sequence data is available and does not suggest information about the repeat region itself.

Table 4.9 Observed sequence length, repeat motif, indels, additional repetitive regions, and changes in the primer sites for locus Bsuil01. Three regions that contain repetitive sequence were identified.

Taxa	Sample	GENOTYPE			Repeat motifs Target region	2nd Region	Undetected short repeat		Indels* 14bp-PRIMER SITE	Primers	
		Fragment length	Observed Seq length	TC			TC	Bsuil01-F		Bsuil01-R	
								5'-GTCTACCCGTCCTCCAGG-3'			5'-AACGTTCTCCTAATTCTCCTCC-3'
<i>H. argenteocinereus</i>	H050	NA	196	(GT) ₇ TT(GT) ₂	(TG) ₇	-	-	X	-	*****TG**	*A**G*****
<i>B. suillus</i>	BS	198	198	(GT) ₁₁	(TG) ₆	-	X	X	X	*****	*****
<i>B. suillus</i>	TM41494	208/210	210	(GT) ₁₄ GC(GT) ₂	(TG) ₅ CG	-	X	X	X	*****	*****
<i>B. janetta</i>	BJ	194	195	(GT) ₆ GC(GT) ₂	(TG) ₆	-	X	X	X	*****	*****
<i>B. janetta</i>	N8	194	195	(GT) ₆ GC(GT) ₂	(TG) ₆	-	X	X	X	*****	*****
<i>G. capensis</i>	GPPH2	206	206	(GT) ₄ AT(GT) ₄ GA(GT) ₂ GC(GT) ₂	(TG) ₆	X	X	X	-	*****A*****	*****
<i>G. capensis</i>	SP6202	206	206	(GT) ₄ AT(GT) ₄ GA(GT) ₂ GC(GT) ₂	(TG) ₆	X	X	X	-	*****A*****	*****
<i>G. capensis</i>	TM38354	206	206	(GT) ₄ AT(GT) ₄ GA(GT) ₂ GC(GT) ₂	(TG) ₆	X	X	X	-	*****	*****
<i>C. hottentotus</i>	MCA324	206	216	(GT) ₆ GCAT(GT) ₄	(TG) ₂₂	-	X	-	-	*****	-----TCCTCC
<i>C. holosericeus</i>	TM38475	NA	204	(GT) ₆ GCAT(GT) ₄	(TG) ₁₄	-	X	-	-	*****	-----TCCTCC
<i>C. holosericeus</i>	SP7552	250	210	(GT) ₅ GCAT(GT) ₄	(TG) ₂₀	-	X	-	-	*****	-----TCCTCC
<i>C. holosericeus</i>	TM41446	NA	212	(GT) ₅ GCAT(GT) ₄	(TG) ₁₂ CG(TG) ₅ CG	-	X	-	-	*****	-----TCCTCC
<i>C. natalensis</i>	CHN2	NA	202	(GT) ₃ ATGTGCAT(GT) ₄	(TG) ₁₆	-	X	-	-	*****T*****	-----TCCTCC
<i>C. natalensis</i>	TM38465	NA	206	(GT) ₃ ATGTGCAT(GT) ₄	(TG) ₁₈	-	X	-	-	*****T*****	-----TCCTCC
<i>C. natalensis</i>	TM41577	NA	212	(GT) ₃ ATGTGCAT(GT) ₄	(TG) ₂₃	-	X	-	-	*****T*****	-----TCCTCC
<i>C. anaomalus</i>	SP7705	NA	214	(GT) ₅ GCAT(GT) ₄	(TG) ₂₁ TA	-	X	-	-	*****C*	-----TCCTCC
<i>C. mechowii</i>	Z9	212	200	(GT) ₁₂ (GC) ₃ AT(GT) ₄	(TG) ₆	-	X	-	-	*****	-----TCCTCC
<i>C. kafuensis</i>	Z10	NA	210	(GT) ₁₅ (GC) ₅ AT(GT) ₄	(TG) ₆	-	X	-	-	*****	-----TCCTCC
<i>C. damarensis</i>	HW3084	208	196	(GT) ₇ (GC) ₅ AT(GT) ₄	(TG) ₇	-	X	-	-	*****	-----TCCTCC
<i>C. anelli</i>	Z4	216/224	206	(GT) ₁₂ (GC) ₆ AT(GT) ₄	(TG) ₆	-	X	-	-	*****	-----TCCTCC
<i>C. amatus</i>	AMATUS2	NA	202	(GT) ₁₂ (GC) ₃ AT(GT) ₄	(TG) ₇	-	X	-	-	*****	-----TCCTCC

NA - no amplification

* X = presence of sequence, - = absence

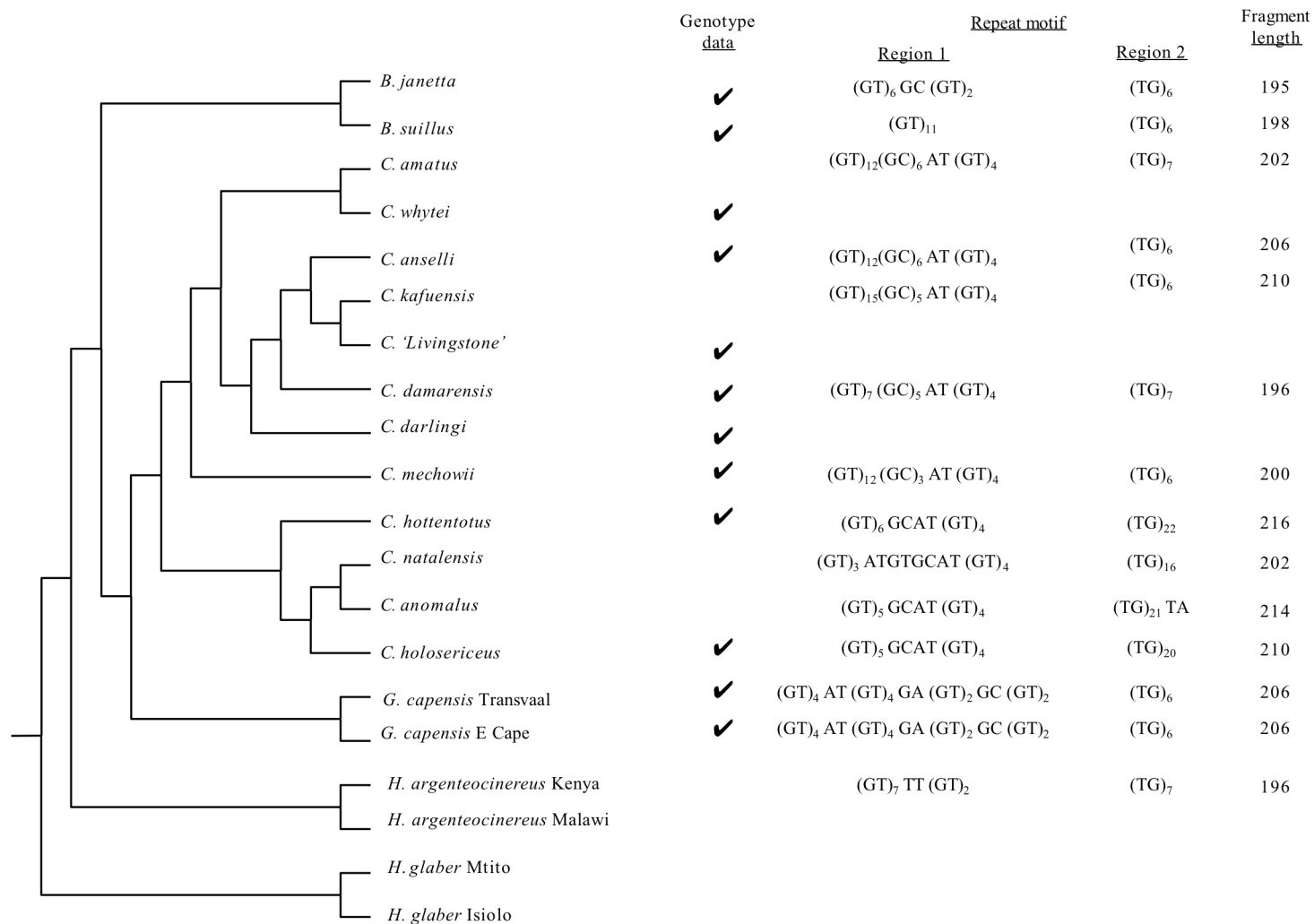


Fig. 4.7 Microsatellite repeat motifs of Bsuil01 plotted on the phylogeny based on Ingram et al. 2004. ✓ indicates successful genotyping amplification. Fragment length was determined from sequencing product size. For species with multiple samples, a representative was selected. Absence of a repeat motif indicates that no sequence data is available and does not suggest information about the repeat region itself.

Table 4.10 Observed sequence length, repeat motif, indels, and changes in the primer sites for locus Bsui104.

Taxa	Sample	GENOTYPE			Indels			Primer
		Fragment length	Observed Seq length	Repeat motif	GG	GG	G	Bsui104-R 5'-TTGCAACACAGAGGAACTGA-3'
<i>H. glaber</i>	L4016	NA	302	GGGGGT	X	X	X	*****A**T*****
<i>B. suillus</i>	BS	NA	339	(GT) ₂₂	X	X	-	*****
<i>B. suillus</i>	TM41494	337/339	339	(GT) ₂₂	X	X	-	*****
<i>B. janetta</i>	BJ	317	319	(GT) ₁₂	X	X	-	*****
<i>G. capensis</i>	TM38353	331	333	GG(GT) ₁₈	X	X	-	**T*****
<i>G. capensis</i>	GPPH2	NA	337	GG(GT) ₂₁	-	X	-	**T*****
<i>C. hottentotus</i>	MCA324	311	311	GGGCAG(GT) ₃ GGGT	X	-	-	*****T**
<i>C. darlingi</i>	DAR4	305	311	(G) ₅ TTCGGTGGGT	X	X	-	*****T**
<i>C. kafuensis</i>	Z10	303	311	(G) ₅ TTCGGTGGGT	X	X	-	*****T**
<i>C. damarensis</i>	HW3084	NA	311	(G) ₅ TTCGGTGGGT	X	X	-	*****T**
<i>C. 'Sekute'</i>	SEK	305	311	(G) ₅ TTCGGTGGGT	X	X	-	*****T**
<i>C. anelli</i>	Z4	303	311	(G) ₅ TTCGGTGGGT	X	X	-	*****T**
<i>C. amatus</i>	AMATUS2	307	311	(G) ₅ TTCGGTGGGT	X	X	-	*****T**

NA - no amplification

* X = presence of sequence, - = absence

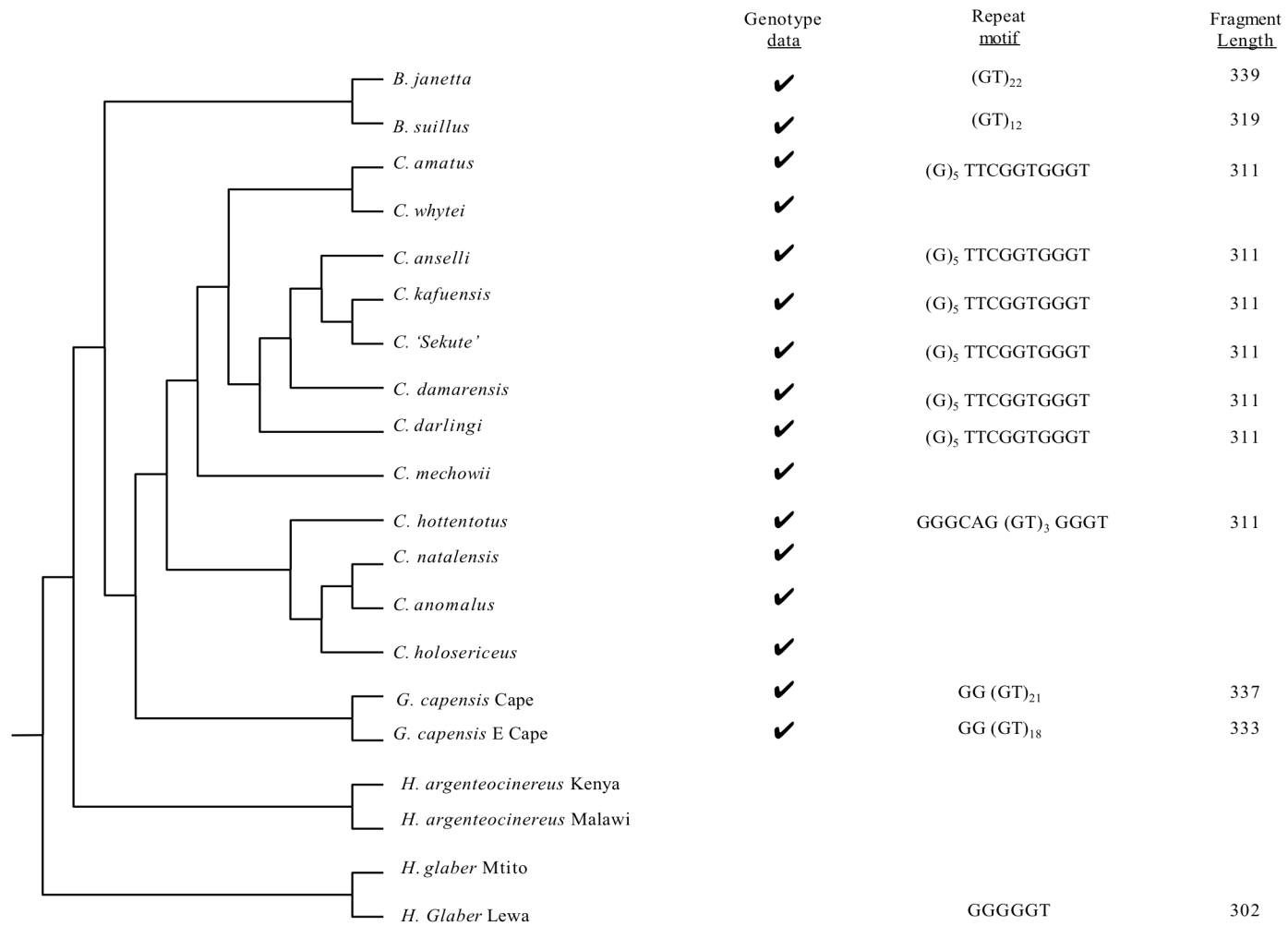


Fig. 4.8 Microsatellite repeat motif of Bsuil04 plotted on the phylogeny based on Ingram et al. 2004. ✓ indicates successful genotyping amplification. Fragment length was determined from sequencing product size. For species with multiple samples, a representative was selected. Absence of a repeat motif indicates that no sequence data is available and does not suggest information about the repeat region itself.

Table 4.11 Observed sequence length, repeat motif, indels, and changes in the primer sites for locus Bsui106.

Taxa	Sample	GENOTYPE			Indels			Primer
		Fragment length	Observed Seq length	Repeat motif	CT/GT	T	CT	Bsui106-R 5' -AACAGTGGAGGAGCTTTGTG-3'
<i>H. argenteocinereus</i>	H050/053	248	245	GC(GT) ₂ GA(GT) ₉ GCG(GT) ₄	CT	-	X	*****
<i>H. argenteocinereus</i>	B4	270	267	(GT) ₃ GA(GT) ₂₁ G(GT) ₄	CT	-	X	*****
<i>H. argenteocinereus</i>	HA25	268	247	(GT) ₃ GA(GT) ₁₁ G(GT) ₄	CT	-	X	*****
<i>H. argenteocinereus</i>	HA24	268	265	(GT) ₃ GA(GT) ₂₀ G(GT) ₄	CT	-	X	*****
<i>B. suillus</i>	BS	240	232	(GT) ₂ GA(GT) ₈ G(GT) ₃	TT	-	X	*****
<i>B. suillus</i>	TM41494	242	234	(GT) ₂ GA(GT) ₈ GGA(GT) ₃	TT	-	-	*****
<i>B. janetta</i>	BJ	242	234	(GT) ₂ GA(GT) ₇ GGA(GT) ₃	TT	-	-	*****
<i>B. janetta</i>	N8	242	234	(GT) ₂ GA(GT) ₉ GGA(GT) ₃	TT	-	-	*****
<i>G. capensis</i>	GPPH2	246	243	(GT) ₂ GA(GT) ₆ G(GT) ₄ GGTATGT	TT	-	X	*****
<i>G. capensis</i>	TM38354	252	247	(GT) ₂ GA(GT) ₁₃ GGTATGT	TT	-	X	*****
<i>G. capensis</i>	TM41550	246	243	(GT) ₂ GA(GT) ₆ G(GT) ₄ GGTATGT	TT	-	X	*****
<i>G. capensis</i>	SP6202	242	241	(GT) ₂ GA(GT) ₅ G(GT) ₄ GGTATGT	TT	-	X	*****
<i>C. holosericeus</i>	TM38475	248/268	246	GTGC(GT) ₁₅ G(GT) ₂	-	X	X	**T*****T*****
<i>C. holosericeus</i>	SP7552	242	240	GTGC(GT) ₁₂ G(GT) ₂	-	X	X	**T*****T*****
<i>C. natalensis</i>	CHN2	234	231	(GT) ₉ G(GT) ₂	-	X	X	**T*****T*****
<i>C. anaomalus</i>	SP7705	252/258	248	(GT) ₁₈ G(GT) ₂	-	-	X	**T*****T*****
<i>C. mechowi</i>	M71	NA	243	(GT) ₂ GA(GT) ₁₁ G(GT) ₃	CT	-	X	*****
<i>C. mechowi</i>	z9	NA	257	(GT) ₂ GA (GT) ₁₈ G(GT) ₃	CT	-	X	*****
<i>C. darlingi</i>	DAR4	NA	255	(GT) ₂ GA (GT) ₁₇ G(GT) ₃	CT	-	X	*****
<i>C. kafuensis</i>	z10	NA	252	(GT) ₁₈ G(GT) ₃	CT	-	X	*****
<i>C. damarensis</i>	HW3084	NA	259	(GT) ₂ GA(GT) ₁₉ G(GT) ₃	CT	-	X	*****
<i>C. damarensis</i>	CHD	NA	265	(GT) ₂ GA(GT) ₂₂ G(GT) ₃	CT	-	X	*****
<i>C. 'sekute'</i>	LIV/Sek	NA	259	(GT) ₂ GA(GT) ₁₉ G(GT) ₃	CT	-	X	*****
<i>C. anelli</i>	Z4	NA	260	(GT) ₂₂ G(GT) ₃	CT	-	X	*****
<i>C. anelli</i>	Z12	NA	250	(GT) ₁₈ G(GT) ₃ GC	CT	-	X	*****
<i>C. amatus</i>	AMATUS2	NA	247	(GT) ₂ GA(GT) ₁₃ G(GT) ₃	CT	-	X	*****

NA - no amplification

* X = presence of sequence, - = absence

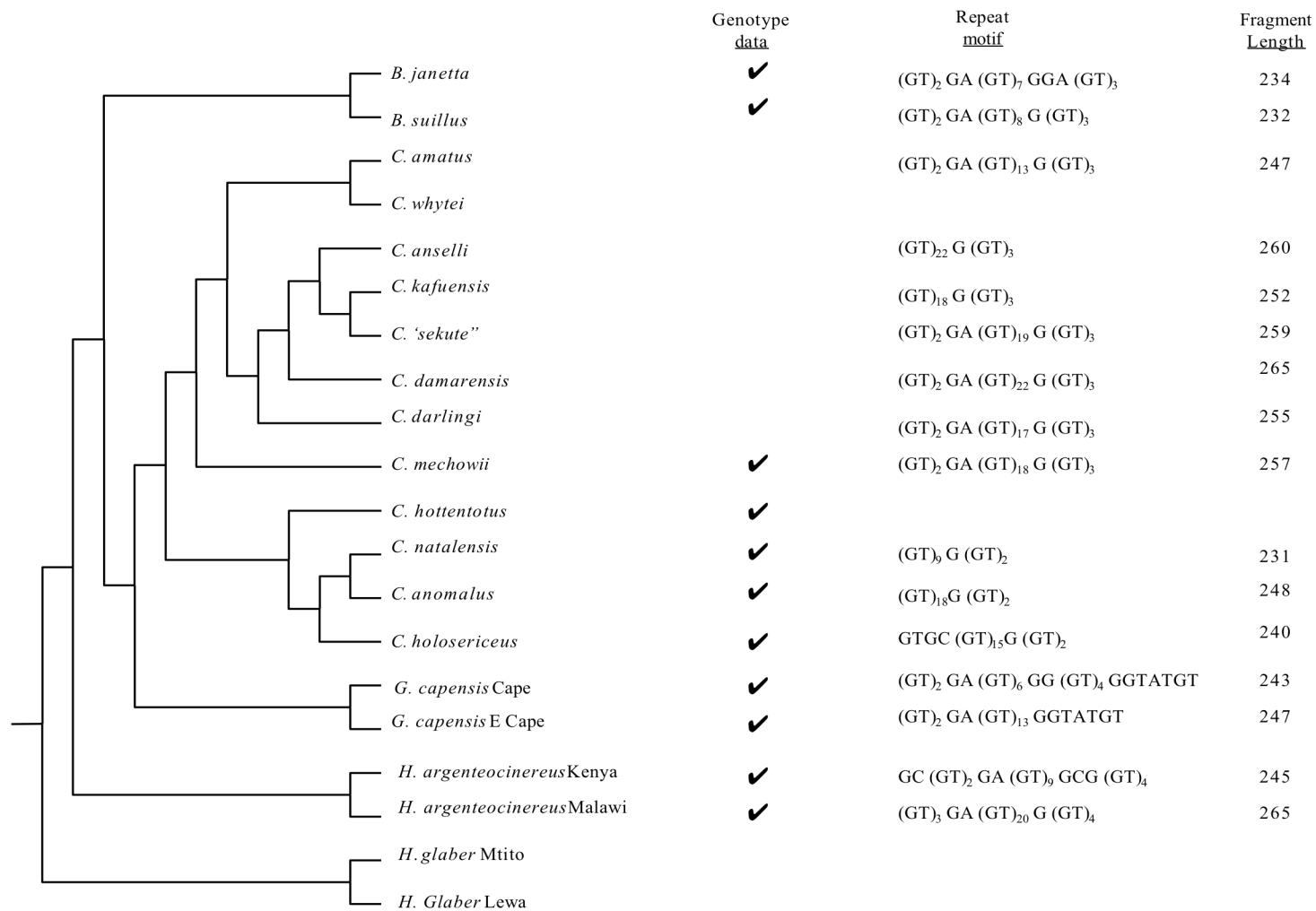


Fig. 4.9 Microsatellite repeat motif of Bsui106 plotted on the phylogeny based on Ingram et al. 2004. ✓ indicates successful genotyping amplification. Fragment length was determined from sequencing product size. For species with multiple samples, a representative was selected. Absence of a repeat motif indicates that no sequence data is available and does not suggest information about the repeat region itself.

Table 4.12 Observed sequence length, repeat motif, indels, and changes in the primer sites for locus Chott01. A SINE/Alu was identified overlapping the primer site of Chott01-F.

Taxa	Sample	GENOTYPE			Indels					Primer		
		Fragment length	Observed Seq length	Repeat motif						Chott01-F (in sine)	Chott01-R	
					AAAC	AC/GC	AA/AT/TT	C	T			T
<i>H. argenteocinereus</i>	H042/H050	NA	279	(GT) ₂₁	-	AC	AA	-	-	-	-----*****A*	*****A*****C****
<i>H. argenteocinereus</i>	SP5566	NA	276	(GT) ₁₉	-	AC	AA	-	-	-	-----**G*****	*****A*****C****
<i>H. argenteocinereus</i>	B4	NA	273	(GT) ₁₇	X	AC	AA	-	-	-	-----*****	*****A*****C****
<i>B. suillus</i>	BS	257	250	(GT) ₁₀ AT(GT) _b	X	GC	--	-	-	-	A****G*****	*****
<i>B. suillus</i>	SP6175	257	250	(GT) ₁₀ AT(GT) _b	X	GC	--	-	-	-	A****G*****C*	*****
<i>B. suillus</i>	TM41493	263	252	(GT) ₁₁ AT(GT) _b	X	GC	--	-	-	-	G****C*****C*	*****C****
<i>B. suillus</i>	TM41450	259	252	(GT) ₁₁ AT(GT) _b	X	GC	--	-	-	-	A****G*****C*	*****C****
<i>B. janetta</i>	BJ	257	250	(GT) ₁₀ AT(GT) _b	X	GC	--	-	-	-	A****G*****C*	*****C****
<i>B. janetta</i>	N8	261	254	(GT) ₁₂ AT(GT) _b	X	GC	--	-	-	-	A****G*****C*	*****
<i>G. capensis</i>	TM38354	275/281	286	(GT) ₂₀	X	GC	--	C	-	-	A****C*-T*****	*****
<i>G. capensis</i>	TM41550	277	286	(GT) ₂₀	X	GC	--	C	-	-	A****C*-T*****	*****
<i>G. capensis</i>	GPPH2	275/277	286	(GT) ₂₀	X	GC	--	C	-	-	A****C*-T*****	*****
<i>C. hottentotus</i>	TM38365/TM38375	277	278	(GT) ₁₈	X	GC	--	-	-	-	*****	*****
<i>C. hottentotus</i>	SP7501	291	292	(GT) ₂₁	X	GC	AT	-	-	-	*****	*****
<i>C. hottentotus</i>	SP6228	273	274	(GT) ₁₆	X	GC	--	-	-	-	*****	*****
<i>C. hottentotus</i>	TM38402	279	280	(GT) ₁₈	X	GC	TT	-	-	-	*****	*****
<i>C. holosericeus</i>	SP7552(H258)	287	284	(GT) ₁₇	X	GC	AT	-	-	-	*****	*****
<i>C. natalensis</i>	CHN2	291	294	(GT) ₂₂	X	GC	AT	-	-	-	*****	*****A
<i>C. anomalus</i>	SP7705	275	268	(GT) ₁₃	X	GC	AT	-	-	-	*****	*****
<i>C. mechowii</i>	MEC2/Z9	285	265	(GT) ₁₄	X	GC	--	-	-	-	A****T*****C**	*****
<i>C. kafuensis</i>	Z10	NA	285	(GT) ₁₁ AT(GT) ₁₀	X	--	--	-	X	-	A****T*****GA**	*****
<i>C. damarensis</i>	HW3084/CHD	NA	292	(GT) ₁₁ (AT) ₂ (GT) ₁₂	X	--	--	-	X	X	A****T*****GA**	*****
<i>C. damarensis</i>	SP7654	NA	290	(GT) ₂₄	X	--	--	-	X	X	A****T*****GA**	*****
<i>C. 'sekute'</i>	SEK	NA	281	(GT) ₁₀ AT(GT) _b	X	--	--	-	X	-	A****T*****GA**	*****
<i>C. anelli</i>	Z12	NA	283	(GT) ₁₁ AT(GT) _b	X	--	--	-	X	-	A****T*****GA**	*****
<i>C. anelli</i>	Z1/MAZUBUKU	NA	281	(GT) ₁₀ AT(GT) _b	X	--	--	-	X	-	A****T*****GA**	*****
<i>C. amatus</i>	AMATUS2	NA	268	(GT) ₁₃	X	--	--	-	-	-	A****T*****C**	*****

NA - no amplification

* X = presence of sequence, - = absence

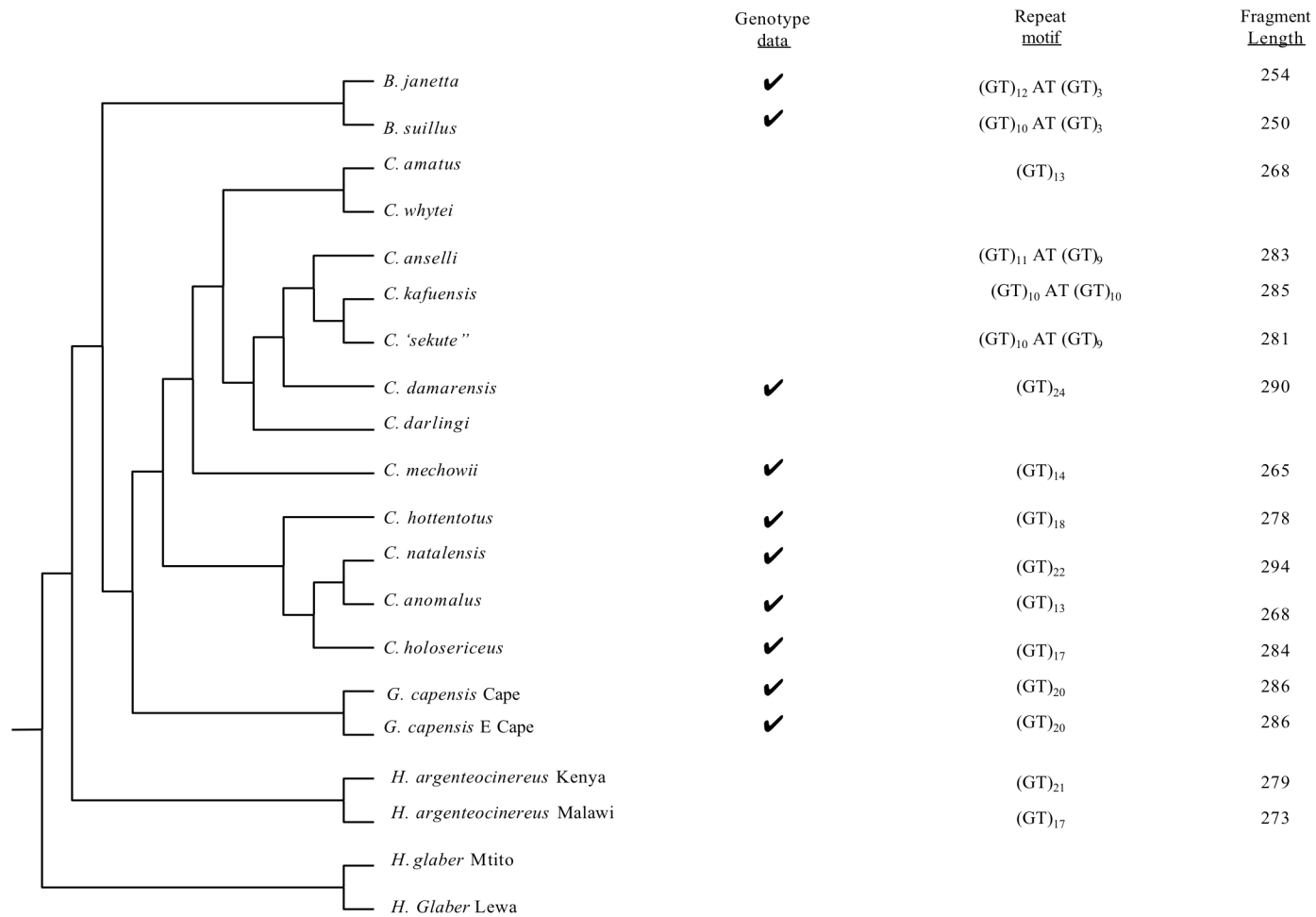


Fig. 4.10 Microsatellite repeat motif of Chott01 plotted on the phylogeny based on Ingram et al. 2004. ✓ indicates successful genotyping amplification. Fragment length was determined from sequencing product size. For species with multiple samples, a representative was selected. Absence of a repeat motif indicates that no sequence data is available and does not suggest information about the repeat region itself.

Table 4.13 Observed sequence length, repeat motif, indels, and changes in the primer sites for locus Chott03.

Taxa	Sample	GENOTYPE			Primer -Chott03-R 5'-ATGTT CAGGACCTACAGGAGG-3
		Fragment length	Observed Seq length	Repeat motif	
<i>H. argenteocinereus</i>	H050	158	157	GC(GT) ₂ CT(GT) ₆ CT(GT) ₄ CTGTGCT(CA) ₂ CG	***C*****A***
<i>H. argenteocinereus</i>	HA24/143	158	157	GC(GT) ₂ CT(GT) ₆ CT(GT) ₄ CTGTGCT(CA) ₂ CG	***C*****A***
<i>C. hottentotus</i>	TM38375	210	209	(GT) ₂ (GC) ₅ (GT) ₄ (GCGT) ₃ (GT) ₄ GCGTGC(GT) ₂ GC(GT) ₃ GCGTGCAT(GT) ₂ (GC) ₃ G	*****
<i>C. hottentotus</i>	MCA324	206/208	205	(GT) ₂ (GC) ₅ (GT) ₇ GCGTGC(GT) ₂ GC(GT) ₃ (GC) ₅ (GT) ₅ GC(GT) ₅ (GC) ₅ A	*****
<i>C. holosericeus</i>	sp7552	216/238	215	(GT) ₂ (GC) ₆ (GT) ₁₂ (GC) ₃ (GT) ₁₄ (GC) ₂ (GT) ₅ (GC) ₅ A	*****
<i>C. anaomalus</i>	SP7705	182	185	(GT) ₂ (GC) ₃ ACGCCT(GT) ₂ GCGTGC(GT) ₃ GCGTGCAT(GT) ₂ (GC) ₆ G	*****
<i>C. mechowii</i>	M71	206/208	165	GC(GT) ₁₂ GC(GT) ₃ GC(GT) ₂ GCGT(GC) ₂ ATGCA	*****C*****
<i>C. mechowii</i>	Z9	164/168	163	GC(GT) ₁₁ GC(GT) ₃ GC(GT) ₂ GCGT(GC) ₂ ATGCA	*****C*****
<i>C. kafuensis</i>	Z10	160	157	GC(GT) ₁₂ (GC) ₂ GTGCGT(GC) ₂ ATGCA	*****
<i>C. damarensis</i>	CHD	162/170	161	GC(GT) ₁₄ (GC) ₂ GTGCGT(GC) ₂ ATGCA	*****
<i>C. damarensis</i>	HW3084	160	159	GC(GT) ₁₃ (GC) ₂ GTGCGT(GC) ₂ ATGCA	*****
<i>C. anseli</i>	Z12	160	159	GC(GT) ₁₃ (GC) ₂ GTGCGT(GC) ₂ ATGCA	*****
<i>C. amatus</i>	AMATUS2	154/158	157	(GC) ₈ (GT) ₈ GCGT(GC) ₂ ATGCA	*****

NA - no amplification

* X = presence of sequence, - = absence

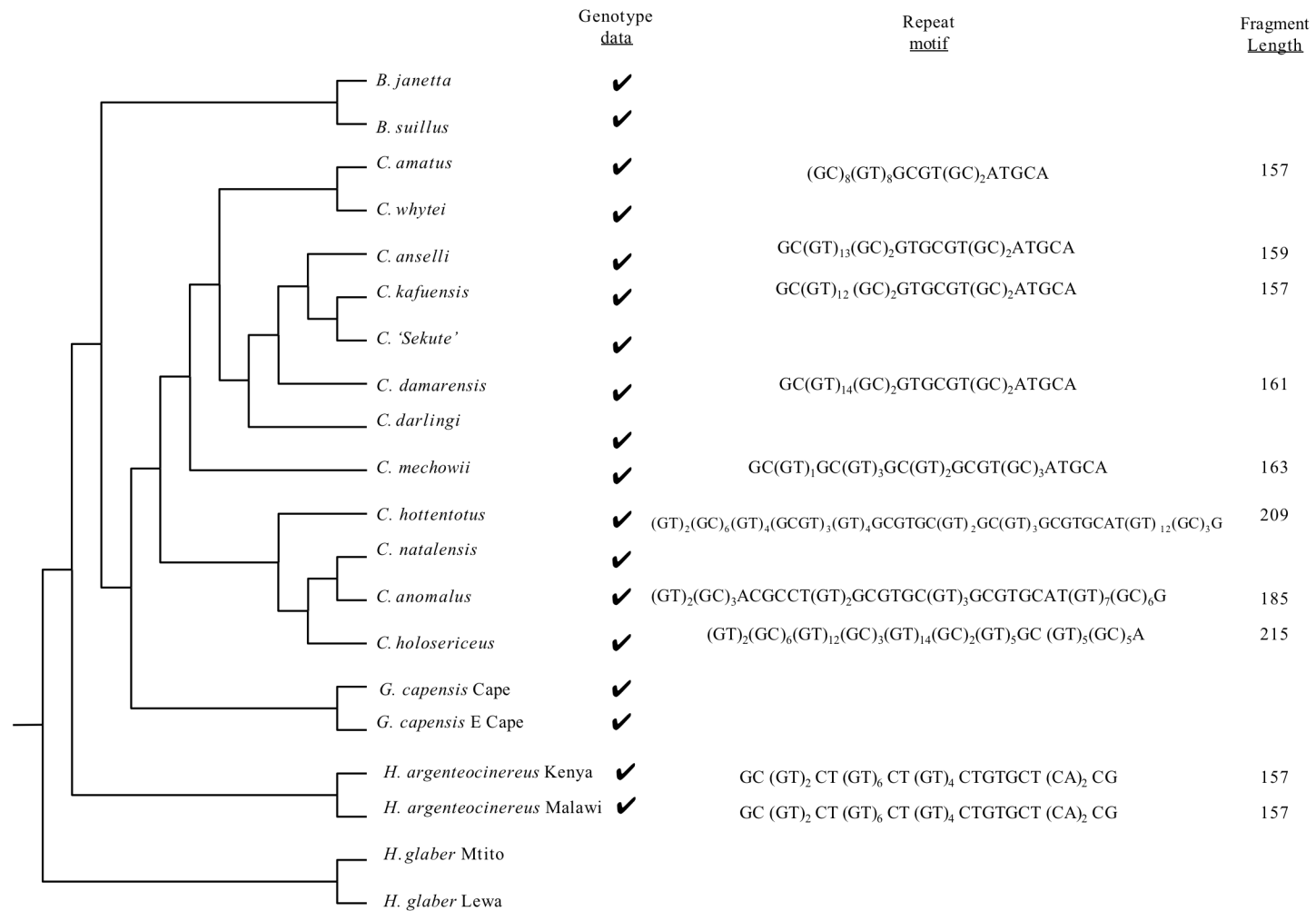


Fig. 4.11 Microsatellite repeat motif of Chott03 plotted on the phylogeny based on Ingram et al. 2004. ✓ indicates successful genotyping amplification. Fragment length was determined from sequencing product size. For species with multiple samples, a representative was selected. Absence of a repeat motif indicates that no sequence data is available and does not suggest information about the repeat region itself.

Table 4.14 Observed sequence length, repeat motif, indels, and changes in the primer sites for locus Chott08.

Taxa	Sample	GENOTYPE			Indels								Primer	
		Fragment length	Observed Seq length	Repeat motif	A	T	G/C	T/C	G	G	Chott08-f	Chott08-R		
											5'-CTCAGCCCCCTCACTACCC-3'	5'-GTGTCCTCCCCCTTTTCTGT-		
<i>H. argenteocinereus</i>	H050/059	121	122	(GT) ₅ GGGT(G) ₇	-	X	G	C	X	X	*****CA*****	T*****		
<i>H. argenteocinereus</i>	H772	121	122	(GT) ₅ GGGT(G) ₇	-	X	G	C	X	X	*****CA*****	T*****		
<i>H. argenteocinereus</i>	HA24	125	125	(GT) ₆ GGC(G) ₈	X	X	G	T	X	X	*****CA*****	T*****		
<i>H. argenteocinereus</i>	HA143	NA	124	(GT) ₇ C(G) ₇	X	X	G	T	X	X	*****CA*****	T*****		
<i>B. suillus</i>	BS	121	113	(GT) ₇ (G) ₆	-	-	-	-	-	X	*****	T*****		
<i>C. hottentotus</i>	MCA324	115	117	(GT) ₆ (G) ₇	-	-	-	C	X	X	*****	*****		
<i>C. hottentotus</i>	TM38375	139/141	140	(GT) ₂₀ GG	-	-	-	C	X	X	*****	*****		
<i>C. hottentotus</i>	TM38365	121	122	(GT) ₁₁ GG	-	-	-	C	X	X	*****	*****		
<i>C. hottentotus</i>	SP7501	115	115	(GT) ₅ (G) ₇	-	-	-	C	X	X	*****	*****		
<i>C. holosericeus</i>	SP7552	115	116	(GT) ₆ (G) ₇	-	-	-	C	X	X	ACT*****_*****	*****		
<i>C. natalensis</i>	CHN2	117	118	(GT) ₄ TT(G) ₁₀	-	-	-	C	X	X	*****	*****T*****		
<i>C. anomalus</i>	SP7705	113	115	(GT) ₅ (G) ₇	-	-	-	C	X	X	*****	*****		
<i>C. mechowii</i>	Z9	115	115	(GT) ₅ (G) ₇	-	-	C	C	X	X	*****C*****	T*****T*****		
<i>C. darlingi</i>	DAR4	111	116	(GT) ₇ (G) ₃	-	-	C	C	X	X	*****C*****	T*****T*****		
<i>C. kafiensis</i>	Z10	115	116	(GT) ₆ (G) ₅	-	-	C	C	X	X	*****C*****	T*****T*****		
<i>C. 'sekute'</i>	SEK/LIV	115	112	(GT) ₆ (G) ₄	-	-	C	C	X	-	*****C*****	T*****T*****		
<i>C. anSELLi</i>	Z4	115	116	(GT) ₆ (G) ₅	-	-	C	C	X	X	*****C*****	T*****T*****		
<i>C. amatus</i>	AMATUS2	115	117	(GT) ₆ (G) ₃	-	-	C	C	X	X	*****C*****	T*****T*****		
<i>C. whytei</i>	B2	111	116	(GT) ₆ (G) ₅	-	-	C	C	X	X	*****C*****	T*****T*****		

NA - no amplification
 * X = presence of sequence, - = absence

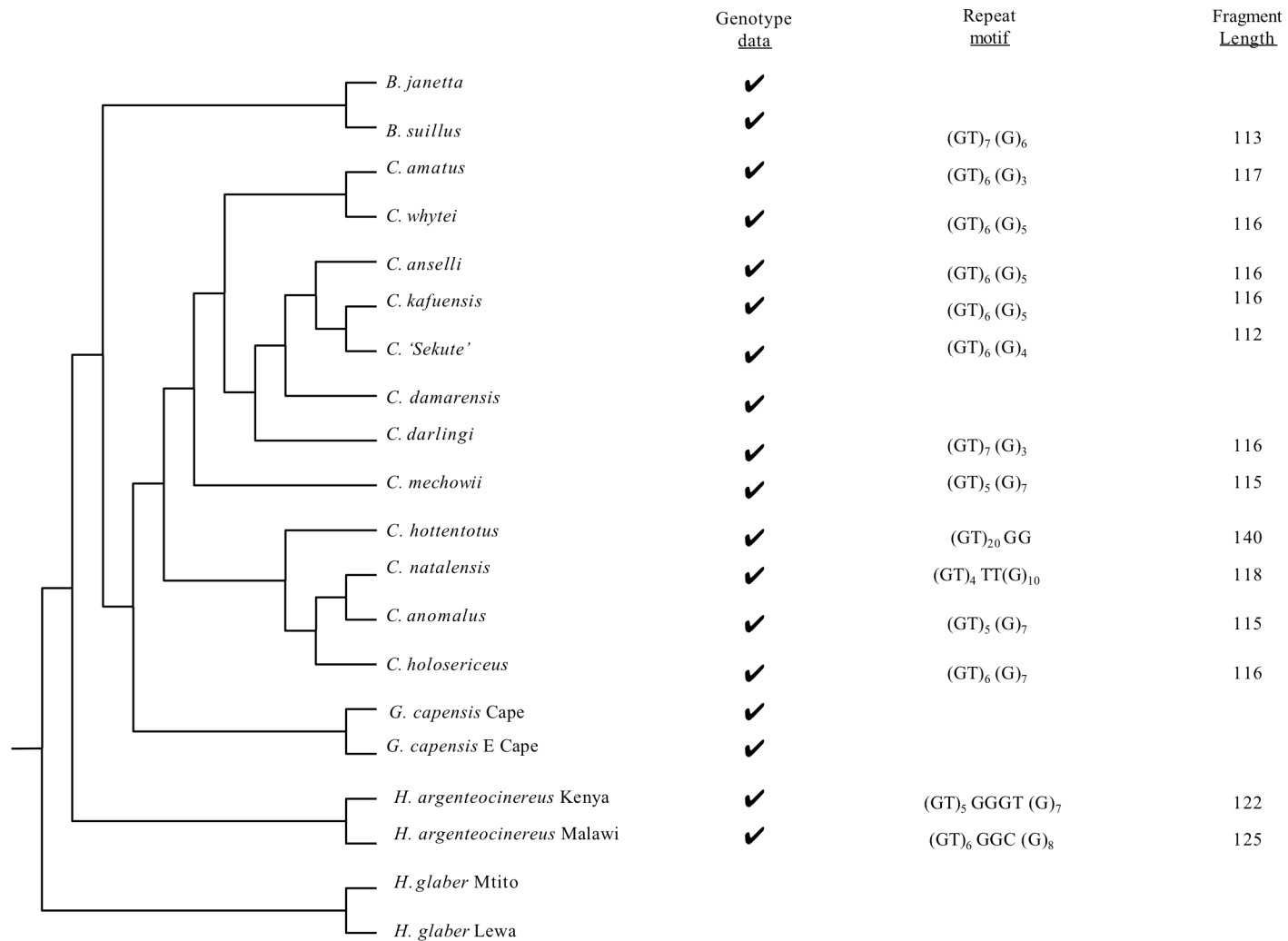


Fig. 4.12 Microsatellite repeat motif of Chott08 plotted on the phylogeny based on Ingram et al. 2004. ✓ indicates successful genotyping amplification. Fragment length was determined from sequencing product size. For species with multiple samples, a representative was selected. Absence of a repeat motif indicates that no sequence data is available and does not suggest information about the repeat region itself.

Table 4.15 Observed sequence length, repeat motif, indels, additional repetitive regions, and changes in the primer sites for locus Cmech03. Included in the genotyping fragment was a CT-rich region

Taxa	Sample	GENOTYPE				Indels		Primer	
		Fragment length	Observed Seq length	Repeat motif	CT-RICH REGION	CTC	GG	5'-CATAAATAAGCAATAGCCCAGC-3'	
<i>B.suillus</i>	BS	286	284	(GT) ₆	CTTC(CTTT) ₂ GTTCTT(CT) ₂ CCTTCTG(CTT) ₂ (CCT) ₂ (CT) ₅ G(CT) ₇		X	-	*****_*****G*
<i>B.suillus</i>	TN39386	290	288	(GT) ₆	CTTC(CTTT) ₂ GTTCTT(CT) ₂ CCTTCTG(CTT) ₂ (CCT) ₂ (CT) ₆ TTCT		X	-	*****_*****G*
<i>B.suillus</i>	TM41494	276/290	275	(GT) ₆	CTTC(CTTT) ₂ GTTCTC(CT) ₂ CCTTCTG(CTT) ₂ (CCT) ₂ (CT) ₅ G(CT) ₇ TTCTGCTGTAT(CT) ₃ CCTCCCACCT		X	-	*****_*****G*
<i>B.janetta</i>	BJ	296	294	(GT) ₆	CTTC(CTTT) ₂ GTTCTT(CT) ₂ CCTTCTG(CTT) ₂ (CCT) ₂ (CT) ₅ G(CT) ₁₂		X	-	*****_*****G*
<i>G.capensis</i>	GPPH2	306/314	289	(GT) ₁₃ GAGTGA	CTTC(CTTT) ₂ GTTCTT(CT) ₂ CCTG (CTT) ₃ (CCT) ₃ (CT) ₄		X	-	_!*****_*****G*
<i>G.capensis</i>	TM38353	294	302	(GT) ₁₅ GA	CTT (CTTT) ₂ GTTCTT(CT) ₂ CCTG (CTT) ₃ (CCT) ₃ (CT) ₄ GCTCTTT(CT) ₃ GCTGTAT(CT) ₃ CCTCCCACC		X	-	*****_*****G*
<i>G.capensis</i>	TM41550	290/294	275	(GT) ₁₂ GAGTGA	CTTC(CTTT) ₂ GTTCTT(CT) ₂ CCTG (CTT) ₃ (CCT) ₃ (CT) ₄		X	-	*****_*****G*
<i>C.hottentotus</i>	MCA324	264	261	(GT) ₅	CTTC(CTTT) ₂ GTTCTT(CT) ₂ C (CTT) ₄ (CCT) ₂ TT(CT) ₃ GCTTTAT(CT) ₃ CCCACCCCT		-	-	_!*****_*****
<i>C.hottentotus</i>	TM38375	266	265	(GT) ₅	CTTC(CTTT) ₃ GTTCTT(CT) ₂ CCTTCTG(CTT) ₃ (CCT) ₂ TT(CT) ₃ GCTTTAT(CT) ₃ CCCACCCCT		X	-	*****_*****
<i>C.hottentotus</i>	TM41446	266	265	(GT) ₅	CTTC(CTTT) ₂ GTTCTT(CT) ₂ CCTTCTG(CTT) ₃ (CCT) ₂ TT(CT) ₃ GCTTTAT(CT) ₃ CCCACCCCT		X	-	*****_*****
<i>C.holosericeus</i>	SP7552	264	262	(GT) ₅	CTTC(CTTT) ₂ GTTCTT(CT) ₂ C (CTT) ₄ (CCT) ₂ TT(CT) ₃ GCTTTAT(CT) ₃ CCCACCCCT		-	-	*****_*****
<i>C.natalensis</i>	CHN2	NA	269	(GT) ₆	TTTC(CTTT) ₂ GTTCTT(CT) ₂ CCTTCTA (CTT) ₃ (CCT) ₂ TT(CT) ₃ GCTTTAT(CT) ₃ CCCACCCCT		X	X	*****_*****
<i>C.anomalus</i>	SP7705	264	261	(GT) ₅	CTTC(CTTT) ₂ GTTCTT(CT) ₂ C (CTT) ₄ (CCT) ₂ TT(CT) ₃ GCTTTAT(CT) ₃ CCCACCCCT		-	-	_!*****_*****
<i>C.mechowii</i>	Z9	290/294	294	TT(GT) ₁₅	CTTC(CTTT) ₂ GTTCTT(CT) ₂ CCTTCTG(CTT) ₃ (CCT) ₂ (CT) ₅ G(CT) ₂ AT(CT) ₃ CCTCCCATCCCT		X	X	*****_*****
<i>C.darlingi</i>	DAR4	282	279	(GT) ₉	CTTC(CTTT) GTT (CT) ₂ CCTTCTG(CTT) ₃ (CCT) ₂ (CT) ₆ G(CT) ₂ ATCTC(CCT) ₂ CCCATCCCT		X	X	*****_*****
<i>C.damarensis</i>	HW3084	284	281	(GT) ₁₁	CTTC(CTTT) ₂ GTT (CT) ₂ CCTTCTG(CTT) ₃ (CCT) ₂ (CT) ₅ G(CT) ₂ ATCTC(CCT) ₂ CCCATCCCT		X	X	*****_*****
<i>C.damarensis</i>	CHD	286	285	(GT) ₁₃	CTTC(CTTT) ₂ GTT (CT) ₂ CCTTCTG(CTT) ₃ (CCT) ₂ (CT) ₅ G(CT) ₂ ATCTC(CCT) ₂ CCCATCCCT		X	X	*****_*****
<i>C.'Sekute'</i>	SEK	290	287	(GT) ₁₄	CTTC(CTTT) ₂ GTT (CT) ₂ CCTTCTG(CTT) ₃ (CCT) ₂ (CT) ₅ G(CT) ₂ ATCTC(CCT) ₂ CCCATCCCT		X	X	*****_*****
<i>C.'Livingstone'</i>	LIV	294	291	(GT) ₁₆	CTTC(CTTT) ₂ GTT (CT) ₂ CCTTCTG(CTT) ₃ (CCT) ₂ (CT) ₅ G(CT) ₂ ATCTC(CCT) ₂ CCCATCCCT		X	-	*****_*****
<i>C.anselli</i>	Z12/4	286/288	285	(GT) ₁₃	CTTC(CTTT) ₂ GTT (CT) ₂ CCTTCTG(CTT) ₃ (CCT) ₂ (CT) ₅ G(CT) ₂ ATCTC(CCT) ₂ CCCATCCCT		X	X	*****_*****
<i>C.amatus</i>	AMATUS2	304	302	(GT) ₂₁	CTTC(CTTT) ₂ GTT (CT) ₂ CCTTCTG(CTT) ₃ (CCT) ₂ (CT) ₅ G(CT) ₂ ATCTC(CCT) ₂ CCCATCCCT		X	X	*****T*****

NA - no amplification

* X = presence of sequence, - = absence

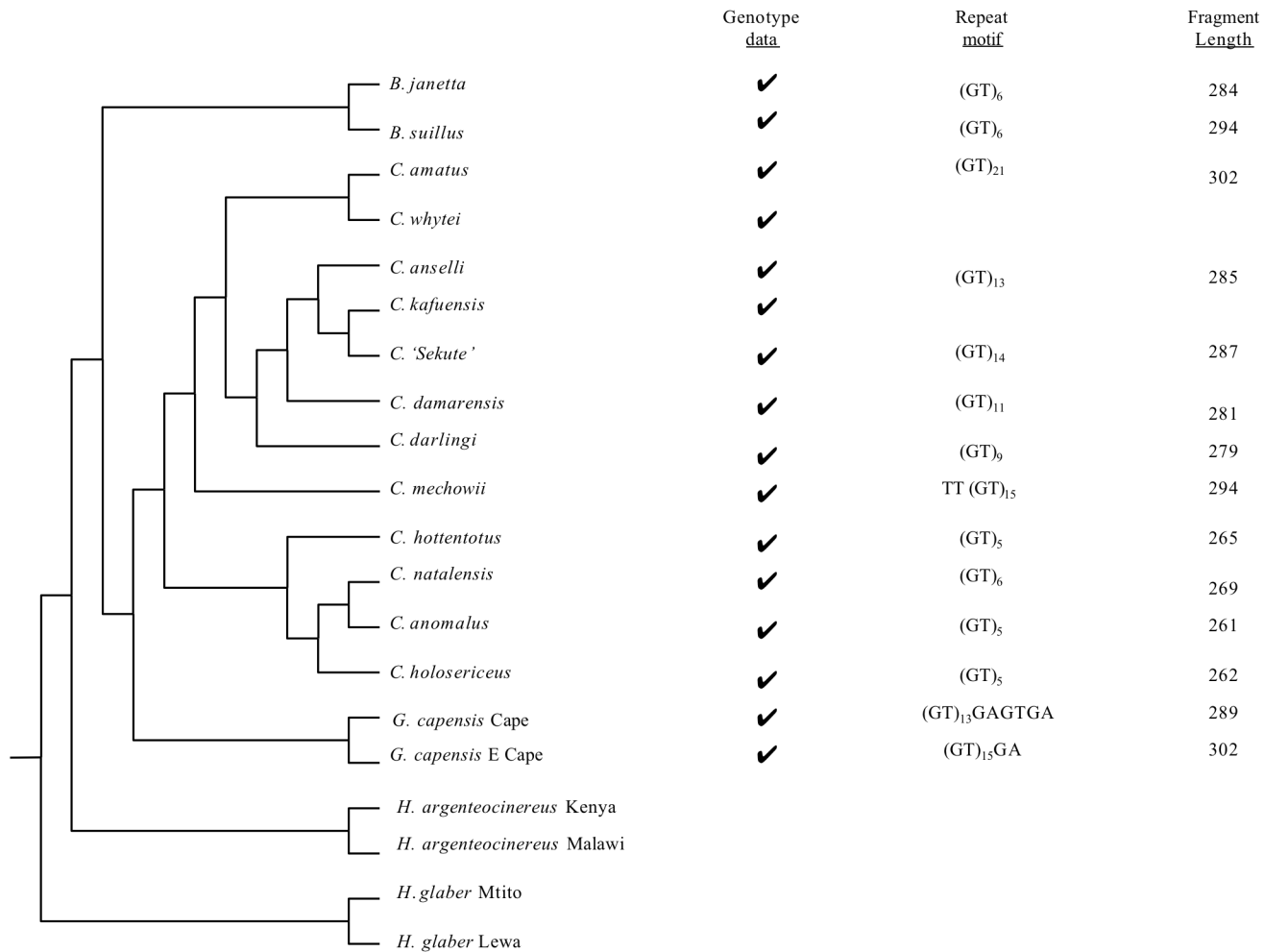


Fig. 4.13 Microsatellite repeat motif of Cmech03 plotted on the phylogeny based on Ingram et al. 2004. ✓ indicates successful genotyping amplification. Fragment length was determined from sequencing product size. For species with multiple samples, a representative was selected. Absence of a repeat motif indicates that no sequence data is available and does not suggest information about the repeat region itself.

Table 4.16 Observed sequence length, repeat motif, indels, additional repetitive regions, and changes in the primer sites for locus Cmech04. Included in the genotyping fragment was an (CAAAA) repeat.

Taxa	Sample	GENOTYPE			Second repetitive region	Indels				Primer Cmech04-R 5'-TCTGACTGGAACCCATCACT-3'
		Fragment length	Observed Seq length	Repeat motif		C	AAT/AAA	GGTGT	TGATTAA/TGGTTAA	
<i>H.glaber</i>	H006	374	374	(T) ₂₀	AACTAG(A) ₅ G(A) ₄ C(A) ₅ C(A) ₅ T	-	-	X	TGATTAA	***G*****
<i>H.glaber</i>	H040	374	374	(T) ₂₀	AACTAG(A) ₅ G(A) ₄ C(A) ₅ C(A) ₅ T	-	-	X	TGATTAA	***G*****
<i>H.glaber</i>	MR1-3835	NA	374	(T) ₂₀	AACTAG(A) ₅ G(A) ₄ C(A) ₅ C(A) ₅ T	-	-	X	TGATTAA	***G*****
<i>H.glaber</i>	MS11	NA	373	(T) ₁₉	AACTAG(A) ₅ G(A) ₄ C(A) ₅ C(A) ₅ T	-	-	X	TGATTAA	***G*****
<i>H.argenteocinereus</i>	H050	430	428	(GT) ₁₃ GC(GT) ₄ GCGTGC(GT) ₅ AT(GT) ₁₁	AA(CAA) ₃ C(A) ₉ CCA	-	AAT	X	TGGTTAA	***G*****
<i>H.argenteocinereus</i>	H045	NA	428	(GT) ₂₀ GC(GT) ₅ AT(GT) ₁₁	AA(CAA) ₃ C(A) ₉ CCA	-	AAT	X	TGGTTAA	***G*****
<i>H.argenteocinereus</i>	H772	434/436	430	(GT) ₂₀ GC(GT) ₅ AT(GT) ₁₂	AA(CAA) ₃ C(A) ₉ CCA	-	AAT	X	TGGTTAA	***G*****
<i>H.argenteocinereus</i>	SP5565	430	482	(GT) ₁₉ (GC) ₄ (GT) ₅ AT(GT) ₁₃ GC(GT) ₄ GCGTGC(GT) ₅ AT(GT) ₁₁	AA(CAA) ₃ C(A) ₁₀ CC	-	AAT	X	TGGTTAA	***G*****
<i>H.argenteocinereus</i>	sp5566	NA	428	(GT) ₁₉ GCGTGC(GT) ₁₆	AA(CAA) ₃ C(A) ₉ CCC	-	AAT	X	TGGTTAA	***G*****
<i>H.argenteocinereus</i>	B4	422/434	413	(GT) ₂ TT(GT) ₂ (GGT) ₂ (GC) ₅ ACGC(GT) ₁₅	AACGTCATCAACATCGAAAAGCC	-	AAT	X	TGGTTAA	***G*****
<i>B.suillus</i>	BS	372	373	GTGA(GT) ₁₂	AA(CAAA) ₅ C(A) ₆ C	-	AAA	-	-	*****T*****
<i>B.suillus</i>	TM38415	378	378	GTGA(GT) ₁₅	AA(CAAA) ₄ C(A) ₉ C	-	AAA	-	-	*****T*****
<i>B.suillus</i>	TM41500	378	379	GTGA(GT) ₁₅	AA(CCAA) ₄ AC(A) ₆ CCCC	-	AAA	-	-	*****T*****
<i>B.suillus</i>	TM39307	374	375	GTGA(GT) ₁₃	AA(CCAA) ₄ (A) ₈ CCCC	-	AAA	-	-	*****T*****
<i>B.janetta</i>	BJ	376/378	376	GTGA (GT) ₁₅	AA(CAAA) ₃ C(A) ₉ CCC	-	AAA	-	-	*****T*****
<i>B.janetta</i>	N8	376	377	GTGA (GT) ₁₅	AA(CAAA) ₃ C(A) ₁₁ CC	-	AAA	-	-	*****T*****
<i>G.capensis</i>	TM39874	362	364	(GT) ₉	AA(CAA) (CAAAA) ₃ C(A) ₉ C	-	AAA	-	-	*****
<i>G.capensis</i>	TM38399	382/386	380	(GT) ₁₇	AA(CAA) ₂ CA(CAAAA) ₂ C(A) ₉ C	-	AAA	-	-	*****C**
<i>C.hottentotus</i>	TM38375	394	375	(GT) ₁₇	AACACCAACAC(CAA) ₂ C(A) ₇ C	-	AAA	-	-	*****
<i>C.hottentotus</i>	H258	378/386	376	(GT) ₁₈	AA(CAC) ₂ (CAA) ₃ C(A) ₈ C	-	AAA	-	-	*****C*****
<i>C.hottentotus</i>	SP7743	376/378	377	(GT) ₁₉	AA CAC (CAA) ₄ C(A) ₇ C	-	AAA	-	-	*****C*****T**
<i>C.hottentotus</i>	SP7501	390	388	(GT) ₂₄	AA(CAC) ₂ (CAA) ₂ C(A) ₇ C	-	AAA	-	-	*****C*****
<i>C.natalensis</i>	TM38464	370/376	369	(GT) ₁₅	AACAC (CAA) ₄ C(A) ₇ C	-	AAA	-	-	*****
<i>C.mechowii</i>	Z9	370/374	402	(GT) ₃₁	AA(CAA) ₃ CAGCAAC(A) ₆ C	-	AAA	-	-	*****
<i>C.mechowii</i>	M69	380	380	(GT) ₂₀	AA(CAA) ₃ CAGCAAC(A) ₆ C	-	AAA	-	-	*****
<i>C.darlingi</i>	DAR4	380/384	400	(GT) ₃₀	AA(CAA) ₃ CAGCAAC(A) ₆ C	-	AAA	-	-	*****
<i>C.kafuensis</i>	Z10	NA	380	(GT) ₂₀	AA(CAA) ₃ CAGCAAC(A) ₆ C	X	AAA	-	-	*****
<i>C.damarensis</i>	SP7576	386	386	(GT) ₂₃	AA(CAA) ₃ CAGCAAC(A) ₆ C	-	AAA	-	-	*****
<i>C.damarensis</i>	SP7591	388	388	(GT) ₂₄	AA(CAA) ₃ CAGCAAC(A) ₆ C	-	AAA	-	-	*****
<i>C.'Mazubuku'</i>	mazubuku	386	388	G (GT) ₂₄	AA(CAA) ₃ CAGCAAC(A) ₆ C	-	AAA	-	-	*****
<i>C.'Sekute'</i>	SEK/SEN/LIV	380/384	384	(GT) ₂₂	AA(CAA) ₃ CAGCAAC(A) ₆ C	X	AAA	-	-	*****
<i>C.anselli</i>	Z1/Z4	384/390	384	(GT) ₂₂	AA(CAA) ₃ CAGCAAC(A) ₆ C	X	AAA	-	-	*****
<i>C.amatus</i>	KAR1	372/390	390	(GT) ₂₅	AA(CAA) ₃ CAGCAAC(A) ₆ C	-	AAA	-	-	*****

NA - no amplification

* X = presence of sequence, - = absence

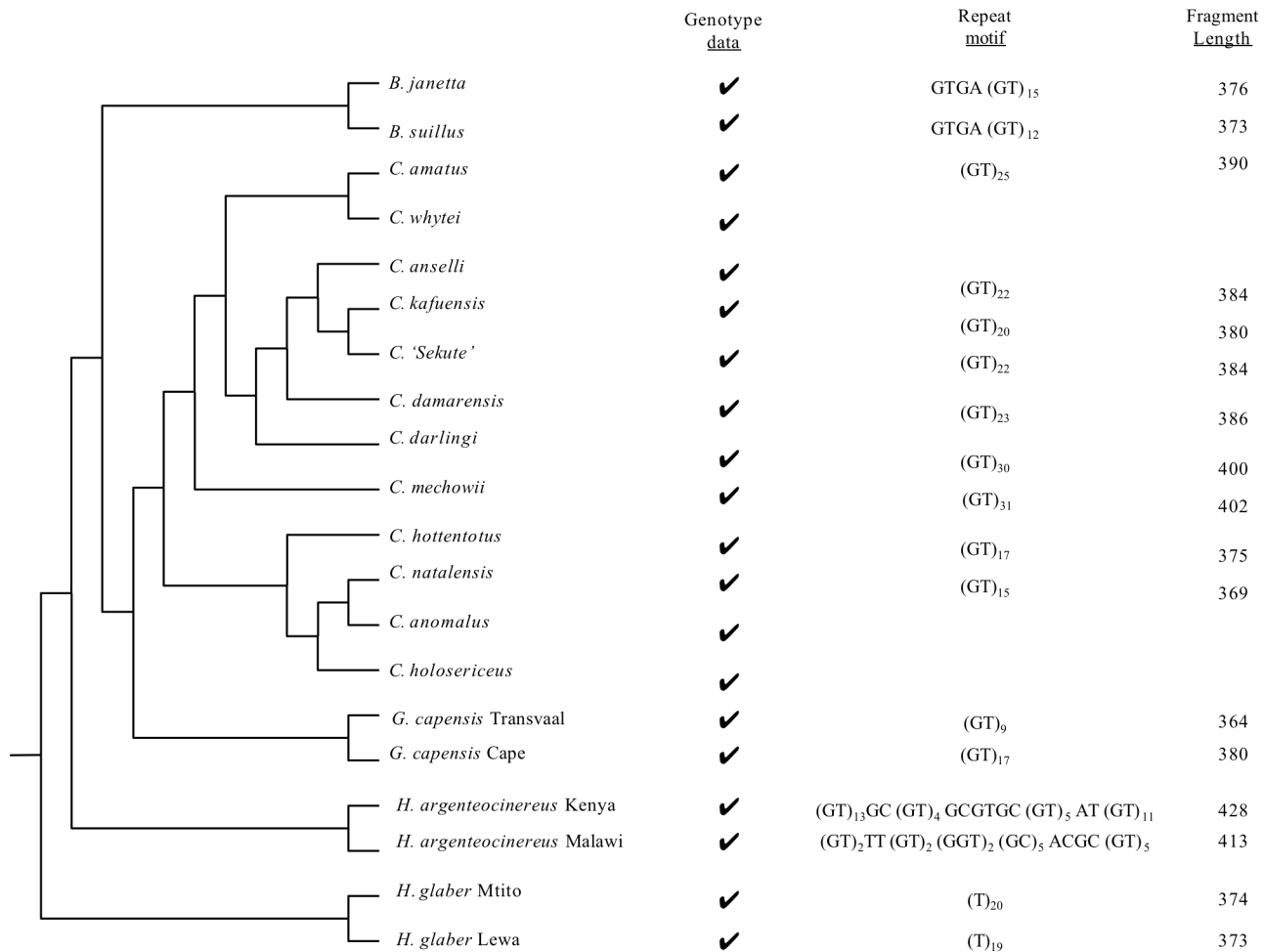


Fig. 4.14 Microsatellite repeat motif of Cmech04 plotted on the phylogeny based on Ingram et al. 2004. ✓ indicates successful genotyping amplification. Fragment length was determined from sequencing product size. For species with multiple samples, a representative was selected. Absence of a repeat motif indicates that no sequence data is available and does not suggest information about the repeat region itself.

Table 4.17 Observed sequence length, repeat motif, indels, and changes in the primer sites for locus Cmech09.

Taxa	Sample	GENOTYPE		Repeat motif	Indels		Primer
		Fragment length	Observed Seq length		TC	C/T	Cmech09-R 5'-CACCCCAACATTATACTCGC-3'
<i>H. argenteocinereus</i>	H050	NA	291	AC(GT) ₆ GC(GT) ₃ GCACGC(GT) ₃ CCATGTGCAC(GT) ₄	-	-	*****G*****A*
<i>H. argenteocinereus</i>	H772	NA	291	AC(GT) ₆ GC(GT) ₃ GCACGC(GT) ₃ CCATGTGCAC(GT) ₄	-	-	*****G*****A*
<i>H. argenteocinereus</i>	HA143	NA	291	AC(GT) ₆ GC(GT) ₂ (GC) ₂ AT(GT) ₂ CCATGTGCAC(GT) ₄	-	-	*****G*****A*
<i>B. suillus</i>	BS	304/306	304	AT(GT) ₃ (GC) ₂ TC(GC) ₂ AT(GT) ₂ CCATGTGCACTT(GT) ₃	X	C	*****
<i>B. suillus</i>	TM41494	304	306	AT(GT) ₂ (GC) ₇ AT(GT) ₂ CCATGTGCACTT(GT) ₃	X	C	*****
<i>B. janetta</i>	BJ	312	312	(GT) ₃ AT(GT) ₃ (GC) ₆ AT(GT) ₂ CCATGTGCACTT(GT) ₃	X	C	*****
<i>B. janetta</i>	N8	298/300	302	AT (GT)10 (GC)7 AT (GT)2 CCATGTGCACTT(GT)3	X	C	*****
<i>G. capensis</i>	TM38354	302	302	(GT) ₁₁ (GC) ₂ AC(GC) ₂ AC(GT) ₃ CCATGTGCACTTGTGCGT	X	C	*****
<i>C. holosericeus</i>	TM41446	NA	304	(GT) ₁₁ (GC) ₆ AT(GT) ₃ CCATGTGCACTT(GT) ₃	-	C	*****A-*
<i>C. natalensis</i>	TM38464	NA	304	(GT) ₁₀ (GC) ₇ AT(GT) ₂ CCATGTGCACTT(GT) ₃	-	C	*****A-*
<i>C. mechowii</i>	Z9	296	296	AT(GT) ₁₀ GC (AC) ₄ AT(GT) ₂ CCATGTGCACTT(GT) ₃	-	C	*****
<i>C. darlingi</i>	DAR4	NA	302	AT(GT) ₂ GC(GT) ₁₀ (GC) ₂ (AC) ₃ (GT) ₃ CCATGTGCACTT(GT) ₃	-	C	*****
<i>C. damarensis</i>	HW3084	NA	302	AT(GT) ₂ GC(GT) ₁₀ (GC) ₂ (AC) ₃ (GT) ₃ CCATGTGCACTT(GT) ₃	-	T	*****
<i>C. damarensis</i>	CHD	306	302	AT(GT) ₂ GC(GT) ₁₀ (GC) ₂ (AC) ₃ (GT) ₃ CCATGTGCACTT(GT) ₃	-	T	*****
<i>C. amatus</i>	AMATUS2	310	306	AT(GT) ₂ GC(GT) ₃ GA(GT) ₄ (GC) ₃ (AC) ₄ (GT) ₃ CCATGTGCACTT(GT) ₃	-	C	*****

NA - no amplification

* X = presence of sequence, - = absence

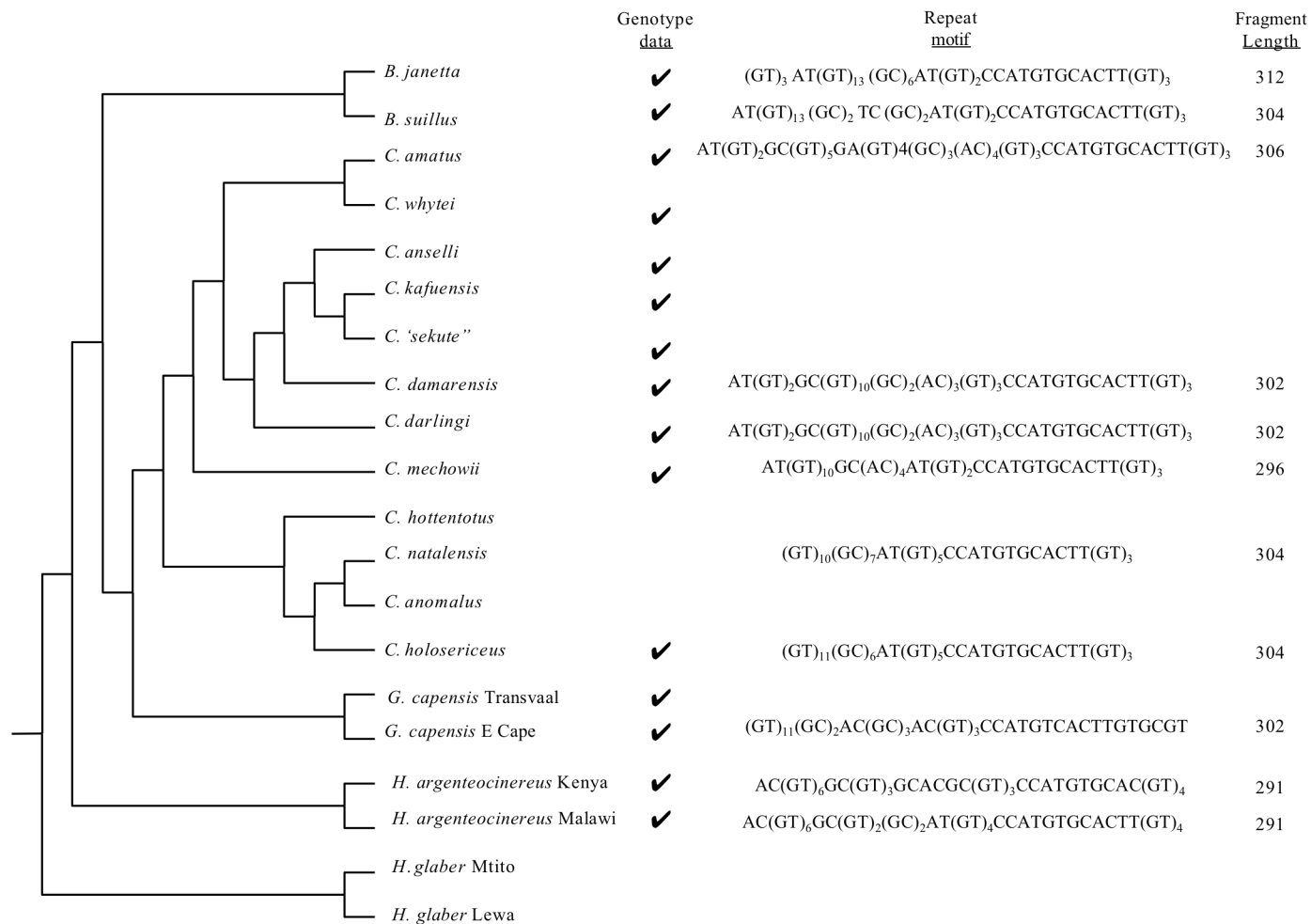


Fig. 4.15 Microsatellite repeat motif of Cmech09 plotted on the phylogeny based on Ingram et al. 2004. ✓ indicates successful genotyping amplification. Fragment length was determined from sequencing product size. For species with multiple samples, a representative was selected. Absence of a repeat motif indicates that no sequence data is available and does not suggest information about the repeat region itself.

Table 4.18 Observed sequence length, repeat motif, indels, additional repetitive regions, and changes in the primer sites for locus Cmech11.

Taxa	Sample	GENOTYPE			Indel immediate indel	CATTCCG	Primers	
		Fragment length	Observed Seq length	Repeat motif			Cmech11-F 5'-GACAGT-GGCCGTAATGTGC-3	Cmech11-R 5'-CCACCTGTGGTTATCTCTCG-
<i>H. argenteocinereus</i>	H050	NA	129	(GT) ₁₆	-----	*****	*****A*****T*****	*****G*G*GT
<i>H. argenteocinereus</i>	HA24	NA	131	(GT) ₁₇	-----	*****	*****A*****T*****	*****G*G*GT
<i>B. suillus</i>	BS	116	117	(GC) ₄ AT(GT) ₅	CTCGCAC	-----	*****A***G**T*****	*****G*A
<i>B. suillus</i>	TM38417	116	117	(GC) ₄ AT(GT) ₅	CTCGCAC	-----	*****A***G**T*****	*****G*A
<i>B. suillus</i>	TM39386	116	117	(GC) ₄ AT(GT) ₅	CTCGCAC	-----	*****A***G**T*****	*****G*A
<i>B. suillus</i>	TM41453	116	117	(GC) ₄ AT(GT) ₅	CTCGCAC	-----	*****A***G**T*****	*****G*A
<i>B. suillus</i>	TM41500	116	117	(GC) ₄ AT(GT) ₅	CTCGCAC	-----	*****A***G**T*****	*****G*A
<i>B. suillus</i>	TM38438	116	117	(GC)4 AT (GT)5	CTCGCAC	-----	*****A***G**T*****	*****G*A
<i>B. janetta</i>	BJ	116	117	(GT)(GC) ₂ AT(GT) ₅	CTCGCAC	-----	*****A***G**T*****	*****G*A
<i>B. janetta</i>	N8	116	117	(GC) ₄ AT(GT) ₅	CTCGCAC	-----	*****A***G**T*****	*****G*A
<i>G. capensis</i>	GPPH2/3	134	130	(GT) ₁₅	CTC----	**C****	*****A**T**T*****	*****GT*
<i>G. capensis</i>	TM38354	NA	136	(GT) ₁₈	CTC----	**C****	*****A**T**T*****	*****GT*
<i>G. capensis</i>	TM38356	136/140	136	(GT) ₁₈	CTC----	**C****	*****A**T**T*****	*****GT*
<i>G. capensis</i>	TM41605	120	140	(GT) ₂₀	CTC----	**C****	**T**A**T**T*****	*****GT*
<i>C. hottentotus</i>	TM38375	132	134	GCGAGCGT(GC) ₆ (GT) ₅	CTCGCGA	**C**T*	*****A*****	*****G**
<i>C. hottentotus</i>	MCA324	132	134	GCGAGCGT(GC) ₆ (GT) ₅	CTCGCGA	**C**T*	*****A*****	*****G**
<i>C. holosericeus</i>	SP7552	132	134	GCGAGCGT(GC) ₆ (GT) ₅	CTCGCGA	**C**T*	*****A*****	*****G**
<i>C. holosericeus</i>	TM41446	132	134	GCGAGC(GT) ₂ (GC) ₂ (GT) ₅	CTCGCGA	**C**T*	*****A*****	*****G**
<i>C. natalensis</i>	CHN2	136	138	GCGAGCGT(GC) ₇ (GT) ₆	CTCGCGA	**C**T*	*****A*****	*****G**
<i>C. anomalus</i>	SP7705	132	132	GCGAGCGT(GC) ₆ (GT) ₅	CTCGCGA	**C**T*	*****A*****	*****G**
<i>C. mechowii</i>	Z9	146/150	150	(GCGA)GTGC(GT) ₁₉	CTCGCGA	**G****	*****A*****	*****G**
<i>C. mechowii</i>	M71	146	154	(GCGA)GTGC(GT) ₂₁	CTCGCGA	**G****	*****A*****	*****G**
<i>C. darlingi</i>	DAR4	144	146	(GCGA)GC(GT) ₁₈	CTCGCGA	**G****	*****A*****	*****G**
<i>C. kafuensis</i>	Z10	146	156	(GCGA)(GC) ₂ (GT) ₂ GC(GT) ₁₈	CTCGCGA	**G****	*****A*****	*****G**
<i>C. damarensis</i>	CHD	144	144	(GCGA)(GC) ₂ (GT) ₂ GC(GT) ₁₃	CTCGCGA	**G****	*****A*****	*****G**
<i>C. damarensis</i>	HW3084	146	146	(GCGA)GCAA(GC) ₂ (GT) ₂ GC(GT) ₁₄	CTCGCGA	**G****	*****A*****	*****G**
<i>C. 'sekute'</i>	LIV	148	148	(GCGA)(GC) ₂ (GT) ₂ GC(GT) ₁₅	CTCGCGA	**G****	*****A*****	*****G**
<i>C. anseli</i>	Z12	150	150	(GCGA)(GC) ₂ (GT) ₂ GC(GT) ₁₆	CTCGCGA	**G****	*****A*****	*****G**
<i>C. anseli</i>	Z4	148	148	(GCGA)(GC) ₂ (GT) ₂ GC(GT) ₁₅	CTCGCGA	**G****	*****A*****	*****G**
<i>C. amatus</i>	AMATUS2/3	152/156	162	(GCGA)(GC) ₂ (GT) ₂ GC(GT) ₂₂	CTCGCGA	**G****	*****A*****	*****G**
<i>C. whytei</i>	B2	142	150	(GCGA)GTGC(GT) ₁₉	CTCGCGA	**G****	*****A*****	*****G**

NA - no amplification

* X = presence of sequence, - = absence

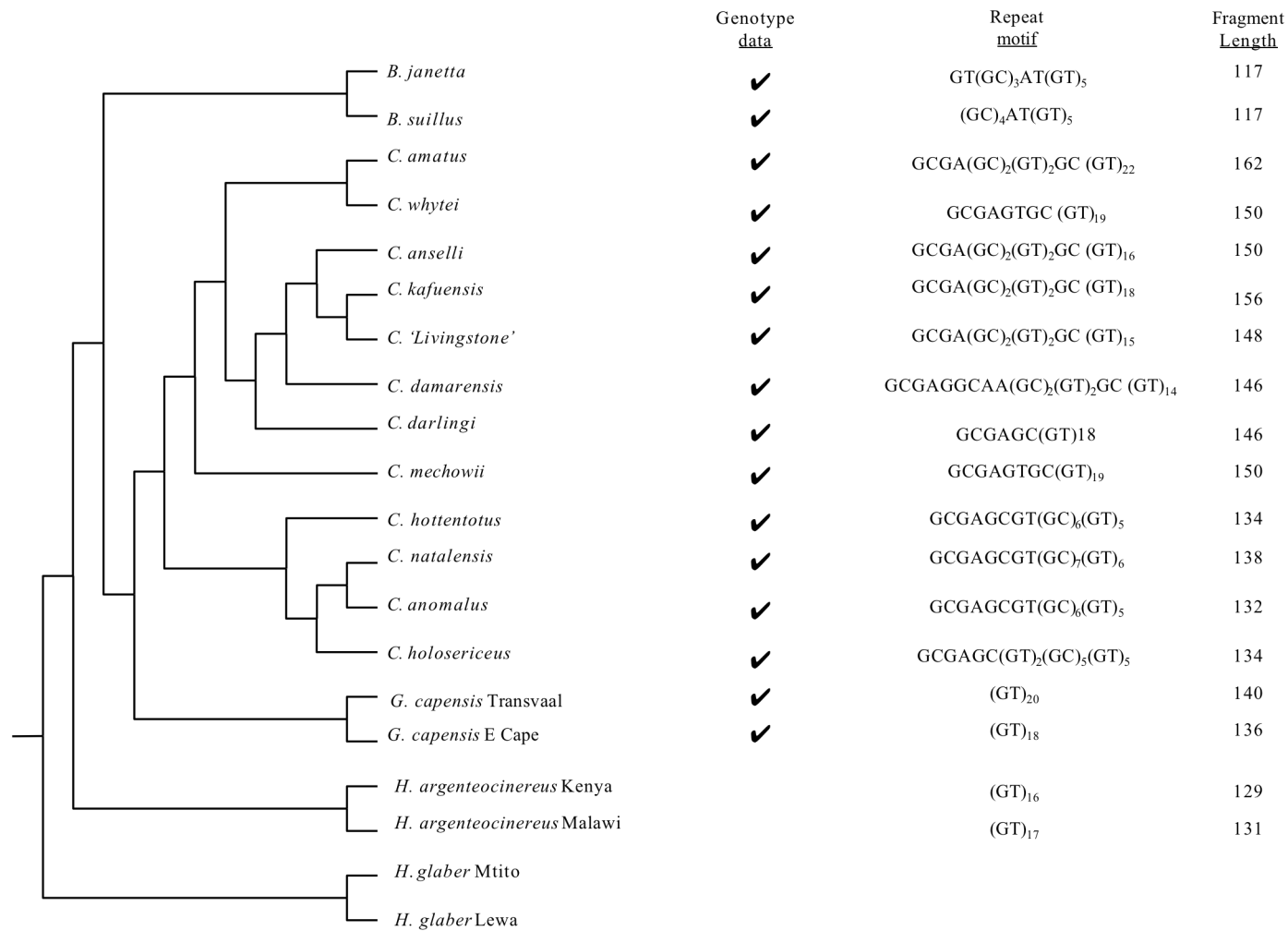


Fig. 4.16 Microsatellite repeat motif of Cmech11 plotted on the phylogeny based on Ingram et al. 2004. ✓ indicates successful genotyping amplification. Fragment length was determined from sequencing product size. For species with multiple samples, a representative was selected. Absence of a repeat motif indicates that no sequence data is available and does not suggest information about the repeat region itself.

Table 4.19 Observed sequence length, repeat motif, indels, and changes in the Hglab10-R primer site for locus Hglab10.

Taxa	Sample	GENOTYPE			Indels			Primer Hglab10-R 5'-TTCTTCTGTTCCTTGTC-3'	
		Fragment length	Observed Seq length	Repeat Motif	G	C/T	GCAACCA		
<i>H. glaber</i>	H006/033/069	304	302	(GT) ₂₁	X	-	-	*****	
<i>H. glaber</i>	MS1	NA	302	(GT) ₂₁	X	-	-	*****	
<i>H. glaber</i>	COL8134	304	302	(GT) ₂₁	X	-	-	*****	
<i>H. glaber</i>	mc16	304	303	(GT) ₂₁	X	C	-	*****	
<i>H. glaber</i>	mr1_3847	294/304	295	(GT) ₁₇	X	C	-	*****	
<i>H. glaber</i>	L4016	294	295	(GT) ₁₇	X	C	-	*****	
<i>H. argenteocinereus</i>	HA24	NA	321	GTTG(GT) ₂ AGGG(GT) ₁₅	AGGG(GT) ₇	-	T	-	***C*****
<i>H. argenteocinereus</i>	HA84	NA	331	GTTG(GT) ₂ AGGG(GT) ₁₃ AT(GT) ₈ AGGG(GT) ₇		-	T	-	***C*****
<i>B. suillus</i>	TM41452	NA	334	(GT) ₂ GCGTAG(GT) ₁₂ TTT(GT) ₁₇		-	-	X	***C*****
<i>B. suillus</i>	TM38419	340	337	(GT) ₂ GCGTAG(GT) ₁₅ TTT(GT) ₁₅		-	-	X	***C*****
<i>B. janetta</i>	BJ	NA	339	(GT) ₂ GCGTAG(GT) ₂₉		-	-	X	***C*****
<i>G. capensis</i>	GPPH3	300/306	306	(GT) ₄ AG(GT) ₁₅		-	-	X	***C*****
<i>G. capensis</i>	TM38354	304/306	304	(GT) ₃ AG(GT) ₁₅		-	-	X	***C*****
<i>G. capensis</i>	TM39874	310	306	(GT) ₄ AG(GT) ₁₅		-	-	X	***C*****
<i>C. hottentotus</i>	MCA324	292	290	(GT) ₄ AG(GT) ₄ GC(GT) ₂		-	-	X	***C*****
<i>C. hottentotus</i>	TM38375	292	290	(GT) ₄ AG(GT) ₄ GC(GT) ₂		-	-	X	***C*****
<i>C. hottentotus</i>	TM41446	292	290	(GT) ₄ AG(GT) ₄ GC(GT) ₂		-	-	X	***C*****
<i>C. holosericeus</i>	SP7519	292	290	(GT) ₄ AG(GT) ₄ GC(GT) ₂		-	-	X	***C*****
<i>C. holosericeus</i>	SP7700	292	290	(GT) ₄ AG(GT) ₄ GC(GT) ₂		-	-	X	***C*****
<i>C. holosericeus</i>	SP7701	292	290	(GT) ₄ AG(GT) ₄ GC(GT) ₂		-	-	X	***C*****
<i>C. holosericeus</i>	SP7552	292	290	(GT) ₄ AG(GT) ₄ GC(GT) ₂		-	-	X	***C*****
<i>C. anomalus</i>	SP7705	292	290	(GT) ₄ AG(GT) ₄ GC(GT) ₂		-	-	X	***C*****
<i>C. mechowii</i>	Z9	314	312	(GT) ₄ AG(GT) ₅ GAT(GT) ₁₃		-	-	X	***C*****
<i>C. darlingi</i>	DAR4	276	326	(GT) ₄ AG(GT) ₄ AT(GT) ₁₀ AT(GT) ₉		-	-	X	***C*****
<i>C. damarensis</i>	HW3053	316/328	340	(GT) ₄ AG(GT) ₄ AT(GT) ₅ TTGT		-	-	X	***C*****
<i>C. damarensis</i>	SP7559	322/332	330	(GT) ₄ AG(GT) ₂₅ TTGT		-	-	X	***C*****
<i>C. damarensis</i>	SP7604	314/324	312	(GT) ₄ AG(GT) ₁₆ TTGT		-	-	X	***C*****
<i>C. damarensis</i>	CHD	300/312	330	(GT) ₄ AG(GT) ₂₅ TTGT		-	-	X	***C*****
<i>C. 'sekute'</i>	SEK	326	324	(GT) ₄ AG(GT) ₄ AT(GT) ₁₇ TTGT		-	-	X	***C*****
<i>C. 'mazubuku'</i>	mazubuku	330	328	(GT) ₄ AG(GT) ₄ AT(GT) ₁₉ TTGT		-	-	X	***C*****
<i>C. 'kasama'</i>	Z5	NA	321	(GT) ₄ AG(GT) ₄ AT(GT) ₁₈		-	-	X	***C*****
<i>C. anelli</i>	Z12	334	332	(GT) ₄ AG(GT) ₄ AT(GT) ₂ TTGT		-	-	X	***C*****
<i>C. amatus</i>	AMATUS2	330	329	(GT) ₄ AG(GT) ₄ AT(GT) ₂		-	-	X	***C*****

NA - no amplification

* X = presence of sequence, - = absence

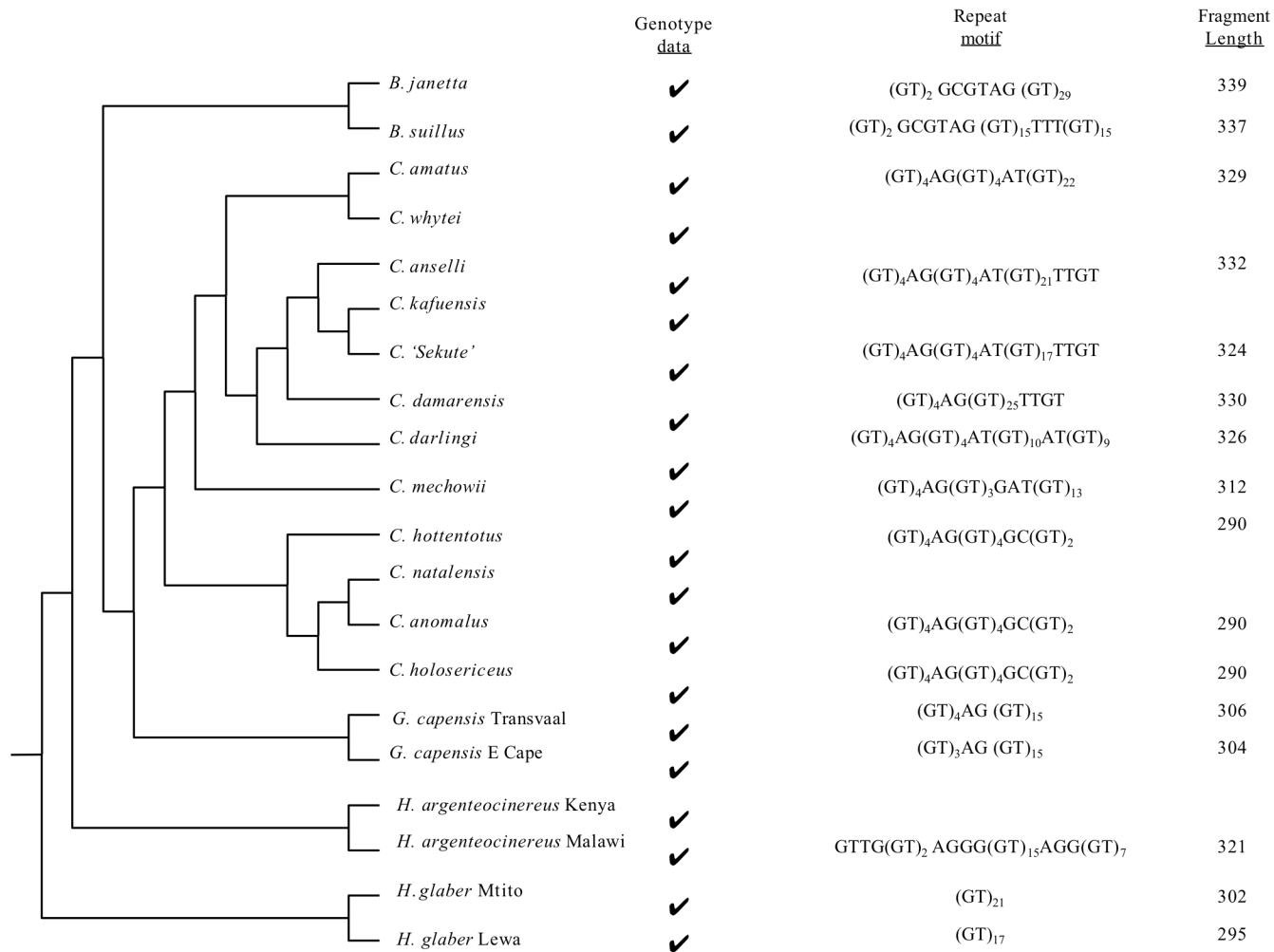


Fig. 4.17 Microsatellite repeat motif of Hglab10 plotted on the phylogeny based on Ingram et al. 2004. ✓ indicates successful genotyping amplification. Fragment length was determined from sequencing product size. For species with multiple samples, a representative was selected. Absence of a repeat motif indicates that no sequence data is available and does not suggest information about the repeat region itself.

genera, while the other three varied between species within both *Cryptomys* and *Coetomys*. Unfortunately, this variation was not documented as errors in genotyping since the genotyping primers did not amplify any individuals of *Coetomys*. Comparison of the repeat motif to the sequencing data showed a lack variation at the repeat motif in all species of *Coetomys* sampled even when there was a difference in genotype that would have been mis-scored with genotype fragment analysis alone (Fig. 4.2).

Mutations in the 3' end of the Harg02-F primer site were documented in *Bathyergus*, *Cryptomys*, and *Coetomys* (Table 4.4; Fig. 4.2). These mutations help explain the lack of amplification of the genotyping fragment in *Bathyergus*, *Coetomys*, and some species of *Cryptomys*.

When RepeatMasker was used to identify any repetitive sequence in the Harg02 sequence, it identified the target region in *Heliophobius* and *Cryptomys*. In both genera, there was variation in the number of repeats. In *Heliophobius*, there were two alleles sequenced, (GTT)₆ and (GTT)₇. Although the genotype fragments were miscalled by two nucleotides from the observed size based on sequencing, the number of repeats was congruent with the genotype allele size of 320 and 323. In *Cryptomys*, the comparison of genotyping and sequencing was puzzling. In the three species with both sequencing information and genotype scores, the genotyping scores were inconsistent, from 3 to 5 bp larger than the fragment length predicted from the sequence. A SINE/Alu element was also identified by RepeatMasker in the Harg02 sequences of *Heliophobius*, *Bathyergus*, and *Coetomys*. Although this element was not identified in *Cryptomys*, it is clear from the sequence alignment that this 54 bp *Alu* element represents a single ancient

Table 4.20 Microsatellite loci with confirmation of null alleles.

Locus	Taxa	Expected allele sizes	Variation at locus	documented change in primer site
Harg02	<i>B. suillus</i>	320	?	yes
	<i>B. janetta</i>	320	?	yes
	<i>C. hottentotus</i>	308/315	yes	yes
	<i>C. mechowii</i>	295	?	yes
	<i>C. kafuensis</i>	289	?	yes
	<i>C. damarensis</i>	295	?	yes
	<i>C. 'Sekute'</i>	295	?	yes
	<i>C. anSELLi</i>	295	?	yes
	<i>C. amatus</i>	297	?	yes
Harg07	<i>B. suillus</i>	588	no	yes
	<i>B. janetta</i>	588	no	yes
	<i>G. capensis</i>	563/599/603	yes	yes
	<i>C. darlingi</i>	627	?	yes
	<i>C. kafuensis</i>	622	?	yes
	<i>C. damarensis</i>	624	?	yes
	<i>C. 'Sekute'</i>	622	?	yes
	<i>C. anSELLi</i>	618	?	yes
	<i>C. amatus</i>	624	?	yes
Gcap01	<i>C. mechowii</i>	122	yes	yes
	<i>C. whytei</i>	132	?	yes
	<i>C. anSELLi</i>	132	?	yes
Gcap07	<i>C. darlingi</i>	226	?	yes
Bsuil01	<i>H. argenteocinereus</i>	196	?	yes
	<i>C. holosericeus</i>	204/212	yes	yes
	<i>C. natalensis</i>	202/206/212	no	yes
	<i>C. anomalus</i>	214	?	yes
	<i>C. kafuensis</i>	210	?	yes
	<i>C. amatus</i>	202	?	yes

Table 4.20 (continued)

Locus	Taxa	Expected allele sizes	Variation at locus	documented change in primer site
Bsuil04	<i>B. suillus</i>	339	?	no (R)
	<i>G. capensis</i>	337	yes	yes
	<i>C. damarensis</i>	311	no	yes
Bsuil06	<i>C. mechowii</i>	243/257	yes	no (R)
	<i>C. darlingi</i>	255	?	no (R)
	<i>C. kafuensis</i>	252	?	no (R)
	<i>C. damarensis</i>	259/265	yes	no (R)
	<i>C. 'Sekute'</i>	259	?	no (R)
	<i>C. anelli</i>	250/260	yes	no (R)
	<i>C. amatus</i>	247		no (R)
Chott01	<i>H. argenteocinereus</i>	273/276/279	yes	yes
	<i>C. kafuensis</i>	285	?	yes
	<i>C. damarensis</i>	290/292	yes	yes
	<i>C. 'Sekute'</i>	281	?	yes
	<i>C. anelli</i>	281/283	yes	yes
	<i>C. amatus</i>	268	?	yes
Cmech03	<i>C. natalensis</i>	269	?	?
Cmech04	<i>H. glaber</i>	374/373	yes	yes
	<i>H. argenteocinereus</i>	428	yes	yes
	<i>C. kafuensis</i>	380	?	no (R)
Cmech09	<i>H. argenteocinereus</i>	291	yes	yes
	<i>C. hottentotus</i>	304	?	yes
	<i>C. natalensis</i>	304	?	yes
	<i>C. darlingi</i>	302	?	no (R)
	<i>C. damarensis</i>	302	?	no (R)
Cmech11	<i>H. argenteocinereus</i>	129/131	yes	yes
	<i>G. capensis</i>	136	yes	yes
Hglab10	<i>H. argenteocinereus</i>	321/331	yes	yes
	<i>B. suillus</i>	334	yes	yes
	<i>B. janetta</i>	339	?	yes
	<i>C. 'Kasama'</i>	321	?	yes

R = only reverse primer included within MFS

insertion event present in all bathyergids with MFS amplification, The presence of this repeat could not be confirmed in *Heterocephalus* since the MFS primers of Harg02 did not amplify in this genus. Sequence divergence of 9.8% between the focal taxon and a representative of *Cryptomys* (TM38464) may explain the lack of identification of this repeat in *Cryptomys* by RepeatMasker. Within the SINE element, there was additional length variation that contributed to fragment length in these taxa. MFS data identified numerous null alleles (Table 4.20).

For Harg03, MFS sequencing efforts recovered sequences for *Heliophobius*, *Bathyergus*, *Georychus*, *Cryptomys*, and *Coetomys*. For each genus, only two individuals from a single species were sequenced (Table 4.5). *Heterocephalus* failed to amplify with either genotyping or sequencing primer sets. RepeatMasker identified the repeat region in all species sampled. The repeat region (GT) is interrupted in all species except for *Cryptomys hottentotus*. In *B. suillus*, *G. capensis*, and *C. mechowii*, the GT repeat is interrupted by an AT, while *Heliophobius* is interrupted with a GC. In addition, three indels were identified in the flanking sequence of Harg03 and these changes all affected fragment length allele size. The MFS sequence revealed homoplasies at this locus. Allele 248 was a homoplastic electromorph in *C.hottentotus* and *C. mechowii* (Table 4.21). When comparing the MFS fragment lengths to the motif sequence, size alone would mis-identify variation at this locus (Fig. 4.3; Table 4.21).

For Harg07, *Heterocephalus* and *Cryptomys* did not amplify the MFS fragment. Although a potential outgroup taxon, (*Hystrix africaeaustralis*: SP7702), successfully amplified, the sequence was not similar to any of the ingroup taxa. The repeat motif was

Table 4.21 Detection of electromorphic homoplasies.

Marker	Allele length	Taxa	motif sequence
Harg03	248	<i>C. hottentotus</i>	(GT)9
		<i>C. mechowii</i>	(GT)3 AT (GT)7
Gcap01	119	<i>H. argenteocinereus</i>	(GT)10 GAGT
		<i>H. argenteocinereus</i>	(GT)9 GAGT
		<i>B. suillus</i>	GTGC (GT)11
		<i>B. suillus</i>	GTGC (GT)10
		<i>C. mechowii</i>	(GT)12
	125	<i>H. argenteocinereus</i>	(GT)13 (GA)2 GT
		<i>C. hottentotus</i>	(GT)14
113	<i>C. damarensis</i>	(GT)6 G (GT)3 GC (GT)4	
	<i>B. suillus</i>	GTGC (GT)8	
Gcap07	234	<i>G. capensis</i>	(GT)10
		<i>C. holosericeus</i>	GTGA (GT)15
		<i>C. natalensis</i>	(GT)17
		<i>C. mechowii</i>	GTGACT (GT)14
		<i>C. kafuensis</i>	GTGACT (GT)15
	236	<i>C. 'livingstone'</i>	GTGACT (GT)13
		<i>C. hottentotus</i>	GTGA (GT)15
	238	<i>C. damarensis</i>	GTGACT (GT)15
		<i>B. janetta</i>	GTGC (GT)4 GC (GT)14
	242	<i>C. amatus</i>	GTGACT (GT)16
		<i>B. suillus</i>	GTGC (GT)4 GC (GT)16
Bsuil01	206	<i>C. 'sekute'</i>	GTGACT (GT)18
		<i>G. capensis</i>	(GT)4 AT (GT)4 GA (GT)2 GC (GT)2
Bsuil06	268	<i>C. hottentotus</i>	(GT)6 GCAT (GT)4
		<i>H. argenteocinereus</i>	(GT)3 GA (GT)11 G (GT)4
	242	<i>H. argenteocinereus</i>	(GT)3 GA (GT)20 G (GT)5
		<i>B. janetta</i>	(GT)2 GA (GT)7 (GGA) (GT)3
		<i>B. janetta</i>	(GT)2 GA (GT)9 (GGA) (GT)4
		<i>G. capensis</i>	(GT)2 GA (GT)5 GG (GT)4 GGTATGT
		<i>C. holosericeus</i>	GTGC (GT)12 G (GT)2
252	<i>G. capensis</i>	(GT)2 GA (GT)13 GGTATGT	
	<i>C. anomalus</i>	(GT)18 G (GT)2	

Table 4.21 (continued)

Marker	Allele length	Taxa	motif sequence
Chott01	277	<i>G. capensis</i>	(GT)20
		<i>C. hottentotus</i>	(GT)18
	291	<i>C. hottentotus</i>	(GT)21
		<i>C. natalensis</i>	(GT)22
Chott03	158	<i>H. argenteocinereus</i>	GC (GT)2 CT (GT)6 CT(GT)4 CT GTGCT (CA)2 CG
		<i>C. amatus</i>	(GC)8 (GT)8 GCGT (GC)2 ATGCA
	160	<i>C. kafuensis</i>	GC (GT)12 (GC)2 GTGCGT (GC)2 ATGCA
		<i>C. damarensis</i>	GC (GT)13 (GC)2 GTGCGT (GC)2 ATGCA
		<i>C. anelli</i>	GC (GT)13 (GC)2 GTGCGT (GC)2 ATGCA
	206/208	<i>C. hottentotus</i>	(GT)2(GC)5(GT)7GCGTGC(GT)2GC(GT)3(GC)5(GT)5GC(GT)5(GC)5A
		<i>C. mechowii</i>	(GC (GT)12 GC (GT)3 GC (GT)2 GCGT (GC)2 ATGCA
Chott08	121	<i>H. argenteocinereus</i>	(GT)5 GGGT (G)7
		<i>B. suillus</i>	(GT)7 (G)6
		<i>C. hottentotus</i>	(GT)11 GG
	115	<i>C. hottentotus</i>	(GT)6 (G)7
		<i>C. hottentotus</i>	(GT)5(G)7
		<i>C. holosericeus</i>	(GT)6 (G)7
		<i>C. mechowii</i>	(GT)5(G)7
		<i>C. kafuensis</i>	(GT)6 (G)5
		<i>C. 'sekute'</i>	(GT)6 (G)4
		<i>C. anelli</i>	(GT)6 (G)5
	111	<i>C. amatus</i>	(GT)6 (G)3
		<i>C. darlingi</i>	(GT)7 (G)3
		<i>C. whytei</i>	(GT)6 (G)5

Table 4.21 (continued)

Marker	Allele length	Taxa	motif sequence
Cmech03	290	<i>B. suillus</i>	(GT)6
		<i>C. 'sekute'</i>	(GT)14
	286	<i>B. suillus</i>	(GT)6
		<i>C. damarensis</i>	(GT)13
		294	<i>G. capensis</i>
<i>C. 'livingstone'</i>	(GT)16		
		<i>C. mechowii</i>	TT(GT)15
Cmech04	374	<i>H. glaber</i>	(T)20
		<i>B. suillus</i>	GTGA(GT)13
	386	<i>C. damarensis</i>	(GT)23
		<i>C. 'mazubuku'</i>	G (GT)24
Cmech11	116	<i>B. suillus</i>	(GC)4 AT (GT)5
		<i>B. janetta</i>	GT (GC)3 AT (GT)5
	132	<i>C. hottentotus</i>	GCGAGCGT (GC)6 (GT)5
		<i>C. holosericeus</i>	GCGAGC(GT) (GC)5 (GT)6
		<i>C. natalensis</i>	GCGAGCGT (GC)6 (GT)5
	144	<i>C. darlingi</i>	GCGAGC (GT)18
		<i>C. damarensis</i>	GCGA (GC)2 (GT)2 GC (GT)13
	146	<i>C. mechowii</i>	GCGAGTGC (GT)21
		<i>C. kafuensis</i>	GCGA (GC)2 (GT)2 GC (GT)18
<i>C. damarensis</i>		GCGAGCAA (GC)2 (GT)2 GC (GT)14	
Hglab10	304	<i>H. glaber</i>	(GT)21
		<i>G. capensis</i>	(GT)3 AG (GT)15
	314	<i>C. mechowii</i>	(GT)4 AG (GT)3 GAT (GT)13
		<i>C. damarensis</i>	(GT)4 AG (GT)16 TTGT
	330	<i>C. 'mazubuku'</i>	(GT)4 AG (GT)4 AT (GT)19 TTGT
		<i>C. amatus</i>	(GT)4 AG (GT)4 AT (GT)22

present in all species of Bathyergidae, although the complexity varied among genera (Table 4.6; Fig. 4.4). In the focal taxon, *Heliophobius*, the repeat motif consisted of a $(GT)_n$ GCTT $(GT)_5$. The repeat region appears to be mutating on only one side of the GCCTT interruption in this genus. In *Georychus*, there were two regions within the microsatellite that are contributing to variation within this species. In *Bathyergus*, the number of repeats was fixed across both species.

Within *Coetomys*, there were two different interruptions in the repeat motif. All had a $(GT)_n$ $(GC)_n$ ATGT in the motif. In *C. darlingi*, *C. damarensis*, *C. 'Sekute'*, and *C. anseli*, there was an additional ATGT interruption between the $(GT)_n$ and the $(GC)_n$ ATGT termination.

Sequencing of the MFS revealed that the Harg07 genotyping primer sites were conserved across the four genera sequenced. Genotyping was not successful in *Bathyergus*, *Georychus*, and *Coetomys* due to a large insertion of 453 bp in the flanking region. This element was not present in the focal species. RepeatMasker recovered a simple dinucleotide repeat in *Heliophobius* and in the 3 genera, another region identified as the repeat class/family LTR/ERV. These are the long terminal repeats of some retrotransposons, similar in structure to retroviruses. Within this region, there was an additional indel that separated *Coetomys* from *Bathyergus* and *Georychus*. Five additional indels were identified in the flanking sequence of Harg07. Four of these were only variable between genera. The fifth indel consisted of a 139 bp insertion in two representatives of *G. capensis*.

3.2.2. *Georychus* (*Gcap*) loci

Two *Georychus* MFS loci (*Gcap01* and *Gcap07*) were sequenced. For *Gcap01*, a thorough sampling of numerous individuals and species in all six genera were sequenced. The sequence from a representative of each genus was searched for any repetitive elements using RepeatMasker. No repetitive sequences were identified in the basal member, *Heterocephalus glaber*. A simple dinucleotide (GT) repeat was identified in the representative of the other 5 genera. The largest repeat (GT)₁₉ was confirmed in *Coetomys anelli*, *C. whytei*, and *Cryptomys hottentotus* and not in the focal taxon as predicted under an ascertainment bias.

Genotyping was successful in all genera but *Heterocephalus*. Changes in both primer sites (*Gcap01-F* = 19%, *Gcap01-R* = 10.5%; Table 4.7) explain the lack of amplification. From the MFS sequencing, no microsatellite was detected at this locus in *Heterocephalus* (Fig.4.5). The flanking sequences, however, were alignable to other taxa, so orthology was assumed. The fragment size predicted by the MFS was within 1-3 bp of the genotyping fragment size in all cases, except for a single individual of *Cryptomys natalensis* (TM38464). This discrepancy cannot be explained by any changes in the flanking sequence.

Two indels were identified in the adjacent flanking region of *Gcap01* (Table 4.7). The first, an additional A was found only in the *Heliophobius* from Malawi. A second 95 bp indel adjacent to the repeat motif (present only in *H. glaber*) was identified as a SINE/ID (ID_RN2). When the SINE/ID fragment was searched with BLAST, a published *C. damarensis* (DMR4) microsatellite sequence (Burland et al. 2004) was

found with a score of 78 bits and a high e-value ($1e-10$). This suggests that the two microsatellite primer sets (Gcap01 and DMR4) are associated with paralogous related SINE/ID elements. With the 95 bp SINE/ID masked from the *H. glaber* sequence, all significant BLAST searches aligned to mRNA sequences associated with PI 3-kinase enhancer long isoform mRNA. Numerous electromorphic homoplasies were identified for allele 113, 119 and 125 (Table 4.21)

The microsatellite and MFS of Gcap07 amplified in all genera but *Heterocephalus*. Genotyping was successful in *Georchus*, *Bathyergus*, *Cryptomys*, *Coetomys*, and *Heliophobius*. Most of the genotype allele sizes were within 1 bp of the predicted size based on MFS sequencing (Table 4.8). One of the *Georchus* samples (GPPH2) had an inconsistent genotype (216/218) with its sequence information (242 bp) the cause of which could not be determined. A *Cryptomys hottentotus* sample (MCA324) also showed inconsistency between genotyping (240 bp) and actual sequence length (234 bp). Amplification was sporadic in *Coetomys* and may be due to mutations in the primer sequence. The genotyping primer region was only confirmed for Gcap07-R and was conserved across *Georchus*, *Bathyergus*, and *Cryptomys*. Mutations in the primer site of *Heliophobius* and *Coetomys* were at different sites (Table 4.8). RepeatMasker identified a simple dinucleotide repeat in the five successfully amplified genera. No other repetitive sequence was identified. A BLAST search found no published sequence of significant similarity. *Georchus* and *Cryptomys natalensis* had perfect (GT) repeats. All other taxa had either interruptions or modifications on the ends of the repetitive element (Table 4.8; Fig. 4.6). Three indels in the flanking sequences

were identified. Two of the indels were the result of poly-As adjacent to the repeat motif. The third indel was the addition of a single nucleotide (A) in *C. damarensis*. Multiple electromorphic homoplasies were identified for allele 234, 236, 238, and 242 (Table 4.21).

3.2.3. *Bathyergus (Bsuil) loci*

Three *Bathyergus* loci (Bsuil01, Bsuil04, and Bsuil06) were sequenced. *Heliophobius*, *Georchus*, *Bathyergus*, *Cryptomys*, and *Coetomys* successfully amplified the MFS of Bsuil01. RepeatMasker detected a dinucleotide (GT) repeat in all genera except *Heliophobius* and *Cryptomys*. RepeatMasker identified a separate dinucleotide (GT) repeat in *Cryptomys*. No repetitive element was identified in *Heliophobius*. When all sequences were aligned, three different and distinct repetitive elements were identified between the genotyping primers, including the two regions identified by RepeatMasker. In a single *Bathyergus suillus* sample (BS), the target microsatellite was a perfect GT repeat, while in all other taxa, the target microsatellite had multiple interruptions in the repeat. In both *Cryptomys* and *Coetomys*, both of the repetitive regions identified by RepeatMasker appear to be mutating (Table 4.11; Fig. 4.7). For the short repeats unrecognized by RepeatMasker, variation was only detectable among genera.

Genotypes across genera could not be compared due to the presence null alleles, impact on fragment length due to indels rather than number of repeats, and the presence of two distinct and mutating repetitive regions in members of this family. Genotyping

was consistent with the sequence length in *Bathyergus* and *Georychus*. However, this was not the case for either *Cryptomys* or *Coetomys*. Sequencing revealed that the priming site of one of the genotyping primers (Bsuil01-R) contained a large indel (14bp) in some taxa (all *Cryptomys* and *Coetomys*) and variation could not be detected by genotyping in all individuals (null alleles; Table 4.20). In addition, the microsatellite was intact in *Heliophobius*, although amplification of the genotyping fragment was unsuccessful. This is most likely due to the changes present in both of the genotyping primers. In the individuals that amplified with the genotyping primers, genotypes were not equal to that of the actual sequence length. Electromorph size homoplasy was identified for at least one allele, 206 (Table 4.21). Additional size homoplasy was seen when comparing genotype sequencing length with repeat motif.

For Bsuil04, the MFS primers did not amplify in *Heliophobius*. RepeatMasker identified a simple dinucleotide repeat in both *Georychus* and *Bathyergus*. Sequencing showed that the repeat was perfect in both genera (Table 4.10; Fig. 4.8). When searched with BLAST, there was no significant similarity to published sequences. In *Coetomys*, the repeat region was replaced by an identical GGGGGTTCGTGTGGGT in all of the species sampled. In *Cryptomys*, the repeat motif was GGGCAG (GT)₃ GGGT. Since only one individual was sequenced, variation within this genus could not be assessed. In *Heterocephalus*, no repetitive sequence was identified and the genotyping primers failed to amplify. Three indels were identified, two of which are distinct across genera. The third was isolated to a loss of GG adjacent to the microsatellite in a single representative of *Georychus* (GPPH2). The genotyping primer Bsuil04-F was conserved in both

species of *Bathyergus*. In *Georchus*, only a single substitution (G→A) was present. In *Cryptomys* and *Coetomys*, there was a change (A→G) in the 2nd position at the 3' end of the primer site. In *Heterocephalus*, two mutation events were observed, both near the 5' end (not in the 3 bp clamp) but may still explain the lack of amplification of genotypes in these two genera (Table 4.10).

All genera amplified the Bsuil06 MFS locus, except *Heterocephalus*.

RepeatMasker identified the simple (GT) dinucleotide repeat in all of the sequenced taxa. The BLAST search did not find any published sequences with significant similarity. In all taxa, the repeat region was interrupted into three different separate sections of (GT) repeats (Table 4.11). In *Heliophobius*, *Bathyergus*, and *Cryptomys*, only one repetitive region was variable within each genus. Within *Coetomys* and *Georchus*, two repetitive sections of the microsatellite changed. The Bsuil06 genotyping primer sites were conserved in all genera, except *Cryptomys*. Even with two mutations within the Bsuil06-R priming site, amplification was successful in *Cryptomys*. In contrast, the Bsuil06-R genotyping primer sites were conserved in *Coetomys*, but did not amplify in any members of the genus (Fig. 4.9). Since the Bsuil06-F primer site was not within the MFS sequence, changes in that region could not be observed.

Three indels were identified within the genotyping fragment of Bsuil06 (Table 4.11). The first indel consisted of a CT or TT sequence present in all taxa but *Cryptomys*. The second indel was the insertion of a single T in two of the three species of *Cryptomys* sampled (*C. holosericeus* and *C. natalensis*). The third indel, a CT insertion, was present in all taxa except for two individuals of *B. janetta* and one *B.*

suillus. Electromorphic size homoplasy, both among and within genera, was detected for three alleles, 242, 252, and 268 (Table 4.21).

3.2.4. *Cryptomys* (Chott) loci

Three *Cryptomys* MSF loci (Chott01, Chott03, and Chott08) were sequenced. The MFS of Chott01 amplified in all genera, except *Heterocephalus*. RepeatMasker identified a simple repeat (GT) in all taxa, as well as two other repetitive elements, an LTR/MaLR (mammalian-apparent LTR) on one side of the repeat region (outside of the genotyping fragment) and a SINE/Alu on the other side starting approximately 80 bp from the repeat. The SINE/Alu was identified in all genera. Although the sequence was present, RepeatMasker failed to recognize the LTR/MaLR in either *Cryptomys* or *Georychus*.

Variation in fragment length of the genotyping fragment was not confined to changes in the dinucleotide motif. Six indels provided additional length variation (Table 4.12; Fig. 4.10). One of the six indels was exclusive to a single genus (*Georychus*). The other five contributed to variation in length both among and within genera. Although not included in Table 4.12, mutations occurred within the SINE/Alu element, most of which contributed to variation in length between genera. There was a deletion of ATTTT seen only in *Heliophobius* (H050) from Kenya that was not shared with *Heliophobius* from Malawi. In both species of *Bathyergus*, there was a 15 bp deletion and in both *Cryptomys* and *Coetomys*, there was a 2 bp (TT) indel. The allele lengths determined via genotyping for the non-focal taxa were inconsistent with the

expected length determined from the sequencing data. This may be due to changes in the stability of the genotyping primers from mutation events combined with the 3' T which is the least discriminating nucleotide increasing the chance for mismatch. Primer Chott01-F was not conserved in any of the sequenced genera. In *Heliophobius*, there was an indel that overlapped with the primer site of Chott01-F and two mutations in the Chott01-R primer site. This explains the lack of amplification with the genotyping primers, documenting null alleles (Table 4.20). In *Bathyergus*, there were changes in both primer sites that may explain the inconsistency of the genotyping lengths. In *Georychus*, although Chott01-R is conserved, numerous mutations affected the forward primer site (three base substitutions and a deletion). This is the only information from the data that could potentially explain the mis-scoring of the genotypes. The Chott01-R primer site in *Coetomys* was conserved, but Chott01-F varied across the species of *Coetomys* (with 3 or 4 substitutions). This is the most likely explanation for the lack of amplification of the genotyping product in *Coetomys*. Electromorphic size homoplasy was detected for two alleles, 277 and 291, both among and within genera (Table 4.21).

The MFS of Chott03 amplified in *Heterocephalus*, *Heliophobius*, *Cryptomys*, and *Coetomys*. An outgroup taxon, *Petromus typicus* (D99), was amplified with these primers. Neither *Petromus* nor *Heterocephalus* were alignable with the other genera or each other. No repetitive element was identified in either. A BLAST search on the *Heterocephalus* (H006) sequence found significant similarity (score= 239, E value = 3e-60) to the large subunit rRNA (LSU/28S). RepeatMasker identified a simple (GT) dinucleotide repeat in *Heliophobius*, *Cryptomys*, and *Coetomys* and a second SINE/MIR

region outside of the genotyping fragment. A BLAST search of these sequences did not find significant similarity with any published sequences. The microsatellite motif was complex in these three genera, consisting of multiple regions of expansion/contraction. No indels were identified within the genotyping fragment. Variation in fragment size, therefore, should only be due to variation in the repeat region. Changes in the primer site were documented for Chott03-R in both *Heliophobius* and *C. mechowii* (Table 4.13; Fig. 4.11). These changes did not appear to be affecting the genotyping product in these taxa. The sequence length determined by the MFS fragments were consistent with the observed genotypes in all cases except one *C. mechowii* (M71). The fragment was 41 nucleotides longer than expected. Electromorphic size homoplasy was identified for at least 3 alleles, 158, 160, and 206/208 (Table 4.21).

The MFS primers for Chott08 amplified in all taxa but *Heterocephalus*, *Georychus*, and *B. janetta*. RepeatMasker did not identify any repetitive sequence in *Heliophobius*, *Bathyergus*, or *Coetomys*. The BLAST search failed to recover any published sequence with significant similarity to the flanking sequence of Chott08. In the focal species, *Cryptomys hottentotus* (TM38375), the repeat region consisted of a simple (GT) dinucleotide repeat flanked by GGG on one side and GG on the other (Table 4.14; Fig. 4.12). In all the other taxa, the GG end was variable, acting as a mononucleotide repeat, while the number of GT repeats was reduced. This poly-G region was variable both among and within genera. The repeat motif was longest in the individual (TM38375) from which the microsatellite locus was designed. Six indels were identified in the genotyping fragment. Four of the six were variable across genera,

while the other two indels were also variable within a genus (*Georychus* and *Coetomys*). Substitutions were identified in both of the genotyping primer sites (Table 4.14). In the Chott08-F site, there were two substitutions in *Heliophobius* and one in *Coetomys*. *Cryptomys holosericeus* had 3 substitutions in the 5' end of the primer site and a deletion in the middle. At the Chott08-R priming site, there was one substitution in the 5' end of the *Heliophobius*, *Bathyergus*, and *Coetomys* sequences. *Coetomys* also had an additional substitution in the center of the primer site. These changes did not appear to have any impacted the amplification of the genotyping locus. Most of the genotypes were consistent with the expected size determined from sequencing the MFS fragment. For the few that did vary, this may be due to slippage of *Taq* polymerase on the stretches of poly-G (Clarke et al., 2001). Electromorphic size homoplasy was detected both among and within genera at three alleles, 111, 115, and 121 (Table 4.21). This is due to the changes in the number of dinucleotide versus mononucleotide repeats.

3.2.5. *Coetomys* (Cmech) loci

Four *Coetomys* MSF loci (Cmech03, Cmech04, Cmech09, and Cmech11) were sequenced. MFS sequences of Cmech03 were generated for all genera, except *Heterocephalus* and *Heliophobius*, neither of which amplified with the genotyping primers. RepeatMasker identified a simple (GT) dinucleotide repeat in *Georychus* and *Coetomys*. A BLAST search failed to find any published sequences with significant similarity to Cmech03. Although not detected by RepeatMasker, the GT repeat was

present in *Bathyergus*, *Georychus*, *Cryptomys*, and *Coetomys*. The GT repeat was longest in the congener, *C. amatus* (amatus2).

RepeatMasker identified an additional CT-rich region within the genotyping fragment in all of the specimens sequenced. This region was fixed in all species of *Coetomys*, except *C. darlingi* (Dar4), which had an additional CT, and *C. mechowii* (Z9 - the individual from which the microsatellite library was constructed) had a TTC in another part of this region. In *Cryptomys*, two different haplotypes were detected with a 3 bp difference. In *Bathyergus* and *Georychus*, this region was variable in length (Table 4.15).

The original genotyping of Cmech03 was only successful for *Bathyergus*, *Georychus*, *Cryptomys*, and *Coetomys* (Fig. 4.13). In *Bathyergus*, polymorphism due to migration of fragment size was observed. This variation was due to mutations in the adjacent CT-rich region. In *Georychus* and *Cryptomys*, variation observed in the fragment analysis contributed to both changes in the number of repeats and within the CT-rich region. Although most of the polymorphism within *Coetomys* was from variation in the number of repeats, mutations within the CT-rich region also contributed to the allele size for *C. darlingi* and *C. mechowii*. In the genotyping primer site of Cmech03, there was a substitution of G→C in the second position of 3' GC clamp in both *Bathyergus* and *Georychus*. Since Cmech03-R was used for both the genotyping and MFS sequencing, changes in that primer site could not be identified. A null allele was identified for *C. natalensis*. Three alleles, 286, 290, and 294, were identified as electromorphic size homoplasies (Table 4.21).

All species were successfully sequenced with Cmech04 MFS primers. RepeatMasker identified the simple (GT) dinucleotide repeat in all taxa, except in *Heterocephalus* where the repeat motif changes from GT to poly-T. The (GT) repeat was perfect in the focal taxon, as well as *Cryptomys*, *Bathyergus* and *Georchus*. In *Heliophobius*, the repeat region had multiple interruptions producing a number of separately variable regions. The largest number of repeats was observed in *Heliophobius* although this was interrupted. RepeatMasker identified an additional repetitive element (CAAAA) in *Georchus* and *Bathyergus*. The BLAST search did not find any published sequences with significant similarity.

Original genotyping data were recovered for all members of the family (Table 4.16; Fig.4.14). In *Heliophobius*, alleles were often greater than 400bp (compared to average of 377 bp for other taxa) and therefore, genotyping was problematic. In *Heterocephalus*, for the individuals that successfully genotyped, the scored fragment length was exactly the same as the sequencing fragment. The fragment lengths recorded as allele sizes in *Bathyergus* were within one base pair of that predicted by the sequencing fragment. In *Georchus*, there was a two base pair difference. The majority of *Cryptomys* samples were within 2 bp, except for *C. hottentotus* (TM38375) that differed by 19 bp. Discrepancies between genotype alleles size and that predicted from the sequence fragment were found within the focal species and some of its congeners. *C. mechowii* (Z9) and *C. darlingi* (DAR4) differed by 28 bp and 20 bp, respectively. There were substitutions in the Cmech04 primer site in at least one representative of each of the other five genera (Table 4.16). In *Georchus* (TM38399), there was a

mutation from A→C in the third base position on the 3' end. In *Cryptomys*, three specimens had a change from A→C in the middle of the primer site and (SP7743) had an additional change from A→T at the third position from the 3' end. In *Bathyergus*, there was a change from C→A in position 8 from the 3' end. In *Heliophobius* and *Heterocephalus*, there was a change in position 15 from A→G.

In addition to the CAAAA repeat identified by RepeatMasker, there were four indels within the genotyping fragment that contributed to size variation at this locus. Three of these indels were only variable across genera. The other one was present in only three species of *Coetomys* and therefore affecting fragment size estimates when making comparisons across species of this genus. Although the CAAA region was fixed in both *Heterocephalus* and *Coetomys*, there was variation at that region within and among the other four genera. Confirmation of a null allele was documented for at least one individual from three different genera, *Heterocephalus*, *Heliophobius*, and *Coetomys* (Table 4.20). For two alleles, 374 and 386, the MFS sequences revealed electromorphic size homoplasies (Table 4.21).

The flanking sequence of Cmech09 amplified in all genera, except *Heterocephalus*. RepeatMasker identified simple repeats in *Coetomys*, *Cryptomys*, *Georychus*, and *Bathyergus*. Although recognized as a simple (GT) repeat, this region was very complex in all taxa, with numerous repeat types and interruptions (Table 4.17; Fig. 4.15). A BLAST search found no significant similarity between the flanking sequence of Cmech09 and any previous published sequence.

The original genotyping primers amplified *Coetomys*, *Georychus*, *Bathyergus*, and *Heliophobius*. Within the genotyping fragment, there were two indels that were variable between genera but fixed within, thus potentially complicating comparisons across genera (Table 4.17). The genotyping and sequenced fragment size were consistent in *Bathyergus* and *Georychus*, within 2 bp. The primer site of Cmech09-R showed some substitutions in the non-focal genera. In *Cryptomys*, it most likely would not amplify due to a mutation at the 3' end of the primer site and an internal deletion at the 3rd bp in at the 3' end (Table 4.17). There were two substitutions in the primer site of *Heliophobius*. Again, this could explain the lack of amplification of the genotype fragment for *Heliophobius*. Genotyping was inconsistent in *Coetomys*. This was unexpected since the primers were designed from *C. mechowii*. Changes in the primer site of Cmech09-F could not be examined since it was used as both the genotyping and MFS primer. Null alleles were documented in *Heliophobius*, *Cryptomys*, and *Coetomys* (Table 4.20).

The Cmech11 MFS primers amplified in all taxa, except *Heterocephalus*. RepeatMasker identified a simple repeat in all taxa except *Cryptomys*, for which no repetitive sequences were found. The BLAST search found significant similarity between sequences published from both human and mouse X chromosome (Score = 62, E value = 1e-06). The flanking sequence immediately adjacent to the repeat had an indel that was unique to each genus (Table 4.18; Fig. 4.16) except *Cryptomys* and *Coetomys* that shared an identical sequence. A second indel (7 bp deletion) was unique to

Bathyergus downstream from repeat but in the genotype fragment. The nucleotide sequence of the 7 bp segment was species-specific for the remaining taxa.

Comparison of the MFS fragment to the genotyping data revealed null alleles in both *Heliophobius* and one *Georychus* (Table 4.5). The genotype data were consistent with the observed fragment lengths of all samples of *Bathyergus*. For *Georychus*, the results were not consistent. Across species of *Cryptomys*, the genotypes were scored two bp shorter than the sequence data revealed, except in *C. anomalus* (SP7705) with identical allele lengths. This documents a case in which some variation remains undetected by the fragment analysis. Genotype data were misleading in *Coetomys*. For samples Z9, Z10, Amatus2, and B2, the genotypes were scored at least 8 -10 bp shorter than the sequence revealed. These discrepancies may be explained by the efficiency of the genotyping primers. Base changes were documented in both primers, Cmech11-F and Cmech11-R, some of which were due to sequence error of the original clone. Neither primer had an exact fit with the sequence from Z9 (the individual from which the primers were designed). In the Cmech11-F site, there was an A present at the seventh position from the 5' end that was undetected during the original primer design. In the Cmech11-R site, there was an error at the third position from the 3' end (T vs. G). This is in the GC-clamp region of the 3' end of the primer and could affect the primers binding. In *Heliophobius*, the genotyping primers did not amplify. This can be explained by the amount of mis-pairing (20% of sequence, all located within the 3' end) at the primer site (Table 4.18). At the Cmech11-R site, *Heliophobius* had 4 substitutions in the last six bases of the primer, affecting the most important binding region for

amplification. Both *Georychus* and *Bathyergus* had substitutions at two of the last three bp, which would affect the efficiency of the primer. This may explain the inconsistent genotypes observed in *Georychus*. Electromorphic size homoplasy was identified for at least 4 alleles, 116, 132, 144, and 146, all of which were genus specific (Table 4.21).

3.2.6. *Heterocephalus (Hglab) loci*

Only one *Heterocephalus* MFS locus provided consistent sequencing results. Hglab10 amplified in all of the six genera of Bathyergidae (Table 4.19). In order to maximize the information for this single Hglab locus, multiple representatives from each genus were included for sequencing.

RepeatMasker identified a simple (GT) dinucleotide repeat in all genera, except for *Cryptomys*. No significant similarity was found between the flanking sequence and any published sequences (NCBI BLAST). In the focal taxon, *Heterocephalus*, the repeat motif was a perfect (GT) dinucleotide repeat. In the other five genera, the repeat motif contained at least one interruption (Table 4.19; Fig. 4.17). *Heliophobius* had multiple interruptions and at least two variable regions in the microsatellite. *Georychus* had a single AG interrupting the (GT) repeat, and in the individuals sampled, only the GT to one side of the interruption showed variation. The interruptions were different between the two species of *Bathyergus*. In both species, there was a GCGTAG interrupting the GT repeat, but in *B. suillus*, there was a second interruption of TTT followed by a third region of GTs. Unlike *Georychus*, the first region was fixed across both species of *Bathyergus* and the second and third regions showed expansions. In all species of

Cryptomys, the repeat motif had two interruptions (AG and GC). There was no variation in this region either among or within any *Cryptomys* species. Within *Coetomys*, the repeat motifs varied across species. All individuals shared the first region of (GT)₄ AG (GT)_n, but the rest of the motif varied across species (Table 4.19; Fig. 4.17). The longest repeat was not detected in the focal taxa as expected. Even though the repeat motif was interrupted in other species sampled, the longest stretches of (GT)_n were present in both *C. damarensis* and *C. amatus*.

Three indels were identified in the genotyping fragment of the Hglab10. The first was a G insertion found only in samples of *Heterocephalus*. The second was variable, with a T present in members of *Heliophobius* and a C in some but not all *Heterocephalus*. The third was a 7 bp indel that differed between *Heterocephalus/Heliophobius* and *Bathyergus/Georychus/Cryptomys/Coetomys*.

Comparison of the genotype allele length from the fragment analysis with the length determined from the sequencing data had mixed results for each genus. Within *Heterocephalus*, the fragment size was within two bases for that expected. Although this did not affect the genotyping size, one of the indels did affect the allele length determined through sequencing. The amplification of Hglab10 was sporadic in *Heliophobius*, so no comparisons could be made. In the three samples of *Georychus*, two were consistent, while the actual fragment length of a third (TM39874) was longer than it would be when scored as a genotype, causing detection of variation when it was not present. Amplification was sporadic in *Bathyergus*, so no confident comparisons could be made. Although varying by two bp, *Cryptomys* had very consistent results

between the genotyping and sequencing data. This locus was fixed across species of this genus, and this was reflected in both datasets. The genotyping data were inconsistent in *Coetomys*. Most species (*C. anelli*, *C. amatus*, *C. mechowii*, *C. darlingi*, *C. 'mazubuku'*, and *C. 'sekute'*) had genotypes that were very consistent with the sequence data, within at most 2 bp. In *C. damarensis*, however, the genotyping results were inconsistent in two of the four samples included. SP7559 and ChD shared at least one allele since their sequences at the repeat motif were exactly the same, but their genotype data were scored differently, 322/332 and 300/312, respectively. Three alleles, 304, 314, and 330, were documented as having electromorphic size homoplasy both among and within genera (Table 4.21).

Across the entire data set, there was a single substitution in the Hglab10-R primer site (Table 4.19). At the fourth position from the 5' end, there was a change from T→C. This substitution was shared among all five non-focal genera. Since Hglab10-F was used in both the genotyping and sequencing reactions, no information about potential changes at that site could be determined. This change in the primer site may explain the problematic amplification of the genotyping fragment in *Heliophobius*, *Bathyergus*, and *Coetomys*, although no issues were observed in the other two genera.

4. Discussion

4.1. Comparison of microsatellite panels based on genotyping data

One advantage of microsatellite loci is their ability to cross-amplify in closely related taxa. When determining if a microsatellite locus was useful in amplifying

members across the family Bathyergidae, a number of criteria were considered: 1) consistency of amplification across genera; 2) number of genera amplified; 3) the number of genera showing polymorphisms for a given locus. For the six panels of microsatellites presented here, none successfully amplified in all taxa. The results were skewed. *Heterocephalus* (Hglab) primers were the most successful, with three loci amplifying in all genera. It should be noted that loci designed from other taxa were least successful in amplifying in *Heterocephalus*, suggesting that isolating these loci from the most basal taxa may recover ancestral and even conserved microsatellites. In contrast to this, *Heliophobius* markers had the lowest success rate in amplifying in other taxa. Only three other loci successfully amplified in all members of the family. The *Cryptomys* locus, Chott05, amplified in all genera, but it was monomorphic in *Heterocephalus*. Two other loci, Gcap10 and Cmech04, showed greater promise of cross-taxon utility, being polymorphic in all genera.

By examining these markers in a phylogenetic context, one would expect that more closely related taxa would have a higher success rate in the amplification of non-specific primers. This was observed in several loci, especially for sister-genera. For example, most *Heterocephalus* loci (67%) amplified in its closest relative, *Heliophobius*. However, no *Heliophobius* markers amplified *Heterocephalus*. *Heliophobius* had the least number of loci that amplified in other taxa, with three loci (of 7) amplifying only in *Heliophobius*. Although the comparisons in this study were limited in size, with only 5 – 7 loci per genus, these results suggest that the assumption that microsatellites will be informative markers in closely related taxa is not necessarily true.

4.2. Comparisons of repeat motifs and the function of sequence data

Direct sequencing of the MFS fragments affords the only method to conclusively examine the evolution of the microsatellite repeat motif (Zhu et al., 2000). By plotting the repeat motifs on the phylogeny, it becomes apparent that interruptions within a repeat motif are phylogenetically informative (Fig. 4.2 – 4.17). The use of multiple sequence alignments provides a means for establishing the true limit of the repetitive element. By default, the presence of a repetitive element is obvious during examination of the original focal taxon during primer design, and most of the observed changes in allele size are attributed to deletion or addition of a few units of repeats (Eckert et al., 2002; Deka et al, 1995), fitting the assumptions of the SMM (Ohta and Kimura, 1973). The majority of mutation at these loci are believed to be from slippage of DNA polymerase which results in the loss or gain of the repeat element (Primmer et al., 1996a; Weber and Wong, 1993; Schlötterer and Tautz, 1992; Levinson and Gutman, 1987). This assumption is clearly violated by the results presented here, for microsatellite evolution in Bathyergidae. Multiple studies, including this one, have documented variation that was not accounted for by changes in the repeat (Blankenship et al., 2002; Macaubas et al., 1997; Deka et al., 1985; Valdes et al., 1993). Additional studies of other natural populations will be necessary to see if this is a general pattern and help to incorporate additional mechanisms that are affecting these regions of DNA.

4.3. *Is ascertainment bias a problem?*

Microsatellite markers are often used because of their ability to be cross-amplified in closely related taxa and the literature is laden with warnings about the potential for an ascertainment bias as a result of methods used in the isolation of the markers (Hutter et al., 1988; Ellegren et al., 1997; Forbes et al., 1995). Since the markers presented here were designed using the same parameters, this bias should be apparent when making comparisons across the six different microsatellite panels. If there is an ascertainment bias, then the number of alleles and maximum allele length should be highest in the focal species (Amos, 1999). This trend was not observed in the data presented here. As shown in Table 4.3, the largest allele, highest number of alleles, and largest range in allele lengths were not identified in the focal species more frequently than in the non-focal species. Looking at each microsatellite panel separately, results could be misleading. For instance, if only *Coetomys* loci had been used, the results suggest an ascertainment bias. While these trends may be isolated to the family Bathyergidae, it does provide a model for investigating the dynamics of microsatellites and effects of primer design protocols.

4.4. *Electromorphic size homoplasy*

Through the use of direct MFS sequencing, electromorphic size homoplasies were detected as changes in the repeat motif in twelve of the sixteen loci sampled, with a total of 32 homoplastic alleles sequenced (Table 4.21). Genotypic fragment length allele size alone was very limited at detecting the amount of variation present at these loci.

When primers are used in taxa beyond their original design, hidden variation at the locus is expected (Culver et al., 2001; Gertsch et al., 1995). In most cases, as expected, the homoplastic events were between different species or genera. In four cases, however, homoplastic electromorphs were discovered within a species, but these were observed in cross-taxon comparisons. In the Chott08 locus, an allele observed in the *C. hottentotus* had different repeat motifs in separate individuals. Considering the limited nature of the intraspecific sampling of this study, these data suggest that the incidence of homoplasy could be much higher than predicted, and caution should be made when accepting fragment length results without confirmation of distinct alleles. Genotyping fragment analysis alone can lead to miscalculations of allele frequencies, deflated measures of heterozygosity within populations, and decreased measures of divergence between populations (Balloux et al., 2000; Hedrick, 1999). This is important to consider when using microsatellite markers for conservation and population genetic studies.

4.5. Null alleles

Like electromorphic size homoplasies, non-amplifying (or null alleles) are believed to predominate when primers are used in cross-specific or cross-generic amplification (Pemberton et al., 1995). Lack of amplification provides no direct information about the locus itself. In general, lack of amplification of the original genotyping fragment, however, shows clear phylogenetic constraint (Figs. 4.2- 4.17). In the sixteen loci sequenced, null alleles were detected at thirteen (Table 4.20). The majority of these null alleles were detected in non-focal species. Only one locus,

Bsuil04, produced a null allele in the focal species. In 100% of the null alleles sequenced, a microsatellite repeat motif was observed. By using MFS sequences, microsatellite repetitive elements can be confirmed and changes in the genotyping primers detected. In 46 of the 58 null alleles detected, mutations in the genotyping primer site explain the lack of amplification.

4.6. Rare genomic changes (RGC)

Rare genomic changes (RGCs) such as indels, gene order, LINES/SINEs, Alu elements, and LTRs, are becoming increasingly important in phylogenetics and comparative genomics (de Jong et al., 2003; Matthee et al., 2001; Okada, 1991; Rokas and Holland, 2000; Springer et al., 2004; Takahashi and Okada, 2002). Arcot et al. (1995) reported an association between *Alu* elements with microsatellite repeats, and suggested that these elements may be the catalyst for microsatellite genesis. In dipterans, a novel mobile element, *mini-me*, has been identified that is believed to be associated with microsatellite genesis (Wilder and Hollocher, 2001). In the present study, multiple indels were present at 14 of the 16 loci sequenced and showed potential for being phylogenetically informative. Three loci had SINE elements, and one locus, Harg07, contained an LTR within the genotyping fragment. In sequences outside of the genotyping fragment, multiple transposable elements and indels were identified (data not shown).

The SINE/Alu element identified by RepeatMasker in one locus in particular (Harg02), is noteworthy. This element was identified in the sequences of *Heliophobius*,

Bathyergus, and *Coetomys*, but not in *Cryptomys*. From the sequence alignment, this 54 bp *Alu* represents a single ancient insertion event. Further inquiry identified this *Alu* as a FLAM_A. FLAM_A and associated 6 bp homology motif (CAAATT – present in all samples sequenced) have been linked with deletion breakpoints associated with human disease (Krawczak and Cooper, 1991; Trarbach et al., 2004). A parsimony analysis of the 54 bp FLAM_A sequence (5 parsimony-informative sites) revealed sequence divergence of 9.8% between the focal taxon and a representative of *Cryptomys* (TM38464), and yielded 18 trees (CI = 1.0, RI = 1.0). Analyzing the nucleotides of this FLAM_A *Alu* provided five parsimony informative characters, while presence/absence of the element alone would have been uninformative. The results of this study contribute to the growing data that support the association of microsatellite repeats with RGCs, and provide a method to isolate these informative sites.

5. Conclusions

This study provides a novel look at the evolution of microsatellites. While previous studies have examined few loci within a phylogenetic context, or made reciprocal comparisons between two species, this study provides a broader picture of how some microsatellite loci are evolving. The number of electomorphic homoplasies, null alleles, and changes within the flanking sequence that impact allele size were markedly high. This study shows the importance of characterizing the entire genotyping fragment across all taxa of interest, and the use of MFS allows for characterization of the repeat motif, RGCs in the flanking sequence, and mutations at the priming sites,

confirming null alleles. While this study was restricted to the family Bathyergidae, there is no reason to believe that these patterns are isolated to this family, especially when other studies examining phylogenetic relationships across Mammalia have utilized nuclear markers that successfully amplify in the Bathyergidae (Murphy et al., 2001).

CHAPTER V

**THE UTILITY OF MICROSATELLITE FLANKING SEQUENCES AS DATA IN
PHYLOGENETIC RECONSTRUCTION**

1. Introduction

Microsatellite loci represent a class of molecular markers ideal for detailed studies of variation within a species (Bowcock et al., 1994; Gardner et al., 2000; Sunnucks, 2000). These molecular markers occur in thousands of copies within the mammalian genome and are distributed throughout autosomes and sex chromosomes (Dietrich et al., 1996; Goodfellow, 1993; Weber and May, 1989). A locus is defined by a specific repeat motif, consisting of multiple, tandem repeat units that vary in size from 2 to 5 nucleotides and flanking sequences specific to a particular chromosomal region (Tautz, 1993; Weber and May, 1989). Variation at microsatellite loci is the consequence of mutations involving insertions and deletions (indels) of specific repeat units during replication, which yield alleles differing in overall length (Weber and May, 1989; Weber and Wong, 1993). Most microsatellite loci are highly polymorphic, owing to a mutation rate ranging between 10^{-5} and 10^{-2} mutations per generation (Edwards et al., 1992; Macaubus et al., 1997). Their distribution throughout the genome and high levels of polymorphism provide a useful means of mapping genomes (Causse et al., 1994; Dib et al., 1996; Su and Willems, 1996) as well as providing markers for epidemiology (Wang et al., 2001), forensics (Edwards et al., 1991), and the establishment of relatedness among individuals (Altet et al., 2001; Queller et al., 1993). Microsatellite loci have

proven useful to population genetics, especially in studies involving the partitioning of genetic variation within and between populations that have experienced fragmentation and/or bottlenecks (Kimmel et al., 1998; Luikart et al., 1998a, b; Rooney et al., 1999; Taylor et al., 1994). As such, these markers have been broadly applied in conservation genetics (Maudet et al., 2002; O’Ryan et al., 1998; Paetkau et al., 1995; Roy et al., 1994; Roy et al., 1996).

One major analytical hurdle associated with microsatellite loci relates to the particular mutation processes responsible for allelic variation at a locus. This process complicates selection of models used to provide accurate estimates of population genetic parameters such as gene flow, population subdivision, and genetic distance between populations (Calabrese et al., 2001; Goldstein and Pollack, 1994; Goldstein et al., 1995b; Kimmel et al., 1998; Slatkin, 1995). In broad scale studies of geographic variation among widespread populations within species, such as humans, selection of both the appropriate model of evolution and the tree/network building method influences the resultant relationships (Goldstein et al., 1995a). Several studies have used distance-based approaches (neighbor-joining) for phylogenetic reconstruction to determine relationships among members of closely related species (Takezaki and Nei, 1996). In the case of the *Peromyscus maniculatus* species complex, ten microsatellite loci successfully approximated the well-corroborated phylogeny (Chirhart et al., 2004). In their study, however, the model selection and the tree building method influenced accuracy.

Problems associated with the use of fragment size data produced for microsatellite loci prevent widespread use of these markers for phylogenetic studies. As phylogenetic distance increases, the probability of homoplasy increases due to back mutations of fragment length (alleles). Therefore, alleles based on fragment size may not be homologous (identical by descent). This is especially troubling given some empirical evidence suggesting a ceiling on the length of alleles (Garza et al., 1995). Another potential source of homoplasy in estimates of allele size based on fragment length relates to insertion/deletion (indel) events in flanking sequences. This results in the convergence of scored allele sizes derived from different motif length + indel combinations (see Chapter IV). Despite problems associated with the use of allele size data at microsatellite loci for phylogeny reconstruction, these loci have the potential of providing a more accurate genome-wide assessment of variation and relatedness among species. For instance, microsatellite loci map to specific chromosomal sites defined by their unique flanking sequences, and they are distributed throughout the genome. Therefore, direct comparisons of nucleotide sequence differences in their flanking regions can be used to reconstruct relationships among species over considerably larger scales of divergence. To date, only a few studies (Arévalo et al., 2004; Ortí et al., 1997; Schlötterer, 2001; Zardoya et al., 1996) have addressed the utility of flanking sequences for phylogeny reconstruction, and these relied on a small number of loci.

The goal of this chapter is to assess the utility of microsatellite flanking sequences in recovering the phylogenetic relationships within and among genera of African mole-rats (Bathyergidae: Rodentia). African mole-rats represent a monophyletic

group endemic to sub-Saharan Africa, and relationships among the genera are well supported by morphological, chromosomal, and nuclear and mitochondrial DNA sequence data (see Chapter II; Allard and Honeycutt, 1992; Faulkes et al., 1997; Ingram et al., 2004; Janecek et al., 1992; Walton et al., 2000). Currently, there are six recognized genera: *Heterocephalus* (1 species) and *Heliophobius* (1 sp), which are restricted in distribution to Eastern Africa; *Bathyergus* (2 sp) and *Georchus* (1 sp), which are limited to southern Africa; *Coetomys* (13 species currently recognized), whose range extends from Ghana in west Africa to southern Sudan and northern Angola in east Africa, and south to Namibia just crossing the border of Botswana into South Africa where it is replaced by *Cryptomys* (5 species currently recognized) which extends to the Cape Province of South Africa (Aguilar, 1993; Burda et al., 1999; Faulkes et al., 1997; Honeycutt et al., 1987; Macholán et al., 1993; Walton et al., 2000). Using the well-resolved phylogeny as a framework, the ability of microsatellite flanking sequences (MFS) to recover the relationships within this family can be assessed. Rather than relying on the flanking sequence of a single microsatellite locus as done in previous studies (Jin et al., 1996; Ortí et al., 1997; Schlötterer, 2001; Zardoya et al., 1996), I designed microsatellite flanking sequence (MFS) loci for each of the six genera, so comparisons could be made on the amount of phylogenetic information that each locus provides, as well as combinations of multiple intra- and cross-taxon loci.

2. Materials and Methods

2.1. Taxon sampling and DNA isolation

For the monotypic genera: *Heterocephalus*, *Heliophobius*, and *Georychus*, a minimum of two individuals were chosen from the extremes of their geographic distribution to increase the chance of assessing the amount of variability within each species. For *Bathyergus*, *Cryptomys*, and *Coetomys*, representatives from a number of species were included. DNA from either frozen liver and/or skin samples preserved in ethanol (70%) was isolated by proteinase-K digestion followed by either phenol/chloroform extraction or QIAGEN DNAEasy spin columns (Qiagen Inc., Valencia, CA).

2.2. Microsatellite flanking region amplification and sequencing

All MFS primer sets (described in Chapter IV) were screened via the polymerase chain reaction (PCR) across all available lineages of Bathyergidae to assess the conservation of each locus. The sequencing efforts focused on loci that successfully amplified across the majority of the taxa. When possible, genotypic homozygotes (determined from original microsatellite genotyping – See Chapter IV), representing multiple localities within each taxon, were sequenced to characterize the microsatellites' repeat motifs and flanking regions. Initial amplification was performed using the external primers that flanked the genotyping fragment. Approximately 20 – 100 ng of template DNA was amplified in 50 μ L reactions using 0.5 μ L of EX-*Taq* polymerase (Takara), 5 μ L of 10X EX-*Taq* Buffer w/ MgCl₂ (Takara), 5 μ L of 2.5 mM dNTPs

(Takara), 0.1 μ M of each primer, and ddH₂O to a final volume. Reaction conditions consisted of an initial denaturation at 94 °C for 5 min, followed by 35 cycles of a 94 °C for 30 sec, 58 °C for 30 sec, and 72 °C for 30 sec, with a final extension at 72 °C degrees for 10 min. Amplification of the correct fragment length was confirmed by electrophoresis of PCR product (5 μ L) with a size standard on 1% agarose minigels, stained with ethidium bromide, and visualized under UV light. When amplification was unsuccessful, additional attempts were made using a gradient block PCR thermal cycler (MJ Research) at annealing temperatures ranging from 50 – 65 °C, with all other reaction parameters remaining identical. PCR products were cleaned using QIAquick Spin PCR purification spin columns and followed a standard protocol (Qiagen Inc., Valencia, CA).

Both strands of the PCR product were sequenced using the PCR primers. Each fragment was sequenced in both directions at least two times for confirmation of the sequence. This was necessary due to decline in quality of the sequence once the repeat motif was encountered. When necessary, the original genotyping primers were used in an attempt to increase the quality of the sequencing across the repeat motif. Cycle sequencing reactions were performed using ABI Prism BigDye Terminator v3.0 chemistry (Applied Biosystems, Foster City, CA), with 25 cycles of 97 °C for 30 sec, 50 °C for 5 sec, and 60 °C for 2 min. Excess terminator dye, oligonucleotides, and polymerase were removed by centrifugation at 3000 rpm through a Sephadex G-50 matrix (Sigma-Aldrich, Inc.). Sequencing reactions were electrophoresed and analyzed on an ABI 377 XL automated sequencer or ABI PRISM® 3100-Avant Genetic Analyzer. Sequence data were imported into SEQUENCHER v4.2 (Gene Codes

Corporation, Ann Arbor, MI) for alignment and contig assembly for each individual. Once the entire sequence was confirmed by overlapping reads, the contigs were exported in FASTA file format. Repeat motifs were masked using RepeatMasker v3.0 (Smit et al., 2004), that identifies the repetitive sequence with lower case so that the repeat could be delimited and masked from further analysis, yet remain in the alignment. All sequences for a locus were initially aligned using SEQUENCHER to establish that fragments were homologous and provided a rough alignment. Each alignment was then imported into MacClade v4.05 (Maddison and Maddison, 2002) and fine-tuned visually using the plain molecular data matrix setting, and saved in NEXUS format for analysis.

2.3. *Data analyses*

Maximum-parsimony (MP) analyses were performed using PAUP* v4.0b10 (Swofford, 2002). Amplification of an outgroup, outside of Bathyergidae, was unsuccessful in all loci and midpoint rooting was applied to all trees. When possible, a branch-and-bound search was performed. If the branch-and-bound search exceeded 24 hours, the run was terminated and the shortest tree length found was used as the maximum tree length for a heuristic search with 1,000 replicate searches, random addition of taxa, and TBR branch swapping, with the steepest descent option not in effect. When equally-weighted searches failed to recover a single MP tree, additional MP analyses were performed with characters successively-weighted (Farris, 1969) by their rescaled consistency index (RC: Farris, 1989). For each locus, the analyses were multi-tiered: 1) all the sequence data, including the repeat sequence, and 2) flanking

sequence alone with the repeat motif removed from analyses by square brackets in the NEXUS file. Bootstrap resampling (Felsenstein, 1985) and decay indices (Bremer, 1988) were used as relative measures of nodal support. Bootstrap analyses were initiated using 1,000 replicates, each with 100 random addition sequences and TBR branch-swapping using PAUP*. Decay indices were generated using MacClade and PAUP*.

To determine the appropriate model of evolution for maximum-likelihood (ML) analyses, the Akaike information criterion (Akaike, 1974) was calculated using MODELTEST v3.06 (Posada and Crandall, 1998). Under the estimated model for each locus, a heuristic search, with 10 random addition sequences and TBR branch-swapping, was used to obtain a ML tree. Bootstrap support for the ML tree was determined using the "fast" stepwise addition option and a minimum of 100 replicates.

To investigate the phylogenetic utility of all MFS loci combined, the datasets were pared down to representatives from each genus and analyzed together with characters coded as missing for incomplete or missing sequences. A minimum of one specimen per genus was selected based on high representation across all data partitions/loci. Identifiable indels across all sixteen loci were coded for representative of each genus in a presence/absence matrix and analyzed using an exhaustive search under MP. Nodal support was assessed using bootstrap proportions.

3. Results

3.1. Success of sequencing effort across MFS loci

Sequence data were recovered for the MFS of 16 microsatellite loci. The number of genera that successfully amplified and sequenced varied across loci (Tables 4.4–4.21). Only three genera (ten species) were successfully sequenced for Chott03. Four loci, Harg02, Harg07, Cmech03, and Chott08, successfully amplified in only four genera (10 – 14 species). Eight loci (Harg03, Bsuil01, Bsuil04, Bsuil06, Gcap07, Cmech09, Cmech11, and Chott01) successfully amplified and sequenced across five genera (6 – 16 species). One non-focal locus (Bsuil04) amplified in *Heterocephalus*, but not in *Heliophobius*. Three loci, Cmech04, Gcap10, and Hglab10, successfully amplified and sequenced all six Bathyergid genera (16 – 17 species).

3.2. Phylogenetic analyses of 16 microsatellite flanking sequences

The average number of characters, number of variable sites, and parsimony-informative characters at each locus were 403 ($R = 194 – 683$), 67 ($R = 13 – 120$), and 46 ($R = 9 – 89$), respectively (Table 5.1). The average percent of variable sites was 16.4% ($R = 6.7 – 26.9\%$). The average percent of variable sites that were parsimony-informative was 66.8% ($R = 25 – 91.5\%$).

Either branch-and-bound or heuristic searches recovered a single parsimonious tree at nine loci (MP trees not shown: CI = 0.864 – 1.0, RI = 0.92 – 1.0; see Figs. 5.1 – 5.9). In eight of these trees (Figs. 5.2 – 5.9), the genera formed well-supported

Table 5.1 Phylogenetic use of microsatellite flanking sequences (MFS).

Locus	# of genera	# of species	# of haplotypes	# of characters	# of variable sites	% variable	# of pars-inf	% pars-inf	# trees	TL	CI	RI	HI	model	I	G	- ln L	# ML trees
Hglab10	6	16	25	412	111	26.9	89	80.2	10	130	0.915	0.975	0.085	TVM+G	-	1.7604	1271.2428	22
Harg02	4	12	15	606	82	13.5	62	75.6	1	89	0.955	0.977	0.045	TrN	-	-	1396.5031	1
Harg03	5	5	8	194	13	6.7	9	69.2	1	14	1	1	0	HKY	-	-	347.35284	1
Harg07	4	10	13	683	73	10.7	53	72.6	1	77	0.974	0.984	0.026	HKY	-	-	1418.2163	1
Bsuil01	5	13	21	365	55	15.1	31	56.4	1	66	0.864	0.92	0.136	K80+G	-	0.3896	900.72252	1
Bsuil04	5	11	11	310	44	14.2	14	31.8	6	59	0.966	0.95	0.05	HKY	-	-	739.38997	3
Bsuil06	5	14	18	277	50	18.1	36	72.0	1	55	0.945	0.978	0.055	GTR	-	-	707.68314	101
Gcap01	6	16	23	493	89	18.1	68	76.4	3	97	0.969	0.988	0.031	K80	-	-	1244.5058	1
Gcap07	5	16	22	318	55	17.3	38	69.1	1 *SA	73	0.822	0.926	0.178	TrN+G	-	0.2234	871.84045	1
Chott01	5	14	20	657	120	18.3	85	70.8	3 *SA	144	0.931	0.975	0.069	K81uf+G	-	0.6229	1148.4598	1
Chott03	3	9	14	253	33	13.0	24	72.7	1	36	0.972	0.984	0.028	HKY	-	-	558.96569	1
Chott08	4	13	18	347	85	24.5	46	54.1	9	94	0.979	0.987	0.071	K81uf	-	-	1008.6729	4
Cmech03	4	14	11	196	22	11.2	20	90.9	1	26	0.923	0.977	0.077	K80	-	-	427.57847	4
Cmech04	6	15	22	382	94	24.6	86	91.5	1	115	0.904	0.972	0.096	K80+G	-	0.7714	1168.6965	1
Cmech09	5	10	14	512	85	16.6	52	61.2	1	95	0.937	0.956	0.063	TrN+G	-	1.0917	1260.4849	2
Cmech11	6	16	30	436	60	13.8	15	25.0	2	64	0.969	0.992	0.031	TrN	-	-	999.01887	1

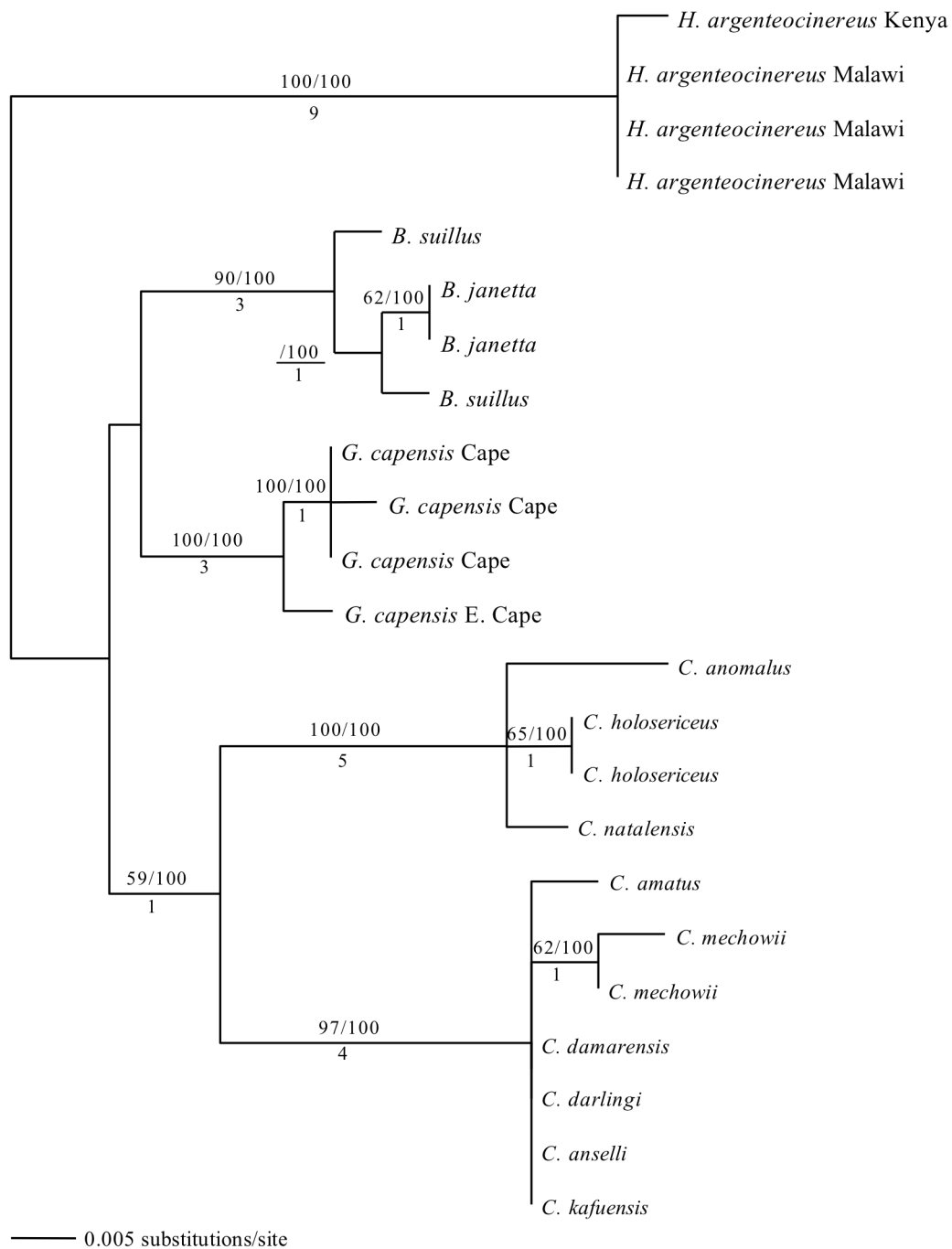


Fig. 5.1 Bsuil06 microsatellite flanking sequence maximum-likelihood phylogeny under GTR (one of 101 trees, $-\ln L = 900.72252$). Midpoint rooting was used. A branch and bound search under maximum-parsimony recovered a similar topology. Value above major branches represent MP bootstrap proportions and ML bootstrap proportions, respectively; values below represent Bremer decay indices.

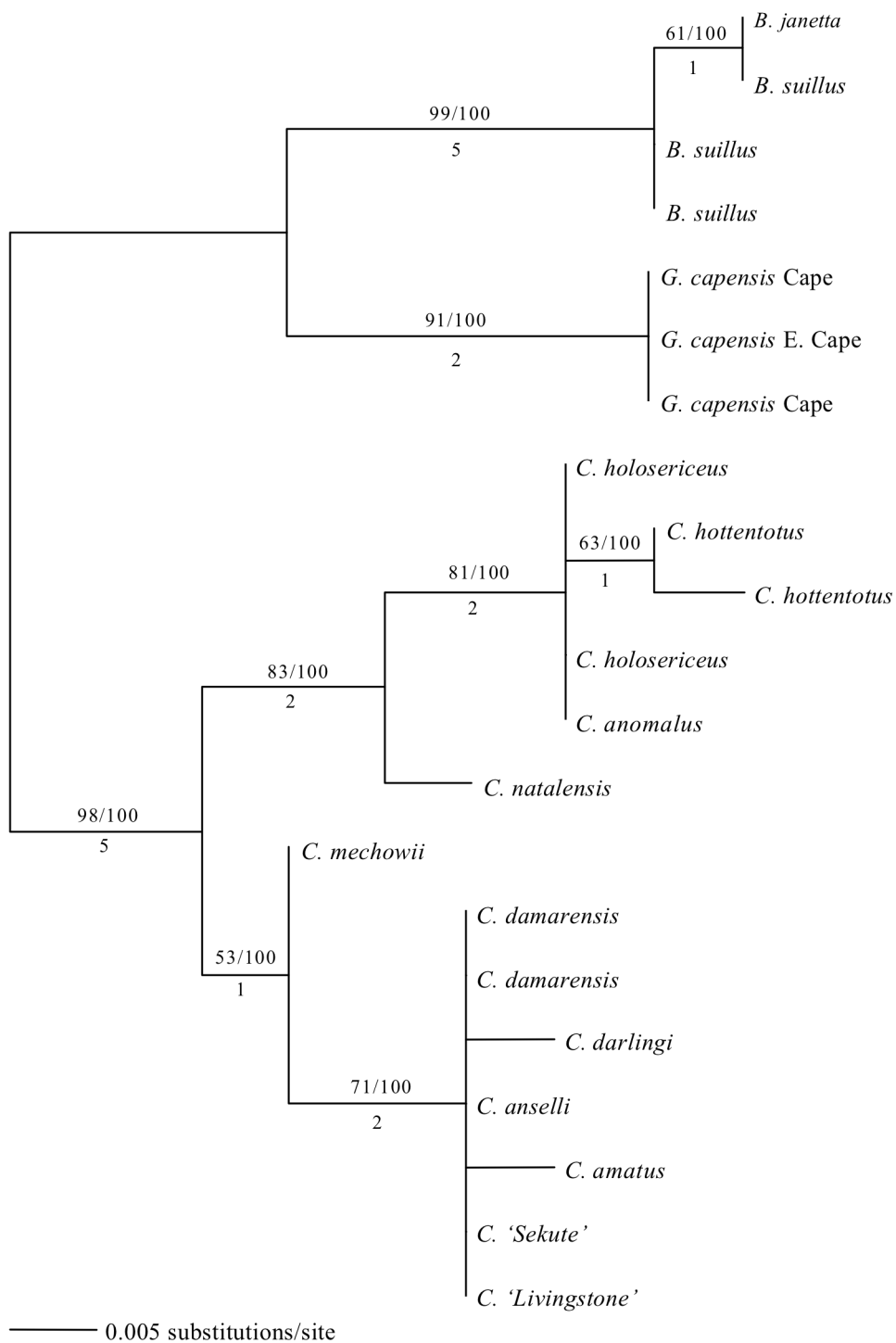


Fig. 5.2 Cmech03 microsatellite flanking sequence maximum-likelihood phylogeny under K80 (one of four trees, $-\ln L = 427.57847$). A branch and bound search under maximum-parsimony recovered the same topology. Value above major branches represent MP bootstrap proportions and ML bootstrap proportions, respectively; values below represent Bremer decay indices.

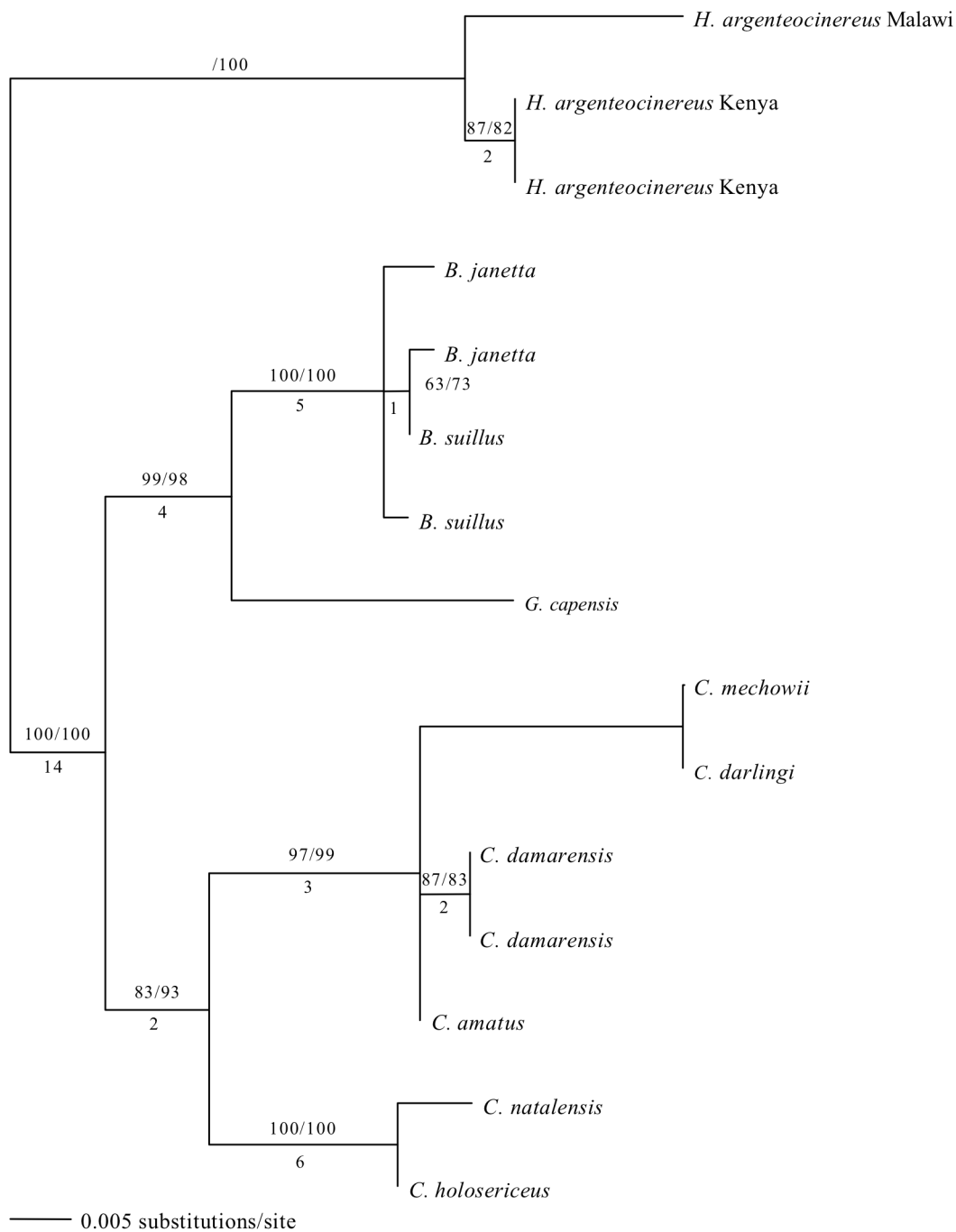


Fig. 5.3 Cmech09 microsatellite flanking sequence maximum-likelihood phylogeny under TrN + G (one of 2 trees, $-\ln L = 1260.48490$, $a = 1.0917$). A branch and bound search under maximum-parsimony recovered the same topology (TL = 95). Value above major branches represent MP bootstrap proportions and ML bootstrap proportions, respectively; values below represent Bremer decay indices.

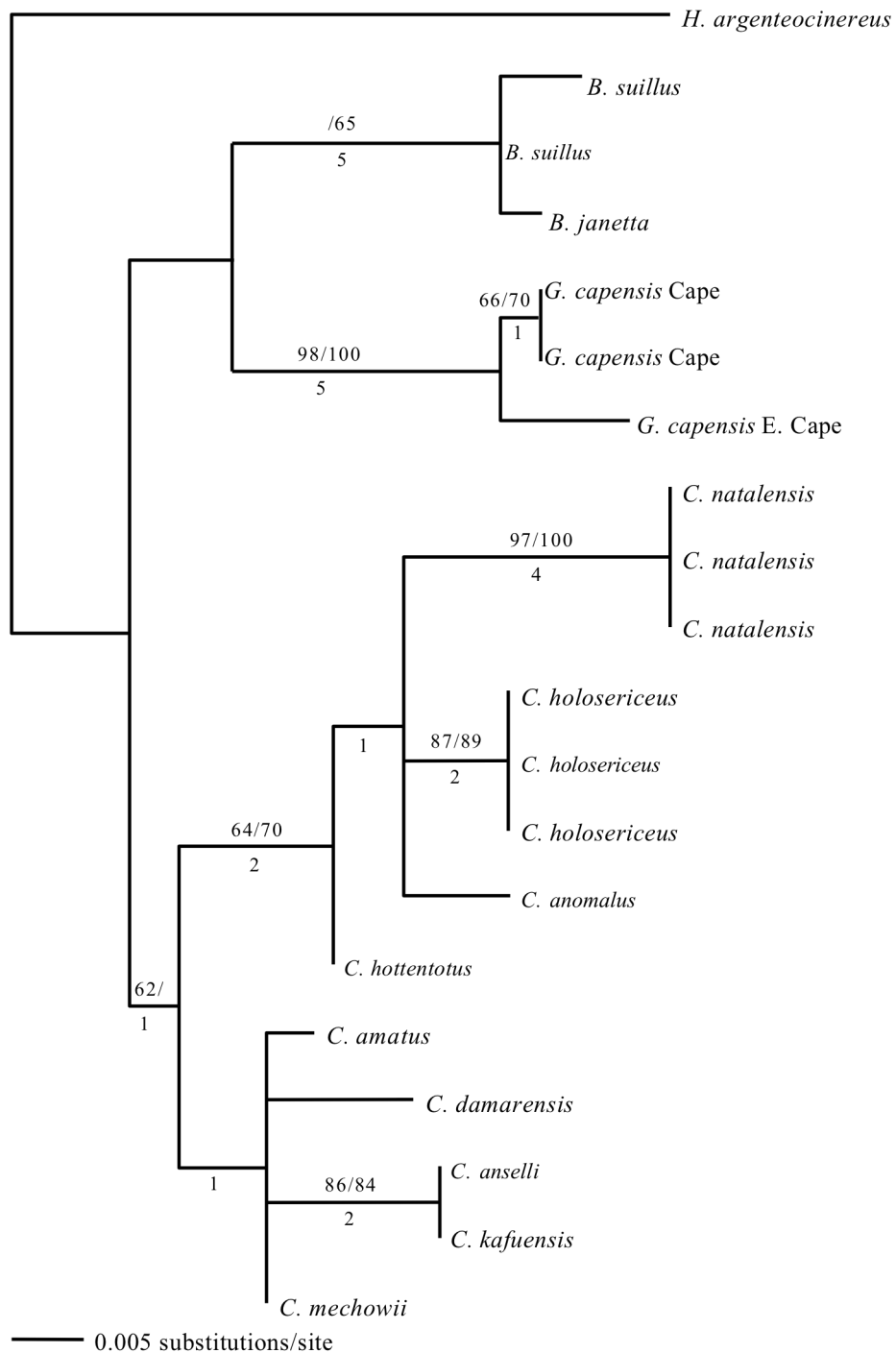


Fig. 5.4 Bsui101 microsatellite flanking sequence maximum-likelihood phylogeny under K80+G ($-\ln L = 900.72252$, $a = 0.3896$). Midpoint rooting was used. A branch and bound search under maximum-parsimony recovered a similar topology (TL = 64). Value above major branches represent MP bootstrap proportions and ML bootstrap proportions, respectively; values below branches represent Bremer decay indices.

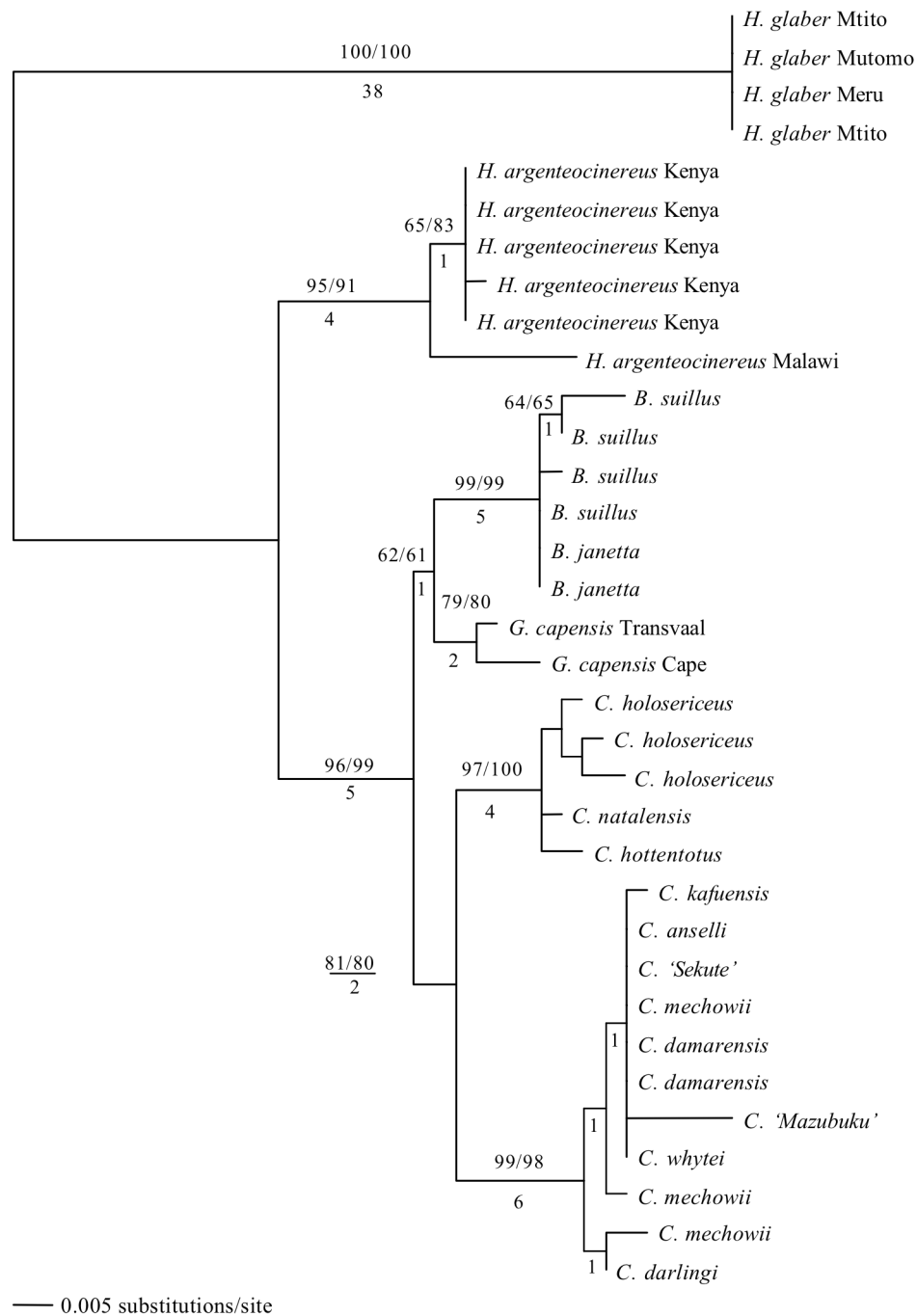


Fig. 5.5 Cmech04 microsatellite flanking sequence maximum-likelihood phylogeny under K80 + G ($-\ln L = 427.57847$, $a = 0.7714$). Midpoint rooting was used. A heuristic search under maximum-parsimony recovered the same topology. Values above major branches represent MP bootstrap proportions and ML bootstrap proportions, respectively; values below represent Bremer decay indices.

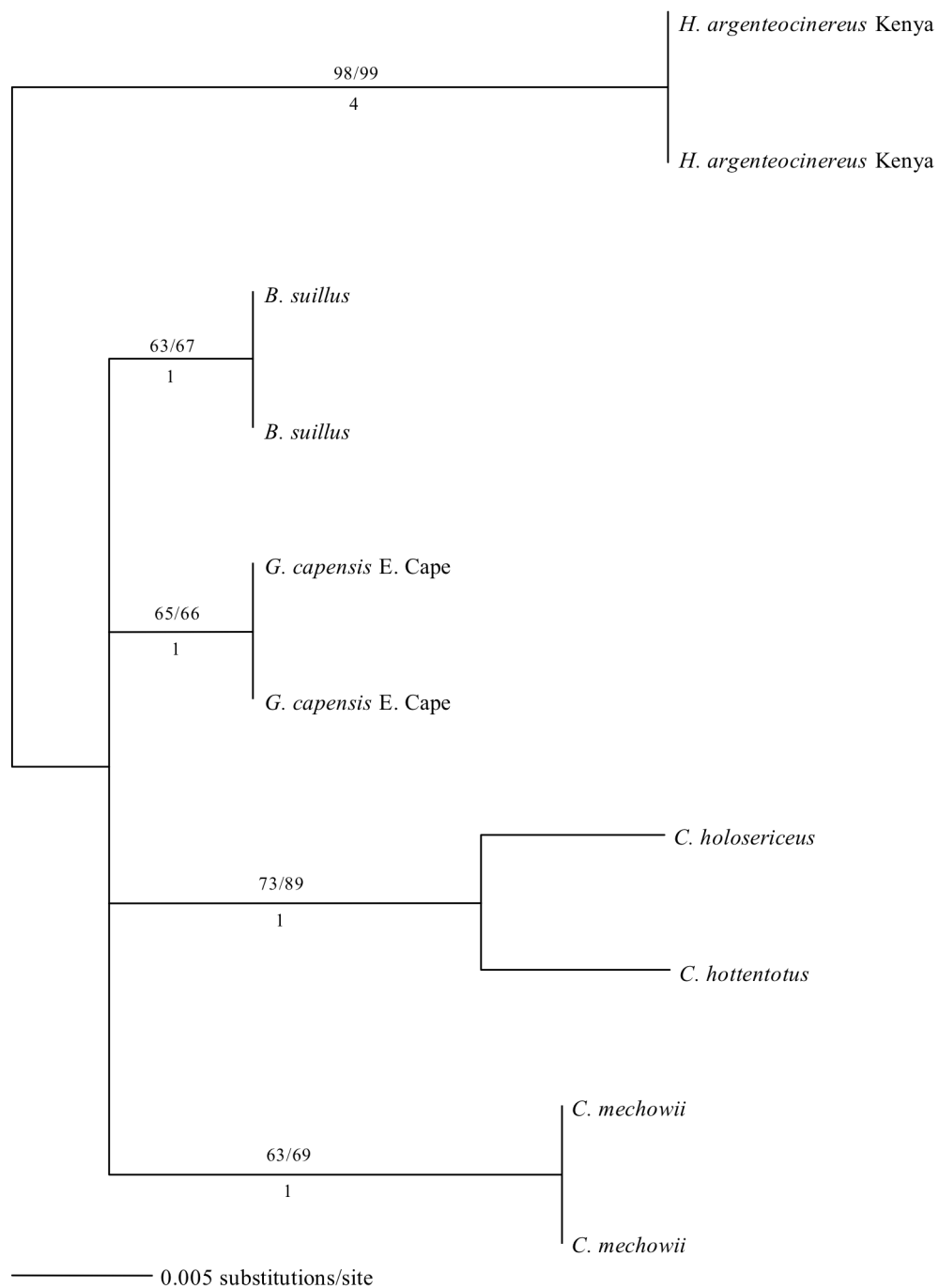


Fig. 5.6 Harg03 microsatellite flanking sequence maximum-likelihood phylogeny under K80 ($-\ln L = 1396.60309$). Midpoint rooting was used. A branch and bound search recovered a similar topology (TL = 14). Values above major branches represent MP bootstrap proportions and ML bootstrap proportions, respectively; values below branches represent Bremer decay indices.

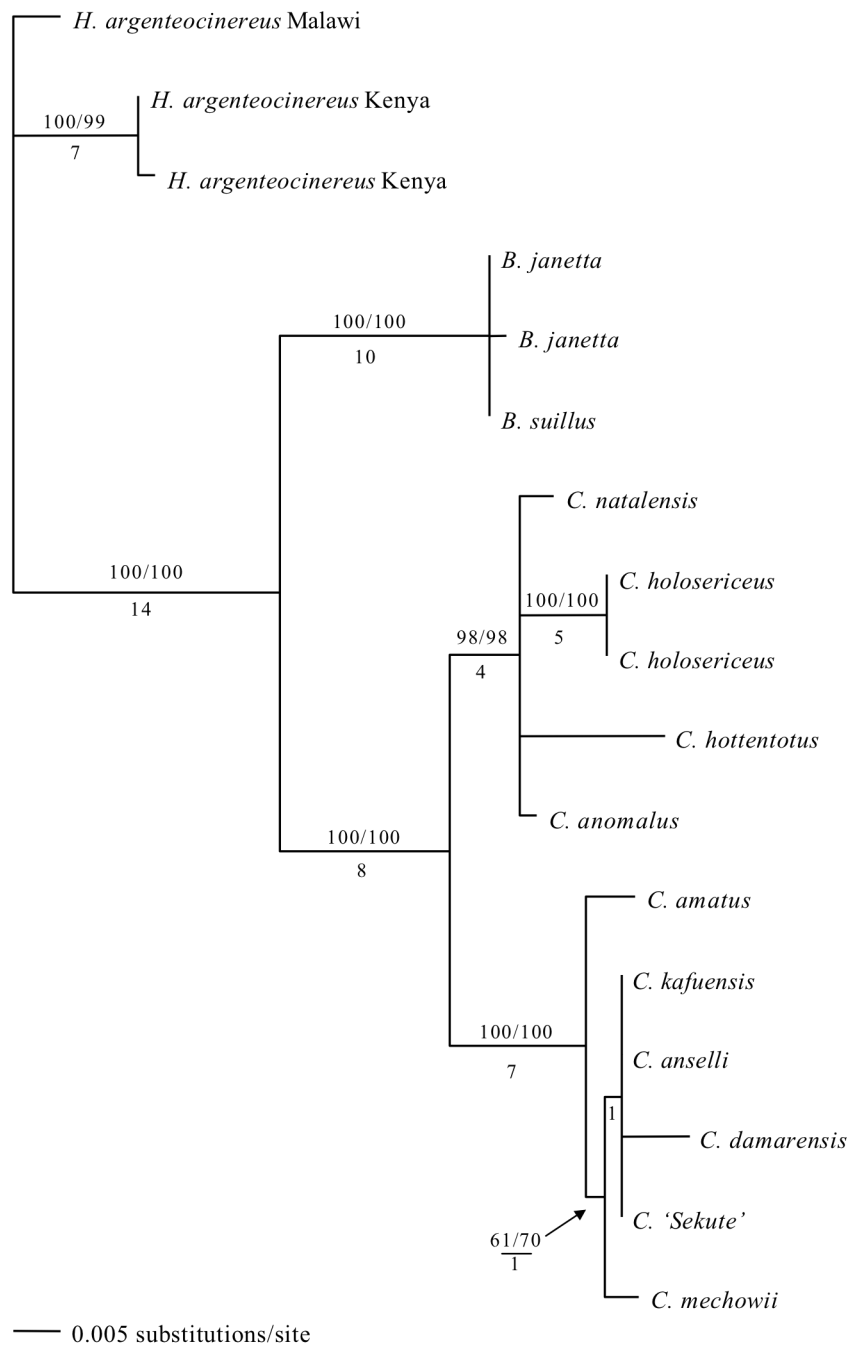


Fig. 5.7 Harg02 microsatellite flanking sequence maximum-likelihood phylogeny under K80 ($-\ln L = 1396.60309$). Midpoint rooting was used. A branch and bound search recovered a similar topology (TL = 89). Values above major branches represent MP bootstrap proportions and ML bootstrap proportions, respectively; values below represent Bremer decay indices.

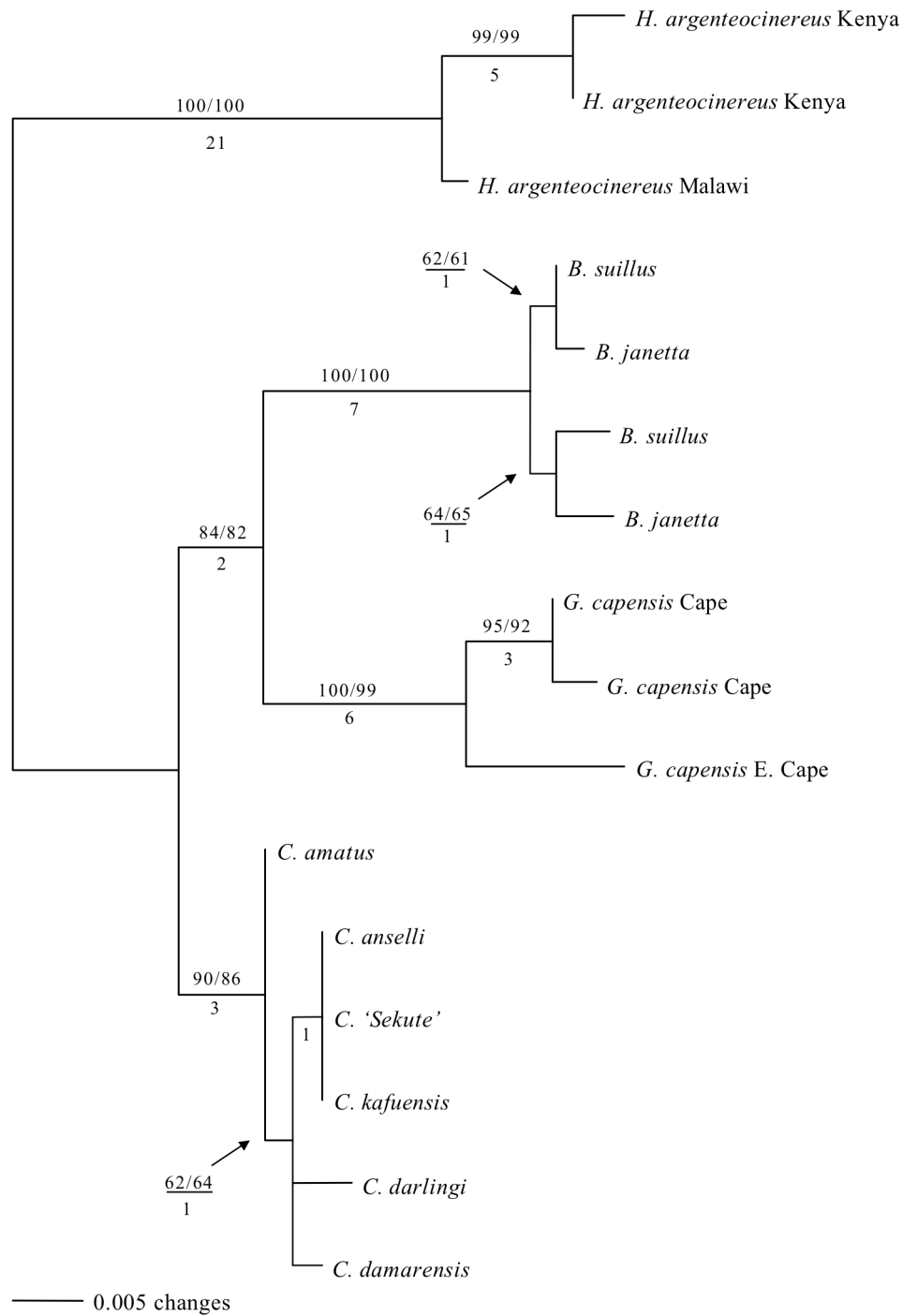


Fig. 5.8 Harg07 microsatellite flanking sequence maximum-likelihood phylogeny under K80 ($-\ln L = 1418.21633$). Midpoint rooting was used. A branch and bound search recovered a similar topology (TL = 76). Value above major branches represent MP bootstrap proportions and ML bootstrap proportions, respectively; values below branches represent Bremer decay indices.

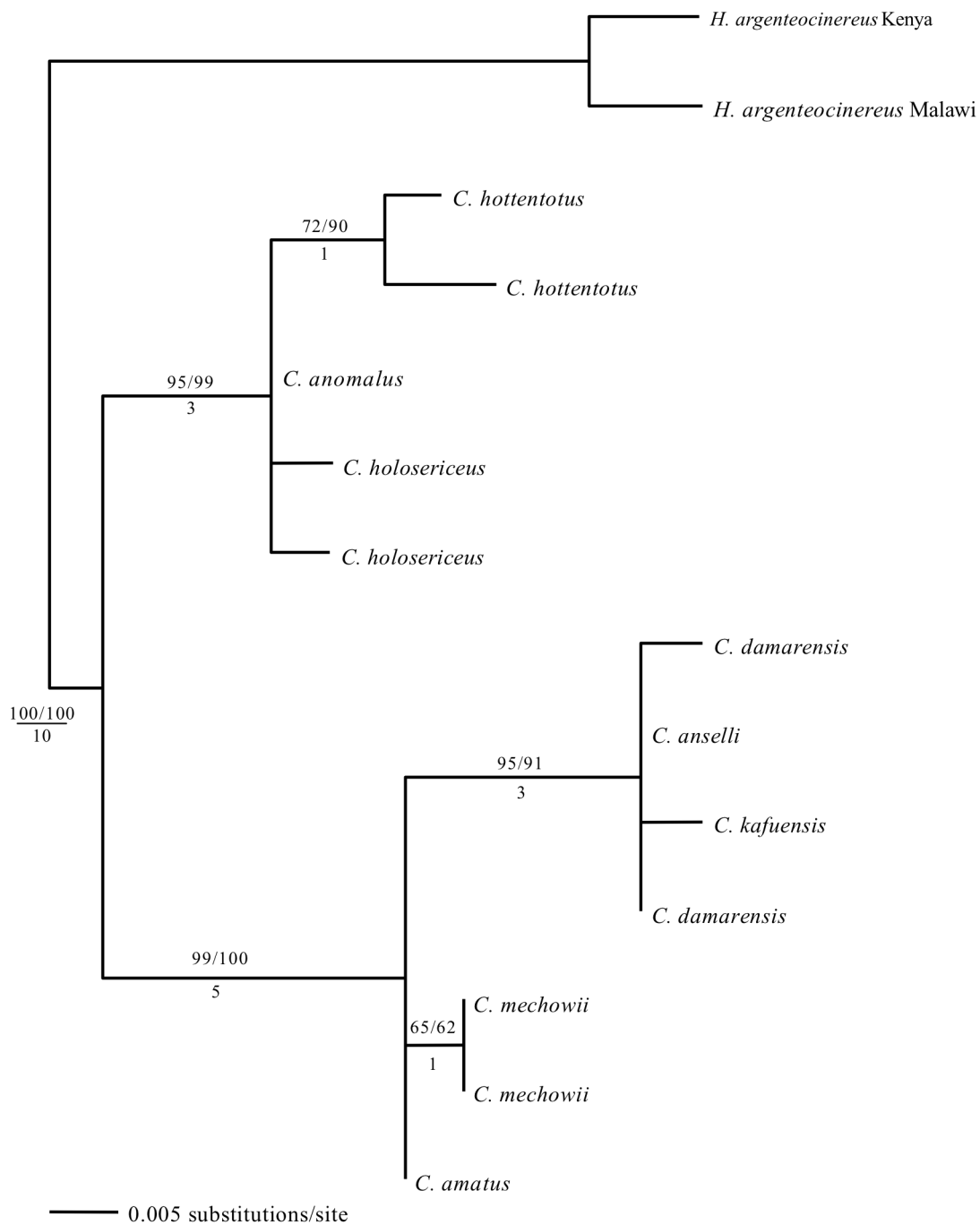


Fig. 5.9 Chott03 microsatellite flanking sequence maximum-likelihood phylogeny under HKY85 ($-\ln L = 558.96569$). Midpoint rooting was used. A branch and bound search under maximum-parsimony recovered the same topologies. Value above major branches represent MP bootstrap proportions and ML bootstrap proportions, respectively; values below represent Bremer decay indices.

monophyletic groups: *Heterocephalus* (Bootstrap proportions (BP) = 100, Decay Indices (DI) = 38), *Heliophobius* (BP = 95 - 100, DI = 4 - 22), *Bathyergus* (BP = 90 - 100, DI = 1 - 10), *Georychus* (BP = 79 - 100, DI = 1 - 6), *Cryptomys* (BP = 64 - 100, DI = 1 - 6), and *Coetomys* (BP = 53 - 100, DI = 1 - 7). For locus Harg03, the five genera formed monophyletic groups, but support was low across *Bathyergus*, *Georychus*, *Cryptomys*, and *Coetomys* (Fig. 5.6: CI = 1.0, RI = 1.0). Gcap07 recovered a single most-parsimonious tree when successively-weighted parsimony was used (not shown: CI = 0.822, RI = 0.926; see Fig. 5.10). Chott01 recovered 3 equally parsimonious trees when successive-weighting was used (not shown: CI = 0.931, RI = 0.975; see Fig. 5.11). For Chott08, nine equally-parsimonious trees were recovered (not shown: CI = 0.979, RI = 0.987; see Fig. 5.12). Two equally-parsimonious trees were recovered for Cmech11 (not shown: CI = 0.969, RI = 0.992; see Fig. 5.13). Three equally-parsimonious trees were recovered for Gcap01, with strong support for monophyly of all genera (not shown: CI = 0.969, RI = 0.988; see Fig. 5.14). For Bsuil04, six equally-parsimonious trees were recovered (not shown; see Fig. 5.15). Ten equally-parsimonious trees were recovered for Hglab10 (not shown: CI = 0.966, RI = 0.95; see Fig. 5.16).

The models of evolution varied across each locus (Table 5.1), ranging from very simple: K80 (Kimura, 1980), with equal base frequencies and two substitution rates (transitions vs. transversions) to a complex submodel of the general time reversible model: TVM+ Γ (GTR: Tavaré, 1986; TVM: Posada and Crandall, 1998) with unequal base frequencies, five substitution rates (4 transversion + 1 transversion), and among-site rate variation estimated by the gamma distribution. Compared with the results from the

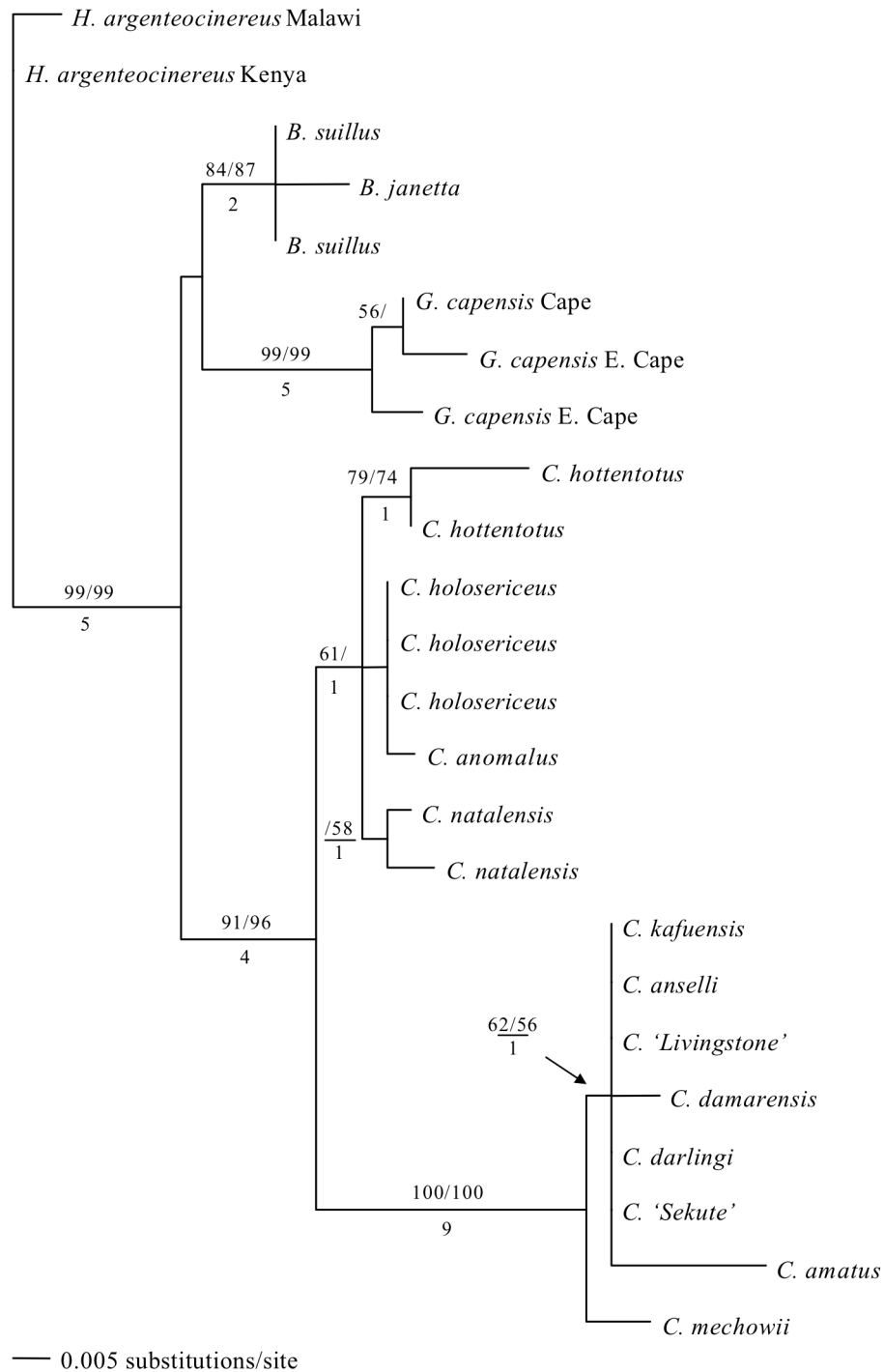


Fig. 5.10 Gcap07 microsatellite flanking sequence maximum-likelihood phylogeny under K80 ($-\ln L = 1244.5058$). *Heliophobius* was used as the outgroup. Successively weighted maximum-parsimony (by RC) recovered a similar topology. Values above major branches represent MP bootstrap proportions and ML bootstrap proportions, respectively; values below represent Bremer decay indices.

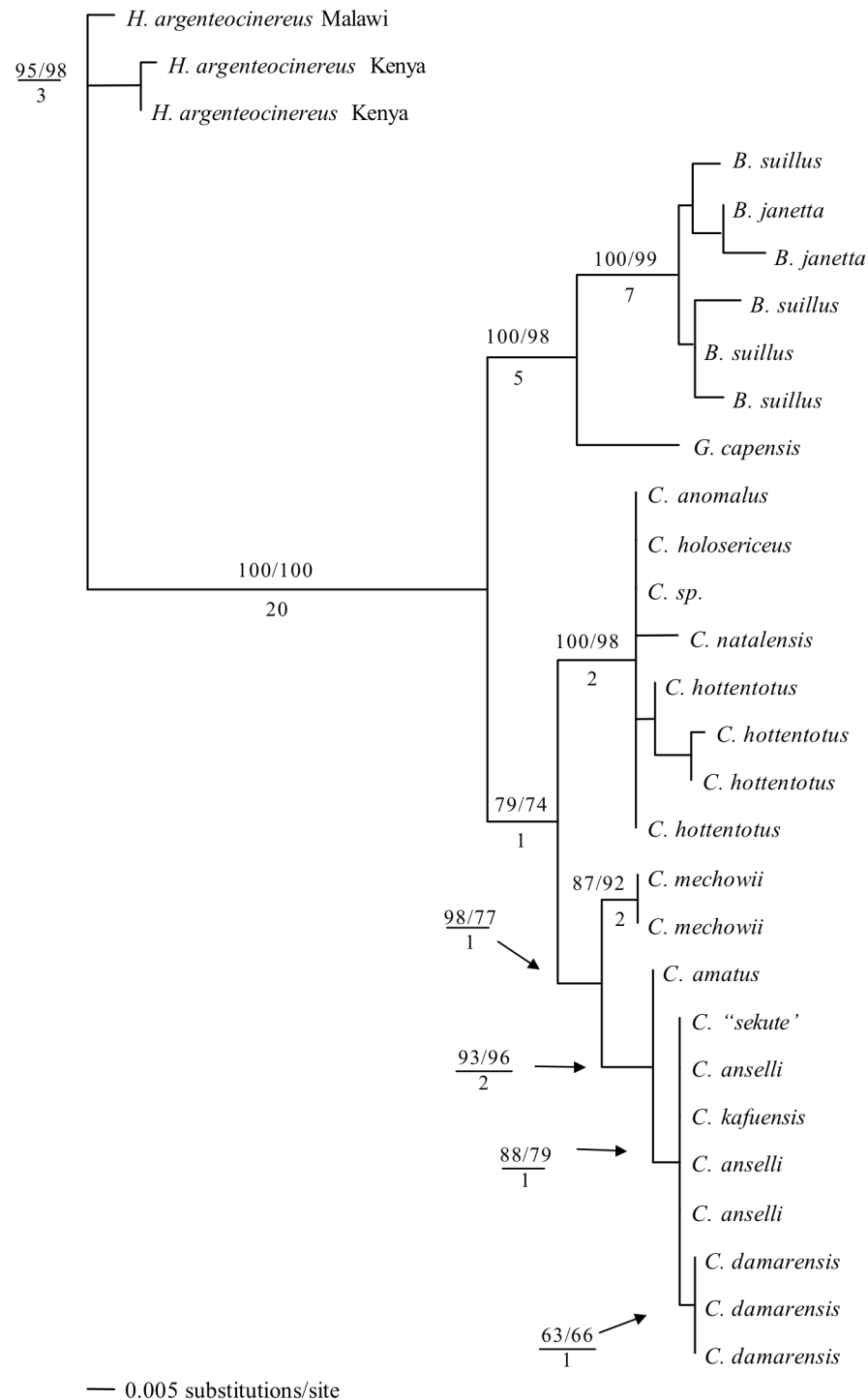


Fig. 5.11 Chott01 microsatellite flanking sequence maximum-likelihood phylogeny under K81uf + G ($-\ln L = 1148.45978$, $a = 0.6229$). Successively-weighted maximum-parsimony (by RC) recovered the same topologies. Value above major branches represent MP bootstrap proportions and ML bootstrap proportions, respectively; values below represent Bremer decay indices.

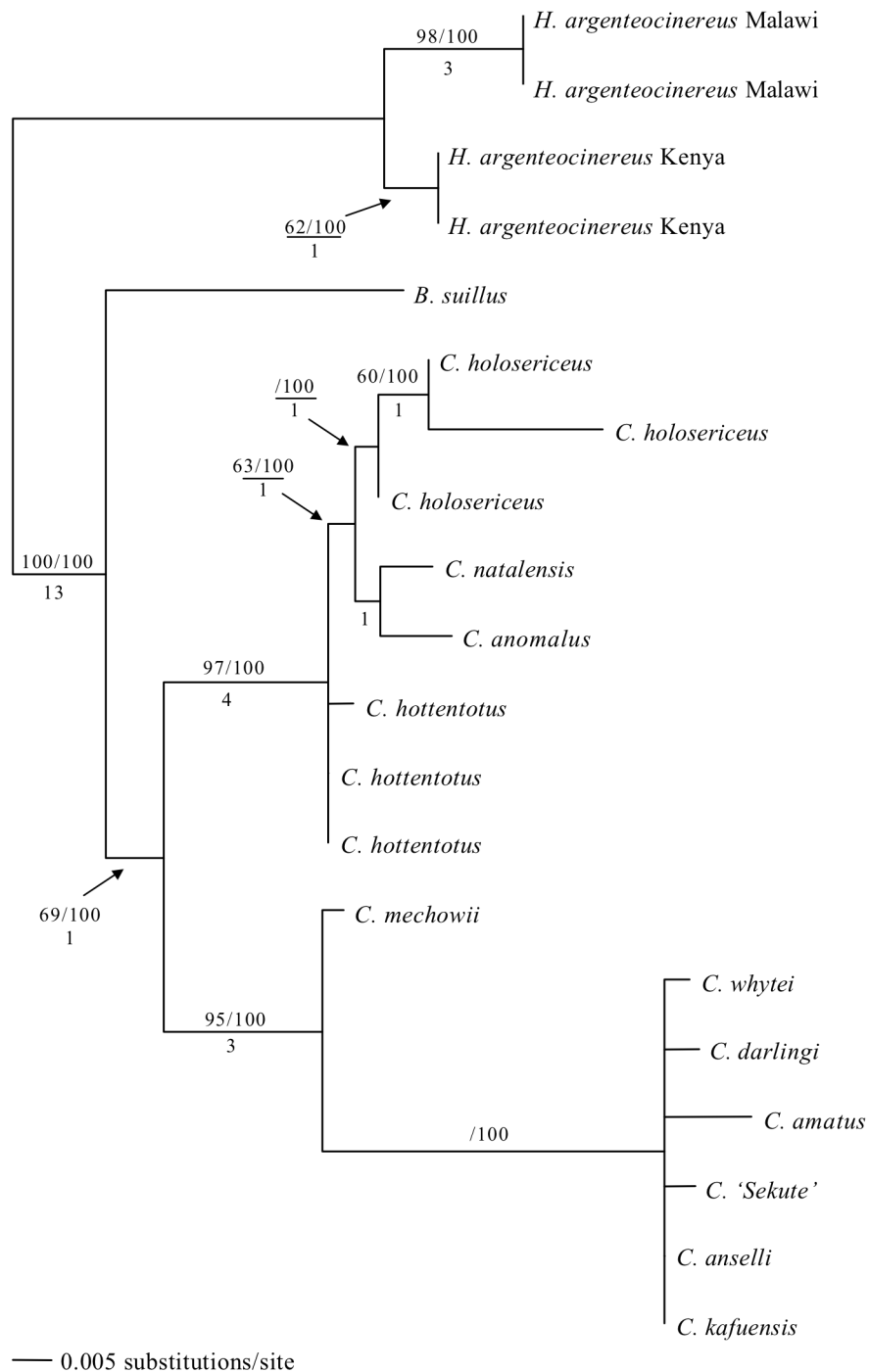


Fig. 5.12 Chott08 microsatellite flanking sequence maximum-likelihood phylogeny under GTR (one of four trees, $-\ln L = 558.96569$). *Heliophobius* was set as the outgroup. Successively weighted maximum-parsimony recovered 9 trees, including this topology. Value above major branches represent MP bootstrap proportions, and ML bootstrap proportions, respectively; values below represent Bremer decay indices.

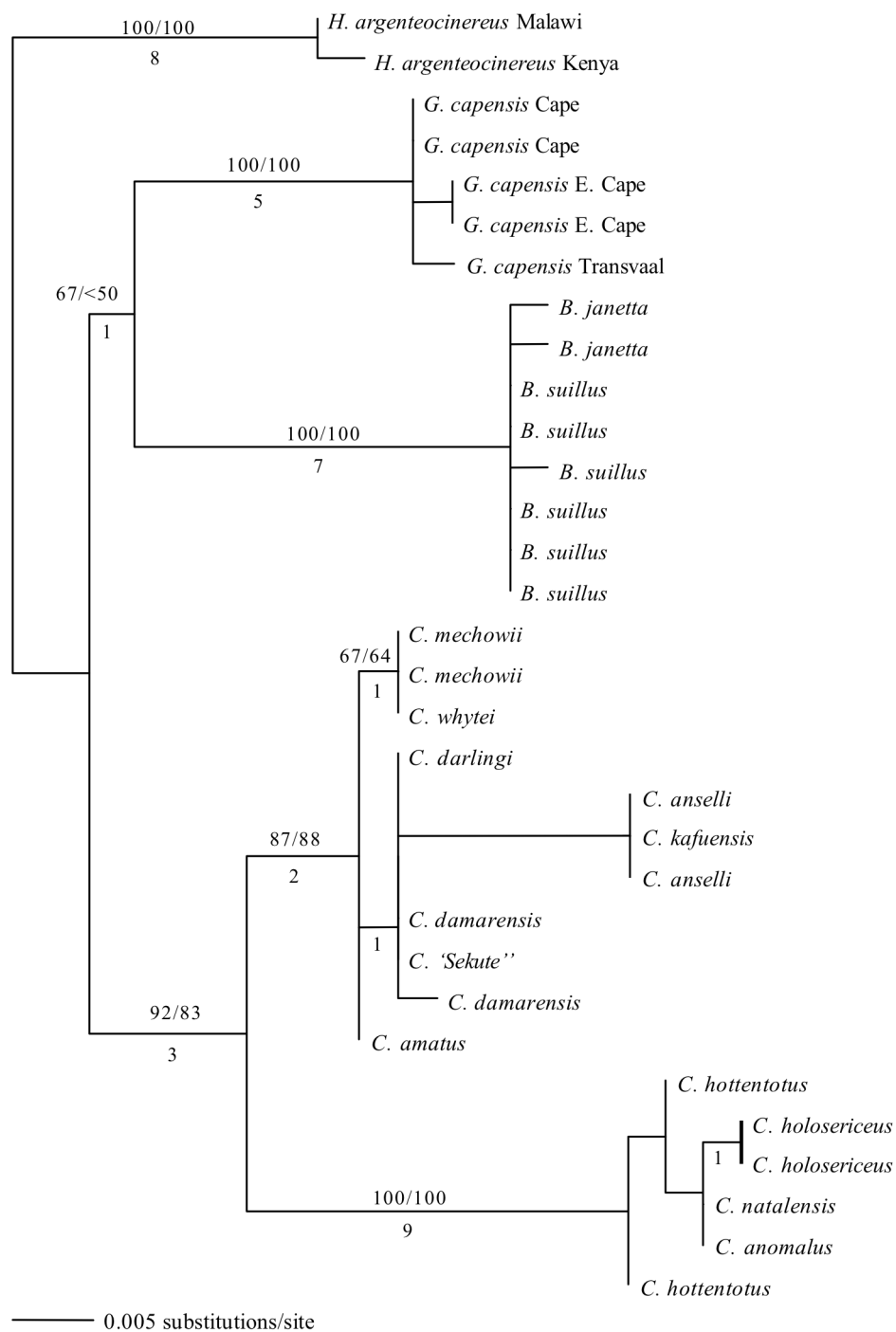


Fig. 5.13 Cmech11 microsatellite flanking sequence maximum-likelihood phylogeny under TrN (one of 202 trees, $-\ln L = 999.01887$). *Heliophobius* was used as the outgroup. A heuristic search under maximum-parsimony recovered similar topologies (6 trees). Value above major branches represent MP bootstrap proportions, value below represents ML bootstrap proportions.

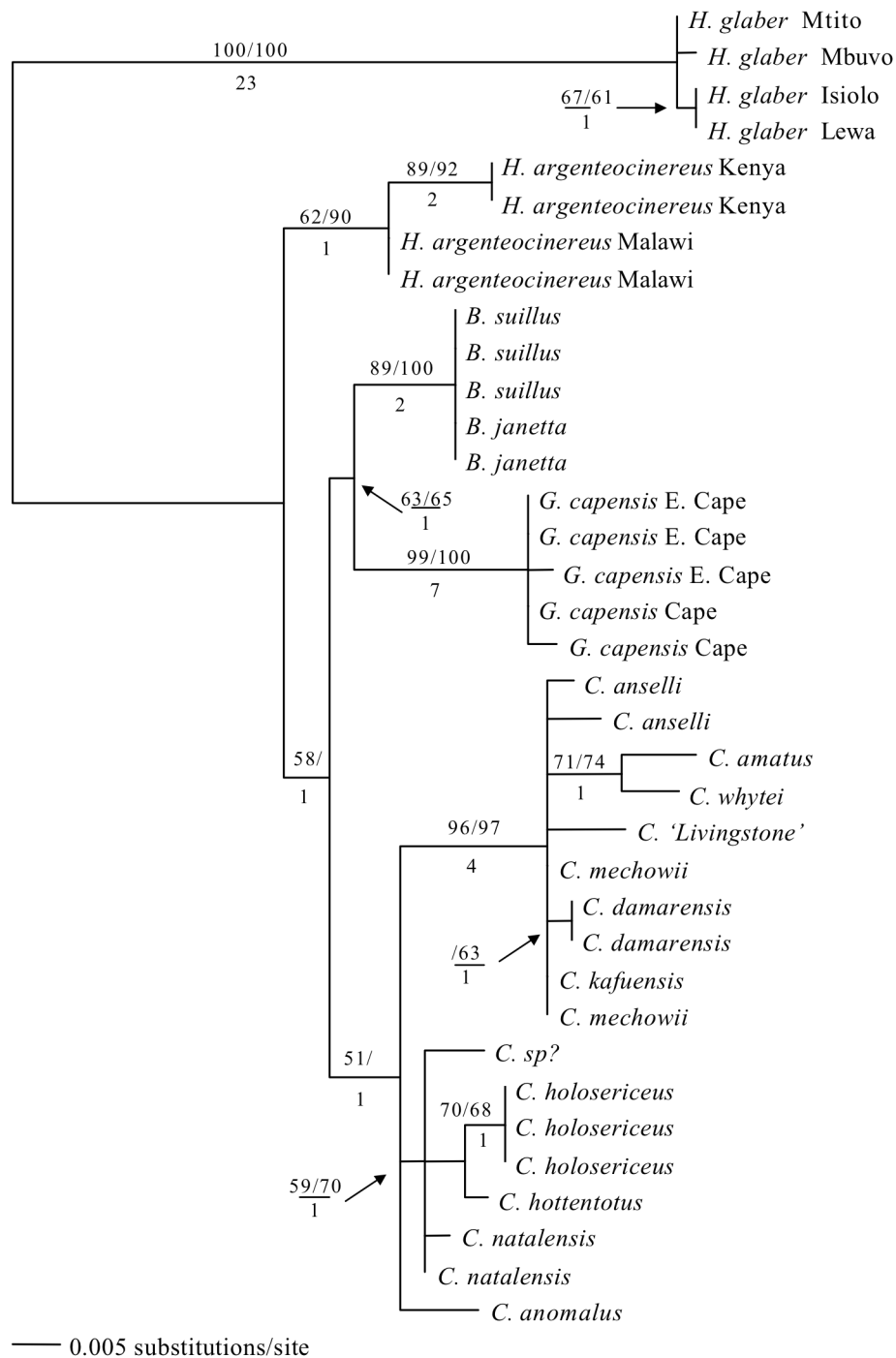


Fig. 5.14 Gcap01 microsatellite flanking sequence maximum-likelihood phylogeny under K80 ($-\ln L = 1244.5058$). A branch and bound search under maximum-parsimony recovered a similar topology (3 trees). Values above major branches represent MP bootstrap proportions and ML bootstrap proportions, respectively; values below represent Bremer decay indices.

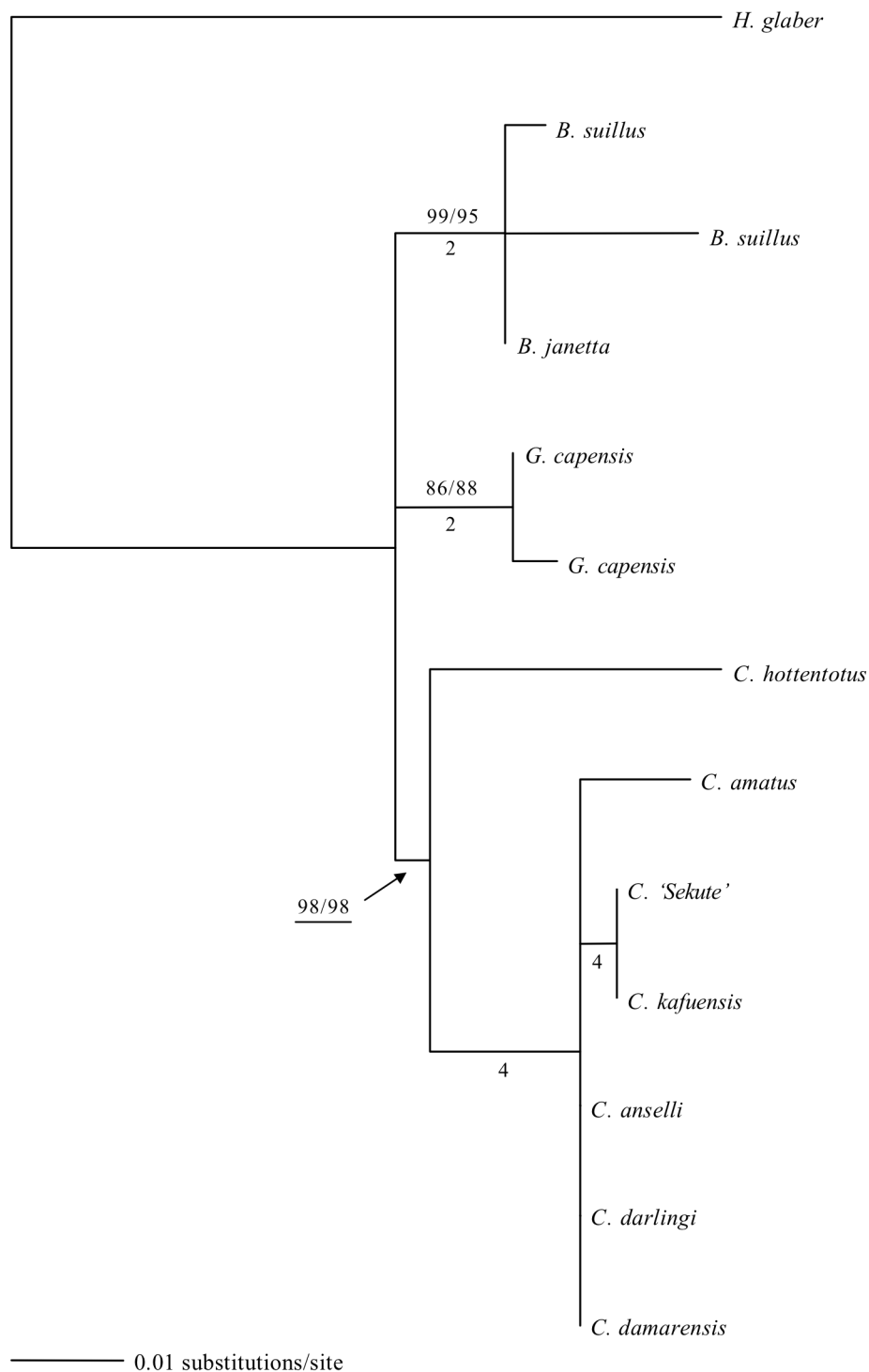


Fig. 5.15 Bsuil04 microsatellite flanking sequence maximum-likelihood phylogeny under HKY85 (one of three trees, $-\ln L = 739.38997$). Successively-weighted maximum-parsimony (by RC) recovered the same topologies. Value above major branches represent MP bootstrap proportions and ML bootstrap proportions, respectively; values below represent Bremer decay indices.

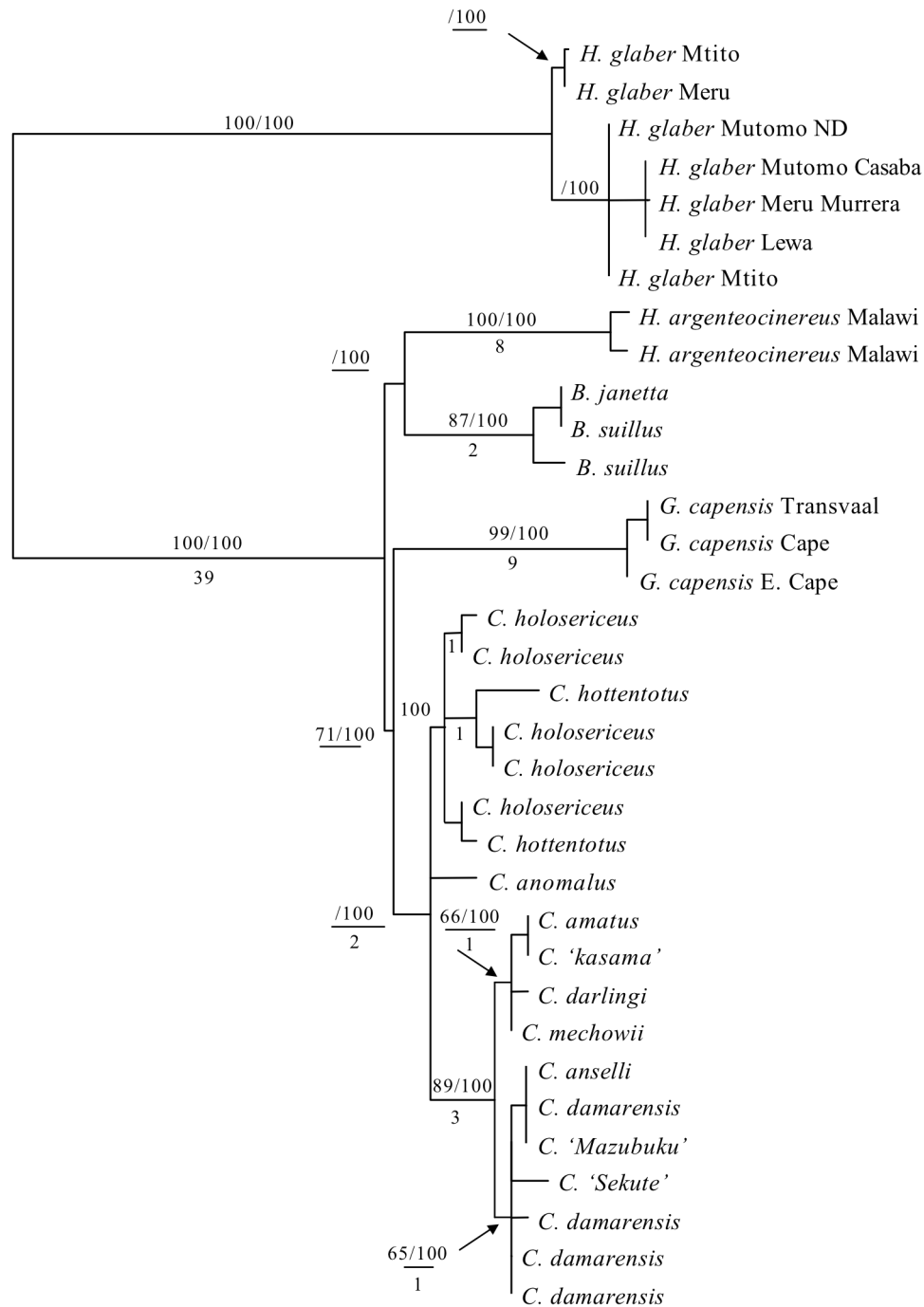


Fig. 5.16 Hglab10 microsatellite flanking sequence maximum-likelihood phylogeny under K80 (one of 22 trees, $-\ln L = 1396.60309$, $a = 1.7604$). *Heterocephalus* was used as the outgroup. A heuristic search recovered similar topologies (10 trees; TL = 130). Values above major branches represent MP bootstrap proportions and ML bootstrap proportions, respectively; values below represent Bremer decay indices.

parsimony analysis, in which 9 loci each recovered a single tree, a different set of ten loci recovered single trees using their respective models under ML (Table 5.1). Under ML, Gcap01 recovered a single tree (Fig. 5.14) versus three from MP. This topology was consistent with the 12S/TTR phylogeny (Fig. 2.4), with the exception of a non-monophyletic *Cryptomys*. Similarly, a single tree was also recovered under ML for Cmech11, versus two MP trees (Fig. 5.13), with strong support for monophyly of all included genera (ML BP = 87 – 100). Three loci (Cmech09, Cmech03, and Bsuil06) that recovered single MP trees, recovered multiple trees under ML (Fig. 5.1 – 5.3). The most extreme example was Bsuil06 that recovered 101 trees under ML (Fig. 5.1). The differences among the 101 trees were small changes in branch lengths and branching patterns within *Coetomys*.

3.3. Combined data sets

Due to the variable success of amplification across the available samples, the sets of taxa analyzed per locus were quite different, limiting the possibilities for combined analyses of the 16 MFS loci. Two separate combinations of loci were analyzed: 1) a set of 3 loci (Cmech04, Gcap01, and Hglab10) across members of all 6 genera (8 taxa), and 2) all 16 loci for the same 8 taxa, but, with missing data for one or more taxon per partition. The Cmech04/Gcap01/Hglab10 dataset consisted of 1287 characters (238 variable sites; 43 parsimony-informative sites – 18% of variable positions) and recovered single trees under both MP and ML with strong nodal support (CI = 0.973, RI = 0.868; 76–100 MP BP; 69–100 ML BP) (Fig. 5.17). The larger dataset containing

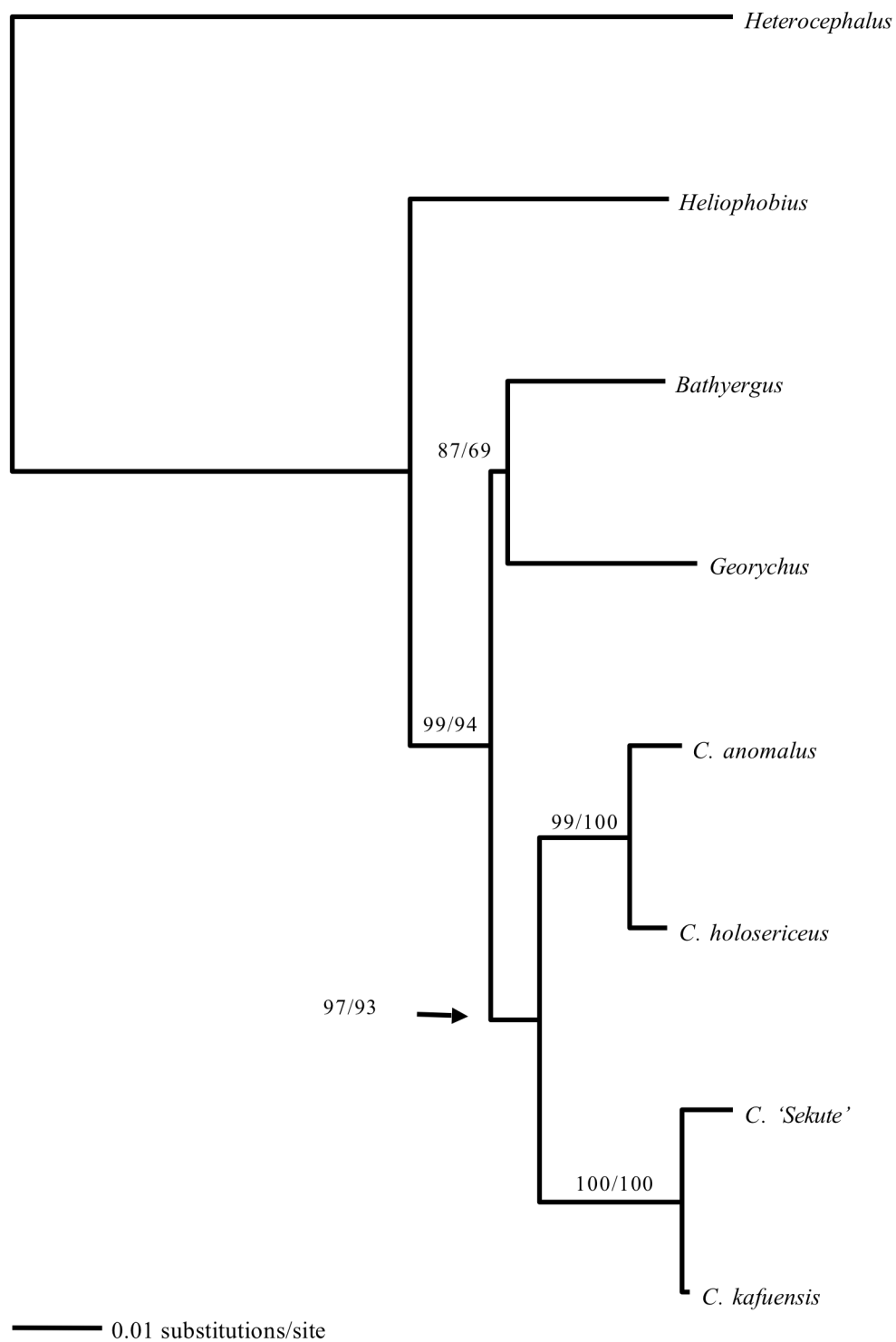


Fig. 5.17 Combined maximum-likelihood phylogeny of Cmech04, Gcap01, and Hglab10 under TVM + G ($-\ln L = 3118.8554$, $\alpha = 1.8738$). A branch and bound search under maximum-parsimony recovered the same topology (TL = 262, CI = 0.973, RI = 0.868). Values above major nodes represent MP and ML bootstrap proportions, respectively.

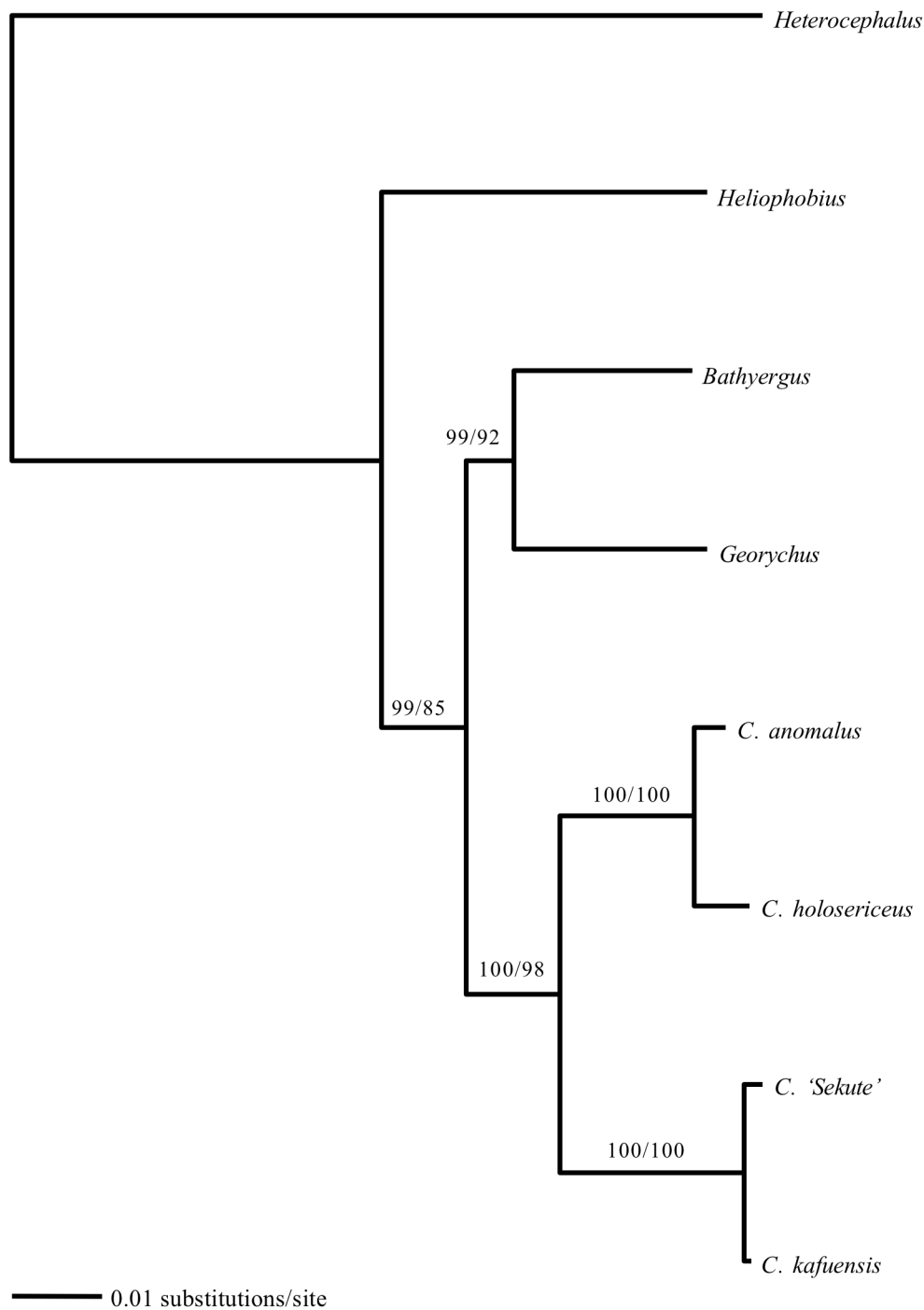


Fig. 5.18 Combined maximum-likelihood phylogeny of all 16 microsatellite flanking sequence (MFS) loci under TVM + G ($-\ln L = 13167.3867$, $\alpha = 1.0101$). Midpoint rooting was used. A branch and bound search under maximum-parsimony recovered the same topology (TL = 883, CI = 0.972, RI = 0.893). Values above major nodes represent MP and ML bootstrap proportions, respectively.

6212 nucleotides (817 variable sites; 199 parsimony-informative sites – 24%) also recovered single trees under MP and ML (Fig. 5.18: CI = 0.972, RI = 0.893).

From the larger combined data set, 96 indel events were coded for presence/absence across the genera and an exhaustive search recovered a single MP tree (not shown; TL = 107, CI = 0.907, RI = 0.545) with weak to strong nodal support for the intergeneric relationships (MP BP = 50 – 89). Of the 96 characters, 20 were parsimony-informative.

4. Discussion

4.1. Utility of flanking sequences in phylogenetic reconstruction

Microsatellite flanking sequences (MFS) were effective in recovering relationships at the generic and sub-generic level (geographic units or species groups) congruent with the phylogeny recovered from 12S/TTR (Chapter II; Ingram et al., 2004). Only one locus, Hglab10, showed any deviation from the expected branching pattern from mtDNA and nDNA (12S/TTR phylogeny: Chapter II; Ingram et al., 2004). For this locus, an unexpected grouping of *Heliophobius* with *Bathyergus*, but excluding *Georchus* was recovered under ML (Fig. 5.16). This relationship was not recovered under maximum-parsimony. The three samples of *Georchus* sequenced for this locus showed numerous fixed differences at sites in which *Heliophobius* and *Bathyergus* shared the symplesiomorphic state with *Heterocephalus*. All other loci recovered strong monophyly for the six genera of Bathyergidae, and most recovered sister relationships of (*Georchus* + *Bathyergus*) and (*Cryptomys* + *Coetomys*).

At the sub-generic level, the majority of loci recovered several of the taxa recommended for recognition in Chapter II. Ten loci show a strong split between populations of *Heliophobius argenteocinereus* separated by the Rift Valley; Kenya and Malawi, respectively. Six loci show strong separation between Cape and eastern populations of *Georychus capensis*. Ten loci recovered some of the expected species groups within *Cryptomys*. Some of the major lineages (*C. anelli* + *C. kafuensis* + *C. 'Sekute'* + *C. 'Livingstone'*; *C. mechowii* + *C. darlingi*; *C. amatus* + *C. whytei*) identified in *Coetomys* (Fig. 2.5) were resolved by nine loci.

4.2. Combined analyses

Both the Cmech04/Gcap01/Hglab10 and complete (16 loci) datasets recovered single trees under both MP and ML with strong nodal support (Figs. 5.17-18: CI = 0.973 and 0.972, RI = 0.868 and 0.893, respectively). The model of evolution determined for each combination was identical (TVM+ Γ), despite differences in the models estimated for each individual partition (Table 5.1).

Identifiable indels across all sixteen loci were coded in a presence/absence matrix that provided 20 parsimony-informative characters that recovered a single tree with the expected generic relationships with low to moderate nodal support (CI = 0.907, RI = 0.545). Given the limited number of taxa and number of missing data in this analysis, the results are encouraging and show promise for use in a larger dataset.

5. Conclusions

The goal of this chapter was to assess the phylogenetic utility of the microsatellite flanking sequences (MFS) isolated for sixteen microsatellite loci from members of the family Bathyergidae. It was not intended to generate an exhaustive analysis of all available samples from members of this family across these loci (6212 nucleotides). The deep relationships at the generic and intergeneric levels were recovered with very strong support (high bootstrap proportions and decay, consistency, and retention indices). Herein, I have described a suitable method for isolating and screening putative phylogenetic markers for use at the family level within Rodentia. The direct sequencing applied in this method can confirm orthology of the loci and has advantages over other types of loci that randomly sample the genome, such as RFLPs or AFLPs (Fleischer, 1996). A number of the loci reported here amplified in all samples tested and are suitable for more detailed studies within this family. Further optimization of the loci, where some taxa showed difficulties in amplification, may provide additional sequences per locus.

CHAPTER VI

SUMMARY

The purpose of this dissertation was to investigate the molecular evolution of microsatellite DNA loci and their flanking regions (MFS) under a phylogenetic context. I selected the endemic African family of mole-rats, Bathyergidae (Rodentia: Mammalia) as my model. In Chapter II, I produced a robust phylogeny for the Bathyergidae based on both mitochondrial (12S rRNA) and nuclear (Transthyretin Intron 1) DNA. The relationships identified in this phylogeny are supported by previous studies of allozymes, karyotypes, morphology, and DNA sequences. As a result of my findings, I proposed the recognition of the *mechowii* species group of *Cryptomys* as the new genus *Coetomys* (Ingram et al., 2004). In addition, I found support for a number of intrageneric relationships including deep divergences between populations of *Heliophobius argenteocinereus* from either side of the Rift Valley, between Cape and eastern populations of *Georychus capensis*, and fine scale resolution at the species/species group level in both *Cryptomys* and *Coetomys*.

In Chapter III, I isolated and characterized microsatellite loci from each of the six genera for use in population genetics level studies. Cross-species application of each locus was tested across a sample of representatives from each genus with varied success. Few studies have examined population level genetic relationships within members of the family and these panels of microsatellite loci will provide tools for further studies.

In Chapter IV, I further characterized the genotyping fragment of the microsatellite loci through the amplification and sequencing of 500 – 800 bp microsatellite flanking sequences (MFS). Direct sequencing of the microsatellite loci revealed rampant electromorphic homoplasy, null alleles, and insertion/deletion (indel) events in both the repeat motif and adjacent flanking region. This evidence adds to the growing body of information regarding problems associated with the acceptance of genotype scores from fragment analysis (Wright et al., 2004; Baliraine et al., 2003; Culver et al., 2001; Ellegren, 2000; Angers and Bernatchez, 1997; Macaubas et al., 1997). A number of the loci isolated were linked with various repetitive elements (LTRs, Alu repeats, SINEs, and MIRs), which as a suite, have been characterized as rare genomic changes (RGCs) that make robust phylogenetic characters (Springer et al., 2004). The method applied in this chapter may be useful in identifying additional RGC markers for phylogenetic use.

In Chapter V, I examined the phylogenetic utility of the genotyping fragments (*sans* repeat element) and their associated MFS regions. Sixteen of the previously described MFS loci were analyzed under standard phylogenetic methods (parsimony and maximum-likelihood). In all but one of the resulting topologies, the MFS loci recovered the expected relationships among the genera of Bathyergidae with moderate to strong nodal support (MP and ML bootstrap proportions, and decay indices). When combined as either: 1) loci sampling all genera (3 loci) or 2) all sixteen loci, with a reduced number of taxa (8), the intergeneric relationships were recovered with strong nodal support. Ninety-six identifiable indel events were coded across the genera in a presence/absence

matrix and recovered a single MP tree with weak to strong nodal support for the intergeneric relationships.

The overall findings of this dissertation suggest that levels of cryptic variation in microsatellite loci is not a trivial issue and should be integrated into studies, particularly those using cross-species markers. Direct sequencing can both confirm the stability of some microsatellites while revealing problems in others. A number of the indels present in the genotyping fragments showed phylogenetic information and can be applied to population genetic studies. Direct sequencing also provides a number of phylogenetically informative characters in the form of nucleotides that show promise in population/species level studies.

REFERENCES

- Adams, J., 2001. Africa during the last 150,000 years. Available at <http://www.esd.ornl.gov/projects/qen/nercAFRICA.html>
- Aguilar, G.H., 1993. The karyotype and taxonomic status of *Cryptomys hottentotus darlingi* (Rodentia: Bathyergidae). *S. Afr. J. Zool.* 28, 201–204.
- Akaike, H., 1974. A new look at the statistical model identification. *IEEE Transactions on Automatic Control* 19,716–722.
- Allard, M.W., Honeycutt R.L., 1992. Nucleotide sequence variation in the mitochondrial 12S rRNA gene and the phylogeny of African mole-rats (Rodentia: Bathyergidae). *Mol. Biol. Evol.* 9, 27–40.
- Allen, G.M., 1939. A checklist of African mammals. *Bull. Mus. Comp. Zool. Harvard Coll.* 83, 425–433.
- Altet, L., Francino, O., Sanchez A, 2001. Microsatellite polymorphism in closely related dogs. *J. Hered.* 92, 276–279.
- Amos, W., 1999. A comparative approach to the study of microsatellite evolution. In: Goldstein, D.B., Schlötterer, C. (Eds.), *Microsatellites: Evolution and Application*. Oxford University Press, New York. pp. 66–79.
- Amos, W., Sawcer, S.J., Feakes, R.W., Rubensztein D.C., 1996. Microsatellites show mutational bias and heterozygote instability. *Nat. Genet.* 13, 390–391.
- Angers, B., Bernatchez, L., 1997. Complex evolution of a salmonid microsatellite locus and its consequences in inferring allelic divergence from size information. *Mol. Biol. Evol.* 14, 230–238.
- Arcot, S.S., Wang, Z., Weber, J.L., Deininger, P.L., Batzer, M.A., 1995. Alu repeats: a source for the genesis of primate microsatellites. *Genomics* 29, 136–144
- Arévalo, E., Zhu, Y., Carpenter, J.M., Strassmann, J.E., 2004. The phylogeny of the social wasp subfamily Polistinae: evidence from microsatellite flanking sequences, mitochondrial COI sequence, and morphological characters. *BMC Evol. Biol.* 4:8.
- Avise, J.C., 1994. *Molecular Markers, Natural History and Evolution*. Chapman & Hall, New York, 551 pp.

- Baliraine, F.N., Bonizzoni, M., Osir, E.O., Lux, S.A., Mulaa, F.J., Zheng, L., Gomulski, L.M., Gasperi, G., Malacrida, A.R., 2003. Comparative analysis of microsatellite loci in four fruit fly species of the genus *Ceratitis* (Diptera: Tephritidae). *Bull. Entomol. Res.* 93, 1–10.
- Balloux, F., Brüner, H., Lugon-Moulin, N., Hausser, J., Goudet, J., 2000. Microsatellites can be misleading: an empirical and simulation study. *Evolution* 54, 1414–1422.
- Bell, G.I., Jurka, J., 1997. The length distribution of perfect dimer repetitive DNA is consistent with its evolution by an unbiased single-step mutation process. *J. Mol. Evol.* 44, 414–421.
- Bennett, N.C., Faulkes, C.G., 2000. *African Mole-Rats: Ecology and Eusociality*. Cambridge University Press, Cambridge, UK, 273pp.
- Bennett, N.C., Jarvis, J.U.M., 1988. The reproductive biology of the Cape mole-rat, *Georychus capensis* (Rodentia, Bathyergidae). *J. Zool. Lond.* 214, 95–106.
- Blankenship, S.M., May, B., Hedgecock, D., 2002. Evolution of a perfect simple sequence repeat locus in the context of its flanking sequence. *Mol. Biol. Evol.* 19, 1943–1951.
- Bowcock, A.M., Ruiz-Linares, A., Tomfohrde, J., Minch, E., Kidd, J.R., Cavalli-Sforza, L.L., 1994. High resolution of human evolutionary trees with polymorphic microsatellites. *Nature* 368, 455–457.
- Braude, S., 2000. Dispersal and new colony formation in wild naked mole-rats: evidence against inbreeding as the system of mating. *Behavioral Ecology* 11, 7–12.
- Bremer, K., 1988. The limits of amino-acid sequence data in angiosperm phylogenetic reconstruction. *Evolution* 42: 795–803.
- Burda, H., 2001. Determinants of the distribution and radiation of African mole-rats (Bathyergidae, Rodentia): ecology or geography? In: Denys, C., Granjon, L., Poulet, A. (Eds.), *African Small Mammals*, IRD Editions, collection Colloques et séminaires, Paris, France. pp. 261–277.
- Burda, H., Honeycutt, R.L., Begall, S., Grütjen, O., Scharff, A., 2000. Are naked and common mole-rats eusocial and if so, why? *Behav. Ecol. Sociobiol.* 47, 293–303.
- Burda, H., Kawalika, M., 1993. Evolution of eusociality in the Bathyergidae: the case of the giant mole-rat (*Cryptomys mehowi*). *Naturwissenschaften* 80, 235–237.

- Burda, H., Zima, J., Scharff, A., Macholán, M., Kawalika, M., 1999. The karyotypes of *Cryptomys anselli* sp. nova and *Cryptomys kafuensis* sp. nova: new species of the common mole-rat from Zambia (Rodentia, Bathyergidae). *Z. Säugetierkd.* 64, 36–50.
- Burland, T.M., Bishop, J.M., O’Ryan, C., Faulkes, C.G., 2001. Microsatellite primers for the African mole-rat genus *Cryptomys* and cross-species amplification within the family Bathyergidae. *Mol. Ecol. Notes* 1, 311–314.
- Calabrese, P.P., Durrett, R.T., Aquadro, C.F., 2001. Dynamics of microsatellite divergence under stepwise mutation and proportional slippage/point mutation models. *Genetics* 159, 839–852.
- Capanna, E., Merani, M.S., 1980. Karyotypes of Somalian rodent populations. 1. *Heterocephalus glaber*. Ruppell, 1842 (Mammalia, Rodentia). *Monit. Zool. Ital. Suppl.* 13, 45–52.
- Causse, M. A., Fulton, T.M., Cho, Y.G., Ahn, S.N., Chunwongse, J., Wu, K., Ziao, J., Yu, Z., Ronald, P.C., Harrington, S.E., 1994. Saturated molecular map of the rice genome based on an interspecific backcross population. *Genetics* 138, 1251–1274.
- Chakraborty, R., Kimmel, M., Stivers, D.N., Davidson, L.J., Deka, R., 1997. Relative mutation rates at di-, tri-, and tetranucleotide microsatellite loci. *Proc. Natl. Acad. Sci. USA* 94, 1041–1046.
- Chirhart, S.E., Honeycutt, R.L., Greenbaum, I.F., 2004. Microsatellite variation and evolution in the *Peromyscus maniculatus* species group. *Mol. Phylogenet. Evol.* 34: 408–415.
- Chitaukali, W.N., Burda, H., Kock, D., 2001. On small mammals of the Nyika Plateau, Malawi. In: Denys, C., Granjon, L., Poulet, A. (Eds.). *African Small Mammals IRD Editions, collection Colloques et séminaires*, Paris, pp. 415–426.
- Chung, M.Y., Ranum, M.P.W., Duvick, L.A., Servadio, A., Zoghbi, H.Y., Orr, H.T., 1993. Evidence for a mechanism predisposing to intergenerational CAG repeat instability in spinocerebellar ataxia type I. *Nat. Genet.* 5, 254–258.
- Cizsek, D., 2000. New colony formation in the “highly inbred” eusocial naked mole-rat: outbreeding is preferred. *Behav. Ecol.* 11, 1–6.

- Clarke, L.A., Rebelo, C.S., Gonçalves, J., Boavida, M.G., Jordan, P., 2001. PCR amplification introduces errors into mononucleotide and dinucleotide repeat sequences. *Mol. Path.* 54, 351–353.
- Clisson, I., Lathuilliere, M., Crouau-Roy, B., 2000. Conservation and evolution of microsatellite loci in primate taxa. *Amer. J. Prim.* 50, 205–214.
- Colson, E., Goldstein, D.B., 1999. Evidence for complex mutations at microsatellite loci in *Drosophila*. *Genetics* 143, 617–627.
- Cooper, G., Rubinsztein, D.C., Amos, W., 1998. Ascertainment bias cannot entirely account for human microsatellites being longer than their chimpanzee homologues. *Human Molec. Genet.* 7: 1425–1429.
- Crawford, A. M., S. M. Kappes, K. A. Paterson, M. J. DeGotari, K. G. Dodds, B. A. Freking, R. T. Stone, Beattie, C. W., 1998. Microsatellite evolution: testing the ascertainment bias hypothesis. *J. Mol. Evol.* 46, 256–260.
- Crozier, R.H., Kaufmann, B., Carew, M.E., Crozier, Y.C., 1999. Mutability of microsatellites developed for the ant *Camponotus consobrinus*. *Mol. Ecol.* 8, 271–276.
- Crow, J.F., 1986. *Basic Concepts in Population, Quantitative, and Evolutionary Genetics*. W.H. Freeman, New York, 273 pp.
- Crow, J.F., Kimura, M. 1970. *An Introduction to Population Genetics Theory*. Harper and Row, New York, 591 pp.
- Culver, M., Menotti-Raymond, M.A., O'Brien, S.J., 2001. Patterns of size homoplasy at 10 microsatellite loci in pumas (*Puma concolor*). *Mol. Biol. Evol.* 18, 1151–1156.
- Davies, K.C., Jarvis, J.U.M., 1986. The burrow systems and burrowing dynamics of the mole-rats *Bathyergus suillus* and *Cryptomys hottentotus* in the fynbos of the south-western Cape, South Africa. *J. Zool.* 209, 125–147.
- de Jong, W.W., van Dijk, M.A.M., Poux, C., Kappé, G., van Rheede, T., Madsen, O., 2003. Indels in protein-coding sequences of Euarchontoglires constrain the rooting of the eutherian tree. *Mol. Phylogenet. Evol.* 28, 328–340
- DeGraaff, G., 1964. A systematic revision of the Bathyergidae (Rodentia) of Southern Africa. Ph.D. dissertation, University of Pretoria, South Africa.

- DeGraaff, G., 1981. The Rodents of Southern Africa. Butterworths, Durban, South Africa.
- Deka, R., Shriver, M.D., Yu, L.M., Ferrell, R.E., Chakraborty, R., 1995. Intra- and interpopulation diversity at short tandem repeat loci in diverse populations of the world. *Electrophoresis* 16, 1659–1664.
- Denys, C., Jaeger, J.-J., 1992. Rodents of the Miocene site of Fort Ternan (Kenya). First part: Phiomysids, bathyergids, sciurids and anomalurids. *Neues Jahrb. Geol. P.-A.* 185, 63–84.
- Dib, C., Raure, S., Fizames, C., Samson, D., Drouot, N., Vignal, A., Millasseau, P., Marc, S., Hazan, J., Seboun, E., Lathrop, M., Gyapay, G., Morissette, J., Weissenbach, J., 1996. A comprehensive genetic map of the human genome based on 5,264 microsatellites. *Nature* 380, 152–154.
- Dietrich, W.F., Miller, J., Steen, R., Merchant, M.A., Damron-Boles, D., Husain, Z., Dredge, R., Daly, M.J., Ingalls, K.A., O'Connor, T.J., 1996. A comprehensive genetic map of the mouse genome. *Nature* 380, 152–154.
- Di Rienzo, A., Peterson, A.C., Garza, J.C., Valdes, A.M., Slatkin, M., Freimer, M.B., 1994. Mutational processes of single-sequence repeat loci in human populations. *Proc. Natl. Acad. Sci. USA* 91, 3166–3170.
- Eckert, K.A., Mowery, A., Hile, S.E., 2002. Misalignment-mediated DNA polymerase beta mutations: comparison of microsatellite and frame-shift error rates using a forward mutation assay. *Biochemistry* 41, 10490–10498.
- Edwards, A., Civitello, A., Hammond, H.A., Caskey, C.T., 1991. DNA typing and genetic mapping with trimeric and tetrameric tandem repeats. *Am. J. Hum. Genet.* 49, 746–756.
- Edwards, A., Hammond, H.A., Jin, L., Caskey, C.T., Chakraborty, R., 1992. Genetic variation at five trimeric and tetrameric tandem repeat loci in four human populations. *Proc. Natl. Acad. Sci. USA* 91, 3166–3170.
- El Nahas, E. M., de Hondt, H.A., Womack, J.E., 2001. Current status of the river buffalo (*Bubalus bubalus* L.) gene map. *J. Heredity* 92, 221–225.
- Ellegren, H., 2000. Microsatellite mutations in the germline; implications for evolutionary inference. *Trends in Genet.* 16, 551–558.

- Ellegren, H., Moore, S., Robinson, N., Byrne, K., Ward, W., Sheldon, B.C., 1997. Microsatellite evolution — a reciprocal study of repeat lengths at homologous loci in cattle and sheep. *Mol. Biol. Evol.* 14, 854–860.
- Ellegren, H., Primmer, C.R., Sheldon, B.C. 1995. Microsatellite “evolution”: directionality or bias? *Nat. Genet.* 11, 360–362.
- Ellerman, J.R., Hayman, R.W., Holt, G.W.C., 1940. The families and genera of living Rodents. The Trustees of the British Museum (Natural History) London 1, 79–95.
- Estoup, A., Cornuet, J.-M., 1999. Microsatellite evolution: inferences from population data. In: Goldstein, D.B., Schlötterer, C. (Eds.), *Microsatellites: Evolution and Application*. Oxford University Press, New York, pp 49–65.
- Estoup, A., Tailliez, C., Cornuet, J.-M., Solignac, M., 1995. Size homoplasy and mutational processes of interrupted microsatellites in two bee species, *Apis mellifera* and *Bombus terrestris* (Apidae). *Mol. Biol. Evol.* 12, 1074–1084.
- Farris, J.S., 1969. A successive approximations approach to character weighting. *Syst. Zool.* 18, 374–385.
- Farris, J.S., 1989. The retention index and homoplasy excess. *Syst. Zool.* 38, 406–407.
- Farris, J.S., Källersjö, M., Kluge, A.G., Bult, C., 1995. Testing significance of incongruence. *Cladistics* 10, 315–320.
- Faulkes, C.G., Abbott, D.H., Mellor, A.L., 1990. Investigation of genetic diversity in wild colonies of naked mole-rats (*Heterocephalus glaber*) by DNA fingerprinting. *J. Zool.* 221, 87–97.
- Faulkes, C.G., Bennett, N.C., Bruford, M.W., O’Brien, H.P., Aguilar, G.H., Jarvis, J.U.M., 1997. Ecological constraints drive social evolution in the African mole-rats. *Proc. R. Soc. Lond. B. Biol. Sci.* 264, 1619–1627.
- Faulkes, C.G., Verheyen, E., Verheyen, W., Jarvis, J.U.M., Bennett N.C., 2004. Phylogeographical patterns of genetic divergence and speciation in African mole-rats (Family: Bathyergidae). *Mol. Ecol.* 13, 613–29.
- Feldman, M.W., Bergman, A., Pollock, D.D., Goldstein, D.B., 1997. Microsatellite genetic distances with range constraints – analytic description and problems of estimation. *Genetics* 145, 207–216.

- Felsenstein, J., 1985. Confidence limits on phylogenies: an approach using the bootstrap. *Evolution* 39, 783–791.
- Filippucci, M.G., Burda, H., Nevo, E., Kocka, J., 1994. Allozyme divergence and systematics of common mole-rats (*Cryptomys*, Bathyergidae, Rodentia) from Zambia. *Z. Säugetierkd.* 59, 42–51.
- Filippucci, M.G., Kawalika, M., Macholán, M., Scharff, A., Burda, H., 1997. Allozyme differentiation and taxonomic status of Zambian giant mole-rats, *Cryptomys mechowii* (Bathyergidae, Rodentia). *Z. Säugetierkd.* 62, 172–178.
- Fitzsimmons, N.N., Moritz, C., Moore, S.S., 1995. Conservation and dynamics of microsatellite loci over 300 million years of marine turtle evolution. *Mol. Biol. Evol.* 12, 432–440.
- Fleischer, R.C., 1996. Application of molecular methods to the assessment of genetic mating systems in vertebrates. In: Ferraris, J.D., Palumbi, S.R. (Eds.), *Molecular Zoology: Advances, Strategies, and Protocols*. Wiley-Liss, New York, pp. 133–161.
- Forbes, S.H., Hogg, J.T., Buchanan, F.C., Crawford, A.M., Allendorf, F.W., 1995. Microsatellite evolution in congeneric mammals: domestic and bighorn sheep. *Mol. Biol. Evol.* 12, 1106–1113.
- Freeman, S., Herron, J.C., 1998. *Evolutionary Analysis*. Prentice-Hall, Englewood Cliffs, NJ.
- Gardner, M.G., Bull, C.M., Cooper, S.J.B., Duffield, G.A., 2000. Microsatellite mutations in litters of the Australian lizard, *Egernia stokesii*. *J. Evol. Biol.* 13, 551–560.
- Garza, J.C., Slatkin, M., Freimer, N.B., 1995. Microsatellite allele frequencies in humans and chimpanzees, with implications for constraints on allele size. *Mol. Biol. Evol.* 12, 594–603.
- George, W., 1979. Conservatism in the karyotypes of two African mole-rats (Rodentia, Bathyergidae). *Z. Säugetierkd.* 44, 278–285.
- Gertsch, P., Pamilo, P., Varvio, S.-L., 1995. Microsatellites reveal high genetic diversity within colonies of *Camponotus* ants. *Mol. Ecol.* 4, 257–260.
- Glaubitz, J.C., 2004. Convert: a user-friendly program to reformat diploid genotypic data for commonly used population genetic software packages. *Mol. Ecol. Notes* 4, 309.

- Glenn, T.C., Staton, J.L., Vu, A.T., Davis, L.M., Bremer, J.R., Rhodes, W.E., Brisbin, I.L., Jr., Sawyer, R.H., 2002. Low mitochondrial DNA variation among American alligators and a novel non-coding region in crocodylians. *J. Exp. Zool.* 294, 312–24.
- Glenn, T.C., Stephan, W., Dessauer, H.C., Braun, M.J., 1996. Allelic diversity in alligator microsatellite loci is negatively correlated with GC content of flanking sequences and evolutionary conservation of PCR amplifiability. *Mol. Biol. Evol.* 13, 1151–1154.
- Goodfellow, P.N., 1993. Viewpoint: microsatellites and the new genetic maps. *Curr. Biol.* 3, 149–151.
- Goldstein, D.B., Pollack, D.D., 1994. Least squares estimation of molecular distance – noise abatement in phylogenetic reconstruction. *Theor. Popul. Biol.* 45, 219–226.
- Goldstein, D.B., Ruiz Linares, A., Cavalli-Sforza, L.L., Feldman, M.W., 1995a. Genetic absolute dating based on microsatellites and the origin of modern humans. *Proc. Nat. Acad. Sci. USA* 92, 6723–6727.
- Goldstein, D.B., Ruiz Linares, A., Cavalli-Sforza, L.L., Feldman, M.W., 1995b. An evaluation of genetic distances for use with microsatellite loci. *Genetics* 139, 463–471.
- Grubb, P., Sandrock, O., Kullmer, O., Kaiser, T.M., Schrenk, F., 1999. Relationships between Eastern and Southern African mammal faunas. In : Bromage, T.G., Schrenk F. (Eds.), *African Biogeography, Climate Change, and Human Evolution*. Oxford University Press, New York, pp. 253–267.
- Harr, B., Zangerl, B., Schlötterer, C., 2000. Removal of microsatellite interruptions by DNA replication slippage: phylogenetic evidence from *Drosophila*. *Mol. Bio. Evol.* 17, 1001–1009.
- Hasagawa, M., Kishino, H., Yano, T., 1985. Dating the human-ape splitting by a molecular clock of mitochondrial DNA. *J. Mol. Evol.* 21, 160–174.
- Hedrick, P.W., 1999. Highly variable loci and their interpretation in evolution and conservation. *Evolution* 53, 313–318.
- Honeycutt, R. L., Allard, M.W., Edwards, S.V., Schlitter, D.A., 1991. Systematics and evolution of the family Bathyergidae. In: Sherman, P.W., Jarvis, J.U.M., Alexander, R.D. (Eds.), *The Biology of the Naked Mole-Rat*. Princeton University Press, Princeton, NJ, pp. 45–65.

- Honeycutt, R.L., Edwards, S.V., Nelson, K., Nevo, E. 1987. Mitochondrial DNA variation and the phylogeny of African mole rats (Rodentia: Bathyergidae). *Syst. Zool.* 36, 280–292.
- Honeycutt, R.L., Nelson, K., Schlitter, D.A., Sherman, P.W., 1991. Genetic variation within and among populations of the naked mole-rat: evidence from nuclear and mitochondrial genomes. In: Sherman, P.W., Jarvis, J.U.M., Alexander, R.D. (Eds.), *The Biology of the Naked Mole-Rat*, Princeton University Press, Princeton, NJ, pp. 195–208.
- Huchon, D., Douzery, E.J., 2001. From the Old World to the New World: a molecular chronicle of the phylogeny and biogeography of hystricognath rodents. *Mol. Phylogenet. Evol.* 20, 238–251.
- Huelsenbeck, J., Ronquist, F., 2001. MrBayes: Bayesian inference of phylogenetic trees. *Bioinformatics* 17, 754–755.
- Hutter, C.M., Schug, M.D., Aquadro, C.F., 1998. Microsatellite variation in *Drosophila melanogaster* and *Drosophila simulans*: a reciprocal test of the ascertainment bias hypothesis. *Mol. Biol. Evol.* 12, 1620–1636.
- Ingram, C.M., Burda, H., Honeycutt, R.L., 2004. Molecular phylogenetics and taxonomy of the African mole-rats, genus *Cryptomys* and the new genus *Coetomys* Gray, 1864. *Mol. Phylogenet. Evol.* 31, 997–1014.
- Janecek, L.L., Honeycutt, R.L., Tautenbach, I.L., Erasmus, B.H., Reig, S., Schlitter, D.A., 1992. Allozyme variation and systematics of African mole-rats (Rodentia: Bathyergidae). *Biochem. Syst. Ecol.* 60, 401–416.
- Jarvis, J.U.M., 1981. Eusociality in a mammal – cooperative breeding in naked mole-rat *Heterocephalus glaber* colonies. *Science* 212, 571–573.
- Jarvis, J.U.M., Bennett, N.C., 1991. Ecology and behavior of the family Bathyergidae. In: Sherman, P.W., Jarvis, J.U.M., Alexander, R.D. (Eds.), *The Biology of the Naked Mole-Rat*. Princeton University Press, Princeton, NJ, pp. 66–96.
- Jarvis, J.U.M., Bennett, N.C., 1993. Eusociality has evolved independently in two genera of bathyergid mole-rats – but occurs in no other subterranean mammal. *Behav. Ecol. Sociobiol.* 33, 253–260.
- Jarvis, J.U.M., O’Riain, M.J., Bennett, N.C., Sherman, P.W., 1994. Mammalian eusociality: a family affair. *Trends Ecol. Evol.* 9, 47–51.
- Jin, L., Macaubas, C., Hallmayer, J., Kimura, A., Mignot, E., 1996. Mutation rate varies

- among alleles at a microsatellite locus – phylogenetic evidence. *Proc. Natl. Acad. Sci. USA* 93, 15285–15288.
- Jordan, P.W., Goodman, A.E., Donnellan, S. 2002. Microsatellite primers for Australian and New Guinean pythons isolated with an efficient marker development method for related species. *Mol. Ecol. Notes* 2, 78–82.
- Karhu, A., Dieterich, J.-H., Savolainen, 2000. Rapid expansion of microsatellite sequences in pines. *Mol. Biol. Evol.* 17, 259–265.
- Kawalika, M., Burda, H., Brüggert, D., 2001. Was Zambia a cradle of the genus *Cryptomys* (Bathyergidae, Rodentia)? A further new ancestral (?) species of *Cryptomys* from Zambia. In: Denys C., Granjon L., Poulet A. (Eds.), *African Small Mammals*. IRD Editions, collection Colloques et séminaires, Paris, pp. 253–261.
- Kim, K.-S., Min, M.-S., An, J.-H., Lee, H., 2004. Cross-species amplification of Bovidae microsatellites and low diversity of the endangered Korean goral. *J. Hered.* 95, 521–525.
- Kimmel, M., Chakraborty, R., King, J.P., Bamshad, M., Watkins, W.S., Jorde, L.B., 1998. Signature of population expansion in microsatellite repeat data. *Genetics* 148, 1921–1930.
- Kimura, M., 1980. A simple method for estimating evolutionary rate of base substitutions through comparative studies of nucleotide sequences. *J. Mol. Evol.* 16, 111–120.
- Kimura, M., Crow, J.F., 1964. The number of alleles that can be maintained in a finite population. *Genetics* 49, 725–738.
- Kimura, M., Ohta, T., 1978. Stepwise mutation model and distribution of allelic frequencies in a finite population. *Proc. Natl. Acad. Sci. USA* 75, 2868–2872.
- Krawczak, M., Cooper, D.N., 1991. Gene deletions causing human genetic disease: Mechanism of mutagenesis and the role of the local DNA sequence environment. *Hum. Genet.* 86, 425–441.
- Lacey, E., Patton, J.L., Cameron, G.N., 2000. *Life Underground: The Biology of Subterranean Rodents*. University of Chicago Press, Chicago.
- Lavocat, R., 1973. Les rongeurs du miocène d'Afrique orientale. I. Miocène inférieur, *Mém. Trav. E.O.H.E. Institut de Montpellier*. 1: 1–284.

- Lavocat, R., 1978. Rodentia and Lagomorpha . In : Maglio, V., Cooke, H.V. (Eds.), Evolution of African Mammals. Harvard Univ Press, Cambridge, MA, pp. 69–89.
- Lavocat, R., 1988. Un rongeur bathyergidé nouveau remarquable du Miocène de Fort Ternan (Kenya). C. R. Acad. Sci. Paris 306, 1301–1304.
- Levinson, G., Gutman, G.A., 1987. Slipped-strand mispairing: a major mechanism for DNA sequence evolution. Mol. Biol. Evol. 4, 203–221.
- Lovegrove, B.G., 1986. Thermoregulation of the subterranean rodent genus *Bathergus* (Bathyergidae). S. Afr. J. Zool. 21, 283–288.
- Luikart, G.L., Sherwin, W.B., Steele, B.M., Allendorf, F.W., 1998a. Usefulness of molecular markers for detecting population bottlenecks via monitoring genetic change. Mol. Ecol. 7, 963–974.
- Luikart, G.L., Sherwin, W.B., Steele, B.M., Allendorf, F.W., 1998b. Distortion of allele frequency distributions provides a test for recent population bottlenecks. J. Hered. 89, 238–247.
- Macaubas, C., Jin, L., Hallmayer, J., Kimura, A., Mignot, E., 1997. The complex mutation pattern of a microsatellite. Genome Res. 7, 635–641.
- Macholán, M., Burda, H., Zima, J., Misek, I., Kawalika, M., 1993. Karyotype of the giant mole-rat, *Cryptomys mechowii* (Bathyergidae, Rodentia). Cytogenet. Cell Genet. 64, 261–263.
- Macholán, M., Burda, H., Zima, J., Misek, I., Kawalika, M., 1998. A new karyotype of a common mole-rat and taxonomical status of *Cryptomys amatus* from Zambia. Z. Säugetierkd 63, 186–190.
- Maddison, D.R., Maddison, W.P., 2002. MacClade 4: Analysis of Phylogeny and Character Evolution. Version 4.0. Sinauer Associates, Sunderland, MA.
- Matthee, C. A., Burzlaff, J. D., Taylor, J. F., Davis, S. K., 2001. Mining the mammalian genome for artiodactyl systematics. Syst. Biol. 50, 367–90.
- Maudet, C., Miller, C., Bassano, B., Breitenmoser-Wursten, C., Gauthier, D., Obexer-Ruff, G., Michallet, J., Taberlet, P. Luikart, G., 2002. Microsatellite DNA and recent statistical methods in wildlife conservation management: applications in Alpine ibex (*Capra ibex* (*ibex*)). Molec. Ecol. 11, 421–436.

- McKenna, M. C., Bell, S.K., Simpson, G.G., 1998. Classification of Mammals Above the Species Level. Columbia University Press, New York.
- Meier, J.-L., 2001. Diversität und Artbildung der Graumulle (*Cryptomys*, Bathyergidae) entlang des oberen Sambesi. M.Sc. Dissertation, University of Essen, Germany.
- Michalakis, Y., Excoffier, L., 1996. A genetic estimation of population subdivision using distances between alleles with special reference for microsatellite loci. *Genetics* 142, 1061–1064.
- Moore, S. S., Sargeant, L.L., King, T.J., Mattick, J.S., Georges, M., Hetzel, J.S., 1991. The conservation of di-nucleotide microsatellites among mammalian genomes allows the use of heterologous PCR primer pairs in closely related species. *Genomics* 10, 654–660.
- Murphy, W., Eizirik, E., Johnson, W.E., Zhang, Y.P., Ryder, E.O., O'Brien, S.J., 2001. Molecular phylogenetics and the origins of placental mammals. *Nature* 409, 614–618.
- Nedbal, M.A., Allard, M.W., Honeycutt, R.L., 1994. Molecular systematics of hystricognath rodent: evidence from the mitochondrial 12S rRNA gene. *Mol. Phylogenet. Evol.* 3, 206–220.
- Nevo, E., 1999. Mosaic Evolution of Subterranean Mammals: Regression, Progression and Global Convergence. Oxford University Press, Oxford, UK.
- Nevo, E., Ben-Shlomo, R., Beiles, A., Jarvis, J.U.M., Hickman, G.C., 1987. Allozyme differentiation and systematics of the endemic subterranean mole rats of South Africa. *Biochem. Syst. Ecol.* 15, 489–502.
- Nevo, E., Capanna, E., Corti, M., Jarvis, J.U.M., Hickman, G.C., 1986. Karyotype differentiation in the endemic subterranean mole-rats of South Africa (Rodentia, Bathyergidae). *Z. Säugetierkd.* 51, 36–49.
- Nevo, E., Filippucci, M.G., Beiles, A., 1990. Genetic diversity and its ecological correlates in nature: comparisons between subterranean, fossorial, and above ground small mammals. In: Nevo, E., Reig, O.A. (Eds.), *Evolution of Subterranean Mammals at the Organismal and Molecular Levels*. Wiley-Liss, New York. pp. 347–366.
- Nevo, E., Reig, O.A. (eds.), 1990. *Evolution of Subterranean Mammals at the Organismal and Molecular Levels*. Wiley-Liss, New York.

- Nowak, R. M., 1999. Walker's Mammals of the World, Volume II, Sixth Edition. Johns Hopkins University Press, Baltimore, pp. 1635–1644.
- Ohta, T., Kimura, M., 1973. A model of mutation appropriate to estimate the number of electrophoretically detectable alleles in a finite population. *Genet. Res.* 22, 201–204.
- Okada, N., 1991. SINEs: short interspersed repeated elements of the eukaryotic genome. *Trends Ecol. Evol.* 6, 358–361.
- Omlin, F.X., 1997. Optic disc and optic nerve of the blind Cape mole-rat (*Georychus capensis*): a proposed model for naturally occurring reactive gliosis. *Brain Res. Bull.* 44, 627–632.
- Oosthuizen, M.K., Cooper, H.M., Bennett, N.C., 2003. Circadian rhythms of locomotor activity in solitary and social species of African mole-rats (Family: Bathyergidae). *J. Biol. Rhythm.* 18, 481–490.
- Ortí, G., Pearse, D.E., Avise, J.C., 1997. Phylogenetic assessment of length variation at a microsatellite locus. *Proc. Natl. Acad. Sci. USA* 94, 10745–10749.
- O’Ryan, C., Harley, E.H., Bruford, M.W., Beaumont, M.A., Wayne, R.K., Cherry, M.I., 1998. Microsatellite analysis of genetic diversity in fragmented South African buffalo (*Syncerus caffer*) populations. *Anim. Conserv.* 1, 85–95.
- Paetkau, D., Calvert, W., Stirling, I., Strobeck, C., 1995. Microsatellite analysis of population structure in Canadian polar bears. *Mol. Ecol.* 4, 347–354.
- Pemberton, J.M., Slate, J., Bancroft, D.R., Barrett, J.A., 1995. Non-amplifying alleles at microsatellite loci: a caution for parentage and population studies. *Mol. Ecol.* 4, 249–25.
- Posada, D., Crandall, K.A., 1998. MODELTEST: testing the model of DNA substitution. *Bioinformatics* 14, 817–818.
- Primmer, C.R., Ellegren, H., 1998. Patterns of molecular evolution in avian microsatellites. *Mol. Biol. Evol.* 15, 997–1008.
- Primmer, C.R., Ellegren, H., Saino, N., Møller, A.P., 1996a. Directional evolution in germline microsatellite mutations. *Nat. Genet.* 13, 391–393.
- Primmer, C.R., Møller, A., Ellegren, H., 1996b. A wide-range survey of cross-species microsatellite amplification in birds. *Mol. Ecol.* 5, 365–378.

- Primmer, C.R., Saino, N., Møller, A.P., Ellegren, H., 1998. Unraveling the processes of microsatellite evolution through analysis of germ line mutations in barn swallows *Hirundo rustica*. *Mol. Biol. Evol.* 15, 1047–1054.
- Queller, D.C., Strassmann, J.E., Hughes, C.R., 1993. Microsatellites and kinship. *Trends Ecol. Evol.* 8, 285–288.
- Raymond, M., Rousset, F., 1995. GENEPOP Version 1.2: population genetics software for exact tests and ecumenicism. *J. Hered.* 86, 248–249.
- Reeve, H.K., Westneat, D.F., Noon, W.A., Sherman, P.W., Aquadro, C.F., 1990. DNA “fingerprinting” reveals high levels of inbreeding in colonies of the eusocial naked mole-rat. *Proc. Natl. Acad. Sci. USA* 87, 2496–2500.
- Roberts, A., 1951. *The Mammals of South Africa*. Trustees of the “Mammals of South Africa” Book Fund, Johannesburg.
- Rokas A., Holland, P.W., 2000. Rare genomic changes as a tool for phylogenetics. *Trends Ecol. Evol.* 15, 454–459.
- Rooney, A.P., Honeycutt, R.L., Davis, S.K., Derr, J.N., 1999. Evaluating a putative bottleneck in a population of bowhead whales from patterns of microsatellite diversity and genetic disequilibria. *J. Mol. Biol.* 48, 682–690.
- Roper, T.J., Bennett, N.C., Conradt, L., Molteno, A.J., 2001. Environmental conditions in burrows of two species of African mole-rat, *Georychus capensis* and *Cryptomys damarensis*. *J. Zool.* 254, 101–107.
- Rosevear, D.R., 1969. *The Rodents of West Africa*. Trustees of the British Museum (Natural History), London.
- Roy, M.S., Geffen, E., Smith, D., Ostrander, E.A., Wayne, R.K., 1994. Patterns of differentiation and hybridization in North American wolflike canids, revealed by analysis of microsatellite loci. *Mol. Biol. Evol.* 11, 553–570.
- Roy, M.S., Geffen, E., Smith, D., Wayne, R.K., 1996. Molecular of pre-1940 red wolves. *Conserv. Biol.* 10, 1413–1424.
- Rubinsztein, D.C., Amos, W., Leggo, J., Goodburn, S., Jain, S., Li, S.-H., Margolis, R.L., Ross, C.A., Ferguson-Smith, M.A., 1995. Microsatellite evolution – evidence for directionality and variation in rate between species. *Nat. Genet.* 10, 337–343.

- Sanderson, M.J., 2003. r8s: inferring absolute rates of molecular evolution and divergence times in the absence of a molecular clock. *Bioinformatics* 19, 301–302.
- Schlötterer, C., 2001. Genealogical inference of closely related species based on microsatellites. *Genet. Res.* 78, 209–212.
- Schlötterer, C., Tautz, D., 1992. Slippage synthesis of simple sequence DNA. *Nuc. Acids Res.* 20, 211–215.
- Scharff, V.A., Macholán, M., Zima, J., Burda, H., 2001. A new karyotype of *Heliophobius argenteocinereus* (Bathyergidae, Rodentia) from Zambia with field notes on the species. *Mamm. Biol.* 66, 376–378.
- Schug, M.D., Hutter, C.M., Wetterstrand, K.A., Gaudette, M.S., Mackay, T.R.C., Aquadro, C.F., 1998. The mutation rates of di-, tri-, and tetranucleotide repeats in *Drosophila melanogaster*. *Mol. Biol. Evol.* 15, 1751–1760
- Shao, Z., Lek, S., Chang, J., 2005. Complex mutation at a microsatellite locus in sturgeons: *Acipenser sinensis*, *A. schrenckii*, *A. gueldenstaedtii*, and *A. baerii*. *J. Applied Ichth.* 21, 2–7.
- Sherman, P.W., Jarvis, J.U.M., Alexander, R.D., 1991. *The Biology of the Naked Mole-Rat*. Princeton University Press, Princeton, NJ, 518 pp.
- Shriver, M.D., Jin, L., Chakraborty, R., Boerwinkle, E., 1993. VNTR allele frequency distributions under the stepwise mutation model. *Genetics* 134, 983–993.
- Shimodaira, H., Hasagawa, M., 1999. Multiple comparisons of log-likelihoods with applications to phylogenetic inference. *Mol. Biol. Evol.* 16, 1114–1116.
- Sibley, R.M., Meade, A., Boxall, N., Wilkinson, M.J., Corne, D.W., Whittaker, J.C., 2003. The structure of interrupted human AC microsatellites. *Mol. Biol. Evol.* 20, 453–459.
- Slatkin, M., 1995. A measure of population subdivision based on microsatellite allele frequencies. *Genetics* 139, 457–462.
- Smit, A.F.A., Hubley, R., Green, P., 2004. RepeatMasker Open–3.0. Available at <http://www.repeatmasker.org>.
- Smith, M.F., 1998. Phylogenetic relationships and geographic structure in pocket gophers in the genus *Thomomys*. *Mol. Phylogenet. Evol.* 9, 1–14.

- Sorenson, M.D., 1999. TreeRot, version 2. Boston University, Boston, MA.
- Springer, M.S., Douzery, E., 1996. Secondary structure and patterns of evolution among mammalian mitochondrial 12S rRNA molecules. *J. Mol. Evol.* 43, 357–73.
- Springer, M.S., Stanhope, M.J., Madsen, O., de Jong, W.W., 2004. Molecules consolidate the placental mammal tree. *Trends Ecol. Evol.* 19, 430–438.
- Strand, M.T., Prolla, A., Liskay, R.M., Petes, T.D., 1993. Destabilization of tracts of simple repetitive DNA in yeast by mutations affecting DNA mismatch repair. *Nature* 365, 274–276.
- Streisinger, G., Okada, Y., Emrich, J., Newton, J., Tsugita, A., Terzaghi, E., Inouye, M., 1966. Frameshift mutations and the genetic code. *Cold Spring Harbor Symposium on Quantitative Biology* 31, 77–84.
- Su, X.Z., Willems, T.E., 1996. Towards a high-resolution *Plasmodium falciparum* linkage map-polymorphic markers from hundreds of simple sequence repeats. *Genomics* 33, 431–444.
- Sudman, P.D., Hafner, M.S., 1992. Phylogenetic relationships among middle American pocket gophers (genus *Orthogeomys*) based on mitochondrial DNA sequences. *Mol. Phylogenet. Evol.* 1, 17–25.
- Sullivan, J., Swofford, D.L., 1997. Are guinea pigs rodents? The importance of adequate models in molecular phylogenetics. *J. Mamm. Evol.* 4, 77–86.
- Sumbera, R., Burda, H., Chitaukali, W.N., Kubova, J., 2003. Silvery mole-rats (*Heliophobius argenteocinereus*, Bathyergidae) change their burrow architecture seasonally. *Naturwissenschaften* 90, 370–373.
- Sunnucks, P., 2000. Efficient genetic markers for population biology. *Trends Ecol. Evol.* 15, 199–203.
- Swofford, D.L., 2002. PAUP*. Phylogenetic Analysis Using Parsimony (*and Other Methods). Version 4. Sinauer Associates, Sunderland, MA.
- Synmonds, V.V., Lloyd, A.M., 2003. An analysis of microsatellite loci in *Arabidopsis thaliana*: mutational dynamics and application. *Genetics* 165, 1475–1488.
- Tajima, F., 1993a. Unbiased estimation of evolutionary distance between nucleotide-sequences. *Mol. Biol. Evol.* 10, 677–688.

- Tajima, F., 1993b. Simple methods for testing the molecular evolutionary clock hypothesis. *Genetics* 135, 599–607.
- Takahashi, K, Okada, N., 2002. Mosaic structure and retropositional dynamics during evolution of subfamilies of short interspersed elements of African cichlids. *Mol. Biol. Evol.* 19, 1303–1312.
- Takazaki, N., Nei, M., 1996. Genetic distances and reconstruction of phylogenetic trees from microsatellite DNA. *Genetics* 144, 389–399.
- Tautz, D., 1993. Notes on the definition and nomenclature of tandemly repetitive DNA sequences. In: Pena, S.D.J., Chakraborty, R., Epplen, J.T., Jeffreys, A.J. (Eds.), *DNA Fingerprinting: State of the Science*. Birkhauser, Basel. pp. 21–28.
- Tavaré, S., 1986. Some probabilistic and statistical problems in the analysis of DNA sequences. *Lect. Notes Math. Life Sci.* 17, 57–86.
- Taylor, A.C., Sherwin, W.B., Wayne, R.K., 1994. Genetic variation of microsatellite loci in bottlenecked species: the northern hairy-nosed wombat (*Lasiorhinus krefftii*). *Mol. Ecol.* 3, 277–290.
- Tenora, F., Baru, V., Proke, M., Sumbera, R., Koubkov, B., 2003. Helminths parasitizing the silvery mole-rat, *Heliophobius argenteocinereus* (Rodentia: Bathyergidae) from Malawi. *Helminthologia* 40, 153–160.
- Thomas, D.S.G., Shaw, P.A., 1988. Late Cainozoic drainage evolution in the Zambezi basin: geomorphological evidence from the Kalahari rim. *J. Afr. Earth Sci.* 7, 611–618.
- Thomas, O., 1910. List of mammals from Mount Kilimanjaro, obtained by Mr. Robin Kemp, and presented to the British Museum by Mr. C. D. Rudd. *Ann. Mag. Nat. Hist.* 8, 303–316.
- Thompson, J.D., Gibson, T.J., Plewniak, F., Jeanmougin, F., Higgins, D.G., 1997. The CLUSTAL X windows interface: flexible strategies for multiple sequence alignment aided by quality analysis tools. *Nuc. Acids Res.* 25, 403–405.
- Trarbach, E.B., Monlleo, I.L., Porciuncula, C.G.G., Fontes, M.I.B., Baptista, M.T.M., Hackel, C., 2004. Similar interstitial deletions of the *KAL-1* gene in two Brazilian families with X-linked Kallmann Syndrome. *Genet. Molec. Biol.* 27, 337–341.
- Tsuzuki, T., Mita, S., Maeda, S., Aracki, S., Shimada, K., 1985. Structure of the human prealbumin gene. *J. Biol. Chem.* 260, 2224–2227.

- Valdes, A.M., Slatkin, M., Freimer, N.B., 1993. Allele frequencies at microsatellite loci: the stepwise mutation model revisited. *Genetics* 133: 737–749.
- van Oppen, M.J.H., Rico, C., Turner, G.F., Hewitt, G.M., 2000. Extensive homoplasy, nonstepwise mutations, and shared ancestral polymorphism at a complex microsatellite locus in Lake Malawi Cichlids. *Mol. Biol. Evol.* 17, 489–498.
- Walton, A.H., Nedbal, M.A., Honeycutt, R.L., 2000. Evidence from intron 1 of the nuclear transthyretin (Prealbumin) gene for the phylogeny of African mole-rats (Bathyergidae). *Mol. Phylogenet. Evol.* 16, 467–474.
- Wang, R., Zheng, L., Toure, Y.T., Dandekar, T., Kafatos, F.C., 2001. When genetic distance matters: measuring genetic differentiation at microsatellite loci in whole-genome scans of recent and incipient mosquito species. *Proc. Natl. Acad. Sci. USA* 98, 10769–10774.
- Weber, J.L., 1990. Informativeness of human (dC-dA)_n · (dG-dT) polymorphisms. *Genomics* 7, 524–530.
- Weber, J.L., May, P.E., 1989. Abundant class of human DNA polymorphisms which can be typed using the polymerase chain reaction. *Am. J. Hum. Genet.* 44, 388–396.
- Weber, J.L., Wong, C., 1993. Mutation of human short tandem repeats. *Hum. Mol. Genet.* 2, 1123–1128.
- White, F., 1983. *The Vegetation of Africa*. UNESCO, Paris.
- Wilder, J., Hollocher, H., 2001. Mobile elements and the genesis of microsatellites in dipterans. *Mol. Biol. Evol.* 18: 384–392.
- Williams, S.L., Schlitter, D.A., Robbins, L.W., 1983. Morphological variation in a natural population of *Cryptomys* (Rodentia, Bathyergidae) from Cameroon. *Ann. Mus. Roy. Afr. Centr. Sc. Zool.* 237, 159–172.
- Wright, T.F., Johns, P.M., Walters, J.R., Lerner, A.P., Swallow, J.G., Wilkinson, G.S., 2004. Microsatellite variation among divergent populations of stalk-eyed flies, genus *Cyrtodiopsis*. *Genet. Res. Camb.* 84, 27–40.
- Yang, Z., 1994. Estimating the pattern of nucleotide substitution. *J. Mol. Evol.* 39, 105–111.
- Yeh, F.C., Boyle, T.J.B., 1997. Population genetic analysis of co-dominant and dominant markers and quantitative traits. *Belg. J. Bot.* 129, 157.

- Zardoya, R., Vollmer, D.M., Craddock, C., Streelman, J.R., Karl, S., Meyer, A., 1996. Evolutionary conservation of microsatellite flanking regions and their use in resolving the phylogeny of cichlid fishes (Pisces: Perciformes). *Proc. R. Soc. Lond. B Biol. Sci.* 263, 1589–1598.
- Zhivotovsky, L.A., Feldman, M.W., 1995. Microsatellite variability and genetic distances. *Proc. Natl. Acad. Sci. USA* 92, 11549–11552.
- Zhu, Y., Queller, D.C., Strassman, J.E., 2000. A phylogenetic perspective on sequence evolution in microsatellite loci. *J. Mol. Evol.* 50: 324–338.

APPENDIX

No.	Species	Locality	Coordinates	Source ^b	Accession numbers ^c	
					12S rRNA	TTR
	<i>Petromus typicus</i>	SA ^a : Cape Province, Farm Riemvasmaak		H550	M63571	AF159313
	<i>Thyromys swinderianus</i>	SA: Kwazulu-Natal, Durban Colony		H571	M63570	AF159312
1	<i>Heterocephalus glaber</i>	Kenya: Machakos District, 8 km N, 3 km W of Mtito Andei	2° 37' S, 38° 03' E	M63563	M63563	AF159324
2	<i>Heterocephalus glaber</i>	Kenya: Machakos District, 8 km N, 3 km W of Mtito Andei	2° 37' S, 38° 03' E	H025	AY427071	
3	<i>Heterocephalus glaber</i>	Kenya: Machakos District, 8 km N, 3 km W of Mtito Andei	2° 37' S, 38° 03' E	H035	AY427072	
4	<i>Heterocephalus glaber</i>	Kenya: Isiolo District, Buffalo Springs National Reserve		H874	AY427074	
5	<i>Heterocephalus glaber</i>	Kenya: Machakos District, 1.5 km NW of Kathakani		H791	AY427075	AF159325
6	<i>Heterocephalus glaber</i>	Kenya: Isiolo District, Buffalo Springs National Reserve		H871	AY427073	AF159326
7	<i>Heliophobius argenteocinereus</i>	Kenya: Rift Valley Province, Athi River		M63562	M63562	AF159323
8	<i>Heliophobius argenteocinereus</i>	Malawi: Blantyre	14° 47' S, 35° 04' E	B4	AY427067	
9	<i>Heliophobius argenteocinereus</i>	Malawi: Nyika	10° 26' S, 33° 51' E	B3	AY427068	
10	<i>Heliophobius argenteocinereus</i>	Malawi: Nyika	10° 26' S, 33° 51' E	B1	AY427069	
11	<i>Heliophobius argenteocinereus</i>	Zambia: Luano Valley	14° 40' S, 29° 55' E	Z13	AY427070	
12	<i>Bathyergus janetta</i>	Namibia: Oranjemund (Orange River)	28° 33' S, 16° 24' E	M63565	M63565	AF159320
13	<i>Bathyergus janetta</i>	Namibia: Boesmanberg, Locality 4, Diamond 1 Area		B.j. Male Nam	AY427016	
14	<i>Bathyergus suillus</i>	SA: Western Cape, Swellendam	34° 01' S, 20° 27' E	M63564	M63564	AF159321

No.	Species	Locality	Coordinates	Source ^b	Accession numbers ^c	
					12S rRNA	TTR
15	<i>Bathyergus suillus</i>	SA: Western Cape, University Western Cape	33° 54' S, 18° 39' E	TM38370	AY427017	
16	<i>Bathyergus suillus</i>	SA: Western Cape, Lilydale	33° 56' S, 18° 46' E	TM38374	AY427018	
17	<i>Bathyergus suillus</i>	SA: Western Cape, Langebaan, Postberg Nature Reserve	33° 07' S, 18° 00' E	TM41452	AY427019	
18	<i>Bathyergus suillus</i>	SA: Western Cape, Langebaan, West Coast National Park	39° 09' S, 18° 56' E	TM41500	AY427020	
19	<i>Georychus capensis</i>	SA: Kwazulu-Natal, Nottingham Road	29° 22' S, 29° 59' E	M63566	M63566	AF159318
20	<i>Georychus capensis</i>	SA: Western Cape, Cape Town	33° 56' S, 18° 28' E	GC5	AY429592	AF159319
21	<i>Georychus capensis</i>	SA: Eastern Cape, Port Elizabeth	33° 42' S, 26° 05' E	TM38354	AY427065	
22	<i>Georychus capensis</i>	SA: Kwazulu-Natal, Wakkerstroom District	27° 17' S, 30° 16' E	TM39874	AY427066	
23	<i>Coetomys amatus</i>	Zambia: Chibale Valley	13° 35' S, 30° 05' E	AMATUS1	AY427021	AY426994
24	<i>Coetomys anelli</i>	Zambia: Mungule	15° 20' S, 28° 10' E	Z1	AY427022	AY426995
25	<i>Coetomys anelli</i>	Zambia: Mungule	15° 20' S, 28° 10' E	Z2	AY427023	AY426996
26	<i>Coetomys anelli</i>	Zambia: Lusaka		Z3	AY427024	AY426997
27	<i>Coetomys anelli</i>	Zambia: Lusaka		Z12	AY427025	AY426998
28	<i>Coetomys damarensis</i>	Namibia: Okahanja	20° 27' S, 16° 42' E	M63569	M63569	AF159316

No.	Species	Locality	Coordinates	Source ^b	Accession numbers ^c	
					12S rRNA	TTR
29	<i>Coetomys damarensis</i>	SA: North-West, 5 Km E Pomfret	25° 50' S, 25° 34' E	HW3053	AY427026	AY426999
30	<i>Coetomys damarensis</i>	SA: North-West, 5 Km E Pomfret	25° 50' S, 25° 34' E	HW3084	AY427027	
31	<i>Coetomys damarensis</i>	SA: North-West, 5 Km E Pomfret	25° 50' S, 25° 34' E	HW3085	AY427028	
32	<i>Coetomys damarensis</i>	SA: North-West, Farm Elibank	26° 20' S, 24° 53' E	SP7540	AY427029	AY427000
33	<i>Coetomys damarensis</i>	SA: North-West, Constantia Farm 309	27° 17' S, 22° 46' E	SP7658	AY427030	
34	<i>Coetomys damarensis</i>	Zambia: West Bank Zambezi	16° 20' S, 23° 17' E	Wessam0102	AY427031	AY427001
35	<i>Coetomys damarensis</i>	Zambia: West Bank Zambezi	16° 20' S, 23° 17' E	Wessam2-0101	AY427032	
36	<i>Coetomys darlingi</i>	Zimbabwe: Chimanimani	19° 48' S, 32° 50' E	DAR3	AY427033	AY427002
37	<i>Coetomys darlingi</i>	Zimbabwe: Chimanimani	19° 48' S, 32° 50' E	DAR4	AY427034	
38	<i>Coetomys darlingi</i>	Zimbabwe: Mandara, Harare (Museum specimen)	17° 47' S, 31° 09' E	CM40460	AY427035	
39	<i>Coetomys foxi</i>	Cameroon: 13 km S Ngaundere (Museum specimen)	07° 12' N, 13° 36' E	CM59487	AY427036	
40	<i>Coetomys kafuensis</i>	Zambia: Itezhi-tezhi	15° 46' S, 26° 02' E	Z10	AY427037	AY427003
41	<i>Coetomys 'Kasama'</i>	Zambia: Kasama		Z5-Holotype	AY427038	AY427004
42	<i>Coetomys mehowi</i>	Zambia: Ndola		Z6	AY427039	AY427005
43	<i>Coetomys mehowi</i>	Zambia: Chibale Valley	13° 35' S, 30° 05' E	M69	AY427040	

No.	Species	Locality	Coordinates	Source ^b	Accession numbers ^c	
					12S rRNA	TTR
44	<i>Coetomys mechowii</i>	Zambia: Chibale Valley	13° 35' S, 30° 05' E	MEC1	AY427041	
45	<i>Coetomys mechowii</i>	Zambia: Ndola		MEC2	AY427042	
46	<i>Coetomys m.mellandi</i>	Zambia: Solwezi Boma	12° 11' S, 26° 25' E	TM12667	AY427043	
47	<i>Coetomys micklei</i>	Zambia: Kataba		KATJLM0401	AY427044	
48	<i>Coetomys ochraceocinereus</i>	South Sudan: Ivatoku (?) or Bahr-al-Ghazal		C.O.#1	AY427045	
49	<i>Coetomys whytei</i>	Malawi: Nyika	10° 24' S, 33° 50' E	B2	AY427046	AY427006
50	<i>Coetomys whytei</i>	Malawi: Karonga	09° 56' S, 33° 56' E	KAR1	AY427047	AY427007
51	<i>Coetomys anelli</i>	Zambia: sample received from Shimon Simson 7/24/90		H650	AF290211	AF159317
52	<i>Coetomys sp</i>	Zambia: Senanga	15° 58' S, 23° 20' E	SEN	AY427049	AY427009
53	<i>Coetomys sp</i>	Zambia: Sekute		SEKCHF	AY427048	AY427008
54	<i>Coetomys sp</i>	Zambia: Livingstone		LIV0201	AY427050	AY427010
55	<i>Cryptomys hottentotus</i>	SA: Western Cape, Eendekuul	32° 42' S, 18° 53' E	CHH1	M63567	AF159314
56	<i>Cryptomys hottentotus</i>	SA: Western Cape, 28 Km S Clanwilliam	32° 22' S, 18° 58' E	TM38420	AY427056	
57	<i>Cryptomys hottentotus</i>	SA: Western Cape; Algeria Forest, Cederberg	32° 22' S, 18° 58' E	TM38436	AY427055	

No.	Species	Locality	Coordinates	Source ^b	<u>Accession</u> 12S rRNA
58	<i>Cryptomys hottentotus</i>	SA: Western Cape; Langebaan, Postberg Nature Reserve	33° 07' S, 18° 00' E	TM41446	AY427058
59	<i>Cryptomys holosericeus</i>	SA: North-West; Farm Memel	26° 22' S, 24° 46' E	SP7535	AY427059
60	<i>Cryptomys holosericeus</i>	SA: North-West; Farm Elibank	26° 20' S, 24° 53' E	SP7552	AY427060
61	<i>Cryptomys holosericeus</i>	SA: Free State; Henneman	28° 01' S, 26° 59' E	TM38475	AY427061
62	<i>Cryptomys holosericeus</i>	SA: Free State; Henneman	28° 01' S, 26° 59' E	SP7697	AY427062
63	<i>Cryptomys anomalus</i>	SA: Gauteng, Moreleta Nature Reserve	25° 45' S, 28° 12' E	SP7703	AY427063
64	<i>Cryptomys natalensis</i>	SA: Kwazulu-Natal, Pietermaritzburg	29° 36' S, 30° 27' E	CHN5	M63568
65	<i>Cryptomys natalensis</i>	SA: Free State, Ficksburg, Golf Course	28° 53' S, 27° 53' E	TM41573	AY427065
66	<i>Cryptomys natalensis</i>	SA: North-West; Farm Donkeshoek	26° 20' S, 25° 53' E	SP7521	AY427066
67	<i>Cryptomys natalensis</i>	SA: Kwazulu-Natal, Durban, Botanical Gardens	29° 53' S, 30° 58' E	TM38327	AY427067
68	<i>Cryptomys natalensis</i>	SA: Kwazulu-Natal, Durban, Bluff Nature Reserve	29° 55' S, 30° 59' E	TM38461	AY427068
69	<i>Cryptomys natalensis</i>	SA: Mpumalanga, Dullstroom, Verlorenvalle	25° 18' S, 30° 07' E	TM38464	AY427069
70	<i>Cryptomys natalensis</i>	SA: Mpumalanga, Wakkerstroom	27° 17' S, 30° 16' E	TM41610	AY427070
71	<i>Coetomys bocagei</i>	Angola: Lubango	15° S, 13° E	AF012213	AF012213
72	<i>Coetomys kafiensis'</i> choma'	Zambia: Choma (Kalomo-Aguilar)	17° S, 27° E	AF012217	AF012217

No.	Species	Locality	Coordinates	Source ^b	Accession numbers ^c	
					12S rRNA	TTR
73	<i>Cryptomys nimrodi</i>	Zimbabwe: Hillside	20° S, 29° E	AF012219	AF012219	
74	<i>Cryptomys anomalus 'pretoria'</i>	SA: Gauteng, Pretoria	26° S, 28° E	AF012218	AF012218	
75	<i>Coetomys anelli'amatus'</i>	Zambia: Lusaka	15° S, 28° E	AF012216	AF012216	
76	<i>Coetomys darlingi</i>	Zimbabwe: Goromonzi	17° S, 30° E	AF012215	AF012215	
77	<i>Coetomys mehowi</i>	Zambia: Chingola	12° S, 28° E	AF012214	AF012214	

^aSA = South Africa

^bTransvaal Museum - TM, Carnegie Museum - CM, Senckenberg Museum, Frankfurt - SMF

^cGenbank accession numbers

VITA

Colleen Marie Ingram

I. Personal Information

Address: Department of Wildlife and Fisheries Sciences
2258 TAMUS
College Station, TX 77843-2258

II. Education

B.S., Biology, California State University, Long Beach, May 1995

III. Awards & Fellowships

Research Grant: Primate Conservation, Inc. (\$2500.00)2000
Conservation Genetics of Populations of Two Malagasy Primates,
Propithecus diadema and *Propithecus tattersali*

Regents' Fellowship (TAMU)..... 1998 - 1999
Phi Kappa Phi Honor Society..... Inducted 1997
CSULB President's List.....Fall 1994
CSULB Dean's List..... Spring 1995
National Dean's List1994 - 1995

IV. Publications

Kock, D., C. M. Ingram, L. J. Frabotta, H. Burda, and R. L. Honeycutt. 2005. On the nomenclature of Bathyergidae and *Fukomys* n. gen. (Mammalia:Rodentia). *Zootaxa (in Review)*.

Ingram, C. M., H. Burda, and R. L. Honeycutt. 2004. Molecular phylogenetics and taxonomy of the African mole-rats, genus *Cryptomys* and the new genus *Coetomys* Gray, 1864. *Molecular Phylogenetics and Evolution*, 31(3): 997-1014.

Mayor, M. I., J. A. Sommer, M. L. Houck, J. Zaonarivelo, P. C. Wright, C. M. Ingram, S. R. Engel, and E. E. Louis, Jr. 2004. Specific Status of *Propithecus* spp. *International Journal of Primatology*. 25(4): 875-900.